

DOCTORAL THESIS

Optimization and Tech-economic Assessment of Passive Energy-saving Strategies for Opaque Envelopes of Traditional Dwellings in Northeast of Sichuan Hills, China

July 2022

HOU JIAWEN

2019DBB413

The University of Kitakyushu

Faculty of Environmental Engineering

Department of Architecture

Fukuda Laboratory

Abstract

The energy consumption of the building sector occupies nearly 40% of global energy consumption, while in China, the total energy consumption of the whole building process in 2018 was 2.147 billion tce, accounting for 46.5% of the total national energy consumption, of which 1 billion tce was consumed during the building operation phase. Meanwhile, rural buildings contribute 24% of building energy consumption during the operation phase, therefore it is an essential approach to reducing energy consumption and carbon emission by lowering the energy demand of rural buildings. According to the field investigation, traditional dwellings located in northeast of Sichuan hills always have the thermal performance of exterior envelopes which cannot be satisfied with the related energy efficiency standard, thus causing high annual energy demand and a poor indoor thermal environment. In order to determine appropriate energy-saving renovation strategies for traditional dwellings in this region, we carried out a thorough tech-economic evaluation for a set of energy-saving strategies. The main work and results can be summarized as follows.

In **Chapter 1, Research Background and Purpose of the Study**, we reviewed the energy consumption situation for the world and China, and further introduced the share of energy consumption for the building sector in China. Next, we explained the climate background of the research region – northeast of Sichuan hills, and analyzed the challenge of lowering energy consumption in this region. Then we also introduced the current population and economic development of the research region. Based on the previous research background of the research region, we clarified the purpose, significance, and research structure of this study.

In **Chapter 2, Literature Review**, we reviewed a lot of previously published studies to find appropriate energy-saving strategies for traditional dwellings in this region. We summarized the heat transfer process through opaque envelopes of buildings, and then we determined two directions to realize the goal of energy saving based on these fundamental theories. Therefore, the related research on applying insulation system, phase change material (PCM), and solar radiation to reduce the energy demand of buildings were reviewed in the rest parts of this chapter.

In **Chapter 3, Methodology**, we introduced the detailed information about traditional dwellings in this research region based on the field investigation carried on January and July, 2017, and the arrangement of the experimental work, then a base model used for discussing the energy-saving strategies were established and depicted. Next, we also clarified the calculation process of all of the research methods we used in this study, including the core formula for the dynamic simulation program – EnergyPlus, the principle of orthogonal experiment design (OED) and the thorough calculation process of analysis of variance (AVOVA), and the principle and calculation method to obtain a dynamic investment payback period (DPP) and the corresponding economic benefits.

In **Chapter 4, Thermal Performance of the Tested Building**, we analyzed the recorded data of the actual tested building, including the outdoor air temperature and relative humidity, indoor air temperature and relative humidity, outside and inside surface temperatures of exterior walls, and outside and inside surface temperature of the roof. Then we calculated the theoretical values of some basic thermal indicators of exterior envelopes, including the heat transfer coefficient of the present exterior walls and roof, the thermal inertia of the present exterior walls and roof, and the

temperatures of the inner surface of the exterior wall and the inner surface of the roof, and further compared these values with the requirements proposed by the related energy efficiency standard. Moreover, in order to deeply comprehend the indoor environment of the current local traditional dwellings in this region, we also simulated the indoor air temperature during the whole year by EnergyPlus.

In **Chapter 5, Determine Insulation Thickness of Exterior Envelopes for the Traditional Dwellings in Northeast of Sichuan Hills**, we derived the calculation method of the optimum economic thickness of insulation materials for building exterior walls in northeast of Sichuan hills, then calculated the optimal economic thickness for exterior walls of five commonly used insulation materials, including expanded polystyrene (EPS), stone wool board (SW), polyurethane foam (PU), extruded polystyrene (XPS), and phenolic foam (PF). Next, we compared and ranked the importance of all of the factors which could affect the optimum thickness by orthogonal test and analysis of variance (AVOVA). Furthermore, we discussed the correlation between the optimal economic thickness of insulation materials for roofs and the optimal economic thickness of insulation materials for exterior walls and finally, we determined the recommended ratio of their optimal economic thickness.

In **Chapter 6, Parametric and Economic Analysis of Phase Change Materials (PCM) on Energy Saving for Traditional Dwellings in Northeast of Sichuan Hills**, we selected a total of eight parameters of PCM, including location, melting temperature, thickness, phase transition temperature radius, latent heat, density, thermal conductivity, and specific heat, then varied their values in a predetermined range and investigated the effects of their variation on the annual energy demand of traditional dwellings in northeast Sichuan hills, and finally obtained the optimal combination of the parameters of PCM. Furthermore, considering the high cost of PCM, we also discussed a more economic selection of PCM for this study region.

In **Chapter 7, Passive Application of Solar Energy for Traditional Dwellings in Northeast of Sichuan Hills**, we proposed two strategies – Trombe wall (T-wall) and on-top sunspaces (OS) and assessed their energy-saving performances. We discussed the impact of thickness of air cavity, the utilization of shade control, and the glass category of T-wall glazing on the energy-saving effect of T-wall. As for the on-top sunspaces strategy, we also analyzed the influence of the glazing area variation and shade control on the energy-saving effect of the on-top sunspaces strategy. Finally, we determined the optimal parameters of these two strategies.

In **Chapter 8, Tech-economic Analysis of Comprehensive Energy-saving Strategies**, we obtained 15 strategies by making different combinations of four individual strategies proposed in Chapter 5-7 and then, we comprehensively evaluated their energy-saving potential, investment payback period, and economic benefits after 25 years with the help of EnergyPlus and dynamic investment payback period method (DPP). Considering that the building orientation of local traditional dwellings is diverse, we further assessed the influence of building orientation on the energy-saving effects and economic potential. Furthermore, we also took the actual tested building as an example, simulated its annual energy demand pre and post renovation, and calculated the corresponding economic benefits to prove the effective of the recommended energy-saving strategy.

In **Chapter 9, Conclusion**, we summarized the main work and of this study.

TABLE OF CONTENTS

1. Research Background and Purpose of the Study	1-1
1.1 Research background	1-1
1.1.1 Energy consumption background.....	1-1
1.1.2 Climatic background	1-6
1.1.3 Research region background	1-11
1.2 Purpose and significance of this study	1-18
1.2.1 Purpose of this study	1-18
1.2.2 Significance of this study	1-18
1.3 Research structure	1-19
Reference	1-22
2. Literature Review.....	2-1
2.1. Introduction.....	2-1
2.2. Heat transfer process through opaque envelopes of buildings	2-2
2.3. Application effect of insulation system for buildings	2-4
2.4. Application effect of phase change materials for buildings	2-7
2.5. Application effect of renewable energy source for buildings.....	2-9
2.6. Summary	2-9
Reference	2-11
3. Methodology	3-1
3.1 Introduction.....	3-1
3.2 Filed test experiment in this study region	3-1
3.2.1 Description of the survey location	3-1
3.2.2 Description of the experiment	3-2
3.3 Establishment of the base model.....	3-5
3.3.1 Architecture characteristic of traditional dwellings in the study region.....	3-5
3.3.2 Description of the base model.....	3-7
3.4 Numerical simulation	3-9

TABLE OF CONTENTS

3.4.1	Description of simulation program	3-9
3.4.2	Mathematical description of heat balance process for traditional materials..	3-9
3.4.3	Mathematical description of conduction through the wall	3-10
3.4.4	Mathematical description of heat balance process for phase change materials	3-12
3.5	Orthogonal experiment design (OED) and analysis of variance (AVOVA)	3-13
3.6	Dynamic investment payback period model (DPP)	3-14
3.7	Summary	3-15
	Appendix A. Standard orthogonal array of $L_{27}(3^{13})$	3-16
	Reference	3-17
4.	Thermal Performance of the Tested Building	4-1
4.1	Introduction	4-1
4.2	Measurement results of tested building.....	4-1
4.2.1	Measured air temperature analysis	4-1
4.2.2	Measured air relative humidity analysis.....	4-3
4.2.3	Surface temperature of exterior walls of tested building.....	4-7
4.2.4	Surface temperature of roof for the tested building.....	4-12
4.3	Theoretical analysis of current thermal performance of opaque exterior envelopes for tested building	4-14
4.3.1	Theoretical analysis of current thermal performance for opaque exterior envelopes in winter	4-14
4.3.2	Theoretical analysis of current thermal performance for opaque exterior envelopes in summer.....	4-18
4.4	Simulated results of indoor environment throughout the typical year	4-20
4.4.1	Simulation model	4-20
4.4.2	Model validation	4-20
4.4.3	Analysis of simulation results	4-22
4.5	Summary	4-23
	Reference	4-25
5.	Determine Insulation Thickness of Exterior Envelopes for the Traditional Dwellings in Northeast of Sichuan Hills.....	5-1

TABLE OF CONTENTS

5.1	Introduction.....	5-1
5.2	The optimum insulation thickness of exterior walls	5-6
5.2.1	Calculation method of optimum insulation thickness of exterior walls	5-6
5.2.2	Selection of the preferred insulation material	5-9
5.2.3	The impact law of influencing factors on optimum insulation thickness....	5-13
5.2.4	The impact degree of influencing factors on optimum insulation thickness	5-15
5.3	The optimum insulation thickness of roof.....	5-18
5.3.1	Simulation model	5-18
5.3.2	Correlation of optimal economic thickness between insulation for roof and insulation for exterior walls	5-18
5.4	Summary	5-21
	Reference	5-23
	Nomenclature.....	5-28
6.	Parametric and Economic Analysis of Phase Change Materials (PCM) on Energy Saving for Traditional Dwellings in Northeast of Sichuan Hills	6-1
6.1	Introduction.....	6-1
6.2	Materials and methods	6-3
6.2.1	Simulation model	6-3
6.2.2	Model validation	6-5
6.2.3	Evaluation indicator	6-7
6.3	Results and discussion.....	6-7
6.3.1	Effect of PCM melting temperature and location on energy saving	6-7
6.3.2	Effect of PCM thickness on energy saving	6-8
6.3.3	Effect of PCM phase transition temperature radius on energy saving	6-9
6.3.4	Effect of PCM latent heat on energy saving.....	6-10
6.3.5	Effect of PCM density on energy saving.....	6-11
6.3.6	Effect of PCM thermal conductivity on energy saving	6-12
6.3.7	Effect of PCM specific heat on energy saving	6-13
6.3.8	Comparison of energy-saving performance between recommended PCM and present PCM products	6-14

TABLE OF CONTENTS

6.3.9	Economic analysis of PCM selection.....	6-15
6.3.10	Selection of PCM for this study region.....	6-19
6.4	Summary.....	6-20
	Reference.....	6-22
7.	Passive Application of Solar Energy for Traditional Dwellings in Northeast of Sichuan Hills	7-1
7.1	Introduction.....	7-1
7.2	Energy-saving potential of Trombe wall (T-wall) strategy.....	7-3
7.2.1	Description of T-wall.....	7-3
7.2.2	Simulation results.....	7-5
7.3	Energy-saving potential of on-top sunspaces application.....	7-6
7.3.1	Description of on-top sunspaces (OS).....	7-6
7.3.2	Simulation results.....	7-8
7.4	Summary.....	7-9
	Reference.....	7-11
8.	Tech-economic Analysis of Comprehensive Energy-saving Strategies.....	8-1
8.1	Introduction.....	8-1
8.2	Evaluation of energy-saving and economic potential of comprehensive energy-saving strategies.....	8-1
8.2.1	Description of energy-saving strategies.....	8-1
8.2.2	Description of simulation model.....	8-2
8.2.3	Energy-saving and economic potential of energy-saving strategies.....	8-3
8.3	Influence of building orientation on energy-saving and economic potential.....	8-10
8.4	Energy-saving and economic potential for the tested building.....	8-12
8.5	Summary.....	8-14
	Reference.....	8-16
9.	Conclusion.....	9-1

LIST OF FIGURES

Figure 1-1. Share of building sector in the total national energy consumption in 2018 [8].	1-2
Figure 1-2. Share of iron and steel, cement, aluminum products, and others category in energy consumption of the building materials production phase in 2018 [8].	1-3
Figure 1-3. Share of building sector in the total national emission carbon in 2018 [8].	1-4
Figure 1-4. Share of iron and steel, cement, aluminum products, and others category in carbon emission of the building materials production phase in 2018 [8].	1-5
Figure 1-5. Shares of energy consumption in building operation phase for urban residential buildings, rural residential buildings, and public buildings [6].	1-6
Figure 1-6. Shares of carbon emission in building operation phase for urban residential buildings, rural residential buildings, and public buildings [8].	1-6
Figure 1-7. Spatial variation trends of energy consumption during building operation phase [8].	1-10
Figure 1-8. Increase rate of the amount of energy consumption during different periods [8].	1-11
Figure 1-9. Diagram for population density of China [20].	1-12
Figure 1-10. (a) Location of Sichuan province; (b) Location of northeast of Sichuan hills.	1-13
Figure 1-11. Income situation of rural people lived in the study region.	1-14
Figure 1-12. Hourly air temperature throughout whole year of the research region.	1-14
Figure 1-13. Characteristics of monthly temperatures of the research region.	1-15
Figure 1-14. Hourly air relative humidity throughout whole year of the research region.	1-16
Figure 1-15. Hourly solar radiation throughout whole year of the research region.	1-17
Figure 1-16. Difference of direct solar radiation between two Nanchong and Nanjing.	1-18
Figure 1-17. Research structure of this study.	1-21
Figure 2-1. Heat balance of the building [9].	2-2
Figure 3-1. Location diagram and aerial overhead view of Liyuanba Village.	3-2
Figure 3-2. General plan of Liyuanba Village.	3-3
Figure 3-3. Floor plan and photographs of the tested building.	3-4
Figure 3-4. Arrangement of testing points (floor plan diagram).	3-5
Figure 3-5. Floor plan of the base model.	3-7

LIST OF FIGURES

Figure 3-6. Front elevation of the base model.	3-7
Figure 3-7. (a) Side elevation of the base model; (b) Diagram of roof construction; (c) Diagram of exterior walls construction; (d) Diagram of floor construction.	3-8
Figure 3-8 Perspective view of the base model.	3-8
Figure 4-1. (a) Measured air temperature of bedroom on 16th Jan. 2017 and 28th Jul. 2017 and outdoor air temperature on 16th Jan. 2017 and 28th Jul. 2017.	4-3
Figure 4-2. Tested relative humidity of testing room air and outdoor air relative humidity on 28th Jul. 2017.	4-4
Figure 4-3. Frequency of measured relative humidity of testing room air and outdoor air on 28th Jul. 2017.	4-5
Figure 4-4. Tested relative humidity of testing room air and outdoor air relative humidity on 16th Jan. 2017.	4-6
Figure 4-5. Frequency of measured relative humidity of testing room air and outdoor air on 16th Jan. 2017.	4-7
Figure 4-6. Arrangement of testing points (three-dimension diagram).	4-8
Figure 4-7. Indoor and outdoor air temperature, and surface temperature of exterior walls on 16th Jan. 2017.	4-9
Figure 4-8 Indoor and outdoor air temperature, and surface temperature of exterior walls on 28th Jul. 2017.	4-11
Figure 4-9. Indoor air temperature, outdoor air temperature, and surface temperature of the roof on 16th Jan. 2017.	4-13
Figure 4-10. Indoor air temperature, outdoor air temperature, and surface temperature of the roof on 28th Jul. 2017.	4-14
Figure 4-11. Meteorological boundary conditions required for the calculation.	4-19
Figure 4-12. Comparison of measured values and simulated values of tested dwelling.	4-21
Figure 4-13. Simulated annual hourly indoor and outdoor air temperature of the testing room.	4-23
Figure 4-14. Differences of air temperature between the testing room and outside.	4-23
Figure 5-1. (a) Diagram of optimal point of insulation material thickness [15]; (b) Building heating and cooling load and saving rate vs. insulation material thickness of base model [16].	5-2
Figure 5-2. (a) Sichuan province location; (b) the region of northeast of Sichuan; (c) proportion and PCDI of rural population in China and Sichuan [17].	5-3
Figure 5-3. (a) Annual hourly air temperature of Nanchong [39]; (b) diagram of exterior walls construction of traditional dwellings in northeast of Sichuan hills; (c) photographs of traditional	

dwelling in northeast of Sichuan hills.	5-10
Figure 5-4. Impact law of parts of influencing factors on the optimum thickness of PU: (a) discount rate; (b) increase rate of electric price; (c) electric price; (d) insulation material price; (e) service life of insulation material; (f) the heat transfer resistance of exterior wall without insulation.....	5-14
Figure 5-5. The impact law of indoor calculated temperature on optimum thickness.	5-15
Figure 5-6. Economic benefits during service life (25 years) versus the relationship between insulation thickness of roof and insulation thickness of exterior walls.....	5-20
Figure 6-1 Experimental details for performance of natural TCM.	6-6
Figure 6-2. Results of experimental and simulated indoor air temperature.	6-6
Figure 6-3. Effect of PCM location and melting temperature on the energy demand.....	6-8
Figure 6-4. Effect of PCM thickness on the energy demand.	6-9
Figure 6-5. Effect of PCM phase transition temperature radius on the energy demand.....	6-10
Figure 6-6. Effect of PCM latent heat on the energy demand.....	6-11
Figure 6-7. Effect of PCM density on the energy demand.....	6-12
Figure 6-8. Effect of PCM thermal conductivity on the energy demand.	6-13
Figure 6-9. Effect of PCM specific heat on the energy demand.	6-14
Figure 7-1. Diagram of Trombe wall (T-wall) strategy for base building.	7-4
Figure 7-2. Application of Trombe wall (T-wall) on the base model.	7-4
Figure 7-3. Annual heating load and cooling load vs. air cavity thickness and shade control of T-wall.....	7-5
Figure 7-4. Diagram of on-top sunspaces (OS) strategy for base building.....	7-7
Figure 7-5. Application of on-top sunspaces (OS) on the base model.	7-8
Figure 7-6. Energy-saving effect of the OS on heating and cooling load vs. glazing area.	7-9
Figure 8-1. Dynamic payback period of each energy-saving strategy.	8-7
Figure 8-2. Comparison of simple payback period (SPP) and dynamic payback period (DPP) for each energy-saving strategy.	8-8
Figure 8-3. Economic benefits after 25 years of each energy-saving strategy.....	8-10
Figure 8-4. Influence of building orientation on the energy-saving effect of the optimal strategy. 8-	12
Figure 8-5. Diagram of tested building adopted S4 strategy.....	8-13

LIST OF FIGURES

LIST OF TABLES

Table 1-1 Zoning indicators of primary climate zone for building thermal design.....	1-7
Table 1-2 Zoning indicators of secondary climate zone for building thermal design.	1-8
Table 3-1 Information of the testing equipment.	3-4
Table 3-2 Architecture characteristics of traditional dwellings in northeast of Sichuan hills, China.	3-6
Table 3-3 Features of building floor plan of traditional dwellings in northeast of Sichuan hills, China.	3-6
Table 4-1 Characteristic values of measured air temperature in summer and in winter.....	4-2
Table 4-2 Temperature characteristic values of outside and inside surface temperatures in winter.	4-10
Table 4-3 Temperature characteristic values of outside and inside surface temperatures in summer.	4-12
Table 4-4 Thermophysical parameters of wall materials commonly used in traditional dwellings in northeast of Sichuan hills, China [1]......	4-17
Table 4-5 Thermophysical properties of building material for simulation [1].....	4-20
Table 5-1 Building information.....	5-11
Table 5-2 Insulation material information [2, 43].	5-11
Table 5-3 Optimum thickness, energy-saving and economic evaluation of insulation materials.	5-12
Table 5-4 Influencing factors and levels for the orthogonal experiment design.	5-15
Table 5-5 Orthogonal experiment design and test results.	5-16
Table 5-6 Results of ANOVA.....	5-17
Table 5-7 Energy-saving and economic potential by reducing the calculated winter indoor temperature (taking PU as an example).	5-18
Table 5-8 Corresponding energy saving rate of various insulation category and thickness of roof.	5-19
Table 5-9 Dynamic investment payback period (N_p) of various insulation category and thickness of roof.....	5-20
Table 6-1 Setting details of original model.	6-4
Table 6-2 Thermophysical parameters of wall materials.	6-4

LIST OF TABLES

Table 6-3 Range and default value of PCM material parameters used for the parametric analysis.	6-5
Table 6-4. Parameters and the corresponding energy saving rate of different PCM products. ...	6-14
Table 6-5 Dynamic investment payback period and economic benefits of PCM with different parameters.	6-17
Table 6-6 Economic benefits of PCM with different thickness.	6-20
Table 6-7 Economic benefits of PCM with different density.	6-20
Table 7-1 Economic evaluation of different glazing type of T-wall.	7-6
Table 8-1 Contents of each energy-saving strategy.	8-1
Table 8-2 Information of the base model.	8-2
Table 8-3 Thermophysical parameters of materials for simulation [4].	8-3
Table 8-4 Annual energy demand, saved money per year and investment cost of each energy-saving strategy.	8-5
Table 8-5 Unit costs of materials and labor [5-6].	8-6
Table 8-6 Heating load, cooling load, and annual energy demand of building with different orientation.	8-12
Table 8-7 Energy-saving and economic benefits of pre and post renovation for tested building.	8-14

Chapter 1

Research Background and Purpose of the Study

CHAPTER 1. RESEARCH BACKGROUND AND PURPOSE OF THE STUDY

CHAPTER 1. RESEARCH BACKGROUND AND PURPOSE OF THE STUDY

1. Research Background and Purpose of the Study	1-1
1.1 Research background	1-1
1.1.1 Energy consumption background	1-1
1.1.2 Climatic background	1-6
1.1.3 Research region background	1-11
1.2 Purpose and significance of this study	1-18
1.2.1 Purpose of this study	1-18
1.2.2 Significance of this study	1-18
1.3 Research structure	1-19
Reference	1-22

CHAPTER 1. RESEARCH BACKGROUND AND PURPOSE OF THE STUDY

1. Research Background and Purpose of the Study

1.1 Research background

1.1.1 Energy consumption background

Scientific research in recent decades has demonstrated that human activities have a huge impact on the Earth's environment. In the early 1990s, Mathis Wackernagel and William Rees of the University of British Columbia, Canada, introduced the concept of ecological footprint as a measure of our impact on the Earth. Zero footprint means that humans return as much to nature as they take from it. However, since the mid-1980s, humans have taken more resources from nature than they have returned to nature. At the same time, human activities in recent decades have led to a significant increase in the concentration of greenhouse gases in the atmosphere, which has contributed to climate change. Atmospheric carbon dioxide concentrations have risen from 1,760 parts per million (ppm) in 1760, when the industrial revolution began, to 387 ppm in 2009. In 2008, the burning of fossil fuels emitted about 7.9 billion tons of carbon, and about 1.5 billion deforestation produced 9.4 billion tons of carbon dioxide emissions. But since nature relies on the oceans, soil and vegetation to absorb only about 5 billion tons per year, this equates to nearly half of the CO₂ remaining in the atmosphere, thus pushing up CO₂ emission levels [1]. Stix pointed out that without intervention, CO₂ concentrations will easily exceed 500 ppm by 2050 [2]. Reducing carbon emissions and achieving the goal of carbon neutrality is not only responsible for human beings themselves, but also for the entire planet and other species on it.

With the continuous development of countries, the excessive use of energy and industrial production by human beings has caused a large amount of carbon emissions, resulting in the global temperature climbing year by year and the destruction of the ozone layer, which also breaks the ecological balance. According to the U.S. Energy Information Administration (EIA) [3], coal accounts for about 25% of total energy consumption, causing a large amount of carbon dioxide emissions. Currently, most people spend 90% of their daily lives indoors, relying on mechanical heating and air conditioning, making the building industry considered the largest single contributor to world energy consumption and greenhouse gas emissions [4-5]. According to statistics, the global building stock consumes about 40% of the energy and emits one-third of the greenhouse gases [6]. More than 50% of the material raw materials obtained by humans from nature are used to construct various types of buildings and their ancillary facilities, which in turn consume about 50% of the global energy during construction and use.

On September 22, 2020, Chinese President Xi Jinping delivered an important speech at the general debate of the 75th session of the United Nations General Assembly, stating that China will adopt stronger policies and measures to peak CO₂ emissions by 2030 and strive to achieve carbon neutrality by 2060. On 12 December 2020, Chinese President Xi Jinping announced updated 2030 carbon targets at the Climate Ambition Summit, Reduce carbon emissions per unit of GDP by over 65% from the 2005 level. The energy consumption of the building sector occupies nearly 40% of global energy consumption [7], while in China, the energy consumption of the building sector also accounts for a large share of the total national energy consumption.

According to the China Building Energy Consumption Research Report (2020) [8] released by the Energy Consumption Statistics Professional Committee of China Association of Building Energy Efficiency (CABEE) in November 2020, the total energy consumption of the whole building process in 2018 was 2.147 billion tce, accounting for 46.5% of the total Chinese energy consumption. Figure 1-1 shows the share of building sector and other sectors in terms of energy consumption, and the unit adopted to assess the amount of energy consumption is billion tce, while tce stands for standard equivalent coal, and the calorific value of each kilogram of standard equivalent coal in China is 7000 kcal (29307.6 kJ). In addition, the statistics of energy consumption in the building sector are divided into three stages, that is, building materials production phase, building construction phase, and building operation phase. According to Figure 1-1, although energy consumption produced during building construction phase is minor compared to other two building phases (building materials production and building operation phase), it still accounts for about 1.02% of the total national energy consumption, meaning that there is approximately 47 million tce be consumed during the building construction phase. Building materials production phase can consume 23.82% of total national energy consumption, meaning nearly 1.1 billion tce of energy be used to produce building materials in 2018. Furthermore, although the energy consumption amount of building operation phase is less than the building materials production phase, there still about 1 billion tce of energy consumption, that is, about 21.66% of the total energy consumption is contributed by building operation phase. The actual statistic data reveal the fact about the high energy consumption of the building sector, and it is imperative to lower its consumption especially the building materials production phase and building operation phase.

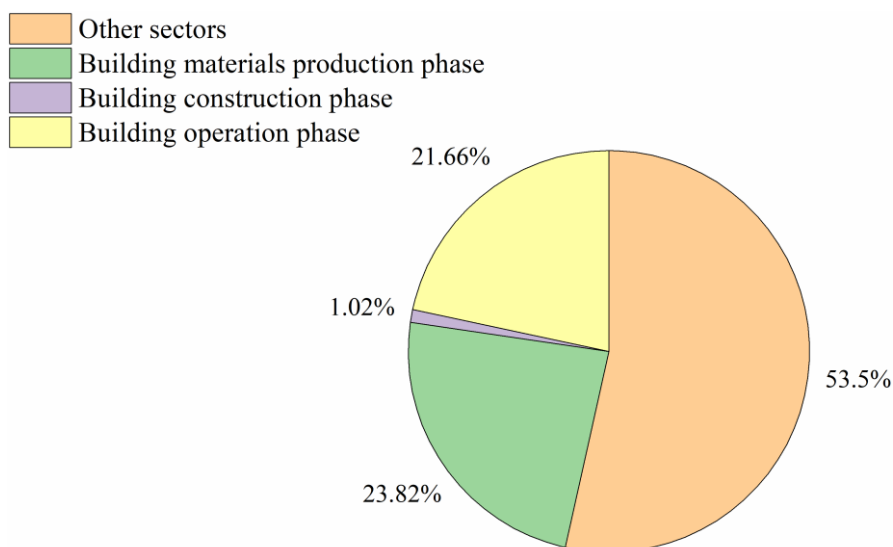


Figure 1-1. Share of building sector in the total national energy consumption in 2018 [8].

We can notice that building material production phase occupies the most share of energy consumption in the whole building sector, and Figure 1-2 shows details of its energy consumption.

At the time of the statistics, building materials were divided into 4 categories, namely iron and steel, cement, aluminum products, and others, and their share of energy consumption in the building materials production phase is 45.56%, 21.3%, 25.5%, and 7.64%, respectively, the corresponding energy consumption is 50.12 million tce, 23.43 million tce, 28.05 million tce, and 8.4 million tce, respectively.

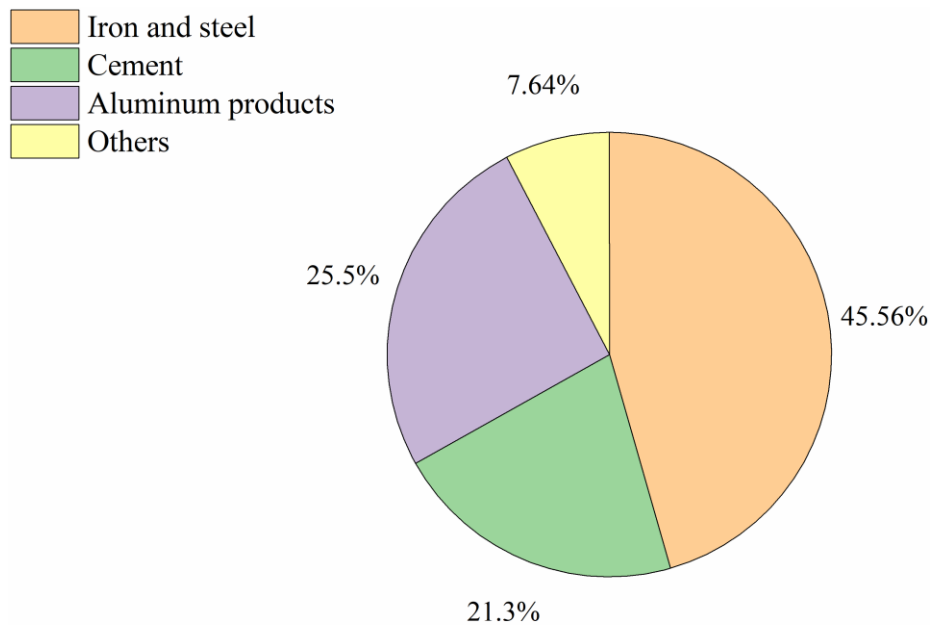


Figure 1-2. Share of iron and steel, cement, aluminum products, and others category in energy consumption of the building materials production phase in 2018 [8].

Expect for the statistic data of energy consumption, which is evaluated by the consumption amount of standard equivalent coal, carbon emission is another crucial indicator used to assess the energy consumption and environmental friendliness of human activities. CABEE also investigated the carbon emission in 2018 and related results are shown in Figure 1-3. Similarly, building sector is divided into three parts and the total carbon emission of the whole building sector in 2018 is 4.93 billion tons of CO₂ (tCO₂), accounting for 51.3% of the national carbon emission in that year. According to Figure 1-3, building materials production phase still occupies the most share of the whole building sector, followed by building operation phase and building construction phase. The proportion of building materials production phase, building operation phase, and building construction phase is 28.3%, 21.88%, and 1.04%, respectively, correspondingly, the amount of carbon emission during these three phases is 139.52 million tons of CO₂, 107.87 tons of CO₂, and 5.13 tons of CO₂.

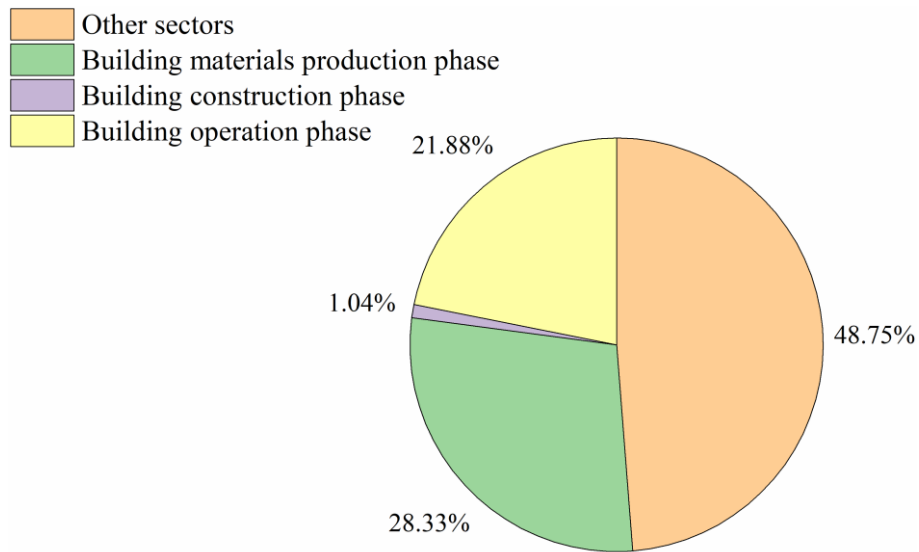


Figure 1-3. Share of building sector in the total national emission carbon in 2018 [8].

Figure 1-4 depicts the share of carbon emissions in the production phase for each category of building material. The ranking of the amount of the share of each category of building materials is the same as the ranking exhibited in the energy consumption statistics, that is, the carbon emission of iron and steel accounts for 48.2% of the total carbon emission of the whole building materials production phase, tightly followed by cement, which counts about 40.8% of the total carbon emission of the whole building materials production phase, then the aluminum products occupies 10%, which is less than that in energy consumption, and finally, others is still the minimum part among these four categories, only accounting for 1%. It can be noticed that the share of cement surges compared to its share in terms of energy consumption (shown in Figure 1-2), and the share of iron and steel category also increases, whereas the shares of aluminum products category and others category drop a lot. Additionally, the exact amount of the carbon emission is 67.25 million tons of CO₂, 56.92 million tons of CO₂, 13.95 million tons of CO₂, and 1.4 million tons of CO₂ for iron and steel category, cement category, aluminum products category, and others category, respectively.

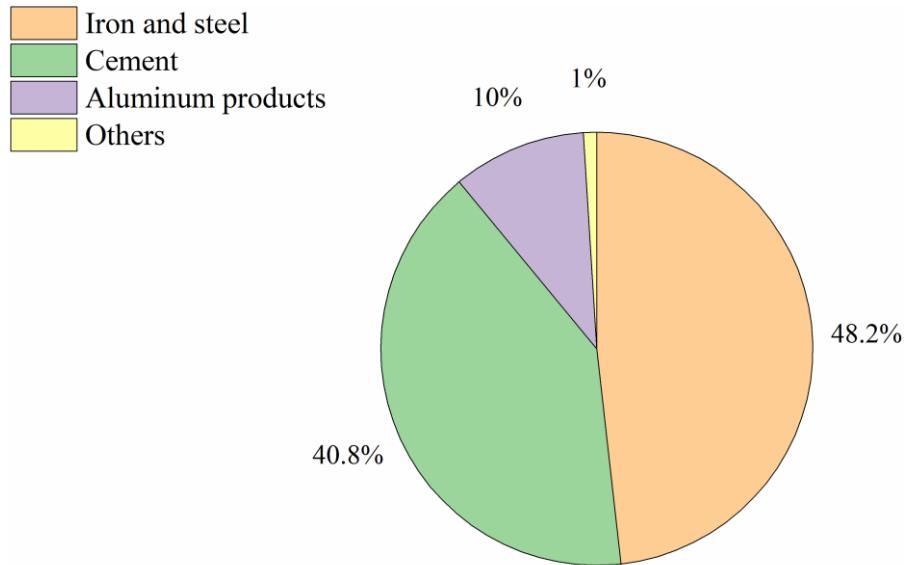


Figure 1-4. Share of iron and steel, cement, aluminum products, and others category in carbon emission of the building materials production phase in 2018 [8].

On March 27, 2021, academician Jiang Yi reported at the 17th Tsinghua University Building Energy Efficiency Academic Week Open Forum that in 2019, there would be 28.2 billion m² of urban residential building area and 537.4 billion kWh of total electricity consumption in operation, and 22.8 billion m² of rural residential building area and 305.4 billion kWh of total electricity consumption in operation. In the future, the electricity consumption will be about twice as much as the current one. Due to the large demand of electricity, even if the full development of wind power photoelectricity, it cannot solve the regulation and balance problem, therefore, energy saving is the basis. As can be seen from the report of academician Jiang Yi, currently, China's rural residential building area accounts for about 45% of the national residential building area, and electricity consumption accounts for about 36% of the national residential building electricity consumption. Therefore, it is important to reduce the energy consumption of rural residential buildings through energy-saving renovation for building energy saving and emission reduction.

Meanwhile, as Figure 1-5 and Figure 1-6 shown, rural buildings contribute 23.78% of building energy consumption and 20.69% of carbon emission during the operation phase, therefore it is an essential approach to achieving carbon neutral by reducing energy consumption of rural buildings. However, it is challenging because the energy demand in rural regions is growing owing to the increased income and desire for a more comfortable indoor thermal environment for local residents. In order to control the building energy consumption, lowering heating and cooling loads is unavoidable since the major portion of the energy consumption in buildings is related to them [9], and globally, energy consumption for space heating and cooling even exceeds 40% and 61% of energy demand in commercial and residential buildings, respectively [10]. Additionally, it is imperative to enhance their thermal performance considering that the heat loss of exterior envelopes

can count for 60%-80% of the total building heat loss [11].

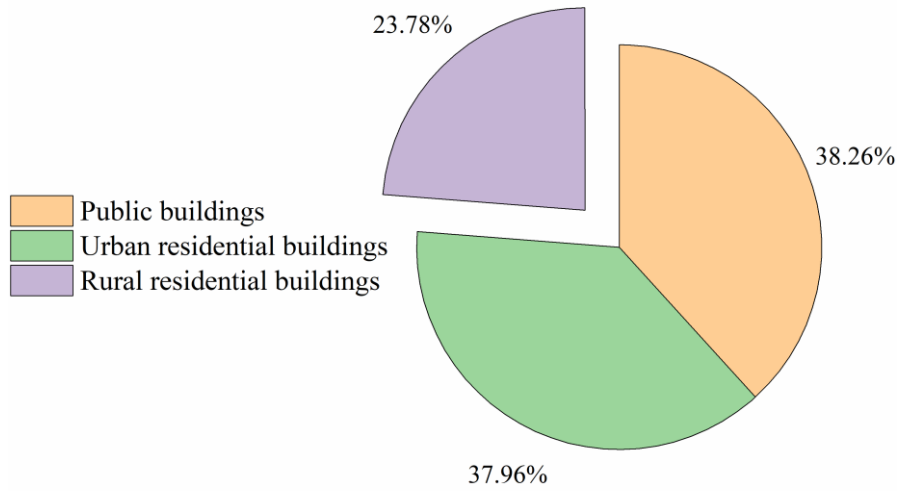


Figure 1-5. Shares of energy consumption in building operation phase for urban residential buildings, rural residential buildings, and public buildings [6].

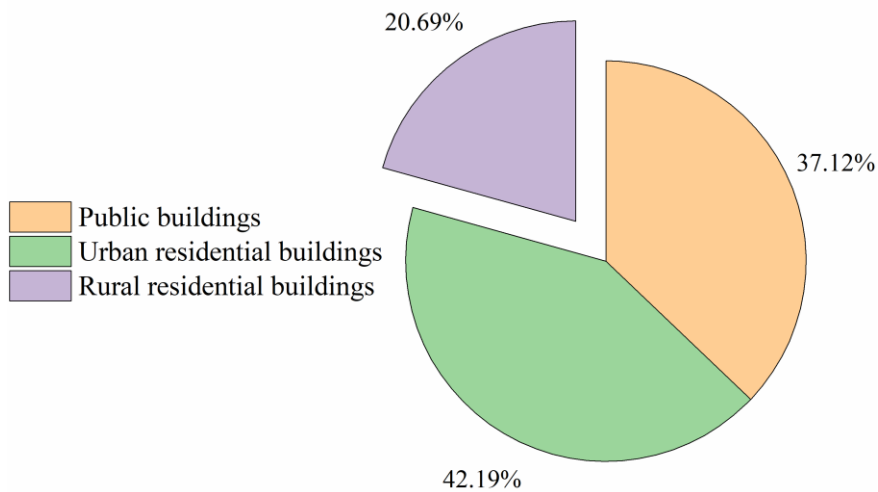


Figure 1-6. Shares of carbon emission in building operation phase for urban residential buildings, rural residential buildings, and public buildings [8].

1.1.2 Climatic background

The building thermal design zone is divided into two levels. The main indicators use the coldest monthly average temperature (t_{min-m}) and the hottest monthly average temperature (t_{max-m}), respectively, refers to the average of the cumulative January average temperature and the cumulative July average temperature. Many climatic factors affect the outdoor air temperature, from years of

statistical data, the coldest (hottest) month of the year is not necessarily always January (July) month. However, exceptions are rare, and the temperature difference is not large, thus the data of January and July are still used. In addition, the "cumulative years" stands for multi-year, refers specifically to the compilation of meteorological data, the use of the previous period of accumulation of consecutive years. The "coldest (hottest) monthly average temperature" refers to the average of the January (July) monthly average temperature for the previous consecutive years (usually more than 10 years). [12] By combining the main indicator and auxiliary indicator shown in Table 1-1, five primary climate zones can be determined, namely severe cold zone (SCZ), cold zone (CZ), hot summer and cold winter zone (HSCW), hot summer and warm winter zone (HSWW), and moderate climate zone (MCZ) .

Table 1-1 Zoning indicators of primary climate zone for building thermal design.

Primary climate zone name	Zoning indicator	
	Main indicator	Auxiliary indicator
Severe cold zone (1)	$t_{min\ m} \leq -10\ ^\circ\text{C}$	$145 \leq d_{\leq 5}$
Cold zone (2)	$-10\ ^\circ\text{C} < t_{min\ m} \leq 0\ ^\circ\text{C}$	$90 \leq d_{\leq 5} < 145$
Hot summer and cold winter zone (3)	$0\ ^\circ\text{C} < t_{min\ m} \leq 10\ ^\circ\text{C}$ $25\ ^\circ\text{C} < t_{max\ m} \leq 30\ ^\circ\text{C}$	$0 \leq d_{\leq 5} < 90$ $40 \leq d_{\geq 25} < 145$
Hot summer and warm winter zone (4)	$t_{min\ m} < 10\ ^\circ\text{C}$ $25\ ^\circ\text{C} < t_{max\ m} \leq 29\ ^\circ\text{C}$	$100 \leq d_{\geq 25} < 200$
Moderate climate zone (5)	$0\ ^\circ\text{C} < t_{min\ m} \leq 13\ ^\circ\text{C}$ $18\ ^\circ\text{C} < t_{max\ m} \leq 25\ ^\circ\text{C}$	$0 \leq d_{\leq 5} < 90$

Due to the vast territory of China, the area of each primary climate zone is very large. For example, the coldest monthly average temperature difference between Mohe, Heilongjiang and Ejina Banner, Inner Mongolia in the same primary climate zone of cold zone (CZ) is 18.3 °C and the value difference of HDD18 is 4110. It is obviously inappropriate to adopt the same design requirements for two regions with such a big difference in coldness. Therefore, the delineation of secondary climate zone adopts HDD18 and CDD26 as the zoning indicators, and subdivides each primary climate zone of building thermal engineering. Throughout the year, the absolute value of the difference between the average daily temperature and the calculated indoor temperature for winter heating (summer cooling) is added up to obtain the number of heating-degree (cooling-degree) day when the average daily outdoor temperature is lower than the calculated winter indoor temperature (higher than the calculated summer indoor temperature), expressed as HDD (CDD) [13] Compared to the zoning indicator of primary climate zone (coldest and hottest monthly average temperatures), this indicator characterizes both the degree of coldness and hotness of the climate and the duration of coldness and hotness. In detail, the heating degree days HDD18 and air conditioning degree days CDD26 are the average values of heating degree days and air conditioning degree days for the calendar year, respectively. Among them, "calendar year" means year by year, especially when compiling meteorological data, used in the previous period of continuous years of each year. HDD18

CHAPTER 1. RESEARCH BACKGROUND AND PURPOSE OF THE STUDY

refers to each year, when the average daily outdoor temperature is lower than the winter heating indoor temperature of 18°C, The difference between the average daily temperature and the calculated winter heating indoor temperature of 18 °C is added up to get the annual number of heating degree days for the year. Then, the number of heating degree days is obtained by calculating the average of the number of HDD18 for each of the previous consecutive years (usually more than 10 years). Similarly, CDD26 refers to each year, when the average daily outdoor temperature is higher than the summer cooling indoor temperature of 26°C, The difference between the average daily temperature and the calculated summer cooling indoor temperature of 26 °C is added up to get the annual number of cooling degree days for the year. And finally, the number of cooling degree days is obtained by calculating the average of the number of CDD26 for each of the previous consecutive years (usually more than 10 years).

Table 1-2 Zoning indicators of secondary climate zone for building thermal design.

Secondary climate zone name	Zoning indicator
Severe cold zone A (1A)	$6000 \leq \text{HDD18}$
Severe cold zone B (1B)	$5000 \leq \text{HDD18} < 6000$
Severe cold zone B (1C)	$3800 \leq \text{HDD18} < 5000$
Cold zone A (2A)	$2000 \leq \text{HDD18} < 3800$ CDD26 ≤ 90
Cold zone B (2B)	CDD26 > 90
Hot summer and cold winter zone A (3A)	$1200 \leq \text{HDD18} < 2000$
Hot summer and cold winter zone B (3B)	$700 \leq \text{HDD18} < 1200$
Hot summer and warm winter zone A (4A)	$500 \leq \text{HDD18} < 700$
Hot summer and warm winter zone B (4B)	$\text{HDD18} < 500$
Moderate climate zone A (5A)	$700 \leq \text{HDD18} < 2000$ CDD26 < 10
Moderate climate zone B (5B)	$\text{HDD18} < 700$

According to Table 1-2, we can determine that the research region – northeast of Sichuan hills belongs to hot summer and cold winter zone A (3A) since its value of HDD18 is 1307 by reviewing the Standard for weather data of building energy efficiency JGJ/T 346-2014 [14]. Meanwhile, the

energy consumption in this climate zone is even higher than that of cold zone [15] since its severe climate characteristics. The average temperature of the hottest month is 25-30 °C (as Table 1-1 shown), about 2°C higher than the places of the same latitude [16]; and the average temperature of the coldest month is 2–7°C, about 8–10°C lower than the places of same latitude [17]. Additionally, the relative humidity in this region is considerably high ranging from 75% to 80% all year round [18]. In order to meet the improving comfort requirements of residents, an increasing number of heating and air-conditioning equipment is used. Moreover, the China Building Energy Consumption Research Report (2020) even reveals this phenomenon that the increasing share of energy consumption in hot summer and cold winter zone.

Figure 1-7 shows the spatial variation trends of energy consumption during building operation phase according to the China Building Energy Consumption Research Report (2020) [8]. Between 2000 and 2018, the share of building energy consumption in hot summer and cold winter zone (HSCW) increased by 6 percentage points, and the share of building energy consumption in northern heating areas decreased by 8 percentage points. In detail, the share of energy consumption during building operation phase for north central heating district is 62%, 60%, 56%, 54%, and 54% for 2000, 2005, 2010, 2015, and 2018 respectively, the corresponding proportion decreases by 8%. By contrast, the share of energy consumption during building operation for hot summer and cold winter zone (HSCW) is 23%, 25%, 28%, 29%, and 29%, respectively. As for the share of energy consumption during building operation for hot summer and warm winter zone (HSWW), it performs a similar variation trend of that of hot summer and cold winter zone (HSCW), that is, its proportion varies from 15% to 17%. From these statistic data, we can notice the increase of energy consumption of hot summer and cold winter climate (HSCW) is significant, thus it's important to reduce the energy consumption of this region.

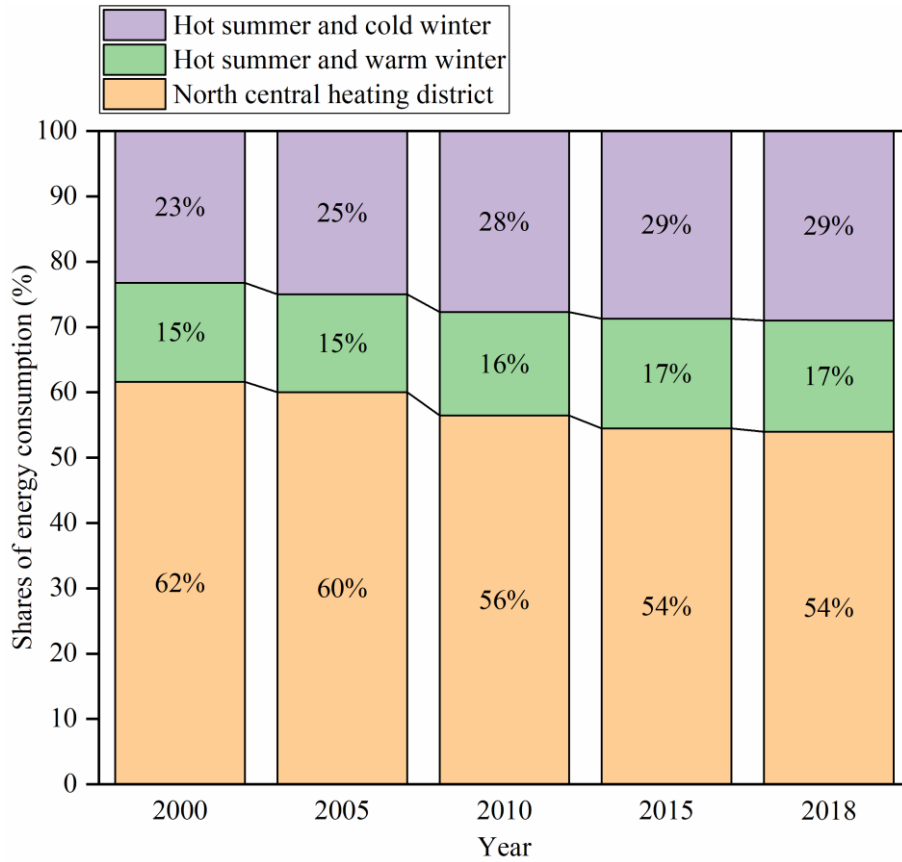


Figure 1-7. Spatial variation trends of energy consumption during building operation phase [8].

Furthermore, the increase rate of the amount of energy consumption can reflect the variation law of energy consumption, and Figure 1-8 displays the related results. From the results, we can note the increase rate of the period of 2000-2005 and 2015-2018 is relatively larger than the period of 2005-2010 and 2010-2015. It is no doubt that the increase rate of the amount of energy consumption presents a development trend, and in detail, the corresponding increase rate of north central heating district, hot summer and warm winter zone (HSWW), and hot summer and cold winter (HSCW) is 8.74%, 10.08%, and 10.32%, respectively.

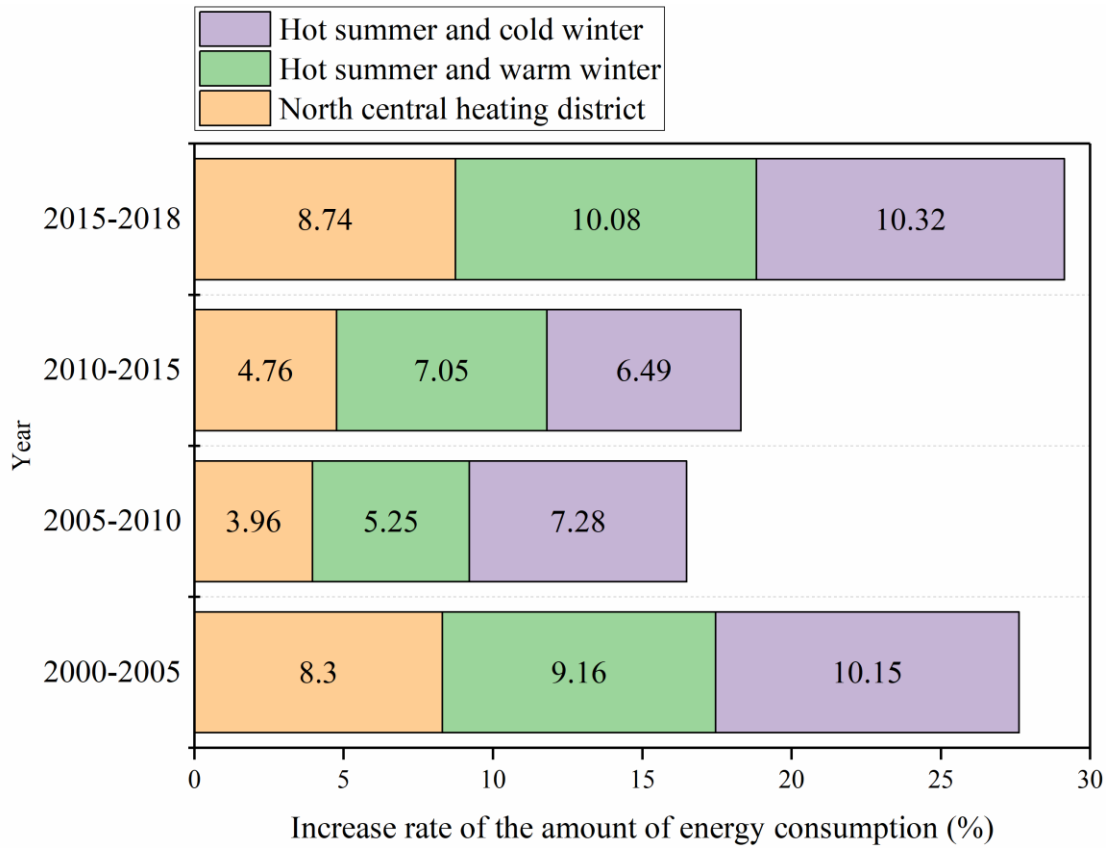


Figure 1-8. Increase rate of the amount of energy consumption during different periods [8].

1.1.3 Research region background

In China, the 12 western provinces, autonomous regions and municipality (hereafter referred to as Western Region) cover an area of about 6,867,000 km² [19], accounting for about 71.5% of the national land area. However, due to natural geography and economic and social reasons, the population density of Western Region are lower than those in the Eastern, Middle and Northeastern regions as Figure 1-9 shown. Moreover, we can notice that Sichuan Basin and surrounding mountainous areas is the most densely populated area in the Western Region.

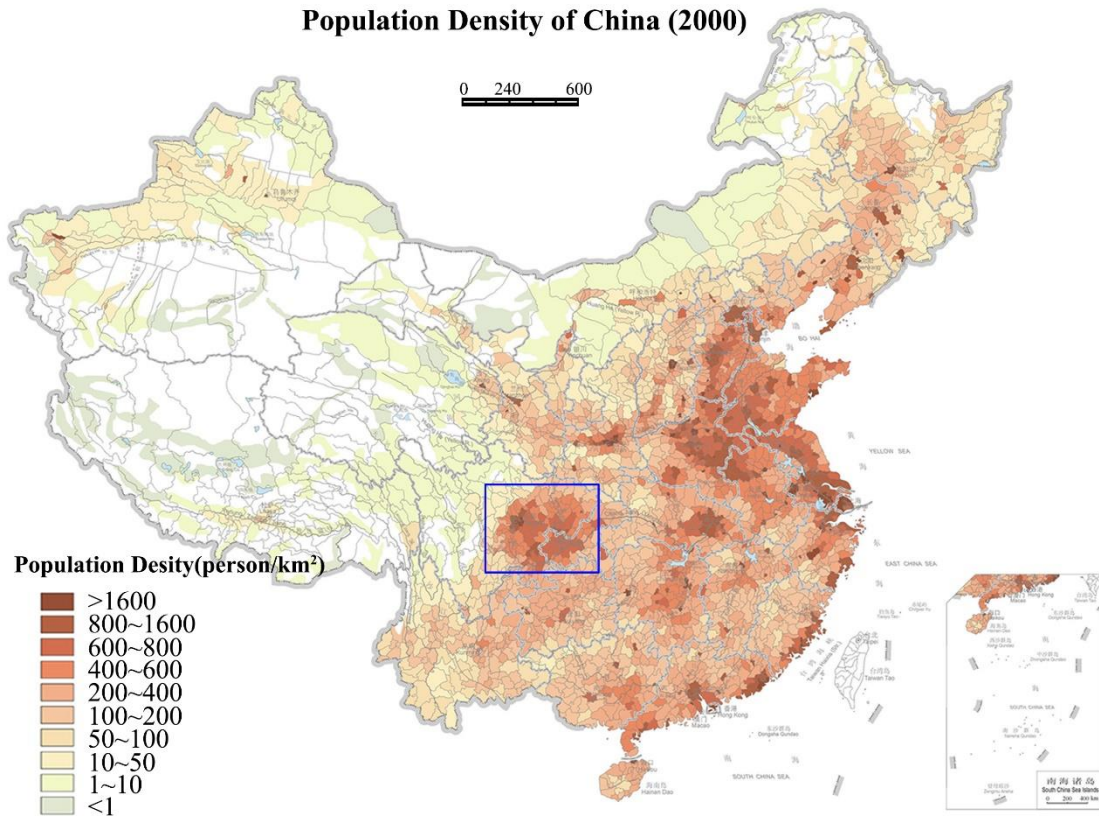


Figure 1-9. Diagram for population density of China [20].

As Figure 1-10 (a) shown, Sichuan Province is located in southwestern China. As for northeast of Sichuan where is basically hilly terrain, normally includes these five cities: Guangyuan, Bazhong, Dazhou, Nanchong and Guang'an. According to the statistics of China Statistical Yearbook [21], the total population of Sichuan Province was 83.75 million, of which, the rural population was 38.7 million by the end of 2019. Compared with the Chinese rural population proportion, which accounts for 39.4% of the total population, the rural population proportion of Sichuan (46.21%) is much higher. Hence, it's very important to focus on the rural area in Sichuan province. In addition to population, economic development is also an important indicator of the level of development of a region and Figure 1-11 can reflect the economic development of rural area in Sichuan.

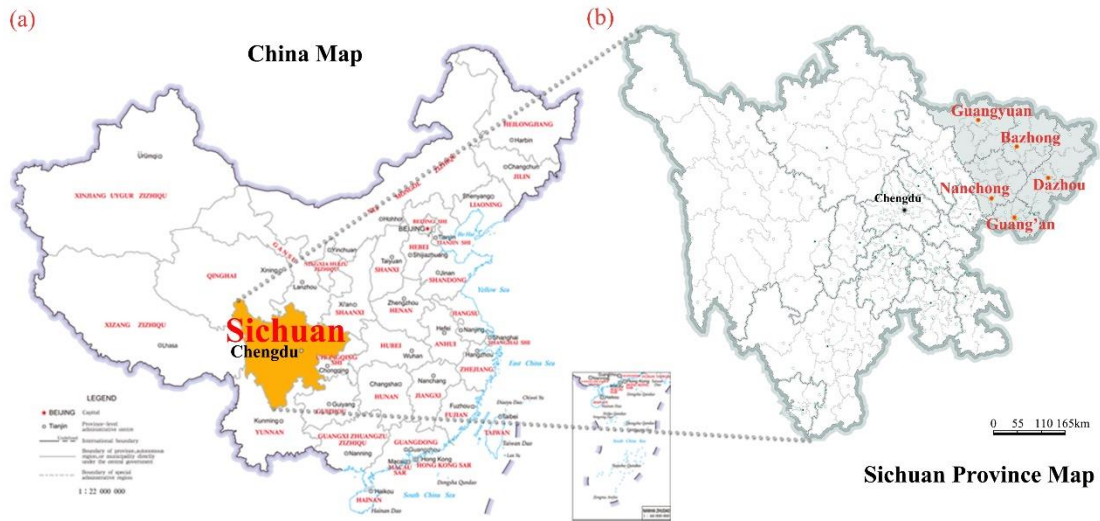


Figure 1-10. (a) Location of Sichuan province; (b) Location of northeast of Sichuan hills.

At the end of 2019, the gross domestic product (GDP) of the Western Region accounted for only 20.8% of total national GDP [21]. The PCDI of urban population and rural populations are 36,040.6 Yuan and 13035.3 Yuan respectively, both lower than the national average – 42,358.8 Yuan and 16,020.7 Yuan [21]. According to the statistics of China Statistical Yearbook (2020) [21], as of the end of 2019, the total population of Sichuan Province was 83.75 million, of which, rural population was 38.7 million. Chongqing has a total population of 31.24 million, with a rural population of 10.37 million. And compared with the national rural population, which accounts for 39.4% of the total population, the rural population in Sichuan Province accounts for 46.21% of the total population in the province, and its proportion is much higher than the national average. In terms of income, the PCDI of the rural population in Sichuan province is 14,670.1 Yuan, which is lower than the national average of 16,020.7 Yuan. Thus, it can be seen that Sichuan Province is not only the most populous province in West Region, but also has a large proportion of rural population and a lower rural economy than the national average. Topographically, the basin located in Sichuan Province is divided into the Chengdu Plain and the mountainous areas. For the cities in the mountainous areas, restricted by the topography and transportation conditions, their economic level is generally lower. For example, according to Sichuan Statistical Yearbook (2020), Bazhong City has an area of 12,293.3 km², which is equivalent to about 86% of the area of Chengdu; however, its GDP per capita in 2019 is 22,716 Yuan, which is only about 20% of the GDP per capita of Chengdu. Besides, the cities located in the mountainous areas have a rural population generally above 60% [22]. For instance, Guangyuan and Bazhong cities located in northeastern Sichuan have 75% and 72% rural populations [22], respectively, and their rural population shares far exceed the provincial average. Although the income of local villagers has gradually increased in recent years, for most rural families, their economic income is still insufficient to support the reconstruction of their houses to improve the living environment quality. Consequently, there are still a large number of primitive rural traditional dwellings. However, with the development of society and economy, the current indoor thermal environment condition of traditional dwellings can no longer satisfy the needs of

modern residents. Thus, improving the living environment for rural residents while minimizing the retrofit cost is a vital issue for these areas.

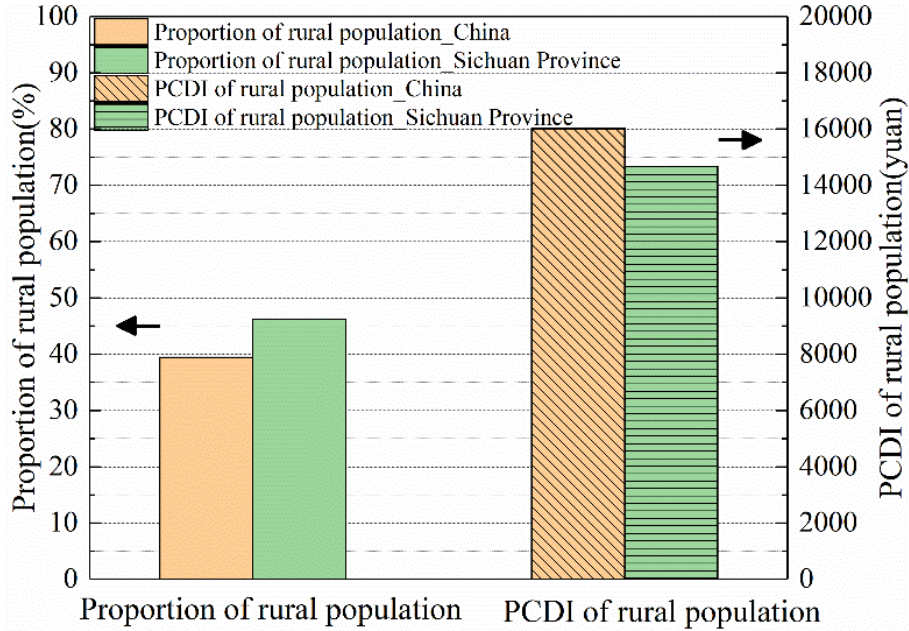


Figure 1-11. Income situation of rural people lived in the study region.

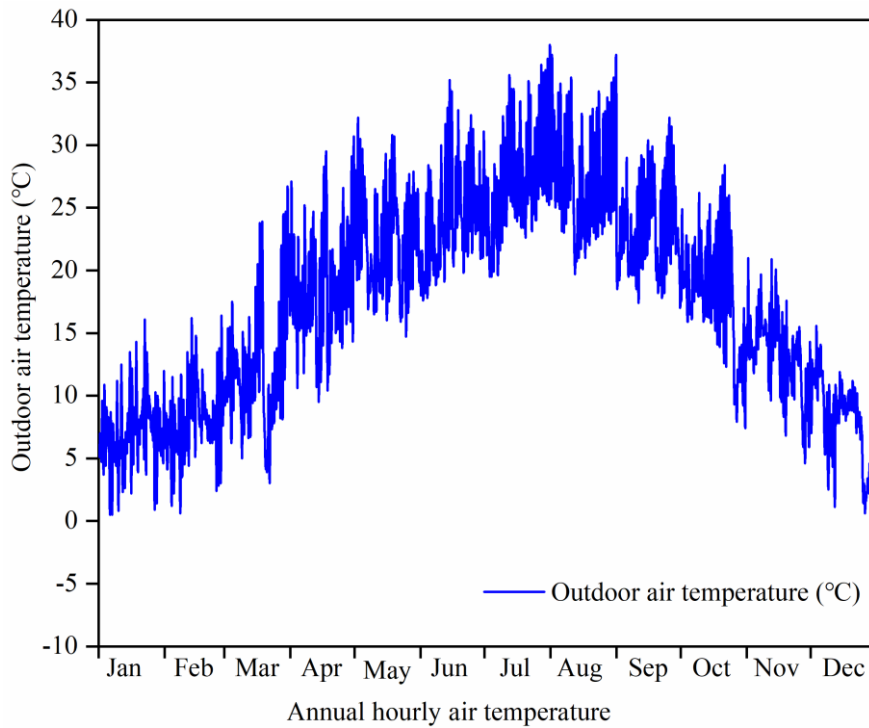


Figure 1-12. Hourly air temperature throughout whole year of the research region.

The weather data of typical meteorological year (TMY) from Nanchong weather station [23] were

analyzed for a more accurate understanding of the local climate. According to the annual hourly temperature in Figure 1-12, the mean temperature of July is about 27.4°C and the highest can achieve 38°C. The mean temperature of January is only 6.9 °C although the temperature is almost above 0°C in winter, while the lowest temperature is minus 0.9°C. In addition, Standard for weather data of building energy efficiency JGJ/T 346-2014 [13] clearly states that the heating degree-day (HDD18) is 1307 °C•d and the cooling degree-day (CDD26) is 156°C•d in this region. This demonstrates that the local demand for heating in winter is higher compared to cooling in summer.

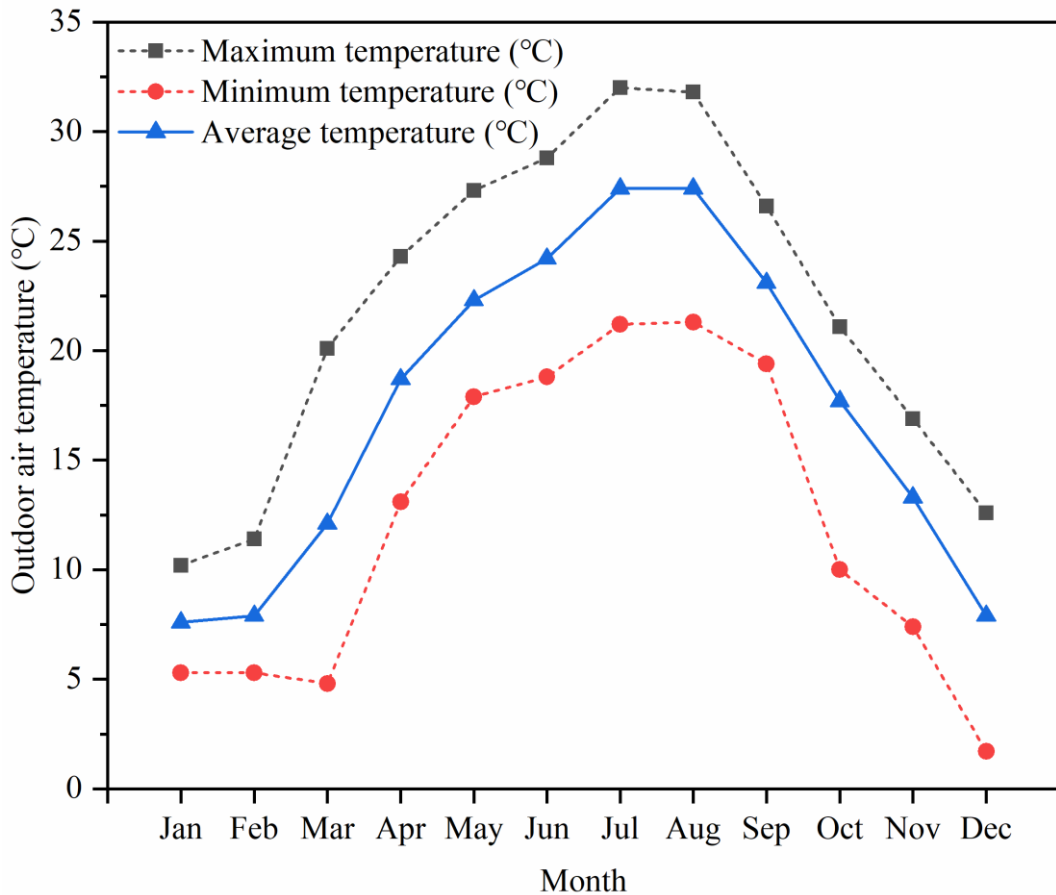


Figure 1-13. Characteristics of monthly temperatures of the research region.

Figure 1-13 shows the characteristics of monthly temperatures of the research region. The mean temperature of July and August is about 25°C and the highest temperature can achieve 36.5°C according to the annual hourly temperature in Figure 2(a). But the mean temperature of December, January and February is only 5.2 °C, while the lowest temperature is minus 4.4°C although the temperature is almost above 0°C in winter. It indicates there is a greater demand for heating.

The local humidity is high throughout the year, with the relative humidity of the air being around 90% in summer and close to 100% in some periods, while in winter the relative humidity is around 50% and below 30% in some periods.

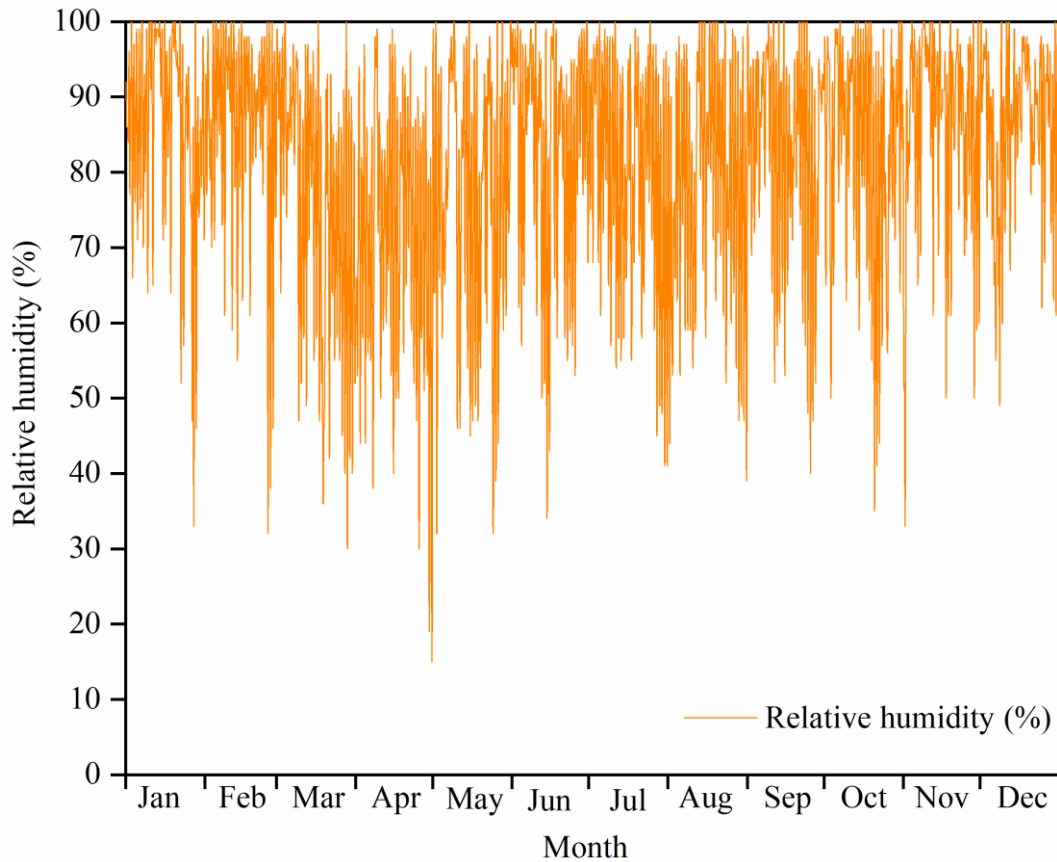


Figure 1-14. Hourly air relative humidity throughout whole year of the research region.

From Figure 1-15, even though the highest hourly solar radiation intensity can reach 1284 Wh/m^2 , there are very few periods of high radiation intensity -- only 22 hours in the year when its value exceeds 1000 Wh/m^2 . So the average hourly solar radiation intensity is only 127 Wh/m^2 throughout the year; while the hourly solar radiation intensity is even lower in winter, with an average value of 77 Wh/m^2 . It is mainly due to the fact that this region belongs to the Sichuan Basin and the topography is basically hilly and mountainous, so it is able to receive low solar radiation with the total annual solar radiation intensity is only 1110 kWh/m^2 .

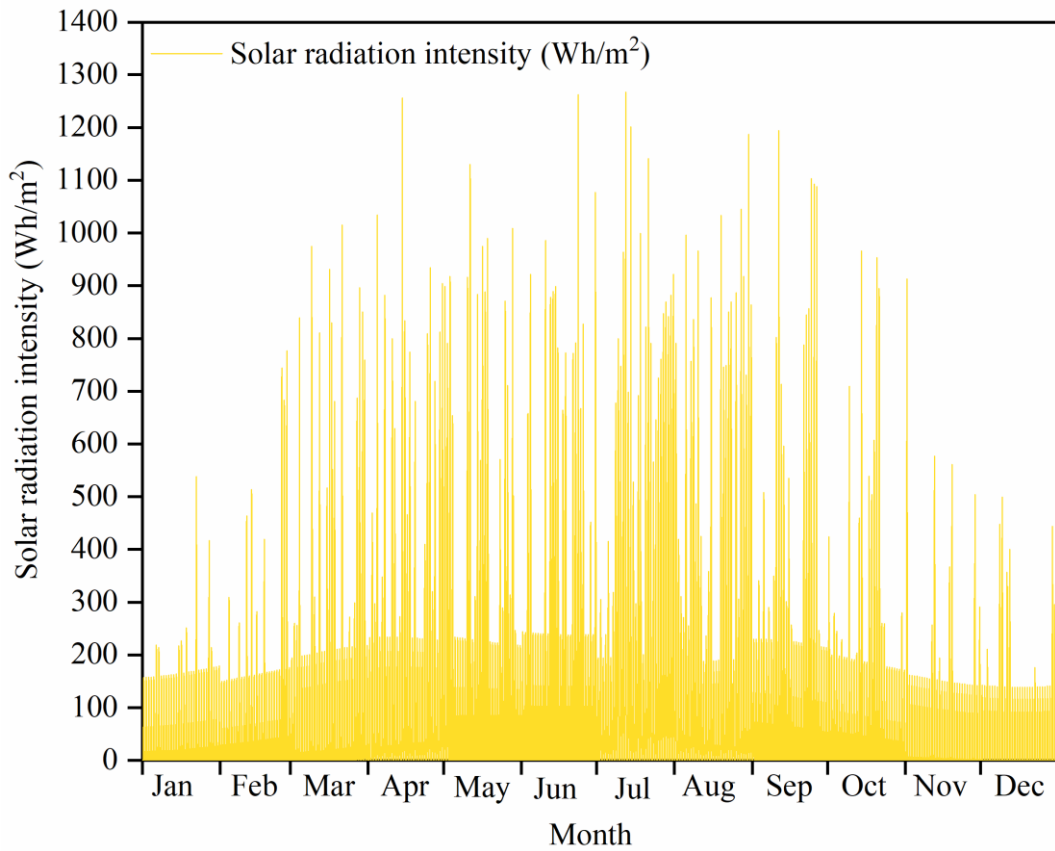


Figure 1-15. Hourly solar radiation throughout whole year of the research region.

Due to the topography, the local cloud cover is thick, the sunshine hours are short, and the solar radiation intensity is low throughout the year. Using the city in the same latitude region - Nanjing as the reference city, comparing the typical annual meteorological data of the two cities, it was found that the annual sunshine hours in the study area was 1588 hours, while the reference city was 1970 hours. Statistics of the hour-by-hour solar radiation intensity difference between the reference city and the study area found that for 1653 hours in the year, the solar radiation intensity of the reference city was greater than that of the study area, and for 1112 hours the solar radiation intensity of the study area was greater. However, when the hour-by-hour solar radiation intensity is summed as Figure 1-16, the direct solar radiation intensity per square meter of ground received in the reference city was 397.14 kWh higher than that in the study area during the whole year.

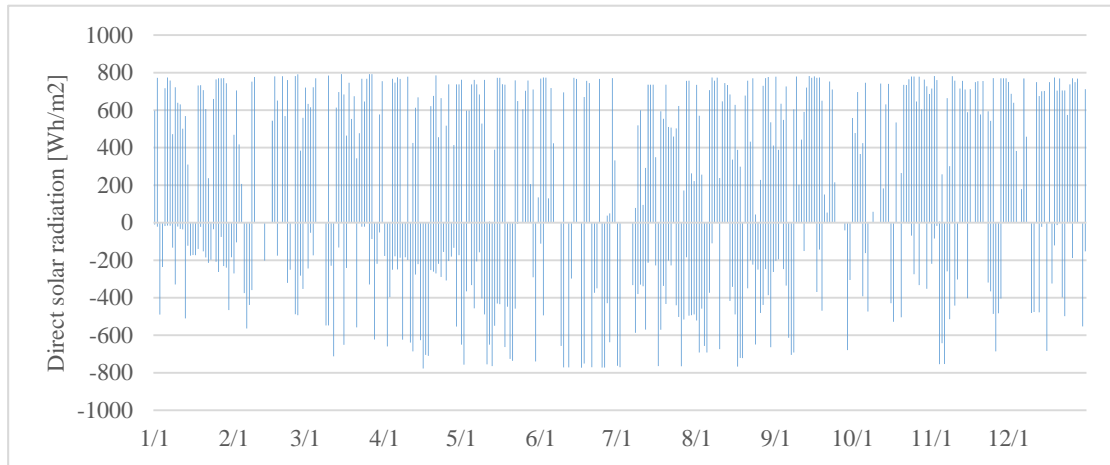


Figure 1-16. Difference of direct solar radiation between two Nanchong and Nanjing.

1.2 Purpose and significance of this study

1.2.1 Purpose of this study

According to the analysis of the energy consumption situation, climate characteristics, and economic background of the study research, we can notice that it's imperative and challenging to lower the energy demand of traditional dwellings in northeast of Sichuan hills, China. Hence we aim to determine appropriate strategies for energy-saving renovation for traditional dwellings in this region. In order to reduce the energy demand and maximum the consequential economic benefits at the same time, we will assess energy demand, the corresponding investment payback period, and economic benefits of the related energy-saving strategies. Finally we will recommend the optimal parameters of energy-saving strategies and the most economic energy-saving strategy.

1.2.2 Significance of this study

In this study, we first propose four individual energy-saving strategy based on the foundational theoretic of heat transfer process of opaque exterior walls, including adding insulation materials for exterior walls and roof, incorporating phase change materials (PCM) into exterior walls, installing Trombe wall (T-wall), and setting on-top sunspaces (OS), then discuss their optimal parameters for maximum the energy-saving effect. Next we obtain a total of 15 strategies by combining these four individual strategies in different methods. Finally we further assess their energy-saving and economic potential. The results of this study can provide the following reference for local decision-makers to select more appropriate strategies of energy-saving renovation.

- Derive the calculation method for optimal economic thickness of insulation materials for exterior walls, and determine the optimal economic thickness of different insulation materials for exterior walls and roof of traditional dwellings in this region.
- Determine the optimal combination of thermophysical parameters of phase change materials (PCM) incorporated with exterior walls to lower energy demand for traditional dwellings in

this region.

- Propose suitable parameters of Trombe wall (T-wall) and on-top sunspaces (OS) to reduce energy demand for traditional dwellings in this region.
- Provide the saving rate of annual energy demand, investment payback period, and economic benefits of 15 energy-saving strategies when they are employed in traditional dwellings located in this region, which can offer useful and relatively accurate reference for local residents and decision-makers.

1.3 Research structure

Figure 1-17 displays the research structure of this study. In general, this study can be divided in three parts. The first part, including Chapter 1, Chapter 2, Chapter 3, and Chapter 4, aims to deeply comprehend the present situation of traditional dwellings in northeast of Sichuan hills, China, and propose four individual energy-saving strategies based on the foundational theories and local situation. The second part, including Chapter 5, Chapter 6, and Chapter 7, aims to evaluate the energy-saving potential and optimal parameters combination of each individual energy-saving strategy. The third part, including Chapter 8 and Chapter 9, aims to assess the energy-saving and economic potential of each energy-saving strategy, and further proves the effective of the recommended strategy by taking the actual tested building as an example. And the following is the main work of each chapter.

In Chapter 1, Research Background and Purpose of the Study:

We review the energy consumption situation for the world and China, and further introduce the share of energy consumption for building sector in China. Next we explain the climate background of the research region – northeast of Sichuan hills, and analyze the challenge for lowering energy consumption in this region. Then we also introduce the current population and economic development of the research region. Based on the previous research background of the research region, we clarify the purpose, significance, and research structure of this study.

In Chapter 2, Literature Review:

We review a lot of previous published studies to find appropriate energy-saving strategies for traditional dwellings in this research region. Firstly, we summary the heat transfer process through opaque envelopes of buildings, and then we determine three directions to realize the goal of energy saving based on these fundamental theories. Therefore, the related research on applying insulation system, phase change material (PCM), and solar radiation to reduce the energy demand of buildings are reviewed in this chapter.

In Chapter 3, Methodology:

We introduce the detail information about traditional dwellings in this research region based on the field investigation and the arrangement of the experimental work, then a base model used for discussing the energy-saving strategies is established and depicted. Next, we also clarify the

calculation process of all of research methods we used in this study.

In Chapter 4, Thermal Performance of the Tested Building:

We analyze the recorded data of the actual tested building. Then we calculate the theoretical values of some basic thermal indicators of exterior envelopes, and further compared these values with the requirements proposed by the related energy efficiency standard. Moreover, in order to deeply comprehend the indoor environment of the current local traditional dwellings in this region, we also simulate the indoor air temperature throughout the whole year by EnergyPlus.

In Chapter 5, Determine Insulation Thickness of Exterior Envelopes for the Traditional Dwellings in Northeast of Sichuan Hills:

We derive the calculation method of the optimum economic thickness of insulation materials for building exterior walls in northeast of Sichuan hills, then calculate the optimal economic thickness for exterior walls of five commonly used insulation materials. Next, we compare and rank the importance of all of the factors which can affect the optimum thickness. Furthermore, we determine the correlation between the optimal economic thickness of insulation materials for roof and the optimal economic thickness of insulation materials for exterior walls.

In Chapter 6, Parametric and Economic Analysis of Phase Change Materials (PCM) on Energy Saving for Traditional Dwellings in Northeast of Sichuan Hills:

We select the total of eight parameters of PCM, including location, melting temperature, thickness, phase transition temperature radius, latent heat, density, thermal conductivity, and specific heat, then vary their values in a predetermined range and investigate the effects of their variation on the annual energy demand, and finally obtain the optimal combination of the parameters of PCM. Furthermore, we also discuss a more economic selection of PCM for this study region considering the high cost of PCM.

In Chapter 7, Passive Application of Solar Energy for Traditional Dwellings in Northeast of Sichuan Hills:

We propose two strategies – Trombe wall (T-wall) and on-top sunspaces (OS) and assess their energy-saving performances and finally, we determine the optimal parameters of these two strategies.

In Chapter 8, Tech-economic Analysis of Comprehensive Energy-saving Strategies:

We obtain 15 strategies by making different combinations of four individual strategies proposed in Chapter 5-7 and then, we comprehensively evaluate their energy-saving potential, investment payback period, and economic benefits after 25 years. Next, we further assess the influence of building orientation on the energy-saving effects and economic potential. In addition, we take the actual tested building as an example, simulate its annual energy demand pre and post renovation to prove the effective of the recommended energy-saving strategy.

In Chapter 9, Conclusion:

CHAPTER 1. RESEARCH BACKGROUND AND PURPOSE OF THE STUDY

We conclude this study.

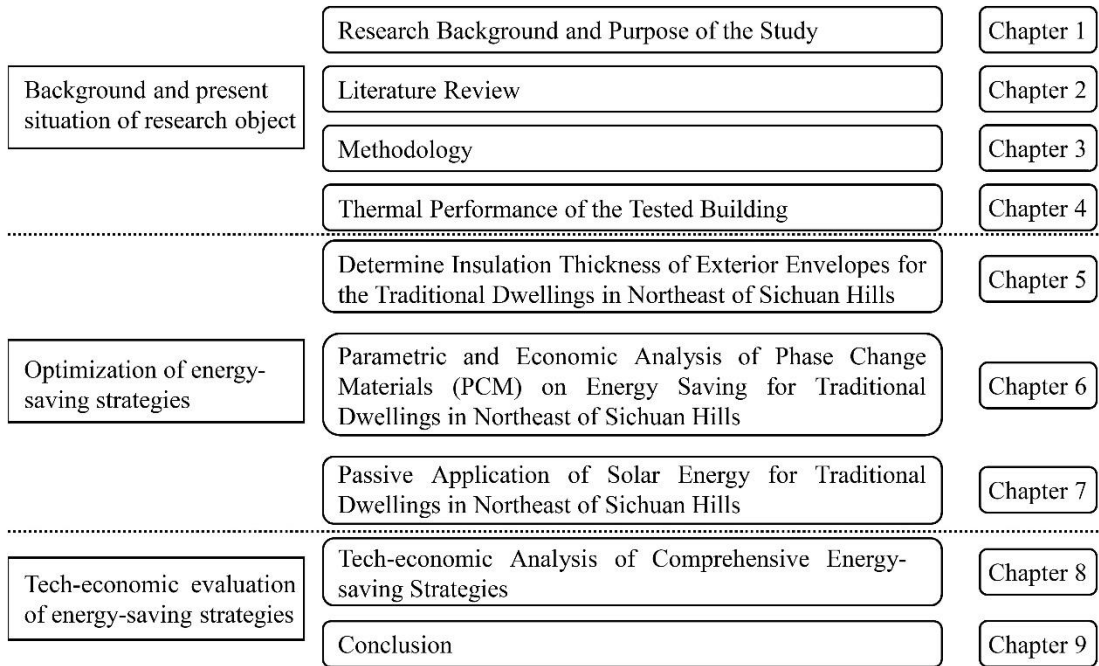


Figure 1-17. Research structure of this study.

Reference

- [1] Lester Brown, *Future at Risk on a Hotter Planet*.(New York: W.W. Norton & Company, 2009).
- [2] *Energy Future Beyond Carbon*, Scientific American (9/2006)
- [3] A. Sieminski. *International energy outlook*. Energy information administration (EIA), 2014, 18.
- [4] A. Allouhi, Y. E. Fouih, T. Kousksou, et al. Energy consumption and efficiency in buildings: current status and future trends. *Journal of Cleaner Production*, 2015, 109: 118-130.
- [5] X. D. Cao, X. L. Dai, J. J. Liu. Building energy-consumption status worldwide and the state-of-the-art technologies for zero-energy buildings during the past decade. *Energy and buildings*, 2016, 128: 198-213.
- [6] R. Rajeevt, H. Kasun, S. Rehan. Improving the energy efficiency of the existing building stock: A critical review of commercial and institutional buildings. *Renewable & Sustainable Energy Reviews*, 2016, 53: 1032-1045.
- [7] N. Zhu, Z. Ma, S. Wang, Dynamic characteristics and energy performance of buildings using phase change materials: a review, *Energy Conversion and Management*. 50 (2009) 3169–3181. doi: <https://doi.org/10.1016/j.enconman.2009.08.019> .
- [8] *China Building Energy Consumption Research Report (2020)*. <https://www.cabee.org/site/content/24021.html>, 2022.
- [9] S.E. Kalnæs, B.P. Jelle, Phase change materials and products for building applications: a state-of-the-art review and future research opportunities, *Energy and Buildings*. 94 (2015) 150–176. doi: <https://doi.org/10.1016/j.enbuild.2015.02.023>
- [10] D. Ürge-Vorsatz, L.F. Cabeza, S. Serrano, C. Barreneche, K. Petrichenko, Heating and cooling energy trends and drivers in buildings, *Renewable and Sustainable Energy Reviews*. 41 (2015) 85–98. doi: <https://doi.org/10.1016/j.rser.2014.08.039>.
- [11] X. Meng, B. Yan, Y. Gao, J. Wang, W. Zhang, E. Long, Factors affecting the in situ measurement accuracy of the wall heat transfer coefficient using the heat flow meter method, *Energy and Buildings*. 86 (2015) 754-765. doi: <https://doi.org/10.1016/j.enbuild.2014.11.005>.
- [12] Ministry of Housing and Urban-Rural Development of the People’s Republic of China, *Code for thermal design of civil building GB50176-2016*, China Architecture & Building Press, Beijing, 2016.
- [13] Ministry of Housing and Urban-Rural Development of the People’s Republic of China, *Standard for weather data of building energy efficiency JGJ/T 346-2014*, China Architecture & Building Press, Beijing, 2014.
- [14] Ministry of Housing and Urban-Rural Development of the People’s Republic of China, *Standard for weather data of building energy efficiency JGJ/T 346-2014*, China Architecture & Building Press, Beijing, 2014.
- [15] Fu X, Han A. *Energy saving of buildings in hot summer and cold winter zone of China*, China Architecture & Building Press, Beijing, 2002.

CHAPTER 1. RESEARCH BACKGROUND AND PURPOSE OF THE STUDY

- [16] X. Liu, Y. Chen, H. Ge, P. Fazio, G. Chen, X. Guo, Determination of optimum insulation thickness for building walls with moisture transfer in hot summer and cold winter zone of China, *Energy and Buildings*. 109 (2015): 361-368. doi: <https://doi.org/10.1016/j.proeng.2017.10.153>.
- [17] J. Yu, C. Yang, L. Tian, D. Liao, A study on optimum insulation thicknesses of external walls in hot summer and cold winter zone of China, *Applied Energy* 86 (2009) 2520–2529. doi: <https://doi.org/10.1016/j.apenergy.2009.03.010>.
- [18] J. Yu, C. Yang, L. Tian, Low-energy envelope design of residential building in hot summer and cold winter zone in China, *Energy Build.* 40 (2008) 1536–1546.
- [19] China Statistical Yearbook (2003)
- [20] Population density of China (2002). <https://www.osgeo.cn/map/m0408>
- [21] China Statistical Yearbook. 2020. <http://www.stats.gov.cn/tjsj/ndsj/2020/indexch.htm>.
- [22] Sichuan Statistical Yearbook. 2020. <http://tjj.sc.gov.cn/tjnj/cs/2020/zk/indexch.htm>.
- [23] Weather Data Download - Sichuan Nanchong 574110 (CSWD). https://energyplus.net/weather-location/asia_wmo_region_2/CHN/CHN_Sichuan.Nanchong.574110_CSWD.

CHAPTER 1. RESEARCH BACKGROUND AND PURPOSE OF THE STUDY

Chapter 2

Literature Review

CHAPTER 2. LITERATURE REVIEW

Chapter 2. Literature Review

2. Literature Review.....	2-1
2.1. Introduction.....	2-1
2.2. Heat transfer process through opaque envelopes of buildings.....	2-2
2.3. Application effect of insulation system for buildings.....	2-4
2.4. Application effect of phase change materials for buildings.....	2-7
2.5. Application effect of renewable energy source for buildings.....	2-9
2.6. Summary.....	2-9
Reference.....	2-11

CHAPTER 2. LITERATURE REVIEW

2. Literature Review

2.1. Introduction

Figure 2-1 depicts the heat balance of a building. Among them, the building envelope plays a pivotal role in maintaining the stability of the indoor environment. The thermal performance of the building envelope determines the amount of heat and cold loads required to maintain the desired indoor thermal environment, thus affecting the amount of building energy consumption. In the study of building envelope energy efficiency, Charles et al. [1] used SIMEB energy simulation software to simulate the effects of different exterior walls, roofs, windows and doors, and airtightness on building energy consumption, and concluded that increasing wall insulation, replacing windows and doors, etc. could reduce the total annual energy consumption by 45%. Mirrahimi et al. [2] conducted a review of studies on the selection of rational parameters for high-rise building envelopes, which include climatic conditions, form, width, length and height, façade, roof, glazing area, shading devices, natural ventilation, and occupant thermal comfort. Zhou et al. [3] used four office buildings in Beijing, Taiwan, Hong Kong, and Berkeley, and by simulating the energy consumption of different combinations of three key energy consumption influencing factors (climate, building envelope, and occupant behavior), they found that the difference in air conditioning and cooling energy consumption increased nearly twofold due to different climate conditions, while occupant behavior led to the largest difference in air conditioning and cooling energy consumption (up to three times). The effect of occupant behavior on air conditioning energy consumption is heterogeneous. The optimal building envelope design differs when the behavior of the occupants in a building varies under similar climatic conditions. In general, the optimal building envelope should be determined based on the people using the building and the surrounding environment. Huo et al. [4] selected four typical cities, Shenyang, Beijing, Chengdu and Guangzhou, to represent different climate regions in China. A quantitative study of the annual load contribution and energy saving contribution of the building envelope under non-stationary conditions was conducted using the finite volume method. The results show that roofs and exterior walls are the focus of energy conservation measures, and exterior wall insulation dominates the energy savings of building models in these four climate zones.

Proper utilization of passive energy-saving strategies can greatly improve the thermal performance of opaque envelopes of buildings. Moreover, passive design not only reduces building costs during the operational phase but can also create significant economic benefits throughout the whole life cycle of the building. Badea et al. [5] calculated the life cycle cost of the passive building under different working conditions and found that the payback period was between 9 and 16 years if the original building used electricity. Tahsidoost and Zomorodian [6] analyzed the economy of different passive strategies and concluded that the payback period was 6-12 years. A study by Zhang et al. [7] found that there was an optimum value between the thickness of insulation material and the total cost per unit of building operation, and the economic cost could be saved by more than 20% by using insulation material with the optimum economic thickness. Furthermore, the whole life cycle cost saving rate of buildings even could up to 52% by using passive design according to the literature review by Song et al. [8]. Hence we need to explore appropriate passive energy-saving

strategies to enhance the thermal performance of opaque exterior envelopes of traditional dwellings in northeast of Sichuan hills, China.

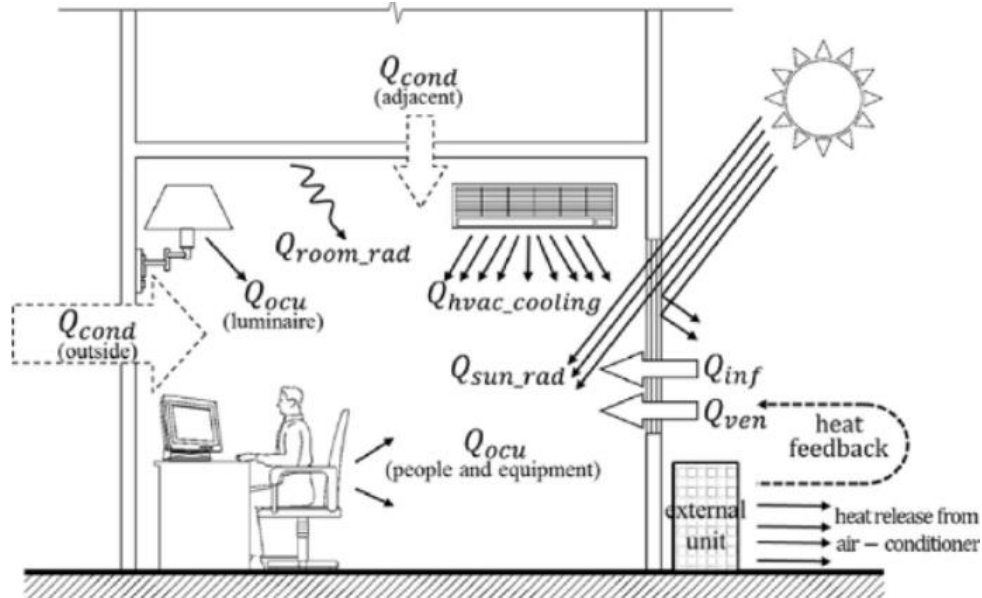


Figure 2-1. Heat balance of the building [9].

2.2. Heat transfer process through opaque envelopes of buildings

It is necessary to find and optimize the main influencing factors based on the heat balance equation to save energy since the high heat loss of building exterior envelopes. Therefore, this subsection describes the heat transfer model of the building exterior envelopes in detail and proposes energy-saving strategies and optimization indexes based on it. In this subsection, Eqs.2-1 to 2-7 describe the heat transfer process of both opaque and transparent exterior envelopes [10]. The heat transfer process of opaque exterior envelope such as walls and roofs can be viewed as a one-dimensional unsteady heat conduction process, and Let x be the coordinate of the thickness direction of the wall, and its heat balance differential equation is:

$$\frac{\partial t}{\partial \tau} = a \frac{\partial^2 t}{\partial x^2} \quad (2-1)$$

$$a = \frac{\lambda}{\rho C} \quad (2-2)$$

where:

t is temperature, °C;

τ is time, s;

a is thermal diffusivity, m²/s;

λ is thermal conductivity, W/(m K);

ρ is density kg/m^3 ;

C is specific heat, $\text{J}/(\text{kg K})$;

It is clear that the thermophysical properties of the envelope materials directly affect the rate and amount of heat transfer in space and time. As for building envelopes, enhancing the overall thermal resistance of the wall is the main means to suppress the impact of outdoor temperature on the indoor. Therefore, reducing the overall heat transfer coefficient of the wall is the main method currently applied, which includes adding insulation materials with lower thermal conductivity or raising the thickness of the wall to improve the thermal inertia. In consideration of the accessibility and practicability of energy-saving renovation of traditional dwellings in northeast of Sichuan hills, thus its application effect and the related optimization process will be thoroughly analyzed in Chapter 5. On other hand, currently there are extensive studies focusing on applying thermal energy storage (TES) to realize energy conservation, where phase change material (PCM) is an effective TES medium due to its large amount of latent heat [11] and broad phase change temperature range [12]. Therefore, the application of PCM has vast potential to reduce energy demand of buildings because it is able to phase change in a particular temperature range and then alleviate the impact of outdoor temperature variation on the indoor environment, thereby lower energy demand for heating and cooling [13,14]. Hence the energy-saving potential and optimization of phase change materials (PCM) also be deeply discussed in Chapter 6.

Then define $x = 0$ as the outside surface of the envelope, and $x = \delta$ as the inside surface of the envelope, the boundary conditions are:

$$\alpha_{out} [t_{out}(\tau) - t(0, \tau)] = -\lambda \left. \frac{\partial t}{\partial x} \right|_{x=0} \quad (2-3)$$

$$\alpha_{in} [t(\delta, \tau) - t_{in}(\tau)] = -\lambda \left. \frac{\partial t}{\partial x} \right|_{x=\delta} \quad (2-4)$$

Initial condition is:

$$t(x, 0) = f(x) \quad (2-5)$$

where:

τ is time, s;

λ is thermal conductivity, $\text{W}/(\text{m K})$;

α_{out} is convective heat transfer coefficient of the outside surface, $(\text{W}/\text{m}^2 \text{ K})$;

α_{in} is convective heat transfer coefficient of the inside surface, $(\text{W}/\text{m}^2 \text{ K})$;

$t_{out}(\tau)$ is outdoor air temperature, $^{\circ}\text{C}$;

$t_{in}(\tau)$ is indoor air temperature, °C;

$t(x,\tau)$ is temperature at each point in the wall , °C.

According to Eqs. 2-3 to 2-4, it is obvious that improving thermal properties of the outside surface of building envelopes and utilizing renewable energy, such as solar radiation, effectively can significantly enlarge the heat gain of building envelopes while keeping the indoor temperature comfortable. It can dramatically lower the heating load for buildings with high heating demand. Therefore, enhancing the heat gain of the exterior surface of the envelope is another focus of the energy-saving strategies proposed in this paper. The mainly current strategies include adding sunrooms, adjusting the solar radiation absorption coefficient of outside surfaces, installing T-wall and setting on-top sunspaces. Taking into account local topographic characteristics and lower economic development of this region, other two passive energy-saving strategies – T-wall and on-top sunspaces which use solar energy to reduce the heating load are proposed and their application effects and optimization parameters are evaluated in Chapter 7.

As for transparent envelope, such as windows. The transient heat gain is:

$$Q_{glazing} = K_{wind} F_{wind} [t_{a,out}(\tau) - t_{a,in}(\tau)] + (SHGC) F_{wind} I \quad (2-6)$$

$$SHGC = \tau + \sum_{k=1}^n N_k a_k \quad (2-7)$$

where:

K_{wind} is the overall heat transfer coefficient of the transparent envelope, W/(m² K);

F_{wind} is the heat transfer area of the transparent envelope, m²;

I is the solar radiation intensity, W/m²;

τ is the overall transmittance of the glazing;

a_k is the absorptance of the k th layer of glazing;

n is the number of glazing layers;

N_k is the rate of inward conduction of solar radiant heat absorbed by the k th layer of glazing.

2.3. Application effect of insulation system for buildings

For the study of thermal performance and insulation of walls, Leccese et al. [15] used an analytical model based on the heat transfer matrix method to predict the dynamic thermal response behavior of internal and external walls of buildings, and using the analytical model, the effect of continuous changes in the location and thickness distribution of insulation materials on dynamic thermal performance (dynamic thermal transmittance, attenuation coefficient and delay time) was demonstrated for different construction schemes. Huang et al. [16,17] established a model for

calculating the thickness of the exterior wall insulation layer and optimizing the thermal performance parameters of the envelope structure by considering the orientation of the building, the window-to-wall ratio, and the type of windows, and verified the feasibility of the model by using an actual building as an example. Xu et al. [18] analyzed the effect of heat transfer coefficient of building envelope on the operation performance of air source heat pump air conditioning system based on the simulation model of air source heat pump air conditioning system established by TRNSYS software, and the results showed that the building load was linearly correlated with the system energy consumption and heat transfer coefficient of the exterior wall, and reducing the heat transfer coefficient of the exterior wall could effectively reduce the system energy consumption. The experimental test carried out by Fang et al. [19] displayed that building envelope insulation offers a saving of up to 23.5% in air conditioning energy consumption. Hu et al. [20] enhance the thermal performance of hollow block walls by filling the insulation material and found the inner surface heat flow of different wall types filled with EPS decreased by 17.96% to 36.6% compared with the wall without filling with EPS. Yu et al [21] used DesignBuilder energy consumption simulation software to simulate the energy consumption of existing residential building facades and three energy-saving retrofit facade systems, and the results showed that not only the same insulation system with different insulation layer thicknesses had different insulation effects, but also different insulation systems with the same insulation layer thickness had different insulation effects. Meng et al. [22,23] and Zhang et al. [24] analyzed the effects of different insulated walls and insulation locations on the thermal response rate and heat flow on the inner surface of the wall and found that although the walls had the same heat transfer coefficient, the closer the insulation was to the inner surface of the wall, the lower its inner surface temperature, the higher the thermal response rate of the wall, and the smallest heat flow value of the inner insulated wall. It was also found that the inner insulated walls and foam concrete walls are suitable for air conditioning intermittent heating conditions, while heavy-duty self-insulation and external insulation are more suitable for air conditioning continuous operation conditions. Compared with continuous operation of air conditioners, the daily cooling load formed by the walls was reduced by 44- 55% during intermittent operation, with the highest energy savings of 52- 65% for internally insulated walls.

Furthermore, scholars around the world have conducted extensive research on the economic thickness of building exterior walls. Daouas [25] investigated the relationship between the optimal insulation thickness of walls with different orientations and building energy efficiency under the combined effect of cold and heat loads for a typical wall structure, and found that east and west facing facades are most favorable for winter heating conditions and north facing facades are least favorable for winter heating conditions, while a cost analysis was conducted with a life cycle of 30 years, resulting in an optimal insulation thickness of south facing facades of 10.1cm, the energy saving rate reaches 71.33%, and the payback period is 3.29 years. It is also pointed out that the wall orientation has less influence on the optimal insulation thickness but more influence on the energy saving effect, and the optimal insulation thickness is influenced by economic parameters such as material price, energy cost, inflation rate and discount rate, and building life. Wang [26] selected Shanghai, Changsha, Shaoguan and Chengdu as four representative geographical areas in the hot-summer and cold-winter regions of China, and calculated and analyzed the optimal insulation thickness of five commonly

used insulation materials for exterior walls (including expanded perlite, polyurethane foam, extruded polystyrene foam, rock wool mat and expanded vermiculite) by combining economic models. Ozel et al. [27] calculated the economic thickness of insulation and found that yearly fuel consumption and emissions are decreased by 68–89.5%. Kurekci [28] predicted energy demand of buildings by heating and cooling degree-day method and used present worth factor (PWF) to calculate annual energy cost. Then the optimum insulation thickness was obtained by minimizing the total heating and cooling cost. Ultimately, they determined the optimum insulation thickness for 81 provincial centers in Turkey. Also by degree-day method and PWF method, Derradji et al. [29] found the optimum insulation thickness in Algeria was 1-2.5cm and its energy savings varied between 0.5 and 1.5 \$/m². Ozel [27] applied implicit finite-difference method to solve the differential equation expressed the transient one-dimensional heat conduction process and then calculated the yearly heating and cooling loads. On this basis, the optimum thickness of different insulation materials for building exterior walls in Elazığ, Turkey was calculated combined the energy demand and the *PWF* method. Results showed the optimum thickness of different insulation materials ranged from 0.054-0.192m and the payback period was between 3.56-8.85 years with a decrease of yearly fuel consumption and emissions by 68-89.5%. Similarly, Rosti et al. [30] employed the numerical solution to calculate the transmission loads and used *PWF* method to evaluate the economy of different insulation materials. They discovered the optimum thickness for different insulation materials was no more than 0.04m based on the analysis of buildings in eight cities representing all climatic zones in Iran. Raimundo et al. [31] simulated energy demand of four buildings with different types of use and different climate context, and used net present value (NPV) method to calculate the equivalent annual cost of the building used during its useful life. Finally, they displayed that 0-0.01m was the range of optimum insulation thickness for building walls in Portugal and revealed that regions with more intense climates require higher thermal insulation thicknesses. With the help of a simulation program (DesignBuilder) and evaluating the insulation material cost by the macroeconomic perspective (only energy costs, insulating material costs and emission costs were considered), Agostino et al. [32] calculated optimum insulation thickness for building walls in Italy and found there were significant differences in the optimal insulation thickness in different cities even though within the same country. For instance, the optimum thickness for insulation materials were 0.08-0.1m and 0.02-0.04m for Milan and Palermo, respectively, while insulation was always disadvantageous for Cairo. For buildings in China, Yu et al. [33] improved heating and cooling degree-day method by considering the effect of solar radiation on building exterior envelopes to predict energy demand, and combined the P_1 - P_2 economic method to calculate the optimum insulation thickness for buildings in HSCW. Finally, they found that 0.053-0.236m was the optimum thickness range for insulation of building walls in HSCW, and the life cycle savings could be up to 39.0-54.4 \$/m² while the payback period was from 1.9 to 4.7 years. Also for buildings in HSCW, Liu et al. [34] used a coupled heat and moisture transfer model to predict building energy consumption and the P_1 - P_2 economic model was combined to evaluate the optimum insulation thickness, and eventually, they found that XPS with 0.081-0.105m could maximize the economic benefits in its service life (16.6-28.5 \$/m²). And in the severe cold and cold zone, Geng et al. [35] analyzed the optimum thickness of vacuum insulation panels for the lightweight building by using dynamic building energy simulation software OpenStudio and the P_1 - P_2 economic model. They found the optimum thickness increases from 3.5mm to 31mm when climate becomes colder and the

saving rate of total cost grown from 40.5% to 47.9%.

2.4. Application effect of phase change materials for buildings

Currently there are extensive studies focusing on applying thermal energy storage (TES) to realize energy conservation, where phase change material (PCM) is an effective TES medium due to its large amount of latent heat [11,36] and broad phase change temperature range [12]. Hence the application of PCM has vast potential to reduce energy demand of buildings because it is able to phase change in a particular temperature range and then alleviate the impact of outdoor temperature variation on the indoor environment, thereby lower energy demand for heating and cooling, and improve occupant thermal comfort [13,14]. Preceding related research has manifested the remarkable contribution of incorporating PCM into building envelopes to control both heating load [37,38] and cooling load [13, 39-40]. The result obtained by Nghana and Tariku [41] demonstrated that the application of PCM can lower heating energy demand by up to 57% during winter. In another optimization study of PCM parameters for U.S. buildings, annual heat gain even could be reduced by 35.6% and 47.2% when the proper transition temperature and location of PCM were adopted in Denver and Billings, respectively [13]. Li et al. [42-44] summarized four typical indoor air conditioning operating conditions by questionnaire survey, on the basis of which Phase Change Material (PCM) was combined with the building envelope to analyze the improvement of the thermal performance of the building envelope, and the results showed that combining PCM with the building envelope could not only improve the indoor thermal environment, but also reduce the heating time and heating energy consumption. For lightweight buildings with air conditioning, the heat load can be reduced by 40% ~ 70% with the addition of phase change materials in the exterior walls, while the cooling load increases slightly in the summer months when the temperature is higher. Young et al. [44] proposed a simple method to quickly evaluate the thermal performance of building envelopes containing PCM or other building materials. Meng et al. [45] also studied the effect of thermal properties of different wall interior finishing materials on the internal surface temperature and heat flow, and found that by reducing the density, heat capacity and thermal conductivity of decorative coatings, the temperature response rate of the coating can be improved and the heat flow value can be reduced, among which, reducing the thermal conductivity of the material has the best energy saving effect. Nevertheless, sometimes the optimal PCM for lowering cooling load may have a negative impact on heating load reduction, and vice versa. For example, also in the study carried out by Kishore et. al. [13], the amount of heat loss increased in Denver and Billings although application of PCM created a remarkable reduction of cooling demand, therefore evaluating thermal performance of PCM based on the whole year period perspective is essential. By evaluating the impact of PCM-drywalls on energy-saving effect for residential buildings in European climates, Soares et. al. [39] concluded that an optimal solution of using PCM to decrease annual energy consumption can be found for each climate, and PCM-drywalls were particularly suitable for Mediterranean climate, even 62% of energy saving could be obtained for the Csb-Coimbra climate, while 10%-46% of energy-saving rate was achieved for other climates. The above studies display the great energy-saving potential of PCM, however, the effect of PCM is not necessarily positive on energy conservation. Tunçbilek et al. [40] found that energy saving can be up to 12.8% when proper

transition temperature and thickness of PCM were adopted under the intermittent cooling operation, whereas any phase transition temperature above 26°C had a negative impact on energy-saving performance of PCM. In addition, Kishore et al. [13,36] also concluded that unsuitable parameters of PCM should not be suggested for energy saving.

Preceding studies demonstrate that the energy-saving performance of PCM is determined jointly by its thermophysical parameters, building construction and the climate background, while inappropriate parameter values even have a negative impact on the exploit of PCM for energy saving, thus the parametric analysis of PCM is imperative. Currently, there are abundant studies about these influencing parameters. Zhou and Eames [47] carried out simulation works for a lightweight building in the UK, optimized the melting temperature of phase change material wallboard and finally found energy-saving rate can be as high as 40% compared to the ordinary building during summer. Except for melting temperature, thermal conductivity and latent heat of PCM were analyzed in the research conducted by Li et al. [48], they concluded the above three parameters can greatly influence the performance of PMC-based walls. Xie et al. [49] discussed the effect of phase change range on the performance of PCM and discovered the optimal phase change range of each month was different, therefore they suggested the performance of PCM should be evaluated during an entire year. In order to acquire a better energy-saving performance of PCM throughout a whole year, Wang et. al. [50] investigated the performance of PCM wallboards in air-conditioned lightweight buildings in Shanghai and optimized melting temperature for different rooms. According to the previous studies, it's no doubt that many parameters related to PCM itself can affect the thermal performance of PCM when it is employed in building envelopes, generally including installation location, phase transition temperature, thickness, latent heat, density, thermal conductivity, and specific heat capacity, however, only a few scholars comprehensively analyzed these parameters rather than only a part of the influencing parameters. Kishore et al. [36] investigated the influence of eight parameters on the thermal performance of PCM, but they aimed to discuss the load modulation caused by PCM. In a numerical study conducted by Liu et al. [51], seven parameters were optimized step by step, and their influences on the performance of lightweight buildings were evaluated.

Based on the above literature review, we can find that the optimal parameters of PCM incorporated into envelopes are greatly affected by the climates and the thermal property of building construction. For example, the optimal melting peak temperature of PCM when it is utilized in warmer climates tends to be higher than that of colder climates [39]. And for the installation position of PCM, it is recommended to be closer to the interior for a heating purpose [52,53] and be installed on the exterior side of walls for the cooling purpose [52], whereas some studies found the mid-element position was better based on annual performance [51, 54]. The disparity of the thermal performance of PCM fitted into different positions displays the proper location of PCM depending on the climate characteristics and the consequential application purpose. Additionally, the thermal property of exterior walls also has a certain impact on the thermal performance of PCM [55,56], indicating that the optimal parameter of PCM employed for buildings with dissimilar construction may be unique even though these buildings are located in the same climate zone. Hence it is

necessary to carefully optimize the relevant parameters of PCM when it is incorporated into building envelopes, thereby improving its thermal performance and contribution to building energy saving. On the other hand, the current economic analysis of the application of PCM is not insufficient [37,38], and sometimes PCM is not even recommended when considering its high cost and long payback period from the economic perspective even though it can lower energy consumption to some extent [56-58], thus economic evaluation of applying PCM is crucial, especially in the rural region where has backward economic development. Furthermore, many common evaluation parameters, such as the investment payback period, economic benefits during particular periods are related to local economic circumstances [56-57,59-61], indicating that the results of economic evaluation are distinctive for different regions even though the same material is employed, thus the economic evaluation should be carried out based on the local economic condition.

2.5. Application effect of renewable energy source for buildings

Using renewable energy can directly reduce the usage of fossil and the most commonly used passive strategy in rural China is solar thermal utilization [62]. Solar radiation is a well-known renewable energy source, but it is also an energy source with low energy density and can only be used intermittently [63]. Si et al. [64] installed the Trombe wall (T-wall) on the south façade of an elementary school dormitory building in Qinghai Province, China, and the experimental and simulation results revealed that this strategy raised the indoor temperature by 4.5°C-10°C in winter, which reduced the building heat load effectively. Zhang et al. [65] did a case study to discuss the effect of T-wall design factors on energy consumption, and the final results showed that up to 72% of annual building energy consumption could be saved by using T-wall with the optimum combination of design factors. Hou [66] analyzed the effect of using additional sunrooms in Tibetan traditional dwellings located in Sichuan Northwestern Plateau by investigation and simulation. The eventual results displayed that installing the additional sunroom with a depth of 1.2m on the south façade could improve indoor temperature by 5°C-10°C in winter. Simoes et al. [67] revealed that T-wall system contributed to a reduction of more than 20% in heating demand without compromising the cooling season in Mediterranean climates. Bevilacqua et al. [68] found that in a moderate climate, such as Pisa, percentage reductions of heating requirements of up to 35.5% for the single-story building have been obtained for the high-insulated building by using T-wall. Wang et al. [69] analyzed the application potential of on-top sunspaces installed on the roof in serve cold zone, and the ultimate results showed that the rational on-top sunspaces could save about 42.8% for total building energy consumption.

2.6. Summary

In this chapter, we review the previous studies about utilization of insulation materials, phase change materials (PCM), Trombe wall and on-top sunspaces to lower energy consumption of building. According to their results, we can conclude that each strategy can reduce energy consumption of building effectively when it is properly utilized, however, we cannot ignore that their energy-saving performance is diverse in different conditions. For instance, the same insulation strategy can lead to varying energy-saving effects in different climatic contexts [64,67-68,70], and for

the identical region, whether or not to consider economy also leads to different decision results [7,27]. Therefore, it is necessary to evaluate the energy-saving effects and economic benefits of energy-saving strategies within local climate characteristics and economic context. On the other hand, the indoor thermal environment of rural buildings in China is usually poor and cannot meet the requirements of Chinese standards [71] and the usage of air conditioning or other means of regulating the indoor thermal environment is becoming more common as residents' economic income increases. But the current evaluation of the application of passive energy-saving strategies, especially the economic evaluation, is not sufficient [62]; while evaluating the energy efficiency and economy of energy-saving strategies in traditional dwellings can help decision-makers to choose appropriate strategies to enhance the thermal performance of the building envelopes, thereby reducing building energy consumption and carbon emissions, as well as decreasing the costs during the building operation phase. Hence we need to evaluate the energy-saving potential of these proposed strategies, and further optimize their related parameters to maximum its energy-saving effect, and then combine the economic evaluation method to conduct the comprehensive tech-economic assessment for these strategies, and the results of the assessment can provide valuable references for local residents and design-makers.

Reference

- [1] A. Charles, W. Maref, C. M. Ouellet-Plamondon, Case study of the upgrade of an existing office building for low energy consumption and low carbon emissions. *Energy and Buildings*, 2019, 183: 151-160.
- [2] S. Mirrahimi, M. F. Mohamed, L. C. Haw, The effect of building envelope on the thermal comfort and energy saving for high-rise buildings in hot-humid climate. *Renewable and Sustainable Energy Reviews*, 2016, 53: 1508-1519.
- [3] X. Zhou, D. Yan, J. J. An, Comparative study of air-conditioning energy use of four office buildings in China and USA. *Energy and Buildings*, 2018, 169: 344-352.
- [4] H. Huo, J. H. Shao, H. B. Huo. Contributions of energy-saving technologies to building energy saving in different climatic regions of China. *Applied Thermal Engineering*, 2017, 124: 1159-1168.
- [5] A. Badea, T. Baracu, C. Dinca, D. Tutica, R. Grigore, M. Anastasiu, A life-cycle cost analysis of the passive House “politehnica” from Bucharest. *Energy and Buildings*, 2014; 80: 542–555. doi: <https://doi.org/10.1016/j.enbuild.2014.04.044>.
- [6] M. Tahsildoost, Z. Zomorodian, Energy, carbon, and cost analysis of rural housing retrofit in different climates. *Journal of Building Engineering*, 2020; 30: 101277. doi: <https://doi.org/10.1016/j.jobee.2020.101277>.
- [7] L. Zhang, Z. Liu, C. Hou, J. Hou, D. Wei, Y. Hou, Optimization analysis of thermal insulation layer attributes of building envelope exterior wall based on DeST and life cycle economic evaluation. *Case Studies in Thermal Engineering*, 2019; 14: 00410. doi: <https://doi.org/10.1016/j.csite.2019.100410>.
- [8] Y. Song, K. S. Darani, A. I. Khdair, G. Abu-Rumman, R. Kalbasi, A review on conventional passive cooling methods applicable to arid and warm climates considering economic cost and efficiency analysis in resource-based cities. *Energy Reports*, 2021; 7: 2784–2820. doi: <https://doi.org/10.1016/j.egy.2021.04.056>.
- [9] M. Han, H. Chen, Effect of external air-conditioner units heat release modes and positions on energy consumption in large public buildings. *Building and Environment*, 2017, 111:47-60. doi: <https://doi.org/10.1016/j.buildenv.2016.10.014>
- [10] Y. Zhu, *Built Environment* (4th Edition). China Architecture & Building Press, Beijing, 2005.
- [11] D. H. Yu, Z. Z. He, Shape-remodeled macrocapsule of phase change materials for thermal energy storage and thermal management, *Applied Energy*. 247 (2019) 503e516. doi: <https://doi.org/10.1016/j.apenergy.2019.04.072>
- [12] E. Solgi, Z. Hamedani, R. Fernando, B. M. Kari, A parametric study of phase change material characteristics when coupled with thermal insulation for different Australian climatic zones,

- Building and Environment. 163 (2019) 106317. doi: <https://doi.org/10.1016/j.buildenv.2019.106317>
- [13] R.A. Kishore, M.V.A. Bianchi, C. Booten, J. Vidal, R. Jackson, Optimizing PCM-integrated walls for potential energy savings in US buildings, *Energy and Buildings*. 226 (2020) 110355. doi: <https://doi.org/10.1016/j.enbuild.2020.110355>
- [14] R. A. Kishore, M.V.A. Bianchi, C. Booten, J. Vidal, R. Jackson, Modulating thermal load through lightweight residential building walls using thermal energy storage and controlled precooling strategy, *Applied Thermal Engineering*. (2020) 115870. doi: <https://doi.org/10.1016/j.applthermaleng.2020.115870>
- [15] F. Leccese, G. Salvadori, F. Asdrubali, et al. Passive thermal behaviour of buildings: Performance of external multi-layered walls and influence of internal walls. *Applied Energy*, 2018, 225: 1078-1089.
- [16] J. E. Huang, H. L. Lv, T. Gao, et al. Thermal properties optimization of envelope in energy-saving renovation of existing public buildings. *Energy and Buildings*, 2014, 75: 504-510.
- [17] J. Huang, H. Lv, W. Feng, Y. Chen, T. Zhou. Thermal Properties Optimization of Envelope in Energy-saving Renovation of Existing Residential Building. *Journal of Civil, Architectural & Environmental Engineering*, 2013, 35(5): 118-124.
- [18] P. Xu, X. Zhai, Influence of climate and building envelope on performance of air source heat pump air conditioning system. *CIESC Journal*, 2016, 67(S2): 208-216.
- [19] Z. Fang, N. Li, B. Li, G. Luo, Y. Huang, The effect of building envelope insulation on cooling energy consumption in summer. *Energy & Buildings*, 2014; 77, 197-205. doi: <https://doi.org/10.1016/j.enbuild.2014.03.030>.
- [20] W. Hu, Y. Xia, F. Li, H. Yu, C. Hou, X. Meng, Effect of the filling position and filling rate of the insulation material on the insulation performance of the hollow block. *Case Studies in Thermal Engineering*, 2021; 26: 101023. doi: <https://doi.org/10.1016/j.csite.2021.101023>.
- [21] Y. Yu, L. Cai, Y. W. Wang, Energy-saving Transformation Research on the External Wall of Existing Residential Buildings in Nanjing Area. *Proceedings of ECOS 2013-the 26th I International Conference on Efficiency, Cost, Optimization, Simulation and Environmental Impact of Energy Systems*. 2013.
- [22] X. Meng, Y. Q. Huang, Y. Cao, et al. Optimization of the wall thermal insulation characteristics based on the intermittent heating operation. *Case Studies in Construction Materials*, 2018, 9: e00188.
- [23] X. Meng, T. Luo, Y. N. Gao, Comparative analysis on thermal performance of different wall insulation forms under the air-conditioning intermittent operation in summer. *Applied Thermal Engineering*, 2018, 130: 429-438.

- [24] L. Zhang, T. Luo, X. Meng, Effect of the thermal insulation layer location on wall dynamic thermal response rate under the air-conditioning intermittent operation. *Case studies in thermal engineering*, 2017, 10: 79-85.
- [25] N. Daouas. A study on optimum insulation thickness in walls and energy savings in Tunisian buildings based on analytical calculation of cooling and heating transmission loads. *Applied Energy*, 2011, 88(1): 156-164.
- [26] X. Wang, Energy Efficiency of Wall in Hot Summer and Cold Winter Zone. *Building Energy Efficiency*, 2014, 42(5): 62-65.
- [27] Ozel M. Cost analysis for optimum thicknesses and environmental impacts of different insulation materials. *Energy & Buildings*, 2012; 49(Jun.), 552-559. doi: <https://doi.org/10.1016/j.enbuild.2012.03.002>.
- [28] N.A. Kurekci, Determination of optimum insulation thickness for building walls by using heating and cooling degree-day values of all Turkey's provincial centers, *Energy and Buildings*. 118 (2016): 197-213. <https://doi.org/10.1016/j.enbuild.2016.03.004>
- [29] L. Derradji, K. Imessad, M. Amara, F.B. Errebai, A study on residential energy requirement and the effect of the glazing on the optimum insulation thickness, *Applied Thermal Engineering*. 112 (2017): 975-985. <http://dx.doi.org/10.1016/j.applthermaleng.2016.10.116>
- [30] B. Rosti, A. Omidvar, N. Monghasemi, Optimal insulation thickness of common classic and modern exterior walls in different climate zones of Iran, *Journal of Building Engineering*. 27 (2020): 100954. <https://doi.org/10.1016/j.jobbe.2019.100954>
- [31] A.M. Raimundo, N.B. Saraiva, A.V.M. Oliveira, Thermal insulation cost optimality of opaque constructive solutions of buildings under Portuguese temperate climate, *Building and Environment*. 182 (2020): 107107. <https://doi.org/10.1016/j.buildenv.2020.107107>
- [32] D. D. Agostino, F. De. Rossi, M. Marigliano, C. Marino, F. Minichiello, Evaluation of the optimal thermal insulation thickness for an office building in different climates by means of the basic and modified "cost-optimal" methodology. *Journal of Building Engineering*, 24 (2019): 100743. <https://doi.org/10.1016/j.jobbe.2019.100743>
- [33] J. Yu, C. Yang, L. Tian, D. Liao, A study on optimum insulation thicknesses of external walls in hot summer and cold winter zone of China, *applied energy*. 86.11 (2009): 2520-2529. <https://doi.org/10.1016/j.apenergy.2009.03.010>
- [34] X. Liu, Y. Chen, H. Ge, P. Fazio, G. Chen, X. Guo, Determination of optimum insulation thickness for building walls with moisture transfer in hot summer and cold winter zone of China, *Energy and Buildings*. 109 (2015): 361-368. <https://doi.org/10.1016/j.proeng.2017.10.153>
- [35] Y. Geng, X. Han, H. Zhang, L. Shi, Optimization and cost analysis of thickness of vacuum insulation panel for structural insulating panel buildings in cold climates, *Journal of Building*

- Engineering. 33 (2021): 101853. <https://doi.org/10.1016/j.jobe.2020.101853>
- [36] R.A. Kishore, M.V.A. Bianchi, C. Booten, J. Vidal, R. Jackson, Parametric and sensitivity analysis of a PCM-integrated wall for optimal thermal load modulation in lightweight buildings, *Applied Thermal Engineering*. 187 (2021) 116568. doi: <https://doi.org/10.1016/j.applthermaleng.2021.116568>
- [37] K. Faraj, M. Khaled, J. Faraj, F. Hachem, C. Castelain, A review on phase change materials for thermal energy storage in buildings: Heating and hybrid applications, *Journal of Energy Storage*. 33 (2021) 101913. doi: <https://doi.org/10.1016/j.est.2020.101913>
- [38] Y. Li, N. Nord, Q. Xiao, T. Tereshchenko, Building heating applications with phase change material: A comprehensive review, *Journal of Energy Storage*. 31 (2020) 101634. doi: <https://doi.org/10.1016/j.est.2020.101634>
- [39] N. Soares, A.R. Gaspar, P. Santos, J.J. Costa, Multi-dimensional optimization of the incorporation of PCM-drywalls in lightweight steel-framed residential buildings in different climates, *Energy and Buildings*. 70 (2014) 411-421. doi: <http://dx.doi.org/10.1016/j.enbuild.2013.11.072>
- [40] E. Tunçbilek, M. Arıcı, Michal. Krajčík, S. Nižetić, H. Karabay, Thermal performance based optimization of an office wall containing PCM under intermittent cooling operation, *Applied Thermal Engineering*. 179 (2020) 115750. doi: <https://doi.org/10.1016/j.applthermaleng.2020.115750>
- [41] B. Nghana, F. Tariku, Phase change material's (PCM) impacts on the energy performance and thermal comfort of buildings in a mild climate, *Building and Environment*. 99 (2016) 221-238. doi: <http://dx.doi.org/10.1016/j.buildenv.2016.01.023>
- [42] Y. R. Li, J. Zhou, E. S. Long, Experimental study on thermal performance improvement of building envelopes by integrating with phase change material in an intermittently heated room. *Sustainable cities and society*, 2018, 38: 607-615.
- [43] Y. R. Li, Y. Wang, X. Meng, Research on indoor thermal environment improvement of lightweight building integrated with phase change material under different climate conditions. *Procedia Engineering*, 2015, 121: 1628-1634.
- [44] Y. R. Li, Y. Wang, X. Meng, Research on thermal performance improvement of lightweight buildings by integrating with phase change material under different climate conditions. *Science and Technology for the Built Environment*, 2017, 23(2): 285-295.
- [45] B. A. Young, G. Falzone, Z. Wei, Reduced-scale experiments to evaluate performance of composite building envelopes containing phase change materials. *Construction and Building Materials*, 2018, 162: 584-595.
- [46] X. Meng, J. F. Du, Y. N. Gao, Effect of inner decoration coating on inner surface temperatures and heat flows under air-conditioning intermittent operation. *Case Studies in Thermal*

- Engineering, 2019, 14: 100503.
- [47] D. Zhou, P. Eames, Phase Change Material Wallboard (PCMW) melting temperature optimisation for passive indoor temperature control, *Renewable Energy*. 139 (2019) 507-514. doi: <https://doi.org/10.1016/j.renene.2019.02.109>
- [48] Z. X. Li, A. A. Al-Rashed, M. Rostamzadeh, R. Kalbasi, A. Shahsavari, M. Afrand, Heat transfer reduction in buildings by embedding phase change material in multi-layer walls: Effects of repositioning, thermophysical properties and thickness of PCM, *Energy Conversion and Management*. 195 (2019) 43-56. doi: <https://doi.org/10.1016/j.enconman.2019.04.075>
- [49] J. Xie, W. Wang, J. Liu, Song Pan, Thermal performance analysis of PCM wallboards for building application based on numerical simulation, *Solar Energy*. 162 (2018) 533-540. doi: <https://doi.org/10.1016/j.solener.2018.01.069>
- [50] H. Wang, W. Lu, Z. Wu, G. Zhang. Parametric analysis of applying PCM wallboards for energy saving in high-rise lightweight buildings in Shanghai, *Renewable Energy*. 145 (2020) 52-64. doi: <https://doi.org/10.1016/j.renene.2019.05.124>
- [51] Z. Liu, J. Hou, X. Meng, B.J. Dewancker, A numerical study on the effect of phase-change material (PCM) parameters on the thermal performance of lightweight building walls, *Case Studies in Construction Materials*. 15 (2021) e00758. doi: <https://doi.org/10.1016/j.cscm.2021.e00758>
- [52] Q. Al-Yasiri, M. Szabó, Incorporation of phase change materials into building envelope for thermal comfort and energy saving: A comprehensive analysis, *Journal of Building Engineering*. 36 (2021) 102122. doi: <https://doi.org/10.1016/j.jobe.2020.102122>
- [53] X. Jin, M.A. Medina, X. Zhang, Numerical analysis for the optimal location of a thin PCM layer in frame walls, *Applied Thermal Engineering*. 103 (2016) 1057-1063. doi: <http://dx.doi.org/10.1016/j.applthermaleng.2016.04.056>
- [54] A. Vukadinović, J. Radosavljević, A. Đorđević, Energy performance impact of using phase-change materials in thermal storage walls of detached residential buildings with a sunspace, *Solar Energy*. 206 (2020) 228-244. doi: <https://doi.org/10.1016/j.solener.2020.06.008>
- [55] Z. Liu, J. Hou, Y. Huang, J. Zhang, X. Meng, B. J. Dewancker, Influence of phase change material (PCM) parameters on the thermal performance of lightweight building walls with different thermal resistances, *Case Studies in Thermal Engineering*. 31 (2022) 101844. doi: <https://doi.org/10.1016/j.csite.2022.101844>
- [56] K. Saafi, N. Daouas, Energy and cost efficiency of phase change materials integrated in building envelopes under Tunisia Mediterranean climate, *Energy*. 187 (2019) 115987. doi: <https://doi.org/10.1016/j.energy.2019.115987>
- [57] X. Mi, R. Liu, H. Cui, S. A. Memon, F. Xing, Y. Lo, Energy and economic analysis of building integrated with PCM in different cities of China, *Applied Energy*. 175 (2016) 324-336. doi:

- <https://doi.org/10.1016/j.apenergy.2016.05.032>
- [58] F. Souayfane, P. H. Biwole, F. Fardoun, P. Achard, Energy performance and economic analysis of a TIM-PCM wall under different climates, *Energy*. 169 (2019) 1274-1291. doi: <https://doi.org/10.1016/j.energy.2018.12.116>
- [59] J. Hou, T. Zhang, Z. Liu, L. Zhang, H. Fukuda, Application evaluation of passive energy-saving strategies in exterior envelopes for rural traditional dwellings in northeast of Sichuan hills, China, *International Journal of Low-Carbon Technologies*. 17 (2022) 342-355. <https://doi.org/10.1093/ijlct/ctac007>
- [60] J. Hou, T. Zhang, Z. Liu, C. Hou, H. Fukuda, A study on influencing factors of optimum insulation thickness of exterior walls for rural traditional dwellings in northeast of Sichuan hills, China, *Case Studies in Construction Materials*. 16 (2022) e01033. doi: <https://doi.org/10.1016/j.cscm.2022.e01033>
- [61] X. Liu, *Engineering Economy (3rd Edition)*, China Architecture & Building Press, Beijing, 2015.
- [62] Lin Y, Zhao L, Yang W, Hao X, Li C. A review on research and development of passive building in China. *Journal of Building Engineering*, 2021; 42: 102509. doi: <https://doi.org/10.1016/j.jobe.2021.102509>.
- [63] J. Liu. *Building Physics (4th Edition)*. China Architecture & Building Press, Beijing, 2009.
- [64] Si P, Lv Y, Rong X, Shi L, Yan J, Wang X. An innovative building envelope with variable thermal performance for passive heating systems. *Applied Energy*, 2020; 269: 115175. doi: <https://doi.org/10.1016/j.apenergy.2020.115175>.
- [65] Zhang L, Hou Y, Liu Z, Du J, Xu L, Zhang G, Shi L. Trombe wall for a residential building in Sichuan-Tibet alpine valley – a case study. *Renewable Energy*, 2020; 156: 31–46. doi: <https://doi.org/10.1016/j.renene.2020.04.067>.
- [66] Hou J (2019). Optimization of indoor thermal environment in winter for traditional Tibetan dwellings in the Sichuan Northwestern Plateau. Master Dissertation, Sichuan Agricultural University, China. doi:<https://doi.org/10.27345/d.cnki.gsnnyu.2019.000693>.
- [67] Simes N, Manaia M, Simes I. Energy performance of solar and trombe walls in mediterranean climates. *Energy*, 2021; 121197.
- [68] Bevilacqua P, Benevento F, Bruno R, Arcuri N. Are trombe walls suitable passive systems for the reduction of the yearly building energy requirements?. *Energy*, 2019; 185, 554-566.
- [69] Wang W, Yuan M, Li Y, Li C. Numerical Investigation on the Impact of an On-top Sunspace Passive Heating Approach for Typical Rural Buildings in Northern China. *Solar Energy*, 2019; 186: 300–310. doi: <https://doi.org/10.1016/j.solener.2019.05.013>.
- [70] Long L, Ye H, Liu M. A new insight into opaque envelopes in a passive solar house: properties

and roles. *Applied Energy*, 2020; 183(dec.1), 685-699.

- [71] Bl A, Ly B, Min Z, Yao C, W A, Zw A. Energy consumption pattern and indoor thermal environment of residential building in rural china. *Energy and Built Environment*, 2020; 1(3), 327-336.

CHAPTER 2. LITERATURE REVIEW

Chapter 3

Methodology

CHAPTER 3. METHODOLOGY

Chapter 3. Methodology

3. Methodology	3-1
3.1 Introduction.....	3-1
3.2 Filed test experiment in this study region	3-1
3.2.1 Description of the survey location	3-1
3.2.2 Description of the experiment.....	3-2
3.3 Establishment of the base model.....	3-5
3.3.1 Architecture characteristic of traditional dwellings in the study region	3-5
3.3.2 Description of the base model.....	3-7
3.4 Numerical simulation.....	3-9
3.4.1 Description of simulation program	3-9
3.4.2 Mathematical description of heat balance process for traditional materials.....	3-9
3.4.3 Mathematical description of conduction through the wall	3-10
3.4.4 Mathematical description of heat balance process for phase change materials..	3-12
3.5 Orthogonal experiment design (OED) and analysis of variance (AVOVA).....	3-13
3.6 Dynamic investment payback period model (DPP)	3-14
3.7 Summary	3-15
Appendix A. Standard orthogonal array of $L_{27} (3^{13})$	3-16
Reference	3-17

CHAPTER 3. METHODOLOGY

3. Methodology

3.1 Introduction

We combine field investigation, numerical simulation, orthogonal design test, and dynamic investment payback period method to evaluate the effectiveness and economical potential of the application of varied energy-saving strategies. In this paper, we aim to introduce all of these methods which are used in the next chapters, and meanwhile, in order to deeply comprehend the current thermal environment and thermal performance of traditional dwellings in this study region, field investigation information and the base model which will be used to analyze energy-saving strategies are also described.

In subsection 3.2, we introduce the location and other brief information of the investigation village, and the detailed construction information of an actual dwelling which was tested is depicted. In subsection 3.3, we explain the establishment process of the base model, which is regarded as the representative model for this study region and will be used in Chapter 4 to Chapter 8 to analyze related energy-saving strategies. In subsection 3.4, we present the brief information and related formulae of the simulation program (EnergyPlus). In subsection 3.5, we explain the detailed process of designing an orthogonal test and the thorough calculation process of analysis of variance (AVOVA). In subsection 3.6, we clarify the calculation method for evaluating the dynamic investment payback period (DPP) and economic benefits over a certain period, which are crucial to assess the economic potential of an energy-saving strategies. Furthermore, subsection 3.7 is the summary part of this chapter.

3.2 Filed test experiment in this study region

3.2.1 Description of the survey location

The Traditional Village Catalogue in China is a national project, which aims to preserve and inherit the traditional architecture culture. The villages selected for the Traditional Village Catalogue have inherited the characteristics of local traditional architecture culture in a great extent, including the building material, building structure, building form and construction. Hence, we carried out a detailed investigation in Liyuanba Village, which was included in the third batch of Traditional Village Catalogue in China in 2014, moreover, the indoor thermal environment and the current thermal performance of the exterior envelopes of the actual traditional dwelling was recorded, and it can help us comprehend the current thermal condition of the local traditional dwellings, and thus some appropriate energy-saving strategies can be put forward and be evaluated based on the actual current situation.

Liyuanba Village is under the jurisdiction of Bazhong City, Sichuan Province, located deep in the Daba Mountains and Figure 3-1 displays its location. As Table 3-1 shown, Bazhong City is located in the northeast corner of Sichuan Province, bordering Shaanxi Province to the north. The city is a typical basin-perimeter mountainous area, located at the southern foot of the Micang Mountains in the Daba Mountain System, with a high north to low south terrain, sloping from north to south. Liyuanba Village of Naixi Township is located in the northwestern part of the township, 3.3

kilometers from the township government, with an area of 8.9 square kilometers and 5 agricultural cooperatives. The number of existing households is 310, with a total population of more than 1,300. Currently, Liyuanba Village has 58 sets of wooden courtyards, built on the mountain, staggered, hidden in the jungle and greenery, including 30 sets of buildings in the 1970s and 1980s, 28 sets of buildings in the Ming and Qing dynasties (5 sets of courtyards, 23 sets of triple courtyards, 20 sets in good condition, and 8 sets in disrepair). Only the foundation and the giant stone lion remain of the Ma clan ancestral hall and theater building. The village has more than 20 ancient tombs of magnificent scale and exquisite carvings, including three Southern Song rock tombs (tombs built by cutting holes in the stone walls), and there are stone inscriptions documented that the tomb was built in the second year of Baoqing (1226 AD). The "Tielincheng" monument at the back of Liyuanba, according to inscriptions, was built in the Ming Dynasty, reinforced and repaired twice during the Jiaqing and Xianfeng years in the Qing Dynasty, and was an important military base of the ancient road of Micang.

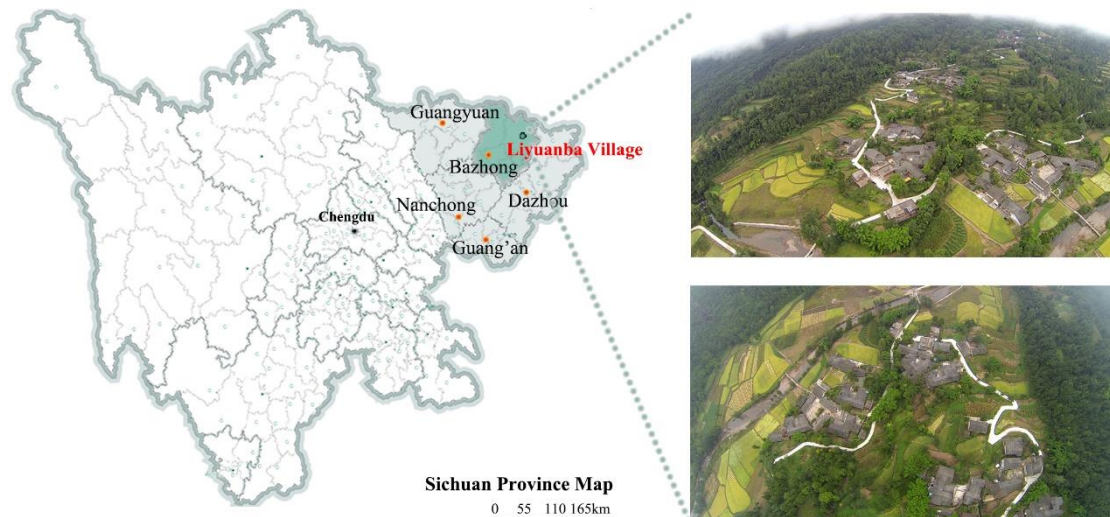


Figure 3-1. Location diagram and aerial overhead view of Liyuanba Village.

3.2.2 Description of the experiment

Figure 3-2 is the general plan of Liyuanba Village, and we can notice that the building orientation of traditional dwellings in Liyuanba Village is not certainly facing south. The main reason is that there is almost hilly or mountainous terrain and there is limited flat ground for people to construct, therefore the orientation of dwellings always follows the topography, which is a common phenomenon in northeast of Sichuan hills, China. In addition, we can see that the plan form of dwellings in this village include quadrangle, triplex, L-shape, - - shape. The main structure of these traditional dwellings in this village is the typical southwestern Chinese wood frame structure, i.e., the wooden structure is used as the building support structure, and the walls only play the role of enclosure, not load-bearing. The building materials are locally sourced, with wood as the doors and windows, and the walls are often rammed earth walls or bamboo and gabion clay walls. Additionally, the tested building is located in the southwest corner of the village, with a quadrangle layout and

two families now living there.

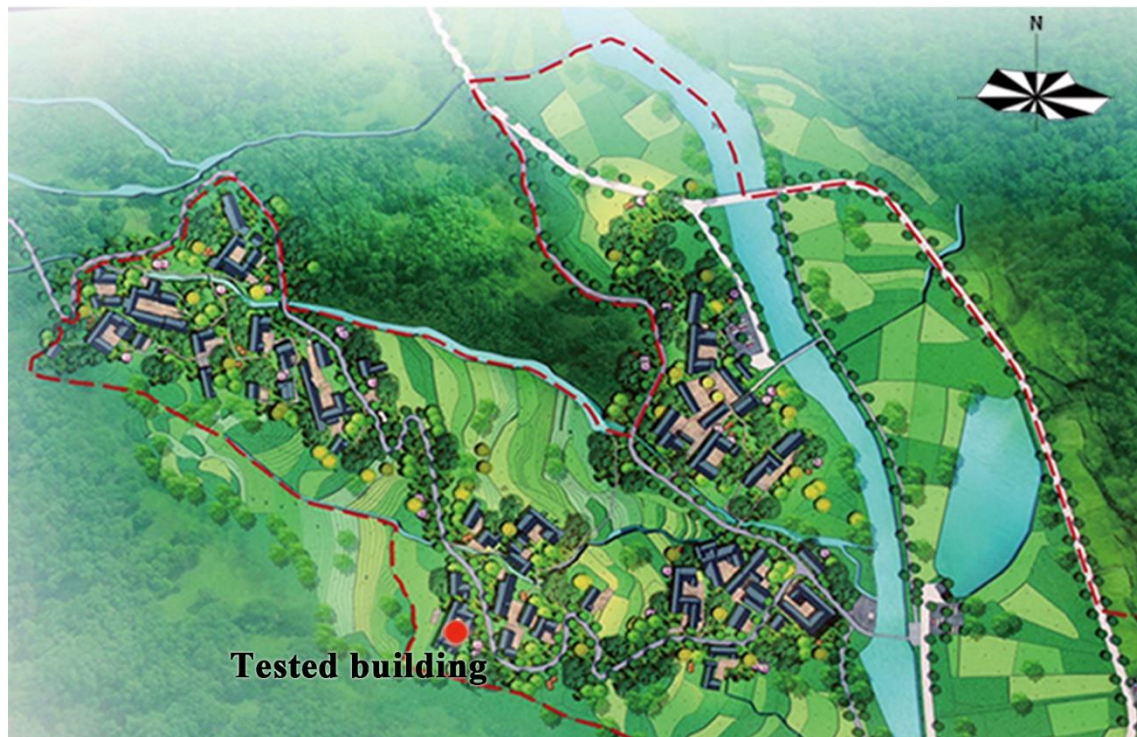


Figure 3-2. General plan of Liyuanba Village.

To fully comprehend the local indoor thermal environment situation, field measurement work was carried out in an actual dwelling located in Liyuanba Village, Tongjiang county, Bazhong. Figure 3-3 displays the floor plan and photographs of the tested building. The floor plan form of this building is complex, and its north has about -60° of angle from the actual north, in other words, the building faces around southeast. Currently, there are two families live in this building. The material of exterior walls is clay or clay mixed with slender bamboo strips. The windows are ordinary single-layer glass with wooden frames. The roof is double-sloped to facilitate drainage, and the roof is covered with small tiles and no roof board, and moreover, the width of the eave projection is generally 0.8m, which can provide shading for the building. The actual tested building is one floor, including the living room, bedroom, kitchen, and storeroom and the floor height is from 2.8m to 3m. Above these main rooms, there is the additional attic as a storage space, whose floor height is between 0.6m to 0.8m. In the past, residents often stored grains, firewood, or farm implements in the attic, but currently, it is underutilized.

Two 72-hour continuous measurement work were accomplished during January 13 to 16, 2017, and July 26 to 29. During the measurement period, the indoor and outdoor air temperature have been automatically recorded by the Testo175 data logger every 30 minutes. The temperature measurement range of the data recorder is $-20-50^\circ\text{C}$, and the measurement accuracy is $\pm 0.4^\circ\text{C}$. Meanwhile, the surface temperature of exterior walls also were be recorded by Testo830 Infrared thermometer (manual record) and JTNT-A/C multi-channel temperature and heat flow tester (auto

record), and more detailed are listed in Table 3-1.

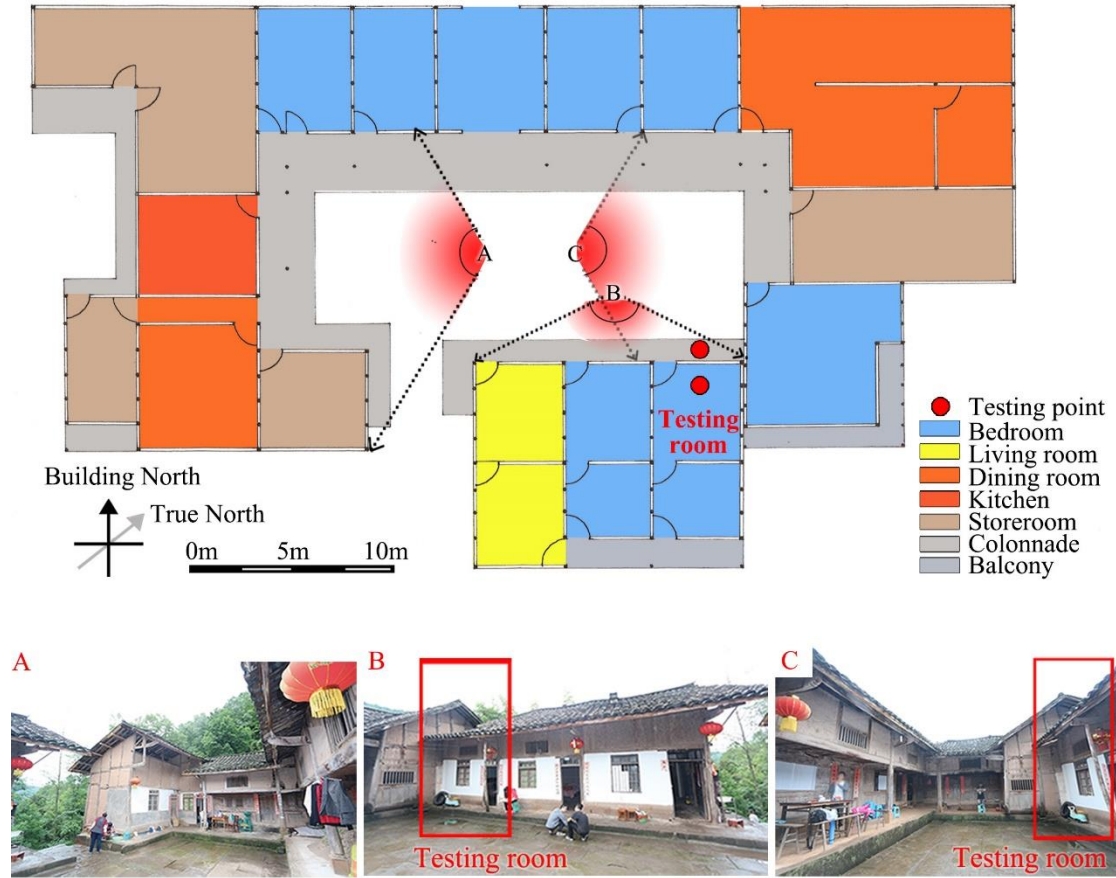


Figure 3-3. Floor plan and photographs of the tested building.

Table 3-1 Information of the testing equipment.

Testing equipment	Testing parameter	Effective range of testing equipment	Testing accuracy	Record method
Testo175 Data loggers	Air temperature	-20-50°C	±0.4°C	Auto
	Relative humidity	0-100%	±2% RH	
Testo830 Infrared thermometer	Surface temperature	0.1-400°C -30-0°C	±1.5°C ±2°C	Manual
JTNT-A/C multi-channel temperature and heat flow tester	Surface temperature	-20-85°C	±0.5°C	Auto

Figure 3-4 shows the arrangement of testing points. One Testo175 data logger is arranged in the testing room, which is used as a bedroom, another one is arranged outdoor. And both devices are 1.5meter high from the ground. P3, P4, P5, P5, P7 are testing points for inside surfaces of exterior

walls, while P8, P9, P10, P11, and P12 are testing points for outside surfaces of exterior wall. Furthermore, these recorded results are thoroughly analyzed in Chapter 4.

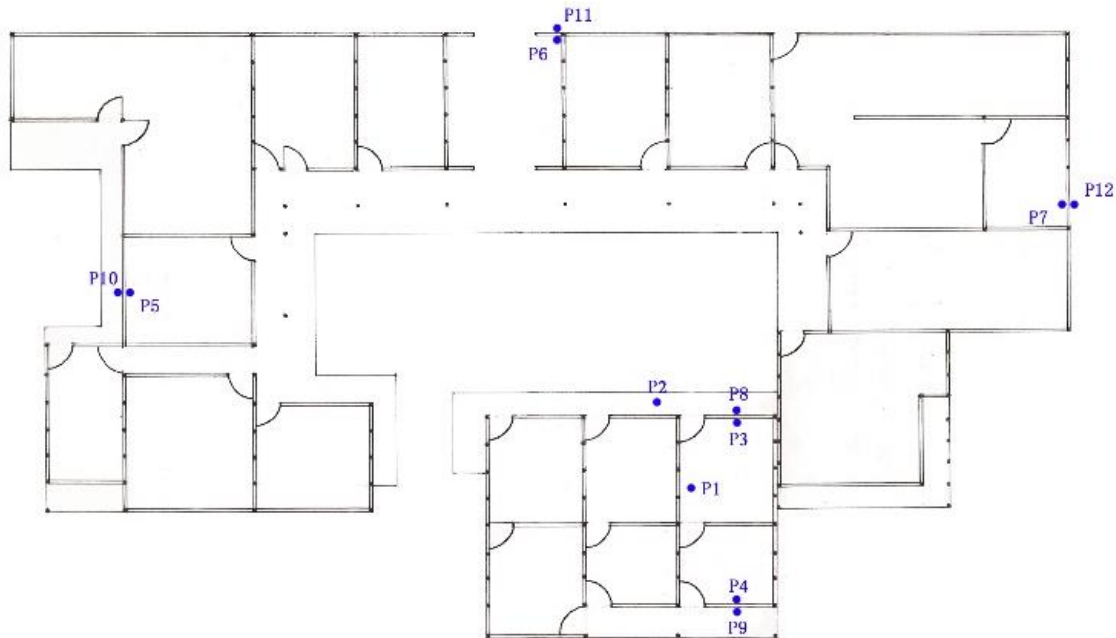


Figure 3-4. Arrangement of testing points (floor plan diagram).











3.3 Establishment of the base model

3.3.1 Architecture characteristic of traditional dwellings in the study region

Within the same climate background and natural resource conditions, the traditional dwellings in northeast Sichuan hills have analogous architectural forms and structures, therefore, we establish a base model according to the common architecture characteristics and construction features of traditional dwellings in this study region, and this base model is regarded as a representative building for this region, and it will be used to evaluate the energy-saving strategies in Chapter 4 to Chapter 8. Considering that the situation of traditional villages can reflect the general condition of the existing traditional dwellings in this region, thus more than 10 traditional villages located in Bazhong and Dazhou were investigated, and the related representative photographs which can show architecture features of local traditional dwellings are summarized in Table 3-2 and Table 3-3.


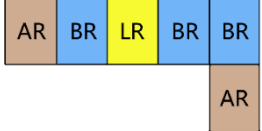
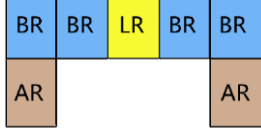
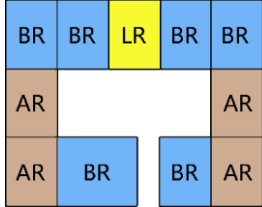








In Table 3-2, the architecture characteristics of traditional dwellings in northeast of Sichuan hills, China are summarized. In this region, the main building structure is column and tie construction, using wooden columns as building support structures. And local clay, wood and stone are the most common materials for envelop construction. Usually, the local dwellings are 1-2 stories, with additional attic as a storage space. Windows and doors are mainly made of wood, supplemented by carved decoration. In recent years, some residents have also installed glass on wooden window frames or updated their windows to aluminum windows.

Table 3-2 Architecture characteristics of traditional dwellings in northeast of Sichuan hills, China.

Structure	Material	Building stoery	Roof structure	Door and window
				
				

In Table 3-3, the floor plan form of local dwellings is classified into four types. As a rule, the number of family members determines the floor plan form. If there is only one family, Type A or Type B generally be utilized. If there are two or more families live together, they would choose Type B, Type C or Type D. For the local residents, the house needs to offer the living room, the bedroom, kitchen and storeroom. On the whole, the width of each room is in the range of 3.9-4.8m, and the depths are 3.9-6m.

Table 3-3 Features of building floor plan of traditional dwellings in northeast of Sichuan hills, China.

Type A	Type B	Type C	Type D
			
			
			

3.3.2 Description of the base model

The dimensional information of the base model is shown in Figure 3-5, Figure 3-6, and Figure 3-7. Considering that this study is concerned with the performance of exterior envelope while the courtyard pattern is not the focus of this paper, and in order to diminish the impact caused by the complexity of the building model, the floor plan form of the base model applies the simplest form (Type A) of local rural traditional dwellings shown in Table 3-3.

Figure 3-5 displays the floor plan and room functions of the base model. It has five rooms, and the number and functions of these rooms can meet the daily needs of local residents. The width of the living room is 4.8m, the rest of the rooms are 4.5m, respectively. The depth of all of the rooms is 6 m. Additionally, the base building faces south.

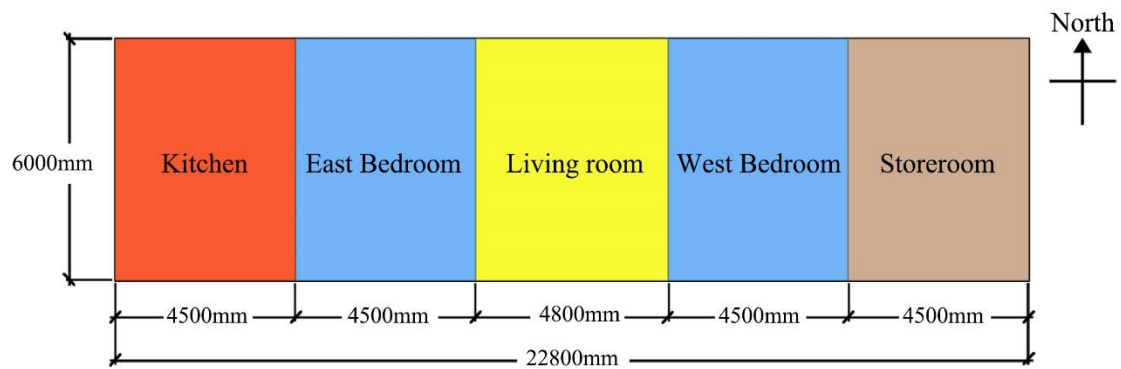


Figure 3-5. Floor plan of the base model.

Figure 3-6 is the front elevation of the base model, it displays that the floor height is 3m, and the maximum height of the attic is 2.1m, which be shown more clear in Figure 3-7(a). The window size is 0.9m × 1.2m, which is commonly used for local dwellings. In accordance with the custom of local dwellings, windows are set only on the south façade.

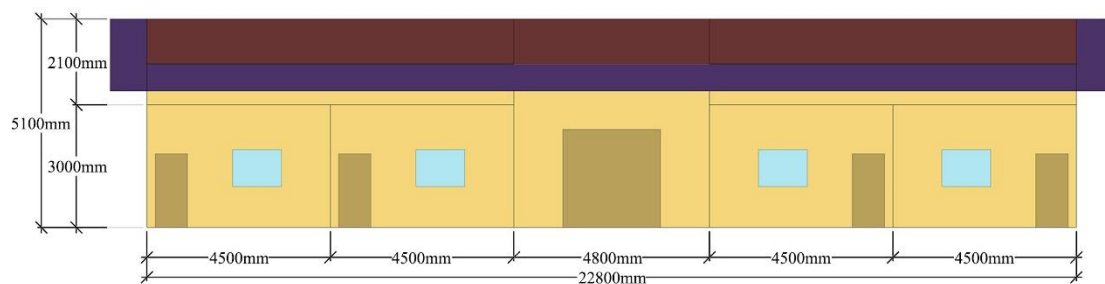


Figure 3-6. Front elevation of the base model.

According to Figure 3-7(a), we can better comprehend the construction of the representative model. The construction form of attic and the projected width of the eaves (1800mm) are consistent with the actual common situation. Furthermore, the construction material and construction for of

the exterior envelopes, including roof, exterior walls, and ground are drawn in Figure 3-7 (b) to (d), respectively.

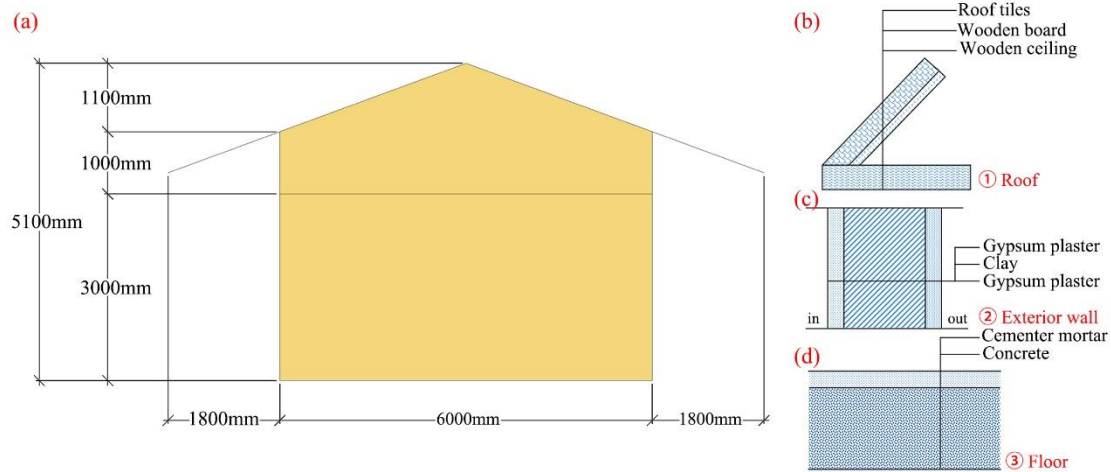


Figure 3-7. (a) Side elevation of the base model; (b) Diagram of roof construction; (c) Diagram of exterior walls construction; (d) Diagram of floor construction.

Finally, the base model is established as its perspective view diagram is shown in Figure 3-8. In the following chapters, we will take this base model as the research object, and the energy-saving effects of some energy-saving strategies will be utilized in this base model, thereby the corresponding effects will be evaluated and help us determine energy-saving strategies that are some appropriate for traditional dwellings in this study region.

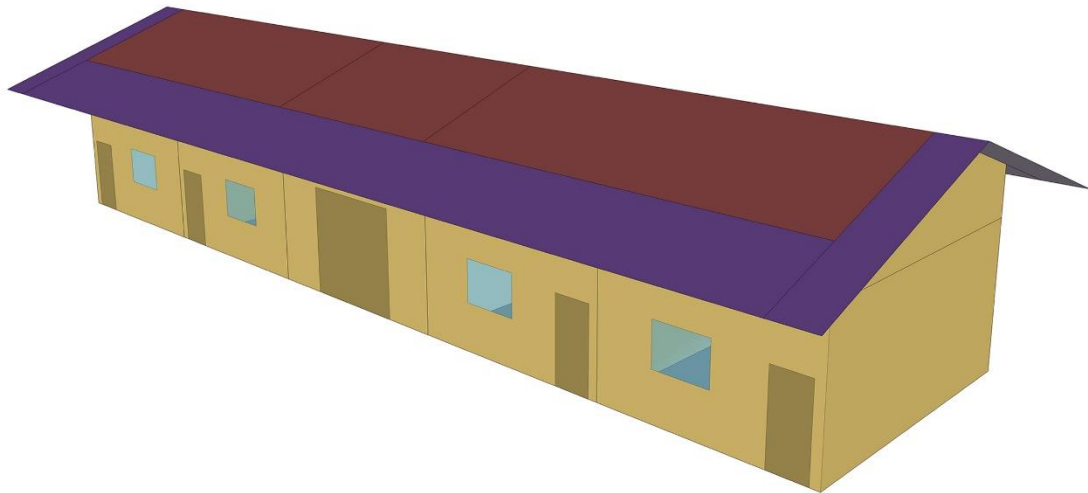


Figure 3-8 Perspective view of the base model.

3.4 Numerical simulation

3.4.1 Description of simulation program

The results of energy consumption predicted by the dynamic simulation program are more accurate compared with the degree-day method due to it adopts time-by-time weather data as the meteorological boundary while the average daily outdoor temperature is used to calculate the difference between indoor and outdoor temperatures in the degree-day method. Commonly used building energy consumption dynamic simulation programs involve DOE-2, EnergyPlus, TRNSYS, DeST, and DesignBuilder. EnergyPlus which is a whole building energy simulation program and was developed by the U.S. Department of Energy (DOE) and Lawrence Berkeley National Laboratory in 1996, was used in this paper to dynamically simulate the building performance under the optimum insulation thickness and obtain the annual cooling and heating load results to access the energy-saving and economic benefits. It applies the conduction transfer functions (CTF) method to compute the thermal conduction of envelope [1] and the airflow pattern can be demonstrated, thus airflow between zones and airflow due to mechanically-induced or natural ventilation can be simulated [2]. In addition, WINDOWS 5 algorithms are employed for calculating the thermal conduction and solar heat gain of the window system [3]. Ultimately, varied data can be outputted, such as indoor air temperature, heating, cooling, and lighting consumption.

3.4.2 Mathematical description of heat balance process for traditional materials

The core of the calculation in EnergyPlus is the basic heat balance principle, and the heating and cooling loads can be predicted by the predictive system energy balance method [4]. The calculation process is as follows.

Firstly, the heat balance on the zone air can be described as Eq. 3-1:

$$C_z \frac{dT_z}{dt} = \sum_{i=1}^{N_{si}} \dot{Q}_i + \sum_{i=1}^{N_{surfaces}} h_i A_i (T_{si} - T_z) + \sum_{i=1}^{N_{zones}} \dot{m}_i C_p (T_{zi} - T_z) + \dot{m}_{inf} C_p (T_{\infty} - T_z) + \dot{Q}_{sys} \quad (3-1)$$

$$C_z = \rho_{air} C_p C_T \quad (3-2)$$

where,

$$\sum_{i=1}^{N_{si}} \dot{Q}_i = \text{sum of the convective internal loads;}$$

$$\sum_{i=1}^{N_{surfaces}} h_i A_i (T_{si} - T_z) = \text{the convective heat transfer from the zone surfaces;}$$

$$\dot{m}_{inf} C_p (T_{\infty} - T_z) = \text{heat transfer due to infiltration of outside air;}$$

$$\sum_{i=1}^{N_{zones}} \dot{m}_i C_p (T_{zi} - T_z) = \text{heat transfer due to interzone air mixing;}$$

\dot{Q}_{sys} = air systems output;

$C_z \frac{dT_z}{dt}$ = energy stored in zone air;

ρ_{air} = zone air density;

C_p = zone air specific heat;

C_T = sensible heat capacity multiplier.

If the air capacitance is neglected, the steady-state system output is:

$$-\dot{Q}_{sys} = \sum_{i=1}^{N_{sl}} \dot{Q}_i + \sum_{i=1}^{N_{surfaces}} h_i A_i (T_{si} - T_z) + \sum_{i=1}^{N_{zones}} \dot{m}_i C_p (T_{zi} - T_z) + \dot{m}_{inf} C_p (T_{\infty} - T_z) \quad (3-3)$$

The heating and cooling loads of zones can be satisfied by air systems to provide hot or cold air. Thus the system energy provided to the zone (\dot{Q}_{sys}) can be formulated from the difference between the enthalpy of supply air and that of air leaving the zone as Eq. 3-4:

$$\dot{Q}_{sys} = \dot{m}_{sys} C_p (T_{sup} - T_z) \quad (3-4)$$

If the air system has sufficient capacity (based on the desired zone air temperature) to meet the zone conditioning requirements, i.e., $\dot{Q}_{sys} = \dot{Q}_{load}$, then the heating and cooling loads (\dot{Q}_{load}) can be predicted by Eq. 3-5:

$$\dot{Q}_{load} = \sum_{i=1}^{N_{sl}} \dot{Q}_i + \sum_{i=1}^{N_{surfaces}} h_i A_i (T_{si} - T_z) + \sum_{i=1}^{N_{zones}} \dot{m}_i C_p (T_{zi} - T_z) + \dot{m}_{inf} C_p (T_{\infty} - T_z) \quad (3-5)$$

3.4.3 Mathematical description of conduction through the wall

The wall conduction process plays a significant role in the overall heat balance procedure since it links the outside and inside heat balance. The most basic time series solution is the response factor equation which relates the flux at one surface of an element to an infinite series of temperature histories at both sides as shown by Eq. 3-6:

$$\dot{q}_{ko}(t) = \sum_{j=0}^{\infty} X_j T_{o,t-j\delta} - \sum_{j=0}^{\infty} Y_j T_{i,t-j\delta} \quad (3-6)$$

where:

q'' = heat flux;

T = temperature;

i = the inside of the building element;

o = the outside of the building element;

t = the current time step;

X, Y = response factors.

Furthermore, Conduction Transfer Functions (CTFs) is embedded in EnergyPlus to depict the wall conduction process. And the general form is shown by the following equation:

$$q''_{ki}(t) = -Z_o T_{i,t} - \sum_{j=1}^{nz} Z_j T_{i,t-j\delta} + Y_o T_{o,t} + \sum_{j=1}^{nz} Y_j T_{o,t-j\delta} + \sum_{j=1}^{nq} \Phi_j q''_{ki,t-j\delta} \quad (3-7)$$

for the inside heat flux, and

$$q''_{ko}(t) = -Y_o T_{i,t} - \sum_{j=1}^{nz} Y_j T_{i,t-j\delta} + X_o T_{o,t} + \sum_{j=1}^{nz} X_j T_{o,t-j\delta} + \sum_{j=1}^{nq} \Phi_j q''_{ko,t-j\delta} \quad (3-8)$$

for the outside heat flux ($q'' = q / A$)

where:

X_j = outside CTF coefficient, $j = 0, 1, \dots, nz$;

Y_j = cross CTF coefficient, $j = 0, 1, \dots, nz$;

Φ_j = flux CTF coefficient, $j = 1, 2, \dots, nq$;

T_i = inside face temperature;

T_o = outside face temperature;

q''_{ko} = conduction heat flux on outside face;

q''_{ki} = conduction heat flux on inside face.

In addition, the subscript of the variables following the comma stands for the time period for the quantity in terms of the time step d . The first terms in the left series have been separated from the rest so that facilitated solving for the current temperature in the solution. The terms of nz and nq depend on the wall structure. These equations state that the heat flux at either face of the surface of any generic building element is linearly related to the current and some of the previous temperatures at both the interior and exterior surface as well as some of the previous flux values at the interior surface.

3.4.4 Mathematical description of heat balance process for phase change materials

The whole building energy simulation program, EnergyPlus, which was developed by the U.S. Department of Energy (DOE) and Lawrence Berkeley National Laboratory in 1996 is employed to simulate building energy consumption in this paper. It applies the conduction transfer functions (CTF) method to compute the thermal conduction of envelope [6]. This has all the usual restrictions of a transformation-based solution: constant properties, fixed values of some parameters, and do not produce results for the interior of the surface. As the energy analysis field moves toward simulating more advanced constructions, such as phase change materials (PCM), it becomes necessary to step back from transformations to more fundamental forms. Accordingly, a conduction finite difference (CondFD) solution algorithm has been incorporated into EnergyPlus.

$$C_p \rho \Delta x \frac{T_i^{j+1} - T_i^j}{\Delta t} = k_w \frac{(T_{i+1}^{j+1} - T_i^{j+1})}{\Delta x} + k_E \frac{(T_{i-1}^{j+1} - T_i^{j+1})}{\Delta x} \quad (3-9)$$

where:

C_p = specific heat of material, J/kg K;

ρ = density of material, kg/m³;

Δx = finite difference layer thickness, m;

Δt = calculation time step;

T = node temperature, °C;

i = node being modeled;

$i+1$ = adjacent node to interior of construction;

$i-1$ = adjacent node to exterior of construction;

$j+1$ = new time step;

j = previous time step.

k_w = thermal conductivity for interface between i node and $i+1$ node, W/(m K);

k_E = thermal conductivity for interface between i node and $i-1$ node, W/(m K).

The finite difference layer thickness (Δx) is determined by the space discretization constant (C), diffusivity of the material (a) and calculation time step (Δt). Additionally, C is basically the inverse of the Fourier Number, and the default value is 3 in the program [5].

$$\Delta x = \sqrt{C a \Delta t} \quad (3-10)$$

Because of the iteration scheme used for CondFD, the node enthalpies get updated each iteration,

and then they are used to develop a variable C_p if a phase change material is being simulated. This is done by including the following equation for C_p :

$$C_p = \frac{h_{i,new} - h_{i,old}}{T_{i,new} - T_{i,old}} \quad (3-11)$$

where h is the specific enthalpy, J/(kg K).

3.5 Orthogonal experiment design (OED) and analysis of variance (AVOVA)

The optimum thickness of insulation materials is affected by a variety of factors, so the multifactor experiment is required to quantify the impact degree of each factor on the optimum thickness. If the full factorial experiment design is employed, the number of the 11-factor with 3-level test is $3^{11}=177147$, which is difficult to implement due to the enormous number of tests. However, the orthogonal experiment design as a kind of fractional factorial experiment, can select representative points which are evenly distributed and can represent the overall situation from the full factorial experiment design, thus effectively reducing the number of tests [7-8].

The orthogonal array is the basis of the orthogonal test, and has the following two important properties [8]: The number of occurrences of different numbers in each column is equal; the number of occurrences of each ordered pair is equal when two numbers in any two columns are considered as an ordered pair in the same row. Influencing factors and their levels should be arranged according to the orthogonal array. It is usually expressed as $L_a(b^c)$, where L represents the orthogonal experimental design, a is the number of rows which represents the total number of trials, b represents the number of levels of factors, and c is the number of columns, which represents the number of factors. The impact degree of each influencing factor on the target value can be quantified by analysis of variance (ANOVA) and its calculation procedure is as follows [8].

Assuming that there are m factors are arranged in an orthogonal array, the total number of trials is n , and the results of the trials are x_1, x_2, \dots, x_n . Assuming that each factor has n_a levels and each level does a trials, then $n=an_a$. The square sum of the total deviation (S_T) and the degrees of the total freedom (f_T) can be expressed as Eqs. 3-12 and 3-13:

$$S_T = \sum_{k=1}^n x_k^2 - \frac{1}{n} \left(\sum_{k=1}^n x_k \right)^2 \quad (3-12)$$

$$f_T = n - 1 \quad (3-13)$$

Taking factor A as an example, Eq. 3-14, Eq. 3-15, and Eq. 3-16 calculate its sum of squares of the deviation (S_A) and the degrees of freedom (f_A). K_i in Eq. 3-15 denotes the sum of the results of the i th level in a trials of the factor. S_A reveals the difference in test results caused when the level of factor A changes, i.e., the effect of factor A on the test results. Further, the sum of squares of the deviation of other factors can be calculated in the same way.

$$S_A = \frac{1}{a} \sum_{i=1}^{n_a} K_i^2 - \frac{1}{n} \left(\sum_{k=1}^n x_k \right)^2 \quad (3-14)$$

$$K_i = \sum_{j=1}^a x_{ij} \quad (3-15)$$

$$f_A = n_a - 1 \quad (3-16)$$

Suppose S_F and f_F are the sum of the squares of the deviations and the sum of the degrees of freedom of all factors, then the squares of the deviations of the experimental errors (S_E) and its degrees of freedom (f_E) can be calculated by Eqs. 3-17 and 3-18:

$$S_E = S_T - S_F \quad (3-17)$$

$$f_E = f_T - f_F \quad (3-18)$$

Finally, F -value of each factor can be obtained by Eq. 3-19, Eq. 3-20, and Eq. 3-21, and the magnitude of this value reveals the degree of influence of each factor on the test results. Further, F -test can be carried out. Still take factor A as an example, give the test level (α) and find out its critical value (F_α) from the F distribution table, then compare the F -value of factor A (F_A) with the critical value (F_α). If $F_A > F_\alpha$, it means that factor A has a significant effect on the test results, and the greater the difference between these two values, the greater the significance of the factor.

$$MS_A = \frac{S_A}{a-1} \quad (3-19)$$

$$MS_E = \frac{S_E}{n-a} \quad (3-20)$$

$$F = \frac{MS_A}{MS_E} \quad (3-21)$$

3.6 Dynamic investment payback period model (DPP)

The dynamic investment payback period (DPP) model was used to calculate the payback period and the economic benefits of insulation materials based on the building energy consumption results obtained from EnergyPlus. Compared with the simple payback period (SPP), which is obtained directly by dividing the initial investment cost by the annual electricity cost savings [9-11], DPP takes into account the time value of money [11-12], expressing as $(P/F, i_0, t')$, so its result is more realistic compared with those of SPP. $(P/F, i_0, t')$ is calculated by Eq. 3-22, and it represents the present worth of the currency in the t^{th} year, while i_0 is the benchmark discount rate used to convert

future anticipated cash flow to present value. With the help of $(P/F, i_0, t')$, the cumulative discounted value of each year can be counted and the dynamic investment payback period (P_D) – the year when the cumulative discounted value becomes non-negative, is able to acquire by Eq. 3-23 [11].

$$(P/F, i_0, t') = \frac{1}{(1+i_0)^t} \quad (3-22)$$

$$P_D = T' - 1 + \frac{\left| \sum_{t=0}^{T'-1} (CI - CO)_t (P/F, i_0, t') \right|}{(CI - CO)_{T'} (P/F, i_0, T')} \quad (3-23)$$

Where P_D is the dynamic investment payback period, year; T' is the number of years with positive cumulative discounted value; t' is the number of the last year with negative cumulative discounted value; CI represents cash inflow, CNY/year, its value equals to annual saving electric charge; CO represents cash outflow, CNY/year, its value equals to the retrofit cost; P/F is present-value compound interest factor; i_0 is the benchmark discount rate, %, its value is 2.8% [13].

3.7 Summary

In this chapter, we introduce the investigation information, including the village and building situation and the testing information, these information can help us deeply comprehend the current thermal situation of the study region. Furthermore, we clarify the detailed process of each method, and in the next chapters, these methods will be utilized and their calculation process will not be explained.

Appendix A. Standard orthogonal array of $L_{27}(3^{13})$

No.	1	2	3	4	5	6	7	8	9	10	11	12	13
1	1	1	1	1	1	1	1	1	1	1	1	1	1
2	1	1	1	1	2	2	2	2	2	2	2	2	2
3	1	1	1	1	2	3	3	3	3	3	3	3	3
4	1	2	2	2	1	1	1	2	2	2	3	3	3
5	1	2	2	2	2	2	2	3	3	3	1	1	1
6	1	2	2	2	3	3	3	1	1	1	2	2	2
7	1	3	3	3	1	1	1	3	3	3	2	2	2
8	1	3	3	3	2	2	2	1	1	1	3	3	3
9	1	3	3	3	3	3	3	2	2	2	1	1	1
10	2	1	2	3	1	2	3	1	2	3	1	2	3
11	2	1	2	3	2	3	1	2	3	1	2	3	1
12	2	1	2	3	3	1	2	3	1	2	3	1	2
13	2	2	3	1	1	2	3	2	3	1	3	1	2
14	2	2	3	1	2	3	1	3	1	2	1	2	3
15	2	2	3	1	3	1	2	1	2	3	2	3	1
16	2	3	1	2	1	2	3	3	1	2	2	3	1
17	2	3	1	2	2	3	1	1	2	3	3	1	2
18	2	3	1	2	3	1	2	2	3	1	1	2	3
19	3	1	3	2	1	3	2	1	3	2	1	3	2
20	3	1	3	2	2	1	3	2	1	3	2	1	3
21	3	1	3	2	3	2	1	3	2	1	3	2	1
22	3	2	1	3	1	3	2	2	1	3	3	2	1
23	3	2	1	3	2	1	3	3	2	1	1	3	2
24	3	2	1	3	3	2	1	1	3	2	2	1	3
25	3	3	2	1	1	3	2	3	2	1	2	1	3
26	3	3	2	1	2	1	3	1	3	2	3	2	1
27	3	3	2	1	3	2	1	2	1	3	1	3	2

Reference

- [1] M.K. Urbikain, M.G. Davies, A frequency domain estimation of wall conduction transfer function coefficients, *Energy & Buildings*. 51. AUG. (2012):191-202. <https://doi.org/10.1016/j.enbuild.2012.05.005>.
- [2] U.S. Department of Energy, EnergyPlus™ version 8.7 documentation input output reference, 2016.
- [3] D.B. Crawley, L.K. Lawrie, F.C. Winkelmann, W.F. Buhl, Y.J. Huang, C.O. Pedersen, R.K. Strand, R.J. Liesen, D.E. Fisher, M.J. Witte, Energyplus: creating a new-generation building energy simulation program, *Energy and Buildings*. 33.4(2001):319-331. [https://doi.org/10.1016/S0378-7788\(00\)00114-6](https://doi.org/10.1016/S0378-7788(00)00114-6).
- [4] Sichuan Statistical Yearbook. 2020. Available at <http://tjj.sc.gov.cn/tjnj/cs/2020/zk/indexch.htm>.
- [5] U.S. Department of Energy, EnergyPlus™ Version 22.1.0 Documentation Engineering Reference, 2022.
- [6] Urbikain M Karmele, Davies M G. A frequency domain estimation of wall conduction transfer function coefficients. *Energy & Buildings*, 2012; 51: 191–202. doi: <https://doi.org/10.1016/j.enbuild.2012.05.005>.
- [7] J. Zhu, D.A.S. Chew, S. Lv, W. Wu, Optimization method for building envelope design to minimize carbon emissions of building operational energy consumption using orthogonal experimental design (OED), *Habitat International*. 37 (2013): 148-154. <https://doi.org/10.1016/j.habitatint.2011.12.006>.
- [8] K. Chen, Design and Analysis of Experiments (2nd Edition), Tsinghua University Press, Beijing, 2005.
- [9] A.A. Serageldin, A. Abdeen, M.S. Ahmed, A. Radwan, S. Ookawara, Solar chimney combined with earth to-air heat exchanger for passive cooling of residential buildings in hot areas, *Solar Energy*. 206(2020):145-162. <https://doi.org/10.1016/j.solener.2020.05.102>
- [10] H. Huang, W.I.B.W.M. Nazi, Y. Yu, Y. Wang, Energy performance of a high-rise residential building retrofitted to passive building standard – A case study, *Applied Thermal Engineering*. 181 (2020): 115902. <https://doi.org/10.1016/j.applthermaleng.2020.115902>
- [11] X. Liu, Engineering Economy (3rd Edition), China Architecture & Building Press, Beijing, 2015
- [12] Y. Geng, X. Han, H. Zhang, L. Shi, Optimization and cost analysis of thickness of vacuum insulation panel for structural insulating panel buildings in cold climates, *Journal of Building Engineering*. 33 (2021): 101853. <https://doi.org/10.1016/j.jobbe.2020.101853>
- [13] L. Zhang, C. Hou, J. Hou, D. Wei, Y. Hou, Optimization analysis of thermal insulation layer attributes of building envelope exterior wall based on DeST and life cycle economic

evaluation, *Case Studies in Thermal Engineering*, 14 (2019): 100410.
<https://doi.org/10.1016/j.csite.2019.100410>.

Chapter 4

Thermal Performance of the Tested Building

CHAPTER 4. THERMAL PERFORMANCE OF THE TESTED BUILDING

Chapter 4. Thermal Performance of the Tested Building

4. Thermal Performance of the Tested Building	4-1
4.1 Introduction.....	4-1
4.2 Measurement results of tested building.....	4-1
4.2.1 Measured air temperature analysis.....	4-1
4.2.2 Measured air relative humidity analysis.....	4-3
4.2.3 Surface temperature of exterior walls of tested building.....	4-7
4.2.4 Surface temperature of roof for the tested building.....	4-12
4.3 Theoretical analysis of current thermal performance of opaque exterior envelopes for tested building	4-14
4.3.1 Theoretical analysis of current thermal performance for opaque exterior envelopes in winter	4-14
4.3.2 Theoretical analysis of current thermal performance for opaque exterior envelopes in summer.....	4-18
4.4 Simulated results of indoor environment throughout the typical year	4-20
4.4.1 Simulation model	4-20
4.4.2 Model validation	4-20
4.4.3 Analysis of simulation results	4-22
4.5 Summary	4-23
Reference	4-25

CHAPTER 4. THERMAL PERFORMANCE OF THE TESTED BUILDING

4. Thermal Performance of the Tested Building

4.1 Introduction

In Chapter 3, we have already introduced the detail information of tested building and measurement work. In this Chapter, we will analyze the present indoor thermal environment and the thermal properties of exterior envelopes of the tested building based on the recorded data. Furthermore, in order to comprehend the thermal situation of local traditional dwellings during a long-time perspective, we simulate the indoor thermal environment throughout a whole year of the tested building by EnergyPlus. Both measured data obtained by an actual experiment and simulated data provided by simulation program can help us comprehend the current thermal environment of local traditional dwellings more accurately and deeply.

In subsection 4.2, we analyze temperature and relative humidity of indoor and outdoor air, then temperatures of inside and outside surfaces for exterior walls and roof are discussed. Considering that the measured data cannot accurately reflect the thermal performance of exterior envelopes, we adopt theoretical method to calculate their thermal parameters, including heat transfer coefficient, thermal inertia, and their thermal performance is also evaluated in subsection 4.3. Moreover, subsection 4.3 depicts temperatures of indoor and outdoor air, and their temperature differences throughout a typical meteorological year. Finally, subsection 4.5 summarizes the related findings observed in this chapter.

4.2 Measurement results of tested building

4.2.1 Measured air temperature analysis

Table 4-1 summarizes the maximum, minimum and mean values of both indoor and outdoor air temperature in summer and in winter. We firstly analyze the summer measured temperature. It can be noticed that the highest indoor temperature (30.5°C) is 6.9°C lower than the outdoor one (37.4°C), while the lowest indoor air temperature (25.1°C) is 2°C higher than the outdoor one (25.1°C). In addition, the indoor temperature fluctuation is more stable than the outdoor – the amplitude of indoor temperature is about 6°C, while that of outdoor temperature is 12.3°C. These temperature differences between indoor room and outdoor environment and the more stable fluctuation of indoor temperature phenomenon reflect the resistance ability for heat transfer of the exterior envelope, revealing that outdoor heat is prevented from conducting into the room to a certain extent due to the thermal resistance of exterior envelopes. But when compare the mean values of the indoor and outdoor temperature in summer, we can find they are 27.5°C and 28.4°C, respectively, and there is only 0.9°C difference among them. Furthermore, Table 4-1 displays more details. During the summer test period, the highest outdoor air temperature occurred at around 16:00, and indoor air temperature achieved its highest value of 30.5°C after about 1 hour. The outdoor air temperature dropped the lowest value (23.1°C), around 3:00, but the indoor lowest temperature is 2°C higher and it appeared around 7:00-8:00. We are also able to realize from Figure 4-1 that room was cooler during 8:00-19:00, and its temperature difference even exceeded 6°C around 13:00, 14:00 and 17:00. It's no doubt that exterior envelopes play a buffer role to some extent to resist outdoor heat enter the

CHAPTER 4. THERMAL PERFORMANCE OF THE TESTED BUILDING

room, but the period of indoor air temperature bellows 26°C is only about 6 hours, even the temperature exceeds 30°C during 3 hours (15:00-17:00). Therefore, the thermal performance of current exterior envelopes still need to be improved to reduce heat gain in summer.

Table 4-1 and Figure 4-1 also summarize the measured temperature in winter. The highest outdoor air temperature only 11.8°C during test period, while the coldest is only 2.3°C around 3:00. And the highest indoor temperature is 11.6°C, while 5.1°C is the lowest value during the test period. As for the mean values of the indoor and outdoor air temperature, the indoor mean air temperature (6.3°C) is only 1.1°C higher than the outdoor (5.2°C). These data reveal that current exterior envelopes cannot greatly resist heat loss from room although the fluctuation of test room (6.5°C) is slightly flatten than that of outdoor environment (9.5°C). Additionally, as the hourly tested temperature shown in Figure 4-1, the indoor air was almost warmer than outdoor throughout the test period, which also reflect the ability for reducing heat loss of exterior envelopes to some degree. However, the phenomenon which cannot be neglected is that the highest value of temperature difference at every moment is only 3.4°C, meaning the temperature in the room is at most 3.4°C higher than outside. The measured data demonstrate that the current thermal performance of exterior envelopes is still poor although they have an insulation effect to some degree. Furthermore, indoor temperature also responds quickly to outdoor temperature variation in both summer and winter, indicating that the current exterior envelopes have not only insufficient insulation properties but also poor thermal storage performance. Therefore, improving thermal performance of exterior envelopes for traditional dwellings in this region is imperative.

Table 4-1 Characteristic values of measured air temperature in summer and in winter

	Measured air temperature in summer		Measured air temperature in winter	
	Indoor air (°C)	Outdoor air (°C)	Indoor air (°C)	Outdoor air (°C)
Maximum	30.5	37.4	11.6	11.8
Minimum	25.1	23.1	5.1	2.3
Mean	27.5	28.4	6.3	5.2

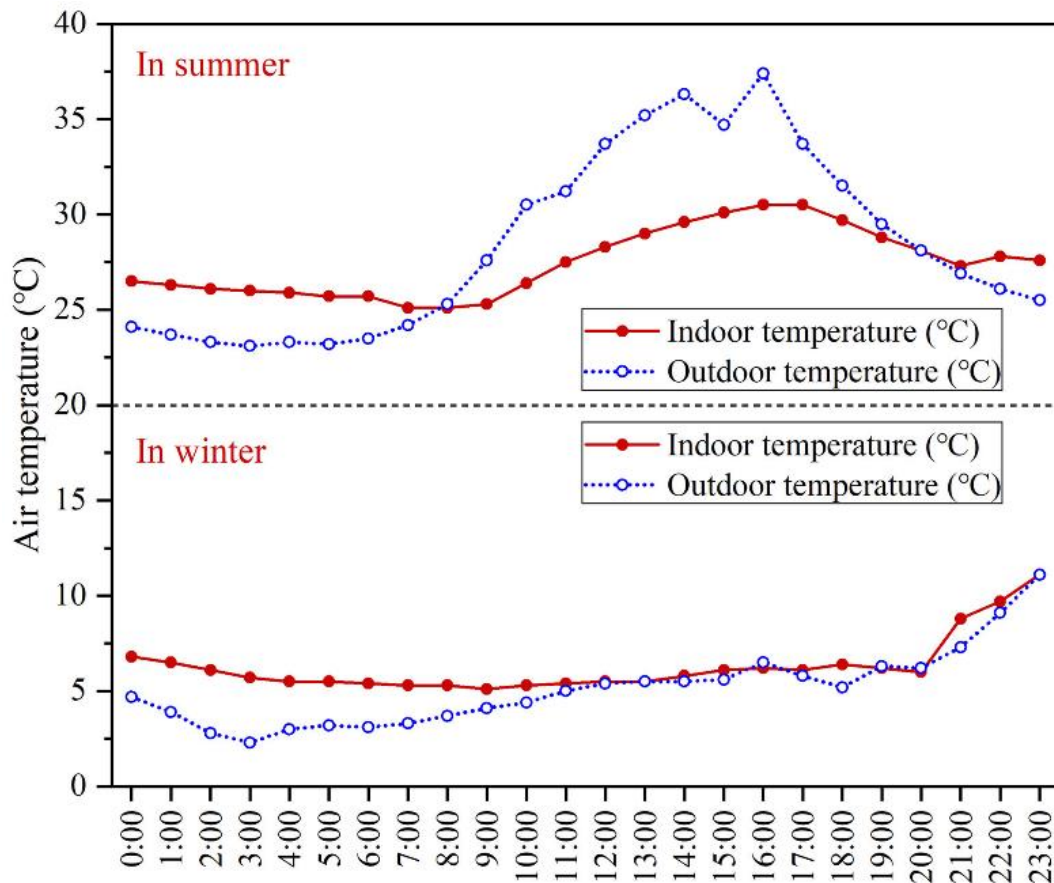


Figure 4-1. (a) Measured air temperature of bedroom on 16th Jan. 2017 and 28th Jul. 2017 and outdoor air temperature on 16th Jan. 2017 and 28th Jul. 2017.

4.2.2 Measured air relative humidity analysis

We also analyze the measured data of the air relative humidity in summer and winter, and Figure 4-2, Figure 4-3, Figure 4-3, and Figure 4-5 depict the variation and frequency of air relative humidity throughout the test period. Firstly, we can see the data measured during summer test period (shown Figure 4-2), the relative humidity exceeded 90% from 00:00 to 8:00, while the maximum relative humidity even up to 96.8% around 6:00. But affected by solar radiation, the relative humidity became to decrease from 9:00, and it dropped the lowest value (56.5%) around 14:00. Then the humidity increased and it exceeded 80% around 21:00. The indoor air humidity shows alike variation trend – the maximum value (86.8%) appeared around 9:00, and the lowest one (71.2%) appeared around 16:00. It is clear that the fluctuation degree of indoor relative humidity (15.6%) is much lower than outdoor relative humidity (41.1%) because of the ability of exterior envelop to resist vapor transfer.

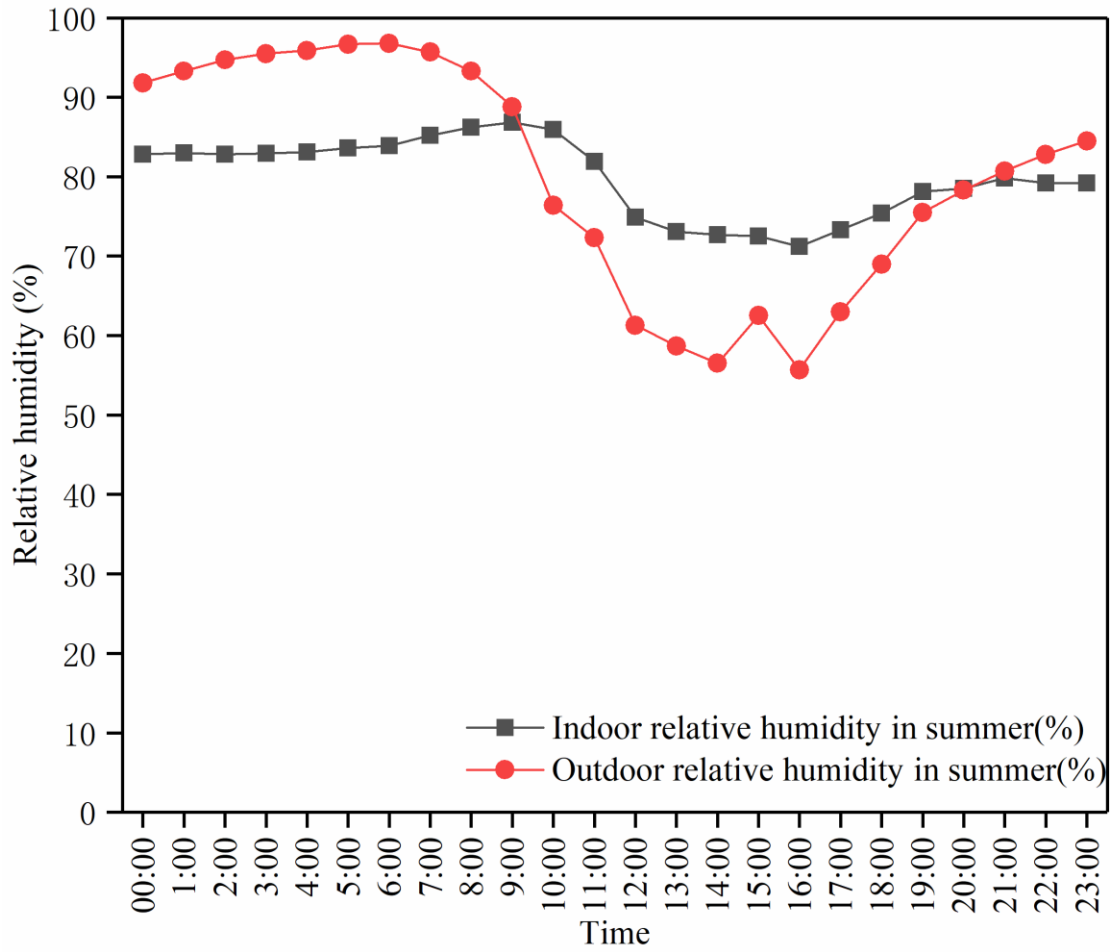


Figure 4-2. Tested relative humidity of testing room air and outdoor air relative humidity on 28th Jul. 2017.

Figure 4-3 displays the frequency of indoor and outdoor air relative humidity during the testing period in summer, and we can see indoor relative humidity was higher than 70% throughout the testing period although its highest value is lower than that of outdoor air. The recorded data demonstrate the air humidity situation of current indoor environment and it will make people feel uncomfortable.

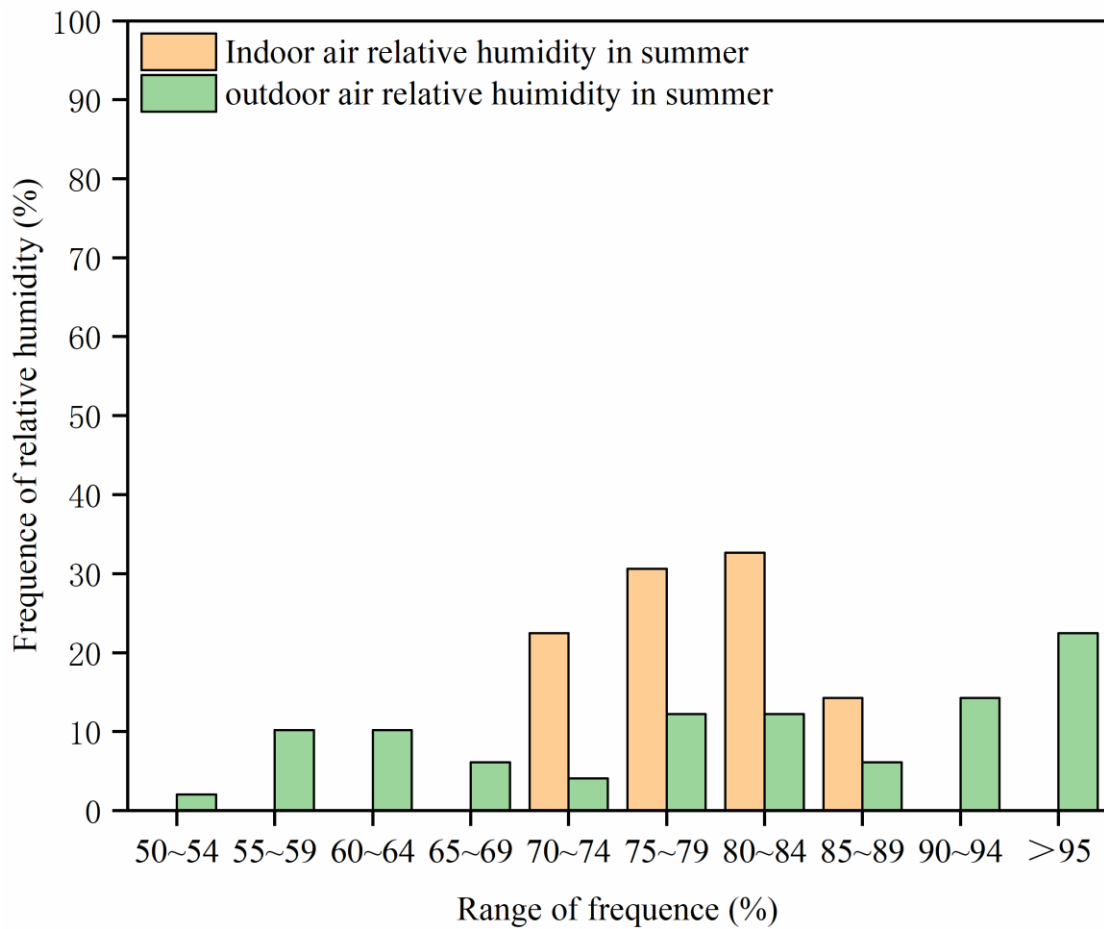


Figure 4-3. Frequency of measured relative humidity of testing room air and outdoor air on 28th Jul. 2017.

According to the variation trend of winter relative humidity shown in Figure 4-4, the highest value of outdoor and indoor relative humidity was 83.2% and 79.1%, respectively, while the lowest relative humidity of outdoor and indoor air was 71.4% and 73.5%, respectively. It can be seen the fluctuation of indoor relative humidity (5.6%) is smaller than outdoor relative humidity (11.8%) because of the resistance of exterior envelopes. And from the frequency statistic results of relative humidity, most of relative humidity values were in the range of 75-79% for both outdoor and indoor air during winter test period.

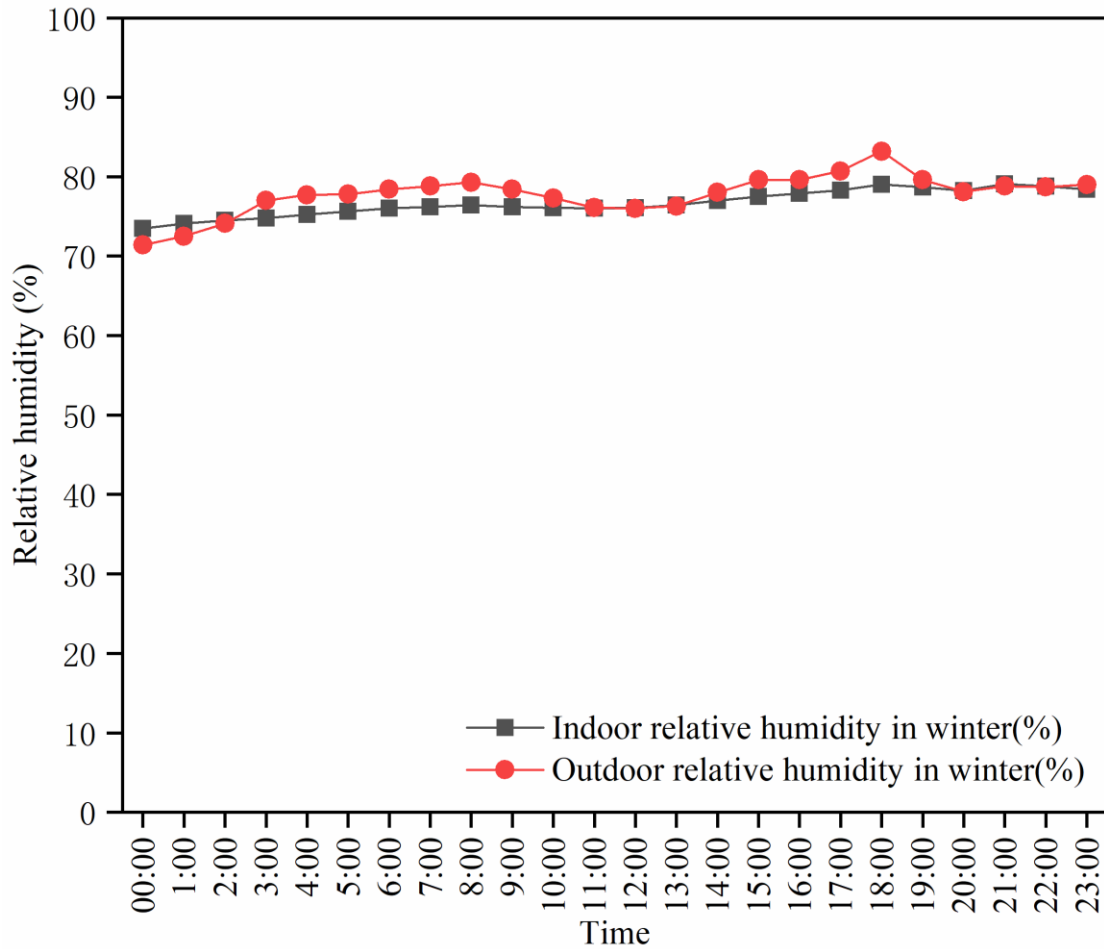


Figure 4-4. Tested relative humidity of testing room air and outdoor air relative humidity on 16th Jan. 2017.

Figure 4-5 displays the frequency of indoor and outdoor air relative humidity, we can see all of the outdoor relative humidity values are more than 70% throughout the winter testing period, indicating the lowest winter relative humidity is much higher than the minimum value of relative humidity during summer testing period, the reason of this phenomenon is that solar radiation in winter is very low for this region because of its basin terrain.

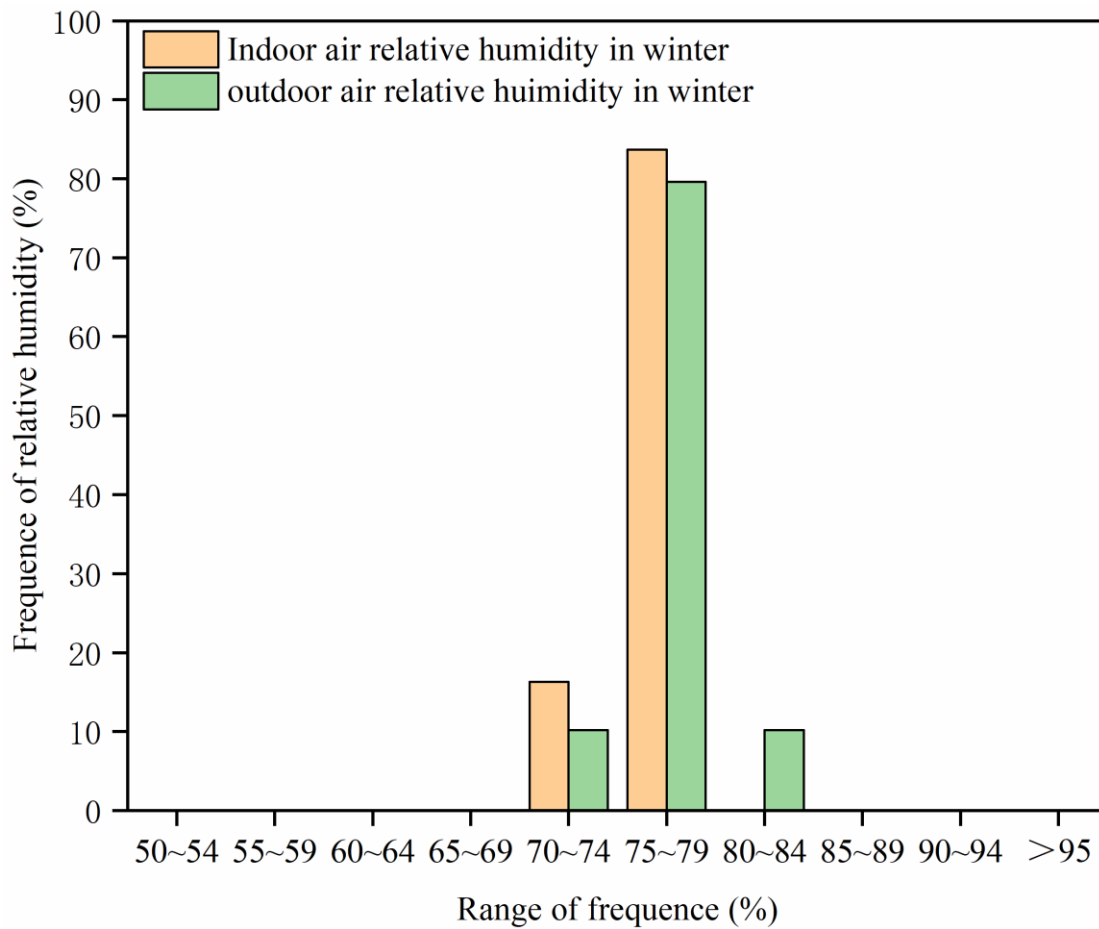


Figure 4-5. Frequency of measured relative humidity of testing room air and outdoor air on 16th Jan. 2017.

4.2.3 Surface temperature of exterior walls of tested building

We also tested the surface temperature of exterior walls of the actual tested dwelling. Figure 4-6 presents the three-dimension diagram of the arrangement of testing point. All of these testing points are higher 1.5 meters than the ground. Among them, P1 and P2 are Testo175 data loggers used to record the indoor and outdoor air temperature and relative humidity, respectively. In addition, P6 and P11 stand for north of building surfaces, P4 and P9 represent south of building surfaces, P5 and P10 stand for west of building surface, and P7 and P12 represent east of building surface. Finally, Figure 4-7 and Figure 4-8 display the hourly surface temperature of exterior walls in different orientation and these data are recorded during 8:00-18:00 on 16th January, 2017 (winter) and 28th July, 2017 (summer), respectively.

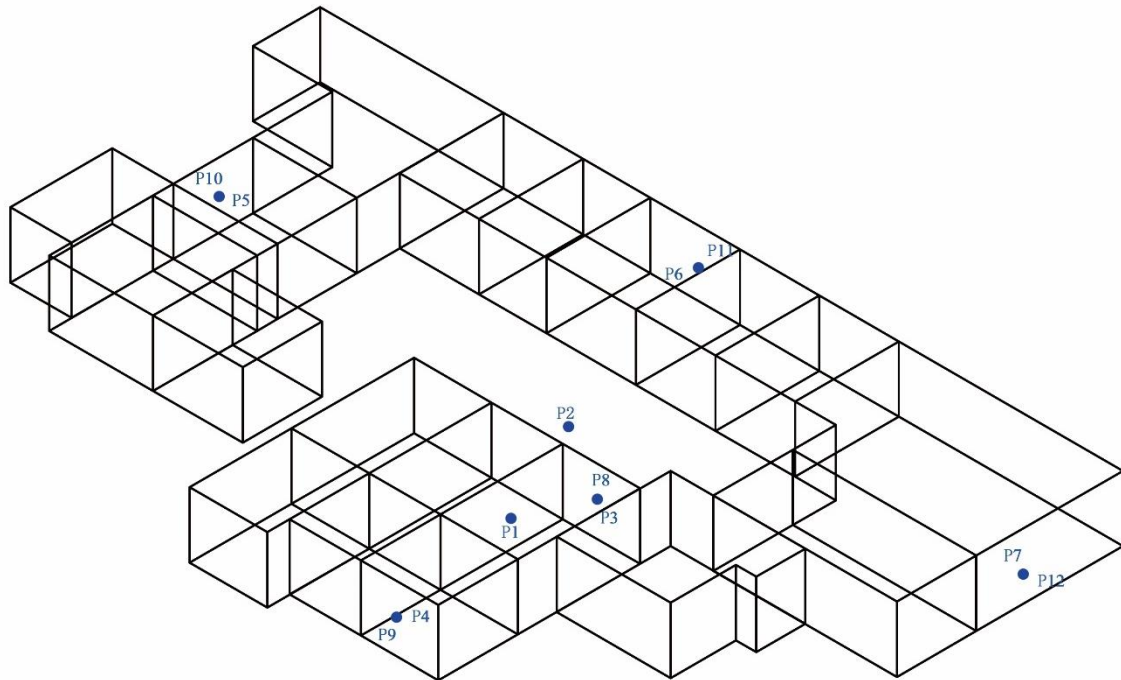


Figure 4-6. Arrangement of testing points (three-dimension diagram).

According to the inside and outside surface temperatures of exterior walls measured in winter, we can note that south wall has a higher temperature than walls faced other orientation. It's no doubt that the southern wall receives the most solar heat in the northern hemisphere, therefore the southern wall has a better performance in winter. Furthermore, the inside surface temperature of south wall can achieve to 16.3°C , which is even 10.1°C and 9.9°C higher than the outdoor and indoor air temperature at the same time, respectively. It displays the effective of the thermal resistance and thermal inertia of the exterior wall, which can prevent heat loss from the room and weaken the impact of temperature fluctuation of outdoor air on the indoor environment. By contrast, the surface temperature of outside surface of northern wall is lowest, but thanks to the thermal resistance of exterior walls, the inside surface of northern wall is about $0.8\text{-}2.3^{\circ}\text{C}$ higher than the outside. Similarly, the thermal resistance of exterior wall has the same effect for the west wall and east wall, and thereby the inside surface temperatures of west and east façade are higher than the outside.

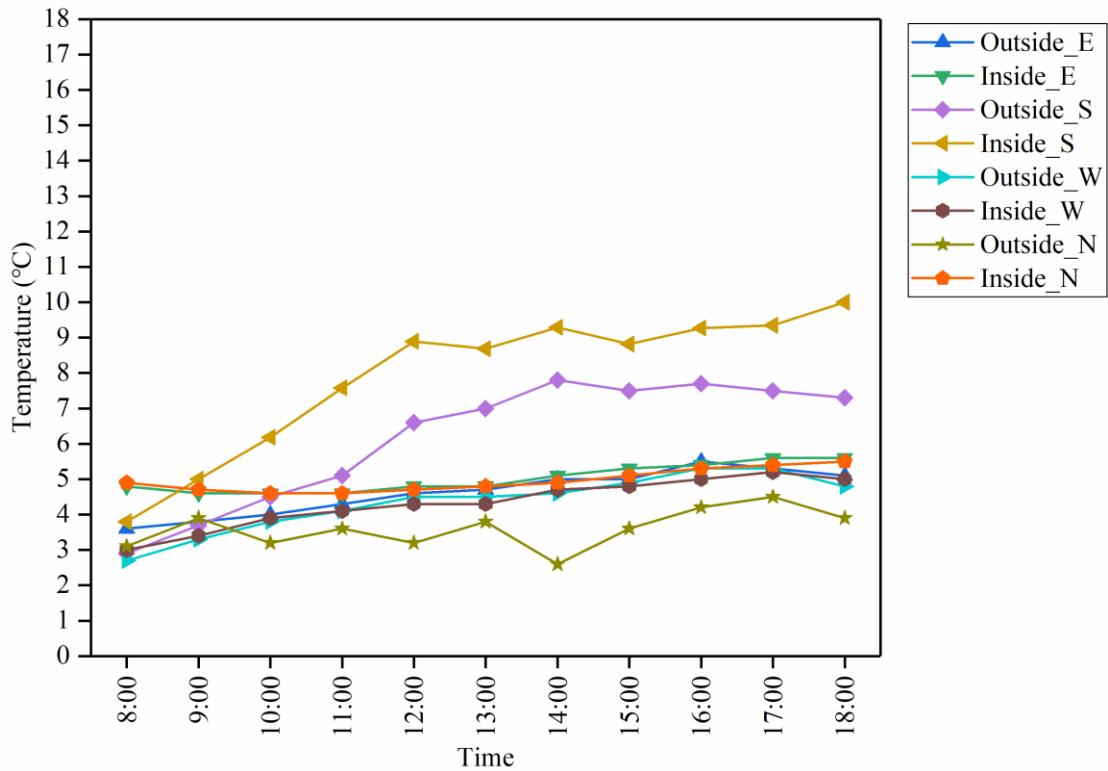


Figure 4-7. Outside and inside surface temperatures of exterior walls on 16th Jan. 2017.

Furthermore, we can better understand the resistance capacity of exterior walls to prevent heat loss from the indoor room according to the mean value of these surface temperature. The mean temperature of the outside surface is 6.1°C, 3.6°C, 4.3°C, and 4.6°C for south, north, west, and east wall, and correspondingly, the inside surface is 7.9°C, 5.0°C, 4.3°C, and 5.0°C, and based on their surface temperature, we can calculate the improved value of the mean temperature is 1.8°C, 1.4°C, 0°C, and 0.4°C for south, north, west, and east walls. The diverse outside temperature value for different orientation façade reflects the effect of solar radiation on the ambient air surround the surface, and no doubt that the solar-air temperature of south wall is highest, therefore the outside temperature of south wall is the maximum one. In addition, the mean temperature of outdoor air is 5.1°C, while the value of indoor air is 5.7°C during the testing period (8:00 - 18:00), and from Table 4-2, we can note that only mean value of outside surface temperature of south wall is higher than that of outdoor air, similarly, only the inside surface of south wall is warmer than the indoor air. It also indicates the importance of solar radiation to increase the thermal performance of the building. Thus we need to find some strategies and which can exploit the solar radiation during winter time and evaluate their energy-saving performance for the building.

Table 4-2 Temperature characteristic values of outside and inside surface temperatures in winter.

	Outside surface temperature (°C)			Inside surface temperature (°C)		
	Maximum	Mean	Minimum	Maximum	Mean	Minimum
South	7.8	6.1	2.9	10.0	7.9	3.8
North	4.5	3.6	2.6	5.5	5.0	4.6
West	5.3	4.3	2.7	5.2	4.3	3
East	5.5	4.6	3.6	5.6	5.0	4.6

In summer, we also recorded the surface temperature of exterior walls during daytime, and the testing period is 6:00-18:00 on 28th July. 2017. Figure 4-8 presents the recorded data, including outdoor and indoor air temperature during 6:00-18:00 on 28th July.2017, and surface temperatures of exterior walls facing varies orientation during testing period. It is apparent that the variation trend of surface temperature is consistent with the outdoor air temperature change trend, and outdoor air is highest after 8:00. South wall has a higher temperature of outside surface before 12:00, however, unlike its performance presented in winter that outside surface of south wall remains the largest during all daytime, the outside surface temperature of west wall exceeds it after 12:00. We can infer the reason of this phenomenon is due to the orientation of the tested building, that is, the building faces around southeast as we shown in Chapter 3. Before 14:00, the inside surface temperatures of south wall, north wall, and east wall are lower than indoor air temperature, whereas inside surface of west wall becomes higher after 11:00 since the west wall absorbs much more solar radiation. Furthermore, the temperature differences between outside and inside surfaces of exterior walls gradually extend after 10:00 and can even up to approximately 3°C, reflecting the insulation function of exterior walls which can prevent heat gain from entering the indoor room. And more detailed data related to the surface temperature of exterior walls can be found in Table 4-3.

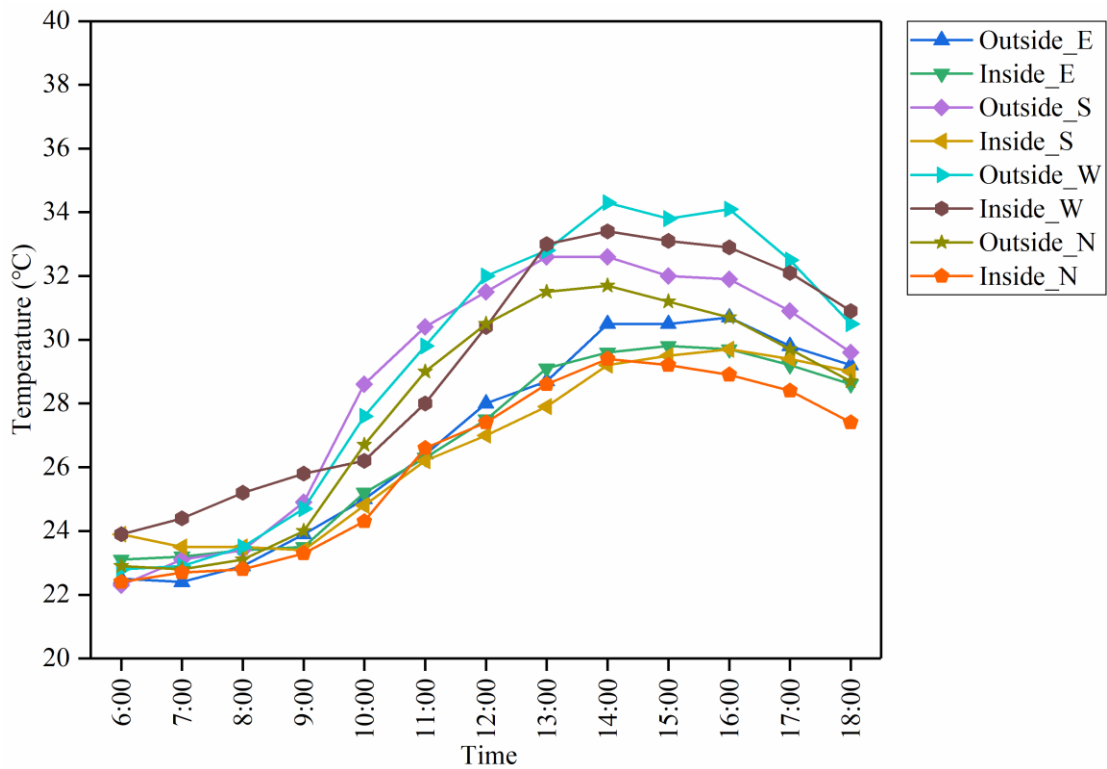


Figure 4-8 Outside and inside surface temperatures of exterior walls on 28th Jul. 2017.

Table 4-3 summaries the temperature of each wall surface, and we can better understand the resistance capacity of exterior walls to prevent heat gain from entering indoor rooms based on these detailed data. Firstly, the mean value of outside temperature of the south, north, west, and east wall is 28.8°C, 27.9°C, 29.3°C, and 27.0°C, respectively, and the mean temperature of outside surface is 26.7°C, 26.3°C, 29.2°C, and 26.8°C for the south, north, west, and east wall. Meanwhile, the mean air temperature of outdoor and indoor air is 31.3°C and 27.9°C during the same period. It is clear that all of mean values of outside surface temperature for exterior walls are lower than the outdoor air, similarly, mean values of inside temperatures for walls with different orientation are smaller than that of indoor air except for the west. Moreover, we can obtain the temperature differences between outside temperature and inside temperature for exterior walls, they are 2.1°C, 1.6°C, 0.1°C, and 0.2°C for south, north, west, and east, respectively. These temperature differences present a likewise performance, that is, the increase of the inside temperature compared to the outside surface temperature is ranked from highest to lowest is the south, north, east, and west.

Table 4-3 Temperature characteristic values of outside and inside surface temperatures in summer.

	Outside surface temperature (°C)			Inside surface temperature (°C)		
	Maximum	Mean	Minimum	Maximum	Mean	Minimum
South	32.6	28.8	22.3	29.7	26.7	23.4
North	31.7	27.9	22.8	31.7	26.3	22.8
West	34.3	29.3	22.8	33.4	29.2	23.9
East	30.7	27.0	22.4	29.8	26.8	23.1

4.2.4 Surface temperature of roof for the tested building

We also recorded the outside and inside surface temperatures of the tested building roofs. Considering that the tested building is enclosed and has sloped roofs, resulting in two roof surfaces for each orientation, therefore weighted average of the roof surface temperatures for each orientation is taken to analyze in this part. Figure 4-9 presents the temperature of outdoor air, indoor air, outside surface of roof, and inside surface of roof during 8:00-18:00 on 16th Jan. 2017. It is obviously that inside surface is warmer than the outside surface of roof while the mean value of inside surface and outside surface is 6.2°C and 3.5°C, respectively. It reflects the thermal resistance of roof to some extents. Furthermore, the maximum and minimum value of temperature difference between inside and outside surface is approximately 6.7°C and 1.3°C, which means the inside surface temperature is at least 1.3°C higher than the concurrent outside surface temperature during the testing period. Additionally, both outside and inside temperature change with the variation of outdoor air, and moreover, their highest value of outdoor air, outside surface, and inside surface of 6.5°C, 5.4°C, and 7.2°C occurs at the same time (16:00), which shows that there is almost not any time lag of roof, and further indicates that the thermal conductivity, the coefficient of heat accumulation, and the thermal inertia of roof are poor to some extents.

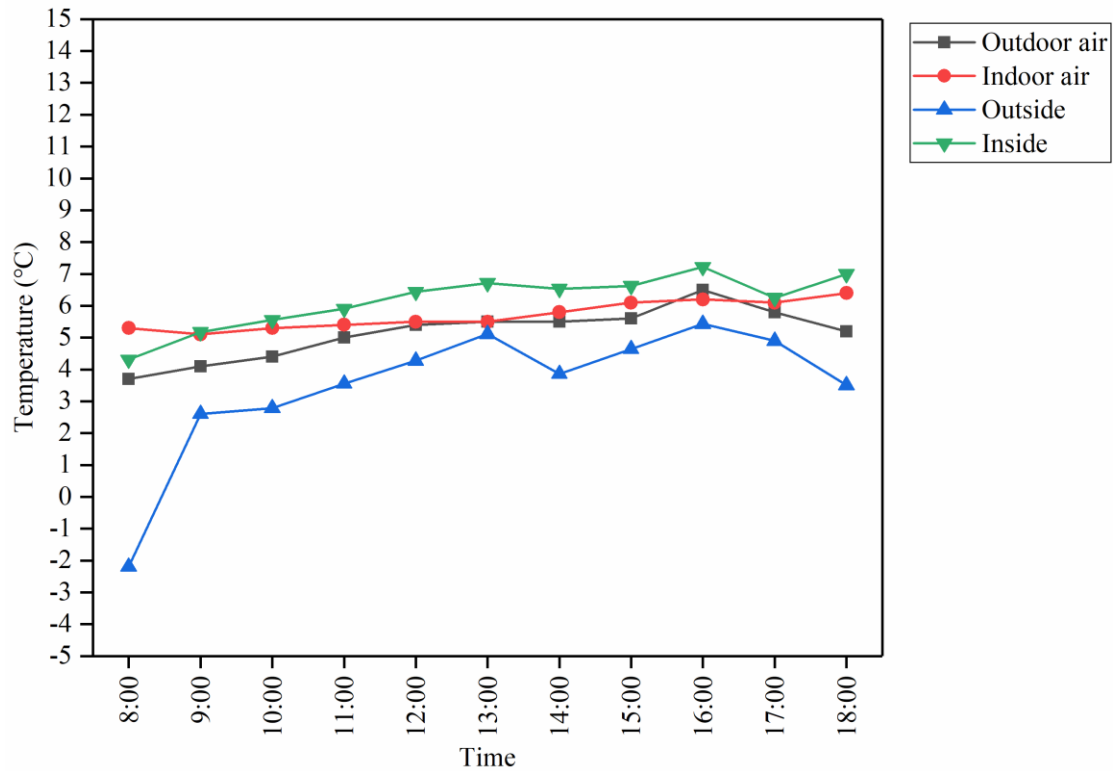


Figure 4-9. Indoor air temperature, outdoor air temperature, and surface temperature of the roof on 16th Jan. 2017.

In summer, the temperature of outdoor air, indoor air, outside surface of roof, and inside surface of roof are recorded during 6:00-18:00 on 28th Jul. 2017. Similarly, weighted average of the roof surface temperatures for each orientation is taken to analyze while Figure 4-10 presents the variation of outdoor air, indoor air, outside surface of roof, and inside surface of roof. It is obviously that inside surface is cooler than the outside surface of roof while the mean value of inside surface and outside surface is 27.5°C and 28.2°C, respectively. It also reflects the ability of roof to prevent heat gain from entering room via roofs to some extents. Furthermore, the maximum and minimum value of temperature difference between inside and outside surface is approximately 1.7°C and 0.1°C, which means the inside surface temperature is at most 1.7°C lower than the concurrent outside surface temperature during the testing period. It proves that the value of thermal conductivity of roof is not as high as enough, thus the heat that outside of roof absorbs from solar radiation cannot be efficiently prevented entering the room.

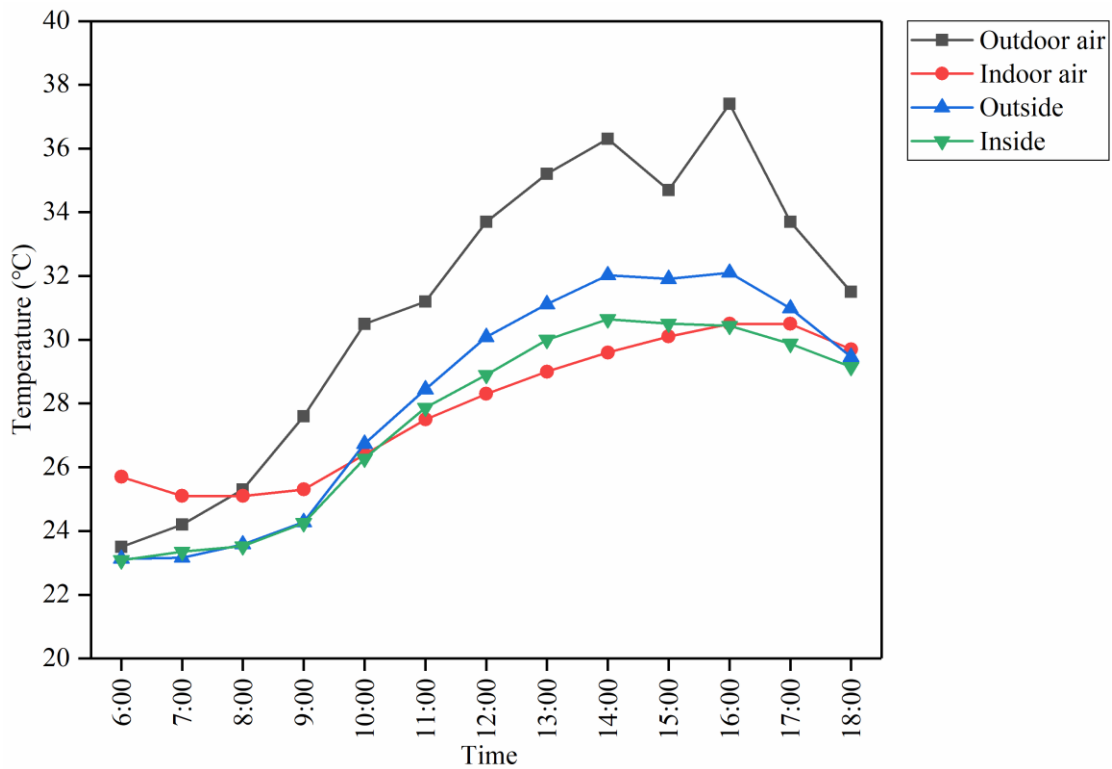


Figure 4-10. Indoor air temperature, outdoor air temperature, and surface temperature of the roof on 28th Jul. 2017.

4.3 Theoretical analysis of current thermal performance of opaque exterior envelopes for tested building

4.3.1 Theoretical analysis of current thermal performance for opaque exterior envelopes in winter

Although we can understand the thermal performance of current exterior envelopes to some extents based on the measured data depicted in subsection 4.2, however, these experimental data cannot exactly reflect the current thermal properties of exterior walls and roofs since the testing period is not as long as enough. Thus we calculate the heat transfer coefficient and thermal inertia of exterior walls by theoretical calculation methods in accordance with the requirements of Code for thermal design of civil building GB 50176-2016 [1], which is one of the Chinese national standards, and the relevant results can help us comprehend the present thermal properties of exterior walls.

Firstly, the heat transfer resistance (R_0) is obtained by Eq. 4-1. The envelope heat transfer resistance is a physical quantity that characterizes the impedance heat transfer capability of the envelope itself plus the air boundary layer on both sides as a whole. Obviously, it is unlike the thermal resistance (R), which is a physical quantity that characterizes the resistance to heat transfer of the envelope itself or one of its layers. Additionally, surface resistance of heat transfer is the thermal resistance of the surface layer of an object during convective and radiant heat transfer process, and is the reciprocal of the surface coefficient of heat transfer.

$$R_0 = R_i + R + R_e \quad (4-1)$$

where:

R stands for thermal resistance of envelope itself, (m² K)/W;

R_i stands for surface resistance of heat transfer of inside surface, (m² K)/W;

R_e stands for surface resistance of heat transfer of outside surface. (m² K)/W.

The thermal resistance of a single homogeneous material layer is calculated by the following equation:

$$R = \delta / \lambda \quad (4-2)$$

where:

δ stands for Thickness of the calculated material, m;

λ stands for thermal conductivity of the calculated material, W/(m K).

Based on the thermal resistance of a single homogeneous material layer, the thermal resistance of the flat wall of the envelope consisting of multiple layers of homogeneous material (R_0) is calculated according to the following formula:

$$R = R_1 + R_2 + \dots + R_n \quad (4-3)$$

where:

R_n stands for thermal resistance of the n^{st} layer material, (m² K)/W.

Then we can obtain heat transfer resistance of the flat wall of the envelope according to the following formula.

$$K = \frac{1}{R_0} = \frac{1}{R_i + R + R_e} \quad (4-4)$$

In Eq. 4-4, according to the requirements of Code for thermal design of civil building GB 50176-2016 [1], the value of R_i equals to 0.11 in both winter and summer, while the value of R_e equals to 0.04 and 0.05 in winter and in summer, respectively.

Thermal inertia reflects the ability of the material layer to resist temperature fluctuations when it receives fluctuating thermal effects, and is denoted by D . And the following formula explains how to calculate thermal inertia (D).

$$D=R S \quad (4-5)$$

where:

R stands for thermal resistance of the calculated material, (m² K)/W;

S stands for coefficient of heat accumulation of the calculated material, W/(m² K).

As the same as the calculation of thermal resistance of the flat wall of the envelope consisting of multiple layers of homogeneous materials (R), thermal inertia of the flat wall of the envelope composed of multiple layers of homogeneous materials (D) is calculated according to the following formula.

$$D=D_1 + D_2 + \dots + D_n \quad (4-6)$$

where:

D_n stands for thermal inertia of the n^{st} layer material.

Additionally, coefficient of heat accumulation (S) is the ratio of the amplitude of the heat flow through the surface to the amplitude of the surface temperature wave when one side of a homogeneous material layer of sufficient thickness is subjected to harmonic heat effects. It can be calculated by the following formula.

$$S = \sqrt{\frac{2\pi\lambda c \rho}{3.6T}} \quad (4-7)$$

where:

λ stands for thermal conductivity of the calculated material, W/(m K);

c stands for specific heat capacity of the calculated material, kJ/(kg K);

ρ stands for density of the calculated material, kg/m³;

T stands for temperature fluctuation cycle, h, and generally $T=24\text{h}$;

π stands for circumference ratio, equals to 3.14.

As we described in Chapter 3, the component materials of the exterior walls are gypsum plaster and clay, while the material of roof is tiles. In addition, thickness of each gypsum plaster layer is 20mm, the thickness of clay is 100mm, and the thickness of roof tiles is 20mm. The thermophysical parameters of these related materials are shown in Table 4-4, meanwhile these values are obtained from Code for thermal design of civil building GB 50176-2016 [1].

Table 4-4 Thermophysical parameters of wall materials commonly used in traditional dwellings in northeast of Sichuan hills, China [1].

	Thermal conductivity λ (W/m K)	Specific heat c (kJ/kg K)	Density ρ (kg/m ³)
Clay	0.76	1.01	1600
Gypsum plaster	0.76	1.05	1500
Roof tiles	0.47	1.01	1200

Suppose the heat transfer coefficients of the exterior wall and the roof is K_{wall} and K_{roof} , respectively, then they can be calculated as the following formulas.

$$K_{wall} = \frac{1}{R_0} = \frac{1}{R_i + R_{gypsum} + R_{clay} + R_{gypsum} + R_e} = \frac{1}{0.11 + \frac{0.02}{0.76} + \frac{0.1}{0.76} + \frac{0.02}{0.76} + 0.04} = 3W / (m^2 \cdot K) \quad (4-8)$$

$$K_{roof} = \frac{1}{R_0} = \frac{1}{R_i + R_{tiles} + R_e} = \frac{1}{0.11 + \frac{0.02}{0.47} + 0.04} = 5.2W / (m^2 \cdot K) \quad (4-9)$$

Next, suppose the coefficient of heat accumulation of the exterior wall and the roof is S_{wall} and S_{roof} , respectively, then they can be calculated by the following formulas.

$$S_{clay} = \sqrt{\frac{2\pi\lambda c\rho}{3.6T}} = \sqrt{\frac{2 \times 3.14 \times 0.76 \times 1.01 \times 1600}{3.6 \times 24}} = 9.44W / (m^2 \cdot K) \quad (4-10)$$

$$S_{gypsum} = \sqrt{\frac{2\pi\lambda c\rho}{3.6T}} = \sqrt{\frac{2 \times 3.14 \times 0.76 \times 1.05 \times 1500}{3.6 \times 24}} = 9.33W / (m^2 \cdot K) \quad (4-11)$$

$$S_{roof} = \sqrt{\frac{2\pi\lambda c\rho}{3.6T}} = \sqrt{\frac{2 \times 3.14 \times 0.47 \times 1.01 \times 1200}{3.6 \times 24}} = 6.43W / (m^2 \cdot K) \quad (4-12)$$

Finally, we can obtain the thermal inertia of the exterior wall (D_{wall}) and the roof (D_{roof}), which can be calculated by the following formulas.

$$D_{clay} = R_{clay} \cdot S_{clay} = \frac{0.1}{0.76} \times \sqrt{\frac{2 \times 3.14 \times 0.76 \times 1.01 \times 1600}{3.6 \times 24}} = 1.24 \quad (4-13)$$

$$D_{gypsum} = R_{gypsum} \cdot S_{gypsum} = \frac{0.02}{0.76} \times \sqrt{\frac{2 \times 3.14 \times 0.76 \times 1.05 \times 1500}{3.6 \times 24}} = 0.25 \quad (4-14)$$

$$D_{wall} = D_{gypsum} + D_{clay} + D_{gypsum} = 1.74 \quad (4-15)$$

$$D_{roof} = R_{roof} \cdot S_{roof} = \frac{0.02}{0.47} \times \sqrt{\frac{2 \times 3.14 \times 0.47 \times 1.01 \times 1200}{3.6 \times 24}} = 0.27 \quad (4-16)$$

According to the Design standard for energy efficiency of residential buildings in hot summer and cold winter zone JGJ 134-2010 [2], the maximum value of heat transfer coefficient of exterior walls and the roof is 1.0 W/(m² K) and 0.8 W/(m² K) when the thermal inertia (D) does not exceed 2.5 ($D \leq 2.5$), while the maximum value of heat transfer coefficient of exterior walls and the roof is 1.5 W/(m² K) and 1.0 W/(m² K) when the thermal inertia (D) is larger than 2.5 ($D > 2.5$). Obviously, the current values of heat transfer coefficient of both exterior walls and roof do not satisfy the minimum requirements of the related standard (JGJ 134-2010). The current poor thermal properties of exterior walls and roof necessitates the improvement of their thermal performance, thus we need to find effective strategies to upgrade their thermal performance to further reduce the heat loss in winter.

4.3.2 Theoretical analysis of current thermal performance for opaque exterior envelopes in summer

According to the Code for Thermal Design of Civil Buildings GB 50176-2016 [1], buildings in hot summer and cold winter zone (HSCW) must be designed to meet the requirements of heat protection in summer and take appropriate account of heat preservation in winter. According to the standard, the maximum temperature of the inside surface of the external wall ($\theta_{i \max Wall}$) and the inside surface of the roof ($\theta_{i \max Roof}$) of the naturally ventilated room should not be higher than the maximum temperature of the highest day of the cumulative annual average daily outdoor temperature ($t_{e \max}$).

In accordance with the requirements of Code for Thermal Design of Civil Buildings GB 50176-2016 [1], the temperature of the inside surface of the external walls and roofs is calculated using a one-dimensional non-stationary method. That is, in the process of heat transfer along the wall thickness direction, if a one-dimensional coordinate system is established at the thickness direction x as the coordinate origin, according to the law of conservation of energy, the dynamic heat transfer process of the wall surface is expressed as the following formula.

$$\frac{\partial T_i}{\partial \tau} = \frac{\partial}{\partial x} \left(\frac{\lambda_i}{\rho_i c_{\rho i}} \cdot \frac{\partial T_i}{\partial x} \right) \quad (4-17)$$

The outside surface of exterior wall is set as " $x=0$ " and the inside surface of exterior wall is set as " $x=\delta$ ", which can be expressed as follows:

$$-\lambda \frac{\partial T}{\partial x} \Big|_{x=0} = a_i (\theta_i - t_i) \quad (4-18)$$

$$-\lambda \frac{\partial T}{\partial x} \Big|_{x=\delta} = a_e (\theta_i - t_i) + \mu I \quad (4-19)$$

where:

T_i stands for the temperature of the i th material, °C;

τ stands for time, s;

ρ_i stands for the density of i th material, kg/m³;

c_{pi} stands for the specific heat of i th material, kJ/(kg K);

μ stands for the solar radiation absorptivity factor of the outside surface of the roof;

I stands for the solar radiation intensity, W/m²;

a_e stands for surface coefficient of heat transfer of outside surface of the roof, W/(m² K), set as 19 W/(m² K) [1];

a_i stands for surface coefficient of heat transfer of inside surface of the roof, W/(m² K), set as 8.7 W/(m² K) [1].

The meteorological boundary conditions required for the calculation include outdoor air hour-by-hour temperature, solar radiation for each orientation, and indoor air temperature, as shown in Figure 4-11 [1].

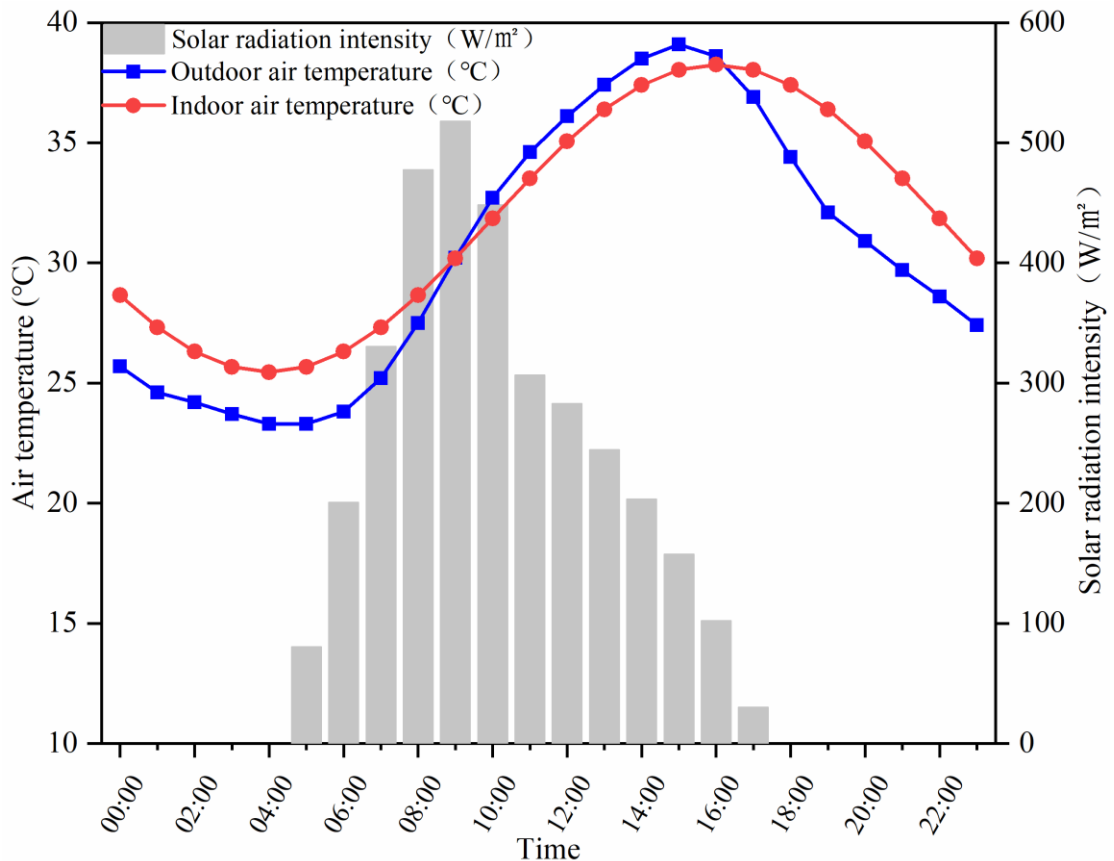


Figure 4-11. Meteorological boundary conditions required for the calculation

By calculation, the temperatures of the inner surface of the exterior wall and the inner surface of the roof are 39.88°C and 40.66°C, respectively. And according to the Code for Thermal Design of Civil Buildings GB 50176-2016 [1], the maximum temperature of the highest day of the highest cumulative annual average daily temperature in the area is 39.10°C. Therefore, the measured thermal insulation performance of the exterior wall and roof of the building do not meet the design requirements proposed by the related standard.

4.4 Simulated results of indoor environment throughout the typical year

4.4.1 Simulation model

In order to learn more indoor environment details for the tested building, we built up a simulation model by EnergyPlus according to the construction information of the tested dwelling. The configuration and construction materials and layers are consistent with the real building. The construction form of exterior walls is gypsum plaster (5mm), clay (100mm) and gypsum plaster (5mm) from outside to inside, the construction form of interior walls is gypsum plaster (5mm), clay (60mm) and gypsum plaster (5mm), while the roof is simply covered with a layer of tiles on the rafters and the construction material of floor is crushed stone concrete. And considering that the poor infiltration of traditional rural buildings in China, the air change hour (ACH) of this model was set as 1.5 h⁻¹. The three dimensional view of this model is shown in Figure 4-12, while Table 4-5 lists the thermophysical properties of building materials which are used in the simulation. Additionally, these values of each parameter are obtained by Code for thermal design of civil building GB50176-2016 [1]. The meteorological boundary is set as weather data of Nanchong station, which was downloaded by the website of EnergyPlus [3]. Its format is Chinese Standard Weather Data (CSWD), which was developed by Dr. Jiang Yi, Department of Building Science and Technology at Tsinghua University and China Meteorological Bureau [4] and it includes annual design data and typical meteorological year data.

Table 4-5 Thermophysical properties of building material for simulation [1]

Building material	Calculation parameters		
	Heat conduction coefficient/ λ (W/m K)	Specific heat capacity/C (kJ/kg K)	Density/ ρ_0 (kg/m ³)
Clay	0.76	1.01	1600
Gypsum plaster	0.76	1.05	1500
Roof tiles	0.47	1.01	1200
Crushed stone concrete	1.28	0.92	2100

4.4.2 Model validation

In the validation phase, the settings of building envelope and people activity schedule were consistent with the actual situation and weather boundary was the actual weather data measured during the testing period. The measured and simulated values of indoor air temperature of the testing room are shown in Figure 4. It is obvious that simulated results are consistent with the trend of the

measured values. Moreover, mean square error (MSE) and root-mean square error (RMSE) were calculated according to Eq. 4-20 and Eq. 4-21 [5]. The value of MSE and RMSE is 1.7 and 1.3, respectively. Meanwhile, the mean value of relative error is 4% while the maximum relative error is 7.7%. These results confirm both the reliability of EnergyPlus and the setting of building envelopes are both rational.

$$MSE = \frac{1}{n} \sum_{i=1}^n (Y_{prediction_i} - Y_i)^2 \quad (4-20)$$

$$RMSE = \sqrt{\frac{1}{n} \sum_{i=1}^n (Y_{prediction_i} - Y_i)^2} \quad (4-21)$$

where,

n is the number of data sets;

$Y_{prediction_i}$ is the set of results predicted by simulation;

Y_i is the set of actual test data.

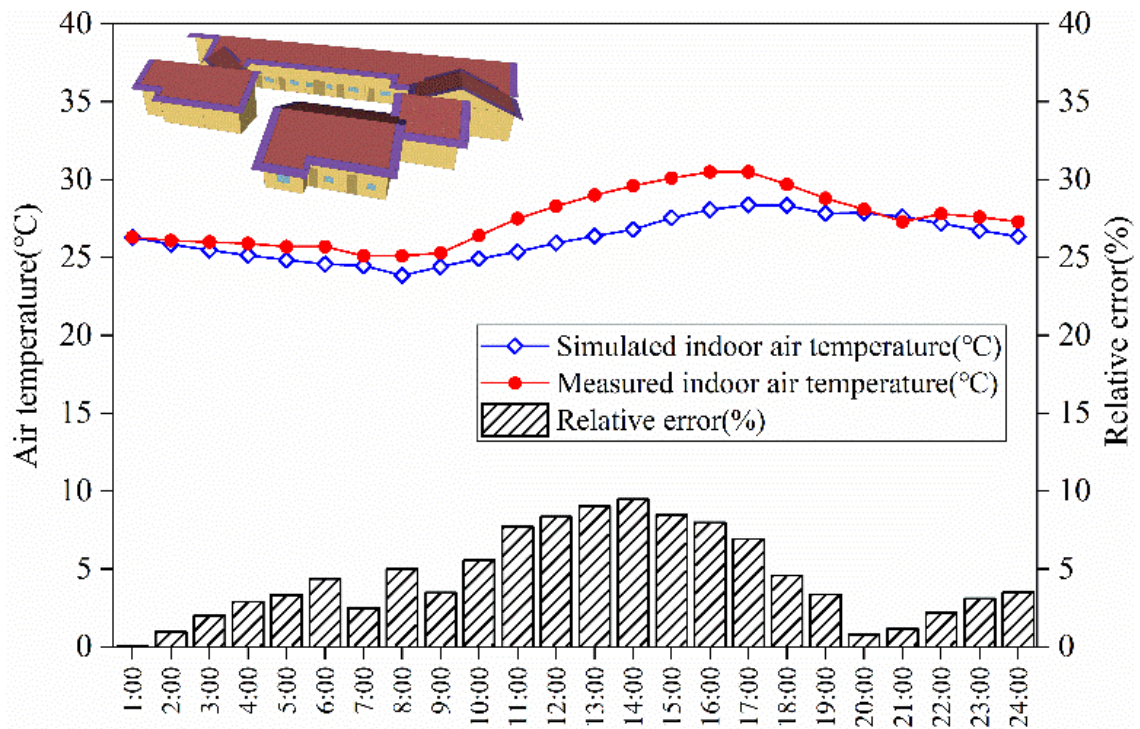


Figure 4-12. Comparison of measured values and simulated values of tested dwelling.

4.4.3 Analysis of simulation results

By the simulation method, we are able to understand the indoor air temperature throughout the whole year better. Figure 4-13 depicts the hourly air temperature of testing room and outdoor environment throughout the typical year. It is no doubt that air in the testing room is warmer than outside during winter and cooler during summer since the resistance of exterior envelopes. Meanwhile, according to the temperature difference between indoor and outdoor air throughout the whole year (the values of the temperature difference are equal to the indoor temperature values minus the outdoor temperature values) shown in Figure 4-14, the highest temperature difference can achieve to 12.4°C and the lowest is -6.0°C , meaning the indoor air is able to warmer than outdoor of 12.4°C in winter and cooler of 6.0°C in summer. However, during January 1st to March 31th and November 1st to December 31th (3624 hours in total), only 109 temperature difference values (corresponding to 109 hours, accounting to about 3% of the total 3624 hours) exceeds 10°C , while about 85.7% of these values are more than 8°C . And during June 1st to August 31th (2208 hours in total), about 59.2% of the total values are below 0°C , indicating the testing room is cooler than outside, but only about 20.1% of the total values are lower than -2°C while there is only 23 hourly values are below -5°C . And because the outdoor temperature is high, which even exceeds 38°C , the indoor air is still higher than 26°C (the indoor calculated temperature used to predict cooling load [1]) and there are 1128 values of hourly indoor temperature are higher than the summer indoor calculated temperature, thereby there still exists cooling load even though the room is cooler than outside in most of the summer time. Similarly, there is an obvious heating load in winter although during the most of time (64% of the 3624 hours) the testing room is warmer than outside at least 5°C . The outdoor air is too cool that even drops to -0.8°C , so the average hourly temperature of the testing room is only 15.3°C during winter, which is lower than the indoor calculated temperature used to predict heating load (18°C). Additionally, the temperature of testing room is lower than 18°C even in the part of time during April and October, and there are 3426 values of hourly indoor temperature are smaller than 18°C . Hence, there are both heating load and cooling load for traditional dwellings in this region, while the heating load is higher because local winter is very cool and last a long period.

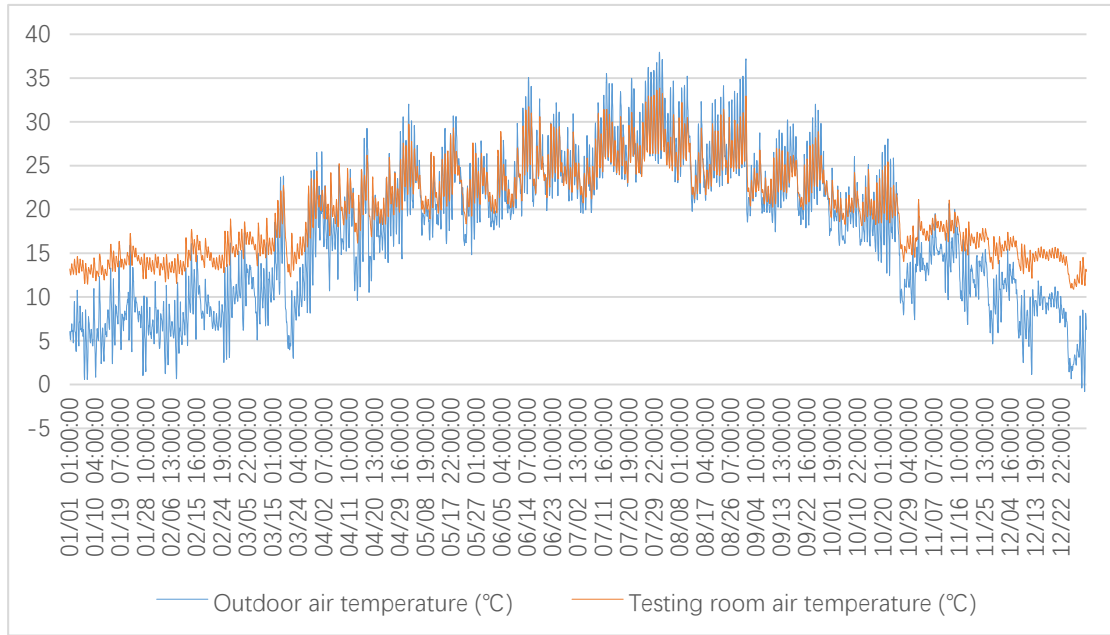


Figure 4-13. Simulated annual hourly indoor and outdoor air temperature of the testing room.

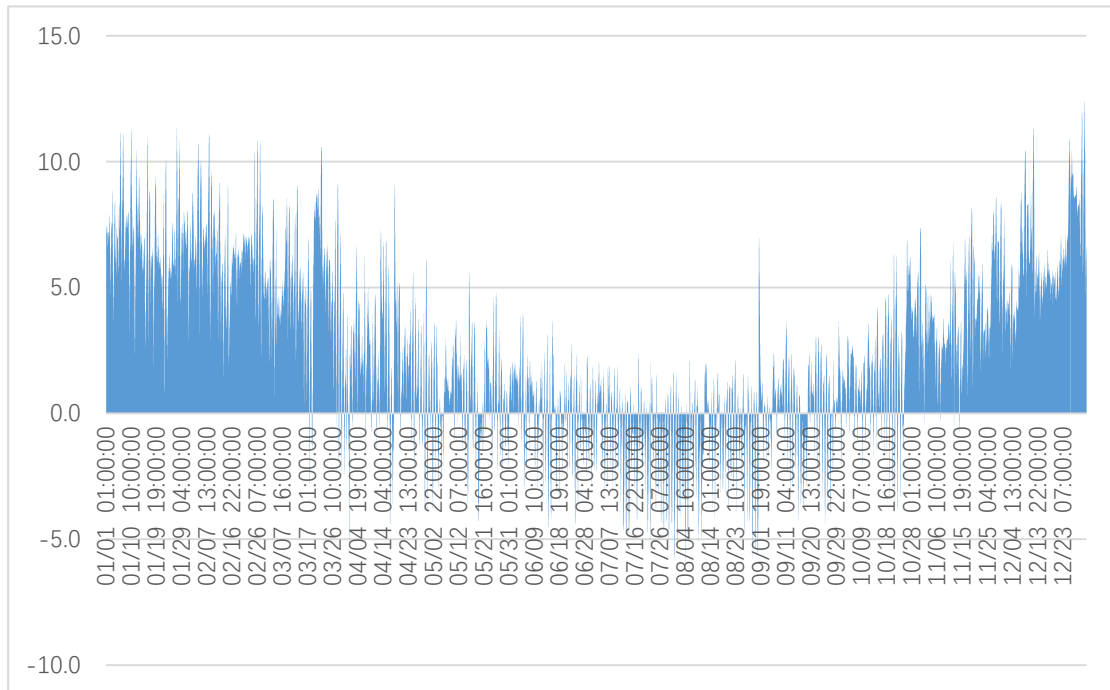


Figure 4-14. Differences of air temperature between the testing room and outside.

4.5 Summary

In this paper, we thoroughly analyze the current indoor thermal environment and thermal performance of an actual traditional dwelling located in northeast of Sichuan hills – the tested

building. Furthermore, we utilize a reliable simulation program aimed to predict building energy performance—EnergyPlus, simulate the indoor air temperature through the whole year for the tested building. From these comprehensive analysis, we can find following facts.

- Although the present exterior envelopes of the tested building performs the ability to resist heat loss in winter and heat gain to some extent, its alleviate degree is not enough to provide an acceptable indoor environment. According to the recorded data, the temperature in the room is at most 3.4°C higher than outside at the same moment during the winter testing period, while the highest temperature of indoor room and outdoor occurs almost at the same time during the summer testing period.
- The current value of heat transfer coefficient of exterior walls (K_{wall}) is 3 W/(m² K), while the value of heat transfer coefficient of roof (K_{roof}) is 5.2 W/(m² K). Meanwhile, the value of the thermal inertia of exterior wall (D_{wall}) is 1.74, while the thermal inertia of roof (D_{roof}) is 0.27. According to the Design standard for energy efficiency of residential buildings in hot summer and cold winter zone JGJ 134-2010 [2], the maximum value of heat transfer coefficient of exterior walls and the roof is 1.0 W/(m² K) and 0.8 W/(m² K) when the thermal inertia (D) does not exceed 2.5 ($D \leq 2.5$), therefore, both heat transfer coefficient of exterior walls (K_{wall}) and eat transfer coefficient of roof (K_{roof}) for the tested building do not meet the related energy efficiency standard.
- According to the Code for Thermal Design of Civil Buildings GB 50176-2016 [1], the maximum temperature of the highest day of the highest cumulative annual average daily temperature in the area is 39.10°C, whereas the temperatures of the inner surface of the exterior wall and the inner surface of the roof are 39.88°C and 40.66°C, respectively, thus both of them do not meet the requirement proposed by the related standard.
- According to the simulated results of indoor temperature of tested building, there are 3426 values of hourly indoor temperature are smaller than the winter indoor calculated temperature (18°C), while 1128 values of hourly indoor temperature are higher than the summer indoor calculated temperature (26°C), meaning there exist a lot of heating load and cooling load for the local actual traditional dwellings.

Reference

- [1] Ministry of Housing and Urban-Rural Development of the People's Republic of China. 2016. Code for thermal design of civil building GB50176-2016. Beijing: China Architecture & Building Press.
- [2] Ministry of Housing and Urban-Rural Development of the People's Republic of China, Design standard for energy efficiency of residential buildings in hot summer and cold winter zone JGJ134-2010, China Architecture & Building Press, Beijing, 2010.
- [3] Weather Data Download - Sichuan Nanchong 574110 (CSWD). https://energyplus.net/weather-location/asia_wmo_region_2/CHN/CHN_Sichuan.Nanchong.574110_CSWD, 2021
- [4] Chinese Standard Weather Data (CSWD). 2021. Available at <https://www.energyplus.net/weather/sources#CSWD>.
- [5] ASHRAE, A. G, Guideline 14-2002: Measurement of Energy and Demand Savings. ASHRAE, Atlanta, 2022.

CHAPTER 4. THERMAL PERFORMANCE OF THE TESTED BUILDING

CHAPTER 5. DETERMINE INSULATION THICKNESS OF EXTERIOR ENVELOPES FOR THE TRADITIONAL DWELLINGS IN NORTHEAST OF SICHUAN HILLS

Chapter 5

Determine Insulation Thickness of Exterior Envelopes for the Traditional Dwellings in Northeast of Sichuan Hills

CHAPTER 5. DETERMINE INSULATION THICKNESS OF EXTERIOR ENVELOPES F
OR THE TRADITIONAL DWELLINGS IN NORTHEAST OF SICHUAN HILLS

Chapter 5. Determine Insulation Thickness of Exterior Envelopes for the Traditional Dwellings in Northeast of Sichuan Hills

5. Determine Insulation Thickness of Exterior Envelopes for the Traditional Dwellings in Northeast of Sichuan Hills

5.1 Introduction	5-1
5.2 The optimum insulation thickness of exterior walls.....	5-6
5.2.1 Calculation method of optimum insulation thickness of exterior walls	5-6
5.2.2 Selection of the preferred insulation material	5-9
5.2.3 The impact law of influencing factors on optimum insulation thickness	5-13
5.2.4 The impact degree of influencing factors on optimum insulation thickness	5-15
5.3 The optimum insulation thickness of roof.....	5-18
5.3.1 Simulation model	5-18
5.3.2 Correlation of optimal economic thickness between insulation for roof and insulation for exterior walls	5-18
5.4 Summary	5-21
Reference	5-23
Nomenclature	5-28

CHAPTER 5. DETERMINE INSULATION THICKNESS OF EXTERIOR ENVELOPES F
OR THE TRADITIONAL DWELLINGS IN NORTHEAST OF SICHUAN HILLS

5. Determine Insulation Thickness of Exterior Envelopes for the Traditional Dwellings in Northeast of Sichuan Hills

5.1 Introduction

The Chinese total energy consumption of the whole building process in 2018 was 2.147 billion tce, accounting for 46.5% of the national total energy consumption, of which 1 billion tce was consumed during the building operation phase, accounting for 21.7% [1]. Northeast of Sichuan belongs to hot summer and cold winter climate zone (HSCW), and both summer and winter insulation is vital for this climate zone considering that the mean temperature of its coldest month is between 0°C and 10°C and its hottest month is between 25°C and 30°C [2]. Meanwhile, the energy consumption in this climate zone is even higher than that of cold zone [3]. On the other hand, rural buildings account for 24% of total building energy consumption when building energy consumption accounting for nearly half of the total national energy consumption [1]. So it is an essential approach to achieve zero carbon emissions by reducing the energy consumption of rural buildings. Enhancing the thermal performance of building exterior envelopes is crucial since their heat loss can account for 60%-80% of the total building heat loss [4]. Presently there are varied means to improve the building exterior envelopes thermal performance, including using insulation material [5], combing energy storage material like phase change material with walls [6,7], employing systems with variable thermal performance [8] and utilizing natural resources by photovoltaic system[9], Trombe wall [10-11] or geothermal heat pumps [12]. While considering the technical development, economic cost and availability, using conventional insulation is still one of the most commonly used energy-saving strategies for buildings in China [5]. It can enhance the thermal performance of exterior envelopes to improve the indoor thermal environment and reduce energy consumption efficiently. However, the cost of insulation will enlarge as insulation thickness increases even though the thermal resistance of exterior envelopes then grows leading to more energy savings for the building. And considering the inescapable fact that the growth of energy-saving rate is not linearly related to the increase in insulation [13], there must be an optimum thickness that can maximize the economic benefits created by insulation during its service life when the economy is considered [13-15]. Figure 5-1(a) displays the correlation between insulation material thickness and related costs, showing the existence of optimal economic thickness of insulation materials. Furthermore, Figure 5-1(b) depicts the annual heating and cooling load and the corresponding energy saving rate of applying EPS in the exterior walls of base model, it clearly presents that the increase rate of energy saving rate caused by insulation materials gradually slows down as the thickness of insulation material becomes thicker, meaning the decrease of energy cost will gradually flat with the increase of insulation material thickness, which is in consistent with the variation law of energy cost shown in Figure 5-1(a).

CHAPTER 5. DETERMINE INSULATION THICKNESS OF EXTERIOR ENVELOPES FOR THE TRADITIONAL DWELLINGS IN NORTHEAST OF SICHUAN HILLS

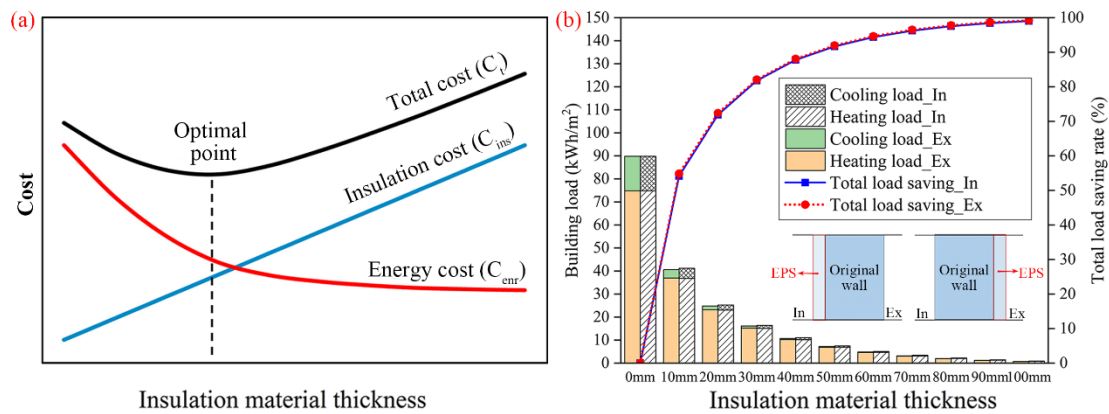


Figure 5-1. (a) Diagram of optimal point of insulation material thickness [15]; (b) Building heating and cooling load and saving rate vs. insulation material thickness of base model [16].

Sichuan province is located in southwestern China and has a large rural population. The total population of Sichuan Province was 83.75 million by the end of 2019, accounting for 46.2% of the total population in the province, and its proportion is much higher than the Chinese average (39.4%) [17,18]. In terms of income, per capita disposable income (PCDI) of the rural population in Sichuan province is 14670.1 CNY, which is lower than the national average of 16020.7 CNY [17, 18]. As for northeast of Sichuan, normally include these five cities: Guangyuan, Bazhong, Dazhou, Nanchong and Guang'an (Figure 1). Its economic development restricted by the hilly terrain and undeveloped transportation conditions is generally lower. For example, Nanchong has an area of 12499.2 km², which is equivalent to about 87% of the area of Chengdu – the provincial capital of Sichuan province but its per capita gross regional product in 2019 is only about 34.9% of Chengdu [18]. Furthermore, rural population shares of this region (74.7%, 72.0%, 66.3%, 70.9% and 74.5% of Guangyuan, Bazhong, Dazhou, Nanchong and Guang'an [18]) far exceed the provincial average (46.2%) and there are still a large number of primitive rural traditional dwellings without insulation construction on exterior walls and the indoor thermal environment can no longer meet the needs of modern residents. Therefore, adding insulation materials for exterior walls with the optimum economic thickness for traditional dwellings in northeast of Sichuan can maximize the economic benefits because it can effectively upgrade the thermal performance of exterior envelopes and it can cut down the energy consumption of buildings while simultaneously minimizing the economic burden imposed on residents by insulation renovation, which is more in line with the reality of the underdeveloped local economy.

CHAPTER 5. DETERMINE INSULATION THICKNESS OF EXTERIOR ENVELOPES FOR THE TRADITIONAL DWELLINGS IN NORTHEAST OF SICHUAN HILLS

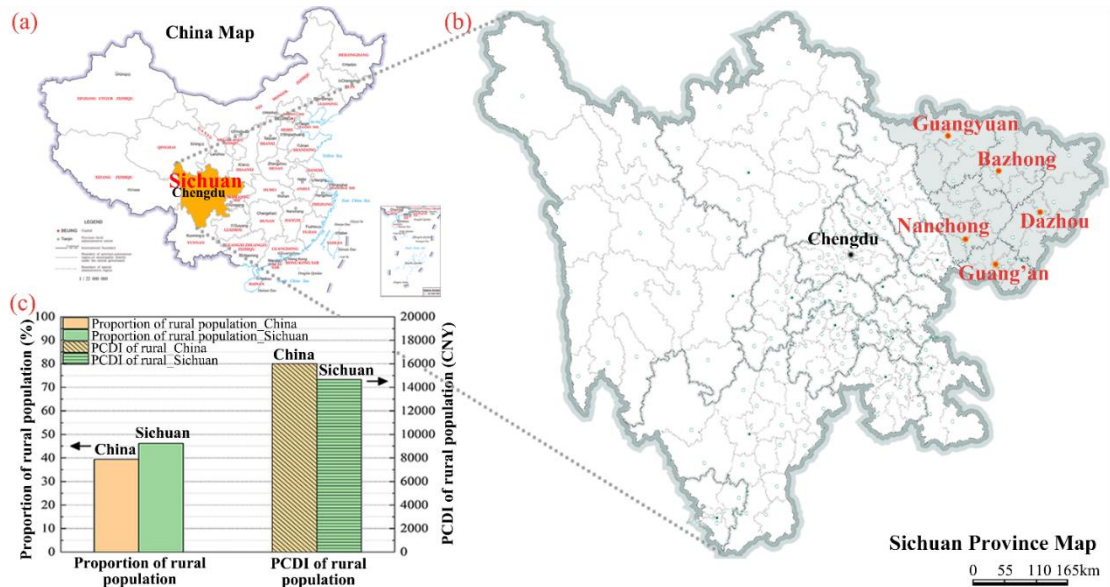


Figure 5-2. (a) Sichuan province location; (b) the region of northeast of Sichuan; (c) proportion and PCDI of rural population in China and Sichuan [17].

Currently, scholars around the world have conducted extensive research on the economic thickness of building exterior walls. Nuri Alpay Kurekci [19] predicted energy demand of buildings by heating and cooling degree-day method and used present worth factor (PWF) to calculate annual energy cost. Then the optimum insulation thickness was obtained by minimizing the total heating and cooling cost. Ultimately, they determined the optimum insulation thickness for 81 provincial centers in Turkey. Also by degree-day method and PWF method, L. Derradji et al. [20] found the optimum insulation thickness in Algeria was 1-2.5cm and its energy savings varied between 0.5 and 1.5 \$/m². Ozel [21] applied implicit finite-difference method to solve the differential equation expressed the transient one-dimensional heat conduction process and then calculated the yearly heating and cooling loads. On this basis, the optimum thickness of different insulation materials for building exterior walls in Elazığ, Turkey was calculated combined the energy demand and the PWF method. Results showed the optimum thickness of different insulation materials ranged from 0.054-0.192m and the payback period was between 3.56-8.85 years with a decrease of yearly fuel consumption and emissions by 68-89.5%. Similarly, Rosti et al. [16] employed the numerical solution to calculate the transmission loads and used PWF method to evaluate the economy of different insulation materials. They discovered the optimum thickness for different insulation materials was no more than 0.04m based on the analysis of buildings in eight cities representing all climatic zones in Iran. Raimundo et al. [22] simulated energy demand of four buildings with different types of use and different climate context, and used net present value (NPV) method to calculate the equivalent annual cost of the building used during its useful life. Finally, they displayed that 0-0.01m was the range of optimum insulation thickness for building walls in Portugal and revealed that regions with more intense climates require higher thermal insulation thicknesses. With the help of a simulation program (DesignBuilder) and evaluating the insulation material cost by the macroeconomic perspective (only energy costs, insulating material costs and emission costs were

CHAPTER 5. DETERMINE INSULATION THICKNESS OF EXTERIOR ENVELOPES FOR THE TRADITIONAL DWELLINGS IN NORTHEAST OF SICHUAN HILLS

considered), D'Agostino et al. [23] calculated optimum insulation thickness for building walls in Italy and found there were significant differences in the optimal insulation thickness in different cities even though within the same country. For instance, the optimum thickness for insulation materials were 0.08-0.1m and 0.02-0.04m for Milan and Palermo, respectively, while insulation was always disadvantageous for Cairo. For buildings in China, Yu et al. [24] improved heating and cooling degree-day method by considering the effect of solar radiation on building exterior envelopes to predict energy demand, and combined the P_1 - P_2 economic method to calculate the optimum insulation thickness for buildings in HSCW. Finally, they found that 0.053-0.236m was the optimum thickness range for insulation of building walls in HSCW, and the life cycle savings could be up to 39.0-54.4 $\$/m^2$ while the payback period was from 1.9 to 4.7 years. Also for buildings in HSCW, Liu et al. [25] used a coupled heat and moisture transfer model to predict building energy consumption and the P_1 - P_2 economic model was combined to evaluate the optimum insulation thickness, and eventually, they found that XPS with 0.081-0.105m could maximize the economic benefits in its service life (16.6-28.5 $\$/m^2$). And in the severe cold and cold zone, Geng et al. [26] analyzed the optimum thickness of vacuum insulation panels for the lightweight building by using dynamic building energy simulation software OpenStudio and the P_1 - P_2 economic model. They found the optimum thickness increases from 3.5mm to 31mm when climate becomes colder and the saving rate of total cost grown from 40.5% to 47.9%. On balance, the related studies of economic thickness of insulation for roof are not insufficient compared to the wall insulation, even though a few research have conducted some exploration, and meanwhile, most current calculation methods of optimal economic thickness of roof insulation materials are similar to that of wall insulation materials.

The previous study shows that calculating the optimum economic insulation thickness for building exterior walls (or roof) is twofold: one is the prediction of the building heating and cooling load demand, and the other is the assessment of the economy using economic models. Further, each part covers several influencing factors. Precisely, regardless of whether theoretical calculations or numerical simulations are used, the building cooling and heating load demands are determined by a conjunction of the climatic conditions, the thermal performance of exterior walls, the operating efficiency of heating and cooling equipment and the indoor temperature setting. While economic evaluation involves factors such as material cost, energy source price, present value of currency and evaluation period. Some researchers discussed the effect of these influencing factors on the result of optimum economic thickness based on acquiring the optimal economic thickness of insulation materials. By comparing the optimum insulation thickness for buildings in Turkey, N.A. Kurekci [19] found that optimum thickness increases with heating degree-day (HDD) and cooling degree-day (CDD) enlarge, respectively. Yu et al. [24] combined HDD , CDD and work efficiency of heating and cooling equipment as a comprehensive factor – DD , and revealed that the optimum insulation thickness was higher for larger DD . In addition, the optimum thickness declines as the overall wall thermal resistance extends [24]. For the economic model, optimum thickness increases as PWF grows [24, 26]. Additionally, Naouel Daouas [27] analyzed the single factor involved in PWF, and discovered that the service life of insulation, inflation rate and energy source cost had a positive relative with the optimum thickness of insulation, while discount rate and insulation material price

CHAPTER 5. DETERMINE INSULATION THICKNESS OF EXTERIOR ENVELOPES FOR THE TRADITIONAL DWELLINGS IN NORTHEAST OF SICHUAN HILLS

had a negative relative with the optimum thickness.

In the published studies, only the variation law of the optimum economic insulation thickness with the change of each influencing factor was discussed on the basis of the optimal thickness calculation, but the comparative analysis of the impact degree of these influencing factors on the value of optimal thickness is scarce. However, we can notice that the variation of the optimal thickness caused by the changing factors varies. For example, according to the results of optimum insulation thickness in Tunisian buildings [27], when inflation rate enlarges from 1% to 5%, the optimum thickness only extends from 0.088m to 0.115m, which only increases about 30% while inflation rate grows 400%. But the service life of insulation material extending from 5 years to 25 years in the same study causes the optimum thickness to enlarge about 130% (from 0.045m to 0.105m). In another study carried by Nuri Alpay Kurekci [19], optimum thickness was able to grow about 30% (from 0.057m to 0.074) when HDD only increased about 56% (from 2828°C d to 4423°C d). These phenomena indicate that each influencing factor has a diverse degree of impact on the optimum thickness of insulation materials. In fact, with the help of full or partial factor tests and statistical analysis, it is available to rank the impact degree of these influencing factors and to analyze their significance on optimum thickness. And based on the results, the most important influencing factor can be optimized so that the value of the optimal thickness can be reduced, and then the investment expenditure on insulation materials can be reduced, which can considerably alleviate the economic burden for the residents. Hence, the optimum thickness of five commonly used insulation materials was firstly determined under the local climate and economic context in this paper based on the degree-days method for predicting building energy consumption and the P_1 - P_2 economic model for assessing the economic circumstance. Then the appropriate insulation materials for local dwellings were recommended by evaluating the energy-saving effect, payback period and economic benefits based on EnergyPlus and dynamic investment payback period model. Furthermore, the most significant effect factor of the optimum thickness was revealed while the importance of all influencing factors was ranked by the orthogonal experiment design and analysis of variance (ANOVA). Finally, the economic and energy-saving potential created by further lowering the optimum insulation thickness were analyzed on the basis of guaranteeing indoor thermal comfort. Analysis in this chapter not only determines the optimum thickness of insulation materials and their energy-saving and economic benefits for traditional dwellings in northeast of Sichuan hills according to the current calculation standard but also reveals the enormous energy-saving and economic potential that can be achieved by rationally modifying the calculation standard based on the actual local circumstance. Additionally, we explore the correlation of the optimal economic thickness between the insulation for roof and the insulation for walls in this region in consideration that the normal calculation method of economic thickness for roof insulation is complex, and the fact that roof insulation and wall insulation exist simultaneously and the corresponding insulation materials are same in the actual project, thereby determining roof insulation thickness based on the result of optimal economic thickness of wall insulation is more convenient and efficiency. Finally, these results can provide a useful reference for residents and policy-makers to make decisions for insulation renovation from a novel perspective.

In this chapter, we have reviewed extensive related studies about optimal economic thickness of

CHAPTER 5. DETERMINE INSULATION THICKNESS OF EXTERIOR ENVELOPES FOR THE TRADITIONAL DWELLINGS IN NORTHEAST OF SICHUAN HILLS

insulation materials for building exterior envelopes, and introduce the related methods and findings, which are shown in section 5.1. Then in section 5.2, we calculate the optimal economic thickness of insulation materials for walls and the impact degree of influencing factors that can affect the results of optimal thickness are evaluated as well. Next, we also discuss the correlation of the optimal economic thickness between the insulation for roof and the insulation for walls in Section 5.3. Finally, section 5.4 summarizes the contents of this chapter.

5.2 The optimum insulation thickness of exterior walls

5.2.1 Calculation method of optimum insulation thickness of exterior walls

The opaque envelopes of buildings are affected by a composite effect of radiation, convection and conduction. Solar radiation is absorbed by the exterior wall surface materials and enters the indoor area, while at the same time, ambient air exchanges heat with the exterior wall surface through convection. Taking the exterior wall in winter heating season as an example, the heat transfer process can be expressed by the following equation:

$$q = U \times (T_{cal} - T_{air}) \quad (5-1)$$

where:

q is the heat loss per unit area of exterior wall, W/m^2 ;

U is the overall heat transfer coefficient of exterior wall, $W/(m^2 \cdot K)$;

T_{cal} is the calculated indoor constant temperature, $^{\circ}C$;

T_{air} is the outdoor air temperature, $^{\circ}C$.

Throughout the year, the absolute value of the difference between the average daily temperature and the calculated indoor temperature for winter heating (summer cooling) is added up to obtain the number of heating-degree (cooling-degree) day when the average daily outdoor temperature is lower than the calculated winter indoor temperature (higher than the calculated summer indoor temperature), expressed as HDD (CDD) [28]. Accordingly, the annual heating energy consumption per unit area of the exterior wall ($Q_{w,H}$) and annual cooling energy consumption ($Q_{w,C}$) can be calculated by Eqs. 5-2 and 5-3, respectively.

$$Q_{w,H} = 86400 \times HDD \times U \quad (5-2)$$

$$Q_{w,C} = 86400 \times CDD \times U \quad (5-3)$$

where:

$Q_{w,H}$ is the annual heating energy demand per unit area of the exterior wall, (J/m^2) ;

$Q_{w,C}$ is the annual cooling energy demand per unit area of the exterior wall, (J/m^2) ;

CHAPTER 5. DETERMINE INSULATION THICKNESS OF EXTERIOR ENVELOPES FOR THE TRADITIONAL DWELLINGS IN NORTHEAST OF SICHUAN HILLS

HDD is heating degree-day, ($^{\circ}C \cdot d$);

CDD is cooling degree-day, ($^{\circ}C \cdot d$).

The internal and external surface heat transfer resistance (R_i and R_e) are considered when calculating the thermal resistance of the wall since there is the convection process between walls and the ambient air, and their values are taken as $0.11(m^2 \cdot K)/W$ and $0.04(m^2 \cdot K)/W$ according to GB50176-2016 [2], respectively. Then the overall heat transfer resistance (R) and heat transfer coefficient (U) of exterior walls can be obtained by Eqs. (4) and (5). The difference of the overall heat transfer coefficient of exterior walls with and without insulation (ΔU) is calculated by Eq. 5-6.

$$R = R_i + R_{wt} + R_{ins} + R_e \quad (5-4)$$

$$U = \frac{1}{R_{wt} + R_{ins}} \quad (5-5)$$

$$\Delta U = \frac{1}{R_{wt}} - \frac{1}{R_{wt} + \frac{x}{\lambda_{ins}}} \quad (5-6)$$

where:

R_i is the heat transfer resistance of internal surface, ($m^2 \cdot K)/W$;

R_{wt} represents the heat transfer resistance of exterior wall without insulation, ($m^2 \cdot K)/W$;

R_{ins} represents the thermal resistance of insulation material, ($m^2 \cdot K)/W$;

R_e is the heat transfer resistance of external surface, ($m^2 \cdot K)/W$;

ΔU is the difference of the overall heat transfer coefficient of exterior wall between exterior walls with insulation and walls without insulation;

λ_{ins} is the thermal conductivity of insulation material, $W/(m \cdot K)$;

x is the thickness of insulation material, m.

In summer, room air conditioners are usually used for air conditioning in residential buildings in HSCW zone. Therefore, the annual cooling electric expense per unit area of exterior walls (E_C) is calculated by Eq. 5-7. EER in this paper is taken as 3.3 according to the provisions of JGJ134-2010 [29].

$$E_C = C_E \times \frac{0.024 \times U \times CDD}{EER} \quad (5-7)$$

where:

CHAPTER 5. DETERMINE INSULATION THICKNESS OF EXTERIOR ENVELOPES FOR THE TRADITIONAL DWELLINGS IN NORTHEAST OF SICHUAN HILLS

C_E is the electricity cost, its value is 0.52 CNY/kWh;

U is the overall heat transfer coefficient of exterior wall, W/(m² K);

CDD is the cooling degree-day, °C·d;

EER is the energy efficiency ratio of the cooling system.

Similarly, the annual heating electric expense per unit area of exterior walls (E_H) is calculated by Eq. 5-8. The heating equipment partly still are electric heaters since there is no centralized heating system in HSCW, so the comprehensive heating energy efficiency quota (η) is lower and is taken as 1.9 [24,29].

$$E_H = C_E \times \frac{0.024 \times U \times HDD}{\eta} \quad (5-8)$$

where:

C_E is the electricity cost, its value is 0.52 CNY/kWh;

U is the overall heat transfer coefficient of exterior wall, W/(m² K);

HDD is the heating degree-day, °C·d;

η is the comprehensive heating energy efficiency quota of the heating system.

P_1 - P_2 economic model proposed by Duffie and Bechman is often used to calculate the economic thickness of insulation materials [24, 30]. It takes into account the time value of money, so P_1 is calculated by Eq. 5-9:

$$P_1 = PWF(N_e, i, d) = \sum_{j=1}^{N_e} \frac{(1+i)^{j-1}}{(1+d)^j} = \begin{cases} \frac{1}{d-i} \left[1 - \left(\frac{1+i}{1+d} \right)^{N_e} \right] & i \neq d \\ \frac{N_e}{1+i} & i = d \end{cases} \quad (5-9)$$

where:

PWF represents the present worth factor;

N_e is the service life of insulation material in this paper, year, its value is 25 years;

i is the increase rate of electricity cost, %, its value is 1% [24];

d is the market discount rate, %, its value is 2.8% [14].

P_2 is the ratio of life cycle expenditures incurred, reflecting the subsequent maintenance costs during the life cycle of the insulation material. It is calculated by Eq. 5-10.

CHAPTER 5. DETERMINE INSULATION THICKNESS OF EXTERIOR ENVELOPES FOR THE TRADITIONAL DWELLINGS IN NORTHEAST OF SICHUAN HILLS

$$P_2 = D + (1 - D) \frac{PWF(N_{min}, 0, d)}{PWF(N_L, 0, m)} + M_s PWF(N_e, i, d) - \frac{R_v}{(1 + d)^{N_e}} \quad (5-10)$$

where:

D is the ratio of down payment to initial investment, %;

M_s is the ratio of first year miscellaneous costs to initial investment, %;

R_v is the ratio of resale value at the end of the analysis period to initial investment, %;

N_L is term of loan, year; and N_{min} is years over which mortgage payments contribute to the analysis period (usually the minimum of N_e and N_L), year.

The cost (C_{ins}) of the insulation renovation for traditional dwellings involves the cost of insulation materials and labor costs, as shown in Eq. 5-11:

$$C_{ins} = C_i x + C_p \quad (5-11)$$

where:

C_{ins} is the retrofit cost of exterior walls insulation, CNY/m²;

C_i is the material cost of insulation, CNY/m³;

C_p is the labor cost of insulation, CNY/m²;

x is the thickness of insulation material, m.

Then, the economic benefit brought by increasing the insulation material (S , CNY/m²) can be calculated by Eq. 5-12:

$$S = P_1 \times C_E \times \left(\frac{0.024 \times \Delta U \times CDD}{EER} + \frac{0.024 \times \Delta U \times HDD}{\eta} \right) - P_2 C_{ins} \quad (5-12)$$

The optimum economic thickness of insulation material (x_{op} , m) is obtained by taking the derivative of S since a greater S implies higher economic benefits, as Eq. (13) shows:

$$x_{op} = \sqrt{\frac{0.024 C_E \times P_1 \times \lambda_{ins}}{P_2 \times C_i} \times \left(\frac{CDD}{EER} + \frac{HDD}{\eta} \right) - R_{wt} \times \lambda_{ins}} \quad (5-13)$$

5.2.2 Selection of the preferred insulation material

5.2.2.1 Simulation model

The weather data of typical meteorological year (TMY) from Nanchong weather station were

CHAPTER 5. DETERMINE INSULATION THICKNESS OF EXTERIOR ENVELOPES FOR THE TRADITIONAL DWELLINGS IN NORTHEAST OF SICHUAN HILLS

analyzed for a more accurate understanding of the local climate. According to the annual hourly temperature in Fig.2 (a), the mean temperature of July is about 27.4°C and the highest can achieve 38°C. The mean temperature of January is only 6.9 °C although the temperature is almost above 0°C in winter, while the lowest temperature is minus 0.9°C. In addition, JGJ/T 346-2014 [28] clearly states that the heating degree-day (HDD18) is 1307 °C d and the cooling degree-day (CDD26) is 156°C d in this region. This demonstrates that the local demand for heating in winter is higher compared to cooling in summer. And in order to grasp the architectural characteristics of local traditional dwellings, field investigation work has been carried out in 2017. The local dwellings are usually 1 story with the additional attic as a storage space. The roof is double-sloped to facilitate drainage, and covered with small tiles and no roof board. The main building structure is column and tie construction, using wooden columns as building support structures. Local clay with a thickness of 60mm-100mm is the most common material for envelope construction and the common construction is displayed in Figure 5-3 (b) and Figure 5-3 (c), and it is notable that there is no sort of insulation materials in exterior envelopes.

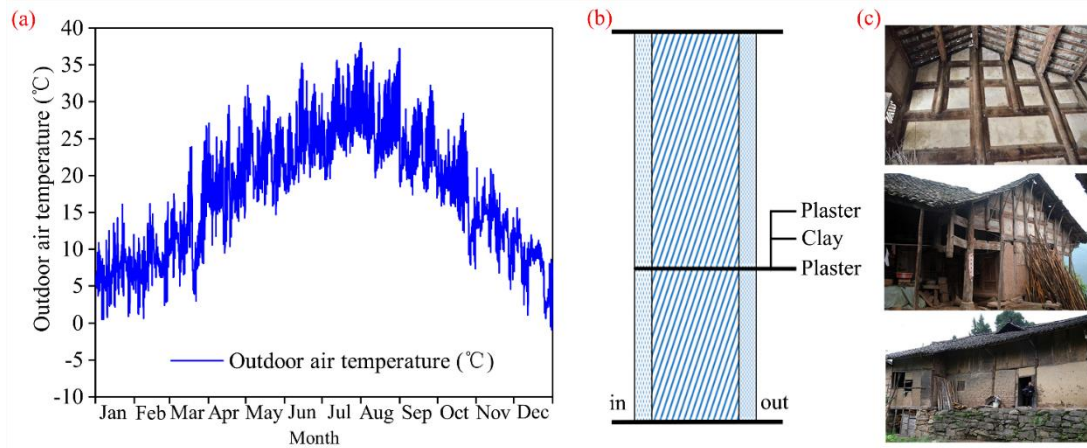
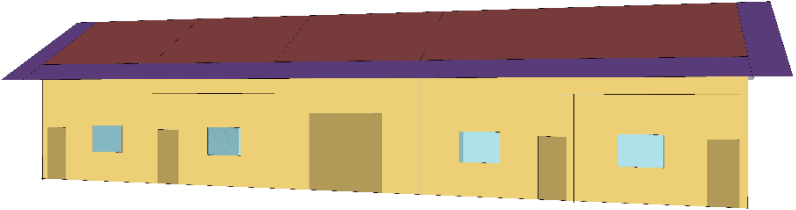


Figure 5-3. (a) Annual hourly air temperature of Nanchong [39]; (b) diagram of exterior walls construction of traditional dwellings in northeast of Sichuan hills; (c) photographs of traditional dwellings in northeast of Sichuan hills.

Table 5-1 displays the model information for the dynamic simulation by EnergyPlus. The construction of exterior walls is the common local construction form. The heat transfer resistance of the roof is only about 0.19(m²-K)/W due to it is covered with only one layer of tiles thus the energy-saving effect will be weakened if the insulation of exterior walls is added with the poor thermal performance of the roof. In addition, the poor airtightness will increase the indoor-outdoor heat exchange and diminish the energy-saving effect of the insulation strategy [40,41]. Therefore, the roof heat transfer coefficient and window airtightness of the simulation model meet the minimum limits required by JGJ134-2010 [29]. The indoor lighting intensity is taken as 7 W/m² according to GB/T50824-2013 [42]. And the calculated indoor temperature in winter and summer is 18°C and 26°C, respectively [2,29]. The thermophysical properties of walls materials are shown in Table 2.

CHAPTER 5. DETERMINE INSULATION THICKNESS OF EXTERIOR ENVELOPES FOR THE TRADITIONAL DWELLINGS IN NORTHEAST OF SICHUAN HILLS

Table 5-1 Building information.

Model description	Detail
Three-dimensional simulation model	
Floor area	217.80 m ²
Height	3m (1F room); 2.8m (attic)
Orientation	South facing
Exterior wall construction	20mm gypsum plaster (outside layer) + 100mm clay +20mm gypsum plaster
Heat transfer coefficient of roof	0.5 [W/ (m ² K)]
Window size	0.9m × 1.2m
Heat transfer coefficient of window	1.63 [W/ (m ² K)]
Airtightness	2.5 [m ³ /(m h)]
Heating load	73.67 kWh/m ²
Cooling load	14.71 kWh/m ²

Five commonly used wall insulation materials are used for analysis, i.e. expanded polystyrene (EPS), stone wool board (SW), polyurethane foam (PU), extruded polystyrene (XPS), and phenolic foam (PF). Table 2 lists their thermophysical properties and material price. In addition, the labor cost is taken as 27.4 CNY/m² referring to the reference price provided by Chengdu Engineering Cost Information [43].

Table 5-2 Insulation material information [2, 43].

Material	Thermal conductivity/ λ ins [W/(m K)]	Density/ ρ (kg/m ³)	Material cost / Ci (CNY/m ³)
Clay	0.76	1600	/
Gypsum plaster	0.76	1500	/
Expanded polystyrene (EPS)	0.039	20	442
Stone wool board (SW)	0.041	60	420
Polyurethane foam (PU)	0.024	35	550
Extruded polystyrene (XPS)	0.030	35	472
Phenolic foam (PF)	0.034	60	400

5.2.2.2 Results and discussion

The optimum thickness of these five insulation materials was obtained according to Eq. (13) (see

CHAPTER 5. DETERMINE INSULATION THICKNESS OF EXTERIOR ENVELOPES FOR THE TRADITIONAL DWELLINGS IN NORTHEAST OF SICHUAN HILLS

Table 5-3). Among them, PU has the lowest thickness, about 28.9% less than the thickest (EPS), but its thermal resistance value [3.38 (m² K)/W] is still higher than that of other insulation materials due to its low thermal conductivity [0.024 W/(m K)]. In addition, XPS and PF have comparable performance with PU with their thermal resistance values are only about 3.3% and 1.8% lower than PU, respectively; while the thermal resistance of EPS and SW are lower than PU by 13.6% and 24.3%, respectively, which have a large difference. It is obvious that the lower the overall heat transfer coefficient of the walls, the better since the priority for local dwellings is to improve the winter insulation performance of the exterior walls because the heating load accounts for about 83.4% of the total cooling and heating loads. Therefore, the wall with PU which has the lowest overall heat transfer coefficient [0.269 W/(m² K)] is best from this perspective.

According to the results of energy demands shown in Table 5-3, it is no doubt that all five insulation materials with optimum economic thickness can effectively lower the cooling and heating load. In detail, the energy-saving rate of cooling load is all around 83%, and the energy-saving rate of the heating load is between 54.8% and 56.9%. In terms of the total heating and cooling loads, PU creates the highest energy-saving rate of 61.4%, followed tightly by PF (61.3%) and XPS (61.2%). As for SW, which has the worst thermal performance, it still saves about 59.4% of the total cooling and heating loads, only about 2% lower than that of the PU even though its related overall heat transfer coefficient is about 14.5% higher than that of the PU. It indicates that the influence of material category on the energy-saving effect is not significant when the optimum thickness is also applied. Hence, it is necessary to combine the economic analysis to select the appropriate insulation materials for local dwellings.

The last two rows of Table 5-3 show the payback period and economic benefits of each insulation material during its service life (25 years). PU creates about 8.3% higher economic benefits (306.7CNY/m²) than the worst economic performer (EPS) during the service life due to its excellent thermal performance even PU is the most expensive material. At the same time, it has the shortest dynamic payback period (7.8 years) of all five insulation materials. As for XPS and PF, their optimum thickness is higher than PU but their price is lower, meanwhile, the difference between the energy-saving effect of both and PU is minor. Therefore, the final economic benefits of XPS and PF are comparable to PU, and their saving amounts are only 2-5CNY/m² lower than PU. The economic benefit of SW is about 4.8% lower than PU while EPS generates the least electric expense savings (283.2CNY/m²) and has the longest payback time (8.7 years). Consequently, PU is the preferred insulation material for traditional dwellings in northeast of Sichuan hills whether in terms of energy-saving effect or economic benefits, followed by PF and XPS.

Table 5-3 Optimum thickness, energy-saving and economic evaluation of insulation materials.

Insulation material	EPS	SW	PU	XPS	PF
Optimum thickness / x_{op} (m)	0.114	0.105	0.081	0.098	0.113
Thermal resistance of insulation / R_{ins} (m ² K/W)	2.91	2.56	3.38	3.25	3.32

Table 5-3 Optimum thickness, energy-saving and economic evaluation of insulation materials (Cont).

Overall heat transfer coefficient of wall / U ($W/m^2 K$)	0.308	0.346	0.269	0.279	0.273
Heating load (kWh/m^2)	32.52 (55.9%)	33.27 (54.8%)	31.77 (56.9%)	31.93 (56.7%)	31.83 (56.8%)
Cooling load (kWh/m^2)	2.49 (83.1%)	2.61 (82.3%)	2.36 (83.9%)	2.39 (83.7%)	2.35 (84%)
Total loads (kWh/m^2)	35.01 (60.4%)	35.88 (59.4%)	34.13 (61.4%)	34.32 (61.2%)	34.18 (61.3%)
Payback period (year)	8.7	8.0	7.8	8.0	7.9
Economic benefits during N_e (CNY/m^2)	283.2	292.1	306.7	301.1	304.6

5.2.3 The impact law of influencing factors on optimum insulation thickness

According to Eq. (13), it is directly seen that the growth of electricity cost (C_E) and increase rate of electricity cost (i) will cause the optimum thickness of insulation material (x_{op}) extends, by contrast, the enlargement of heat transfer resistance of exterior wall without insulation (R_{wt}), material cost of insulation (C_i) and the market discount (d) will lead to x_{op} decrease. Taking PU as an example, Fig. 3 shows links between these factors and x_{op} more clearly. Fig. 3(a) depicts that with the growth of d , implying a currency devaluation, i.e., a decrease in the value of the energy-saving benefits brought by insulation, x_{op} shows a decreasing trend. In Fig. 3(b), x_{op} increases as i enlarges while the larger i is the higher increase speed of x_{op} is. The reason of this positive correlation is that the bigger i indicates the more expensive of electricity cost, so the saving energy caused by insulation material becomes more valuable. Therefore, in order to achieve the highest economic benefits, x_{op} further enlarges. Similarly, the price of electricity (C_E) increases leads to x_{op} become thicker but the increase speed of x_{op} declines with higher C_E . Further, the performances of i and C_E are in harmony with those obtained by Naouel Daouas [27]. In contrast to i and C_E which are related to the electricity cost, higher insulation material cost (C_i) generates the more expensive initial investment, so it results in thinner x_{op} in order to ensure the best economic benefits. The relation of service life of insulation material (N_e) and x_{op} is not plain according to Eq. (13), whereas it's obvious that x_{op} enlarges with N_e extends from Fig. 3(e). Additionally, the growth of x_{op} slows down after the service life reaches about 40 years while the trend is consistent with the results in [27]. As for Fig. 3(f), the increment of R_{wt} means that its contribution to the overall heat transfer resistance of the wall expands while the thermal resistance required to be contributed by the insulation material decreases since the thermal resistance of the base wall (R_{wt}) and the insulation material (R_{ins}) jointly compose the overall heat transfer resistance of the exterior wall. Consequently, an enlargement in R_{wt} will lead to a decrease in the optimum thickness of the insulation material and it is consistent with the results in [15].

CHAPTER 5. DETERMINE INSULATION THICKNESS OF EXTERIOR ENVELOPES FOR THE TRADITIONAL DWELLINGS IN NORTHEAST OF SICHUAN HILLS

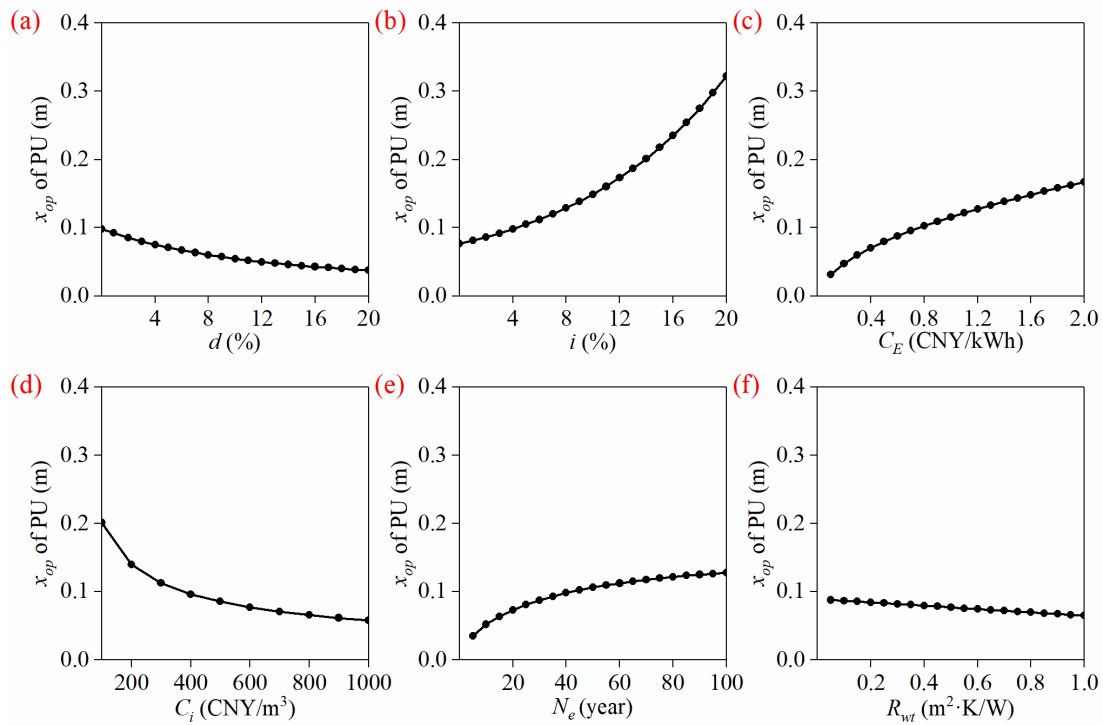


Figure 5-4. Impact law of parts of influencing factors on the optimum thickness of PU: (a) discount rate; (b) increase rate of electric price; (c) electric price; (d) insulation material price; (e) service life of insulation material; (f) the heat transfer resistance of exterior wall without insulation.

The calculated indoor temperatures of rural buildings without any heating and air conditioning measures in HSCW can be taken as 8 °C in winter and 30 °C in summer according to the GB/T 50824-2013 [42]. So Fig. 4 demonstrates the change of PU optimum thickness with the variation of T_{cal} since T_{cal} can affect the optimum thickness by influencing the value of HDD and CDD . The optimum thickness is 0.025m when T_{cal} is taken as 8 °C in winter, which is only about 30% of that when T_{cal} is 18 °C due to the building heating load demand drops dramatically as the T_{cal} decreases. Similarly, the demand for cooling load declines as T_{cal} enlarges in summer since the demand for insulation of the envelope weakens, so the optimum thickness of PU presents a decreasing trend. It is obvious that appropriately lowering the winter and increasing the summer calculated indoor temperature can lessen the optimum thickness of insulation materials, thus saving insulation renovation expenses. However, the optimum thickness of PU (0.078m) is only about 3.7% less than the original state (0.081m) when the summer indoor calculated temperature ups to 30 °C. The reason of this phenomenon is cooling demand in summer only accounts for 16.6% of total heating and cooling loads. By contrast, heating load is 5 time of cooling load, so the focus should be the economic benefit potential caused by lowering T_{cal} in winter. When T_{cal} in winter decreases from 18°C to 8°C, the optimum thickness of PU drops from 0.081m to 0.025m with a decrease rate of 69.1%. The cost of insulation materials correspondingly cut down from 45.1CNY/m² to 13.75CNY/m², which is even saved by about 69.5% and probably more acceptable to local residents with lower incomes.

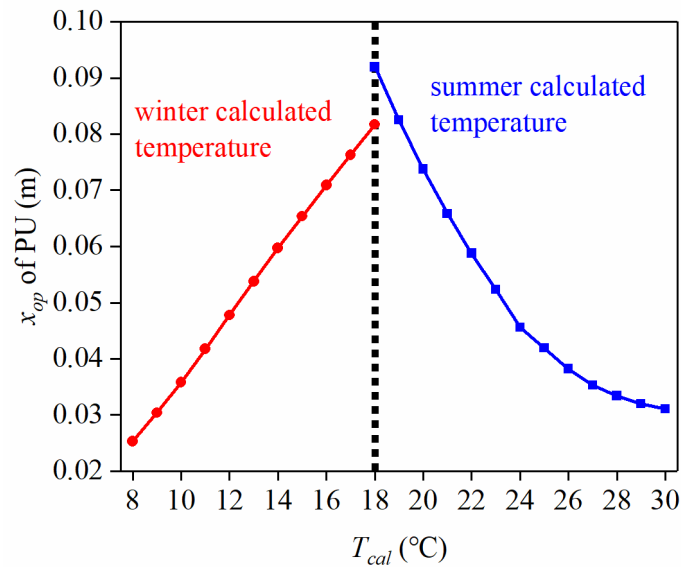


Figure 5-5. The impact law of indoor calculated temperature on optimum thickness.

5.2.4 The impact degree of influencing factors on optimum insulation thickness

Subsection 5.2.3 takes PU as an example and analyses the laws of the variation of optimum thickness with parts of influencing factors, but the impact degree of each influencing factor cannot be judged. Therefore, this section explores the influence degree of each factor on the optimum thickness by the orthogonal experiment design and ANOVA. The optimum thickness of insulation is influenced by 12 factors according to Eq. (13), but there are only 11 variables needed to be discussed in the final because P_2 is taken as a constant value ($P_2=1$) since insulation retrofitting is usually completed in one go and does not involve loan and subsequent maintenance costs. Three levels are taken for each variable (shown in Table 5-4), and among them, the values of CDD and HDD are obtained by statistically counting the weather data since they are determined jointly by the outdoor air temperature and the indoor calculated temperature. In detail, the values of CDD are taken to correspond to the values of $CDD25$, $CDD26$, and $CDD30$, respectively; the values of HDD are taken to correspond to the values of $HDD8$, $HDD14$, and $HDD18$, respectively. The standard orthogonal array $L_{27}(3^{13})$ was employed and it can be found in [38]. Table 5-5 displays the detailed values taken for each test and the corresponding calculation results. $K_1(K_2, K_3)$ denotes the sum of the results of the 1st (2nd, 3rd) level in 9 trials of the factor.

Table 5-4 Influencing factors and levels for the orthogonal experiment design.

Factor	d	i	C_E	C_i	λ_{ins}	R_{wt}	N_e	CDD	HDD	EER	η
levels	%	%	CNY/kWh	CNY/m ³	W/m K	(m ² K)/W	year	°C·d	°C·d	W/W	W/W
1	0.03	0	0.52	400	0.025	0.25	20	193	106	3.2	2
2	0.05	0.01	0.62	500	0.040	0.50	25	129	718	3.4	3
3	0.07	0.02	0.72	600	0.055	0.75	30	10	1327	3.6	4

CHAPTER 5. DETERMINE INSULATION THICKNESS OF EXTERIOR ENVELOPES FOR THE TRADITIONAL DWELLINGS IN NORTHEAST OF SICHUAN HILLS

Table 5-5 Orthogonal experiment design and test results.

No	d	i	C_E	C_i	λ_{ins}	R_{wt}	N_e	CDD	HDD	EER	η	Error	x_{op} m
1	1	1	1	1	1	1	1	1	1	1	1	1	0.030
2	1	1	1	1	2	2	2	2	2	2	2	2	0.058
3	1	1	1	1	3	3	3	3	3	3	3	3	0.065
4	1	2	2	2	1	1	1	2	2	2	3	3	0.045
5	1	2	2	2	2	2	2	3	3	3	1	1	0.104
6	1	2	2	2	3	3	3	1	1	1	2	2	0.018
7	1	3	3	3	1	1	1	3	3	3	2	2	0.069
8	1	3	3	3	2	2	2	1	1	1	3	3	0.027
9	1	3	3	3	3	3	3	2	2	2	1	1	0.085
10	2	1	2	3	1	2	3	1	2	3	1	2	0.050
11	2	1	2	3	2	3	1	2	3	1	2	3	0.047
12	2	1	2	3	3	1	2	3	1	2	3	1	0.010
13	2	2	3	1	1	2	3	2	3	1	3	1	0.071
14	2	2	3	1	2	3	1	3	1	2	1	2	0.006
15	2	2	3	1	3	1	2	1	2	3	2	3	0.090
16	2	3	1	2	1	2	3	3	1	2	2	3	0.009
17	2	3	1	2	2	3	1	1	2	3	3	1	0.028
18	2	3	1	2	3	1	2	2	3	1	1	2	0.115
19	3	1	3	2	1	3	2	1	3	2	1	3	0.066
20	3	1	3	2	2	1	3	2	1	3	2	1	0.025
21	3	1	3	2	3	2	1	3	2	1	3	2	0.033
22	3	2	1	3	1	3	2	2	1	3	3	2	0.002
23	3	2	1	3	2	1	3	3	2	1	1	3	0.054
24	3	2	1	3	3	2	1	1	3	2	2	1	0.053
25	3	3	2	1	1	3	2	3	2	1	2	1	0.037
26	3	3	2	1	2	1	3	1	3	2	3	2	0.084
27	3	3	2	1	3	2	1	2	1	3	1	3	0.020
K_1^2 0.25100.1475 0.1713 0.2125 0.1436 0.2725 0.1096 0.1989 0.0216 0.1866 0.2809 0.1962													
K_2^2 0.1815 0.1962 0.1722 0.1962 0.1875 0.1806 0.2591 0.2190 0.2304 0.1731 0.1648 0.1892 1.301													
K_3^2 0.1399 0.2247 0.2228 0.1576 0.2391 0.1253 0.2125 0.1498 0.4543 0.2052 0.1332 0.1789													

Table 5-6 summarizes ANOVA results based on the 27 tests in Table 5-5. The influence degree of each factor on the optimum thickness was obtained in descending order according to their F value because the magnitude of F value reveals the importance of the influence of the factor on the test results: HDD , N_e , η , R_{wt} , d , λ_{ins} , i , CDD , C_E/C_i , ERR . Furthermore, according to the principle of F test, if the result is smaller than the critical F value, the observed differences among the sample averages could reasonably be due to random chance alone, whereas the result is larger than the critical F value, the observed differences among the sample averages could not reasonably be due to random chance alone [44]. Therefore, among these 11 factors, only HDD is highly

CHAPTER 5. DETERMINE INSULATION THICKNESS OF EXTERIOR ENVELOPES FOR THE TRADITIONAL DWELLINGS IN NORTHEAST OF SICHUAN HILLS

statistically significant and N_e is statistically significant, while the rest of parameters are not statistically significant.

Table 5-6 Results of ANOVA.

Variance source	Square sum of the deviation / S	Degree of freedom / f	Mean square of the deviation/ MS	F value/ F	Critical F value / $F_{\alpha}(f_F, f_E)$	Significance
d	0.00091	2	0.00046	3.54	$F_{0.01}(2,4)=18$	
i	0.00047	2	0.00024	1.85	$F_{0.05}(2,4)=6.94$	
C_E	0.00023	2	0.00012	0.92		
C_i	0.00023	2	0.00012	0.92		
λ_{ins}	0.00067	2	0.00034	2.62		
R_{wt}	0.00158	2	0.00079	6.08		
N_e	0.00189	2	0.00095	7.31		*
CDD	0.00039	2	0.00020	1.54		
HDD	0.01579	2	0.00790	60.77		**
ERR	0.00008	2	0.00004	0.31		
η	0.00163	2	0.00082	6.31		
Error	0.00051	4	0.00013			
Total	0.02438	26				

Considering that if the optimum thickness of the insulation material can be further decreased, which means the cost of insulation renovation is reduced and the economic burden on residents who have lower incomes is lightened, there are potential economic benefits of lowering the optimum insulation thickness. Based on the ANOVA, HDD is the most important influencing factor for the optimum thickness, and meanwhile it presents a positive correlation with optimum thickness according to Eq. (13) and Fig.4. Therefore, the smaller its value, the lower the economic thickness is. Additionally, HDD is determined by both the mean outdoor daily temperature and the calculated winter indoor temperature while the former is fixed and uncontrollable, so reducing the value of HDD can only be achieved by lowering the calculated winter indoor temperature.

The calculated winter indoor temperature of residential buildings in HSCW is taken as 18°C under the current standard JGJ134-2010 [29]. However, one fact that has been revealed by worldwide studies is that long-term thermal history can affect thermal perception [45-49] and people live in different climate zone have different indoor comfort temperatures [47, 49]. Unlike the severe cold and cold zone in China, HSCW is not centrally heated in winter and an investigation by Wu et al. [50] showed that people who long lived in naturally ventilated buildings (approximately 11.8°C ± 3.4 °C in winter) in HSCW has an obvious higher thermal sensation vote than people who long lived in heated space in winter in severe cold condition of 12°C. Moreover, 10°C is found to be the lowest acceptable internal temperature without heating in HSCW [51]. On the other hand, percentage of acceptable votes of rural occupants is higher than that of urban occupants at the same operative temperature in HSCW [52]. Another comparable study on indoor thermal comfort of rural and urban

CHAPTER 5. DETERMINE INSULATION THICKNESS OF EXTERIOR ENVELOPES FOR THE TRADITIONAL DWELLINGS IN NORTHEAST OF SICHUAN HILLS

residents in HSCW conducted by Xiong et al. [53] also revealed that rural residents tend to be more tolerant of cold conditions in winter. Therefore, there exists the possibility of reducing the calculated winter indoor temperature while ensuring indoor comfort for rural traditional dwellings in the northeast of Sichuan hills. Still taking PU as an example (see Table 5-7), if the calculated winter indoor temperature is taken as 16°C [54-55], its optimum thickness is 0.071m and the material cost is reduced by 7.6%. Moreover, the total energy demand is reduced by about 79.1% compared before and after using PU when T_{cal} is 16°C, and the dynamic payback period is 4.8 years while the final economic benefit of PU in its service life (25 years) is 546.6 CNY/m², which is 78.2% improvement than T_{cal} is 18°C. Thus a rational reduction of the calculated winter indoor temperature on the basis of ensuring indoor comfort can reduce insulation renovation expenses while being able to derive greater economic benefits in the long run.

Table 5-7 Energy-saving and economic potential by reducing the calculated winter indoor temperature (taking PU as an example).

T_{cal} (°C)	x_{op} (m)	Pre-retrofit load (kWh/m ²)			Post-retrofit load (kWh/m ²)			C_{ins} (CNY/m ²)	P_D (years)	Economy (CNY/m ²)
		Heating	Cooling	Total	Heating	Cooling	Total			
18	0.081	73.67	14.71	88.38	31.77	2.36	34.13	72	7.8	306.7
16	0.071	32.49	14.71	47.20	7.38	2.48	9.86	66.5	4.8	546.6

5.3 The optimum insulation thickness of roof

5.3.1 Simulation model

Insulation materials discussed in this part are the same as insulation materials analyzed in section 5.2, including expanded polystyrene (EPS), stone wool board (SW), polyurethane foam (PU), extruded polystyrene (XPS), and phenolic foam (PF), and their thermophysical properties and price are shown in Table 5-2. The air change hour of the model is set as 1 h⁻¹ according to the [29]. When calculating the energy demand, the indoor calculated temperature in summer and in winter is 26°C and 18°C, respectively.

In order to explore the links between optimum insulation thickness of roof and optimum insulation thickness of exterior walls, the thickness of insulation materials for exterior walls is 0.114m (EPS), 0.105m (SW), 0.081m (PU), 0.098m (XPS) and 0.113m (PF) according to the optimal thickness of exterior walls displayed in Table 5-3. Then the insulation thickness of roof is set as 0.5 – 3 times of insulation thickness of exterior walls, while the interval is 0.5 time. Meanwhile, the same insulation material is used for exterior walls with the optimal thickness obtained in subsection 5.2. And finally the corresponding energy saving rate, payback period and economic benefits during the service life (25 years) are calculated by EnergyPlus and DIPP.

5.3.2 Correlation of optimal economic thickness between insulation for roof and insulation for exterior walls

The corresponding energy saving rates of various insulation category and thickness of roof are summarized in Table 5-8. It's obvious that no matter what insulation material category, the corresponding saving rate of energy demand increases as the thickness enlarges. Meanwhile, the

CHAPTER 5. DETERMINE INSULATION THICKNESS OF EXTERIOR ENVELOPES FOR THE TRADITIONAL DWELLINGS IN NORTHEAST OF SICHUAN HILLS

acceleration of saving rate gradually slows down as the insulation material becomes thicker, which is consistent with the variation law of insulation thickness of exterior walls, and the saving rate finally remains in a particular value especially after the roof insulation is 2 times the thickness of the wall insulation. Therefore, there must exist the optimum economic thickness for each insulation material.

Table 5-8 Corresponding energy saving rate of various insulation category and thickness of roof.

Times	Saving rate_EPS	Saving rate_SW	Saving rate_PU	Saving rate_XPS	Saving rate_PF
0.5	60%	58%	62%	62%	62%
1	66%	65%	68%	68%	68%
1.5	69%	67%	70%	70%	70%
2	70%	69%	71%	71%	71%
2.5	71%	70%	72%	71%	72%
3	71%	70%	72%	72%	72%

We have already known that there exists optimal point of insulation thickness when the economy is considered from the above analysis of the optimal insulation thickness for exterior walls. Similarly, there exists optimal thickness for each roof insulation material because the price of each insulation material is different while they have alike energy saving performance. Figure 5-6 depicts the economic benefits of each insulation material with different thickness, and we can see no matter what the insulation material category is, the highest benefit appears when the roof insulation is 1.5 times the thickness of exterior walls insulation. And polyurethane foam (PU) also performs the best economy with 586.6 CNY/m², followed by phenolic foam (PF) with 585.7 CNY/m², extruded polystyrene (XPS) with 583.6 CNY/m², stone wool board (SW) with 575.3 CNY/m², and expanded polystyrene (EPS) with 574.4 CNY/m². Additionally, Figure 5-6 also depicts the predicted trend lines (dash lines) of each insulation material and the value of square R is larger than 0.8, showing the predicted trend lines are in good agreement with the calculated values (dots), indicating the relationship between insulation thickness of roof and insulation thickness of exterior walls can be expressed by equations. And it is noticeable that the optimal economic benefits occurs between 1-2 times, but considering the operability in the actual project, we recommend roof insulation is 1.5 times as thick as the exterior walls.

CHAPTER 5. DETERMINE INSULATION THICKNESS OF EXTERIOR ENVELOPES FOR THE TRADITIONAL DWELLINGS IN NORTHEAST OF SICHUAN HILLS

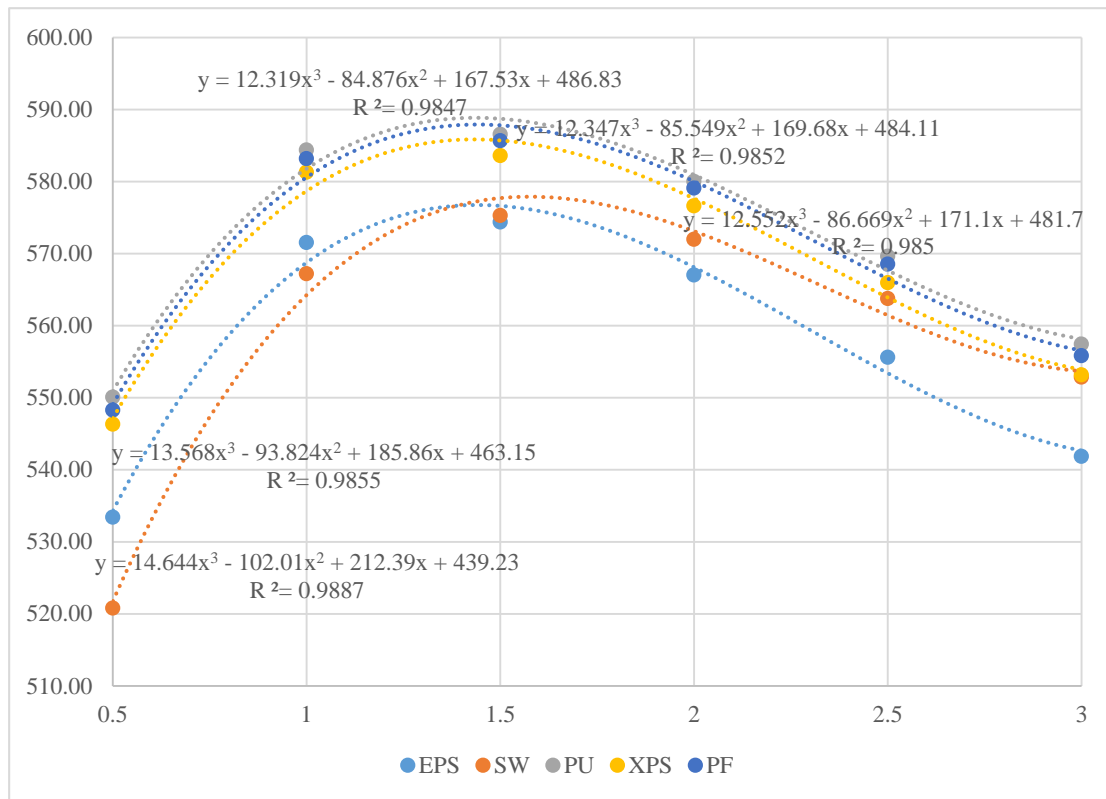


Figure 5-6. Economic benefits during service life (25 years) versus the relationship between insulation thickness of roof and insulation thickness of exterior walls

Table 5-9 displayed the dynamic investment payback period (DPP) of each insulation material with different thickness. It is no doubt that the thicker the insulation material is the longer the payback period is, but these payback period are shorter than that of insulation materials used for exterior walls. Additionally, the payback period of roof insulation is much shorter than that of exterior walls insulation. In detail, when adopt the best ratio of the roof insulation thickness and walls insulation thickness (1.5 times), the longest payback period of roof insulation is only 1.6 years while the shortest payback period of walls insulation material is 7.8 years. The main reason of this phenomenon is that the cost of roof insulation is much cheaper than wall insulation because of the area of roof is about half of the exterior walls.

Table 5-9 Dynamic investment payback period (N_p) of various insulation category and thickness of roof.

Times	N_p _EPS (year)	N_p _SW (year)	N_p _PU (year)	N_p _XPS (year)	N_p _PF (year)
0.5	0.6	0.5	0.5	0.5	0.5
1	1.1	1.0	1.0	1.0	1.0
1.5	1.6	1.4	1.4	1.5	1.4
2	2.1	1.9	1.9	1.9	1.9
2.5	2.6	2.3	2.3	2.4	2.4
3	3.2	2.8	2.8	2.9	2.8

5.4 Summary

Increasing insulation material thickness can enhance the thermal performance of exterior envelopes but there exists the optimum thickness when considering the economy. Northeast of Sichuan hills have a large number of rural traditional dwellings and there is not any insulation material on the exterior envelopes. Adding insulation materials with optimum thickness for exterior envelopes can lighten the economic burden of residents while enhancing their thermal performance and lowering energy consumption. Meanwhile, insulation material used in roof construction is usually the same as the insulation material utilized for exterior walls, thus exploring the correlation between the economic thickness of roof and the economic thickness of exterior walls can help us determine the thickness of roof insulation material more efficiently.

This chapter derived the calculation method of the optimum economic thickness of five commonly used insulation materials for building exterior walls in northeast of Sichuan hills, including expanded polystyrene (EPS), stone wool board (SW), polyurethane foam (PU), extruded polystyrene (XPS), and phenolic foam (PF). Next, we compared and ranked the importance of all of the factors which could affect the optimum thickness by orthogonal test and analysis of variance, and on the basis of these results, the potential energy-saving and economic benefits from changing the most important influencing factor were analyzed. Finally, we discussed the correlation between the optimal economic thickness of insulation material for roof and the optimal economic thickness of insulation material for exterior walls. From the exploration of economic thickness of insulation material for both exterior walls and roof, we can conclude the following results:

- In terms of insulation materials adopted for exterior walls of traditional dwellings in northeast of Sichuan hills, the optimum thickness of expanded polystyrene (EPS), stone wool board (SW), polyurethane foam (PU), extruded polystyrene (XPS), and phenolic foam (PF) is 0.114m, 0.105m, 0.081m, 0.098m and 0.113m, respectively.
- Polyurethane foam is the preferred insulation material among these five commonly used insulation materials in this region. When it is utilized in exterior walls with the corresponding economic thickness, its economic benefit can achieve 306.7 CNY/m² during 25 years while its dynamic payback period is 7.8 years.
- The impact degree of each influencing factor on the optimum thickness in descending order is heating degree-day (*HDD*), service life (N_e), comprehensive heating energy efficiency quota of the heating system (η), heat transfer resistance of exterior wall without insulation (R_{wr}), market discount rate (d), thermal conductivity of insulation material (λ_{ins}), increase rate of electricity cost (i), cooling degree-day (*CDD*), electricity cost (C_E), material cost of insulation

CHAPTER 5. DETERMINE INSULATION THICKNESS OF EXTERIOR ENVELOPES FOR THE TRADITIONAL DWELLINGS IN NORTHEAST OF SICHUAN HILLS

(C_i), energy efficiency ratio of the cooling system (ERR).

- Lowering the calculated winter indoor temperature from 18 °C to 16 °C can save about 7.6% of the insulation renovation expenses, and improve the energy-saving rate and economic benefits by about 29.5% and 78.2%, respectively.
- No matter what the insulation material category is, the highest benefit appears when the roof insulation is 1.5 times the thickness of exterior walls insulation.
- In terms of insulation materials with corresponding economic thickness added on roof construction, polyurethane foam (PU) also performs the best economy with 586.6 CNY/m², followed by phenolic foam (PF) with 585.7 CNY/m², extruded polystyrene (XPS) with 583.6 CNY/m², stone wool board (SW) with 575.3 CNY/m², and expanded polystyrene (EPS) with 574.4 CNY/m².

CHAPTER 5. DETERMINE INSULATION THICKNESS OF EXTERIOR ENVELOPES FOR THE TRADITIONAL DWELLINGS IN NORTHEAST OF SICHUAN HILLS

Reference

- [1] China Building Energy Consumption Research Report (2020). <https://www.cabee.org/site/content/24021.html>, 2021 (Accessed 3 November 2021).
- [2] Ministry of Housing and Urban-Rural Development of the People's Republic of China, Code for thermal design of civil building GB50176-2016, China Architecture & Building Press, Beijing, 2016.
- [3] Fu X, Han A. Energy saving of buildings in hot summer and cold winter zone of China, China Architecture & Building Press, Beijing, 2002.
- [4] X. Meng, B. Yan, Y. Gao, J. Wang, W. Zhang, E. Long, Factors affecting the in situ measurement accuracy of the wall heat transfer coefficient using the heat flow meter method, *Energy and Buildings*. 86 (2015): 754-765. <https://doi.org/10.1016/j.enbuild.2014.11.005>
- [5] Y. Lin, L. Zhao, W. Yang, X. Hao, CQ. Li, A review on research and development of passive building in China, *Journal of Building Engineering*. 42.8(2021):102509. <https://doi.org/10.1016/j.jobe.2021.102509>
- [6] Y. Gao, F. He, X. Meng, Z. Wang, M. Zhang, H. Yu, W. Gao, Thermal behavior analysis of hollow bricks filled with phase-change material (PCM), *Journal of Building Engineering*. 31 (2020): 101447. <https://doi.org/10.1016/j.jobe.2020.101447>
- [7] Z. Liu, J. Hou, X. Meng, B. J. Dewancker, A numerical study on the effect of phase-change material (PCM) parameters on the thermal performance of lightweight building walls. *Case Studies in Construction Materials*. 15 (2021): e00758. <https://doi.org/10.1016/j.cscm.2021.e00758>
- [8] P. Si, Y. Lv, X. Rong, L. Shi, J. Yan, X. Wang, An innovative building envelope with variable thermal performance for passive heating systems. *Applied Energy*. 269(2020): 115175. <https://doi.org/10.1016/j.apenergy.2020.115175>
- [9] B. Huang, K. Xing, S. Pullen, L. Liao, K. Huang, Ecological–economic assessment of renewable energy deployment in sustainable built environment, *Renewable Energy*. 161 (2020): 1328–1340. <https://doi.org/10.1016/j.renene.2020.08.004>
- [10] L. Zhang, Y. Hou, Z. Liu, J. Du, L. Xu, G. Zhang, L. Shi, Trombe wall for a residential building in Sichuan-Tibet alpine valley – a case study. *Renewable Energy*, 156 (2020): 31–46. <https://doi.org/10.1016/j.renene.2020.04.067>
- [11] N. Simes, M. Manai, I. Simes, Energy performance of solar and trombe walls in mediterranean climates, *Energy*. 234 (2021): 121197. <https://doi.org/10.1016/j.energy.2021.121197>
- [12] O. Ozgener, Use of solar assisted geothermal heat pump and small wind turbine systems for heating agricultural and residential buildings, *Energy*. 35 (2010): 262-268. <https://doi.org/10.1016/j.energy.2009.09.018>

CHAPTER 5. DETERMINE INSULATION THICKNESS OF EXTERIOR ENVELOPES FOR THE TRADITIONAL DWELLINGS IN NORTHEAST OF SICHUAN HILLS

- [13] L. Zhang, C. Hou, J. Hou, D. Wei, Y. Hou, Optimization analysis of thermal insulation layer attributes of building envelope exterior wall based on DeST and life cycle economic evaluation, *Case Studies in Thermal Engineering*. 14 (2019): 100410. <https://doi.org/10.1016/j.csite.2019.100410>
- [14] H. Huang, Y. Zhou, R. Huang, H. Wu, Y. Sun, G. Huang, T. Xu, Optimum insulation thicknesses and energy conservation of building thermal insulation materials in Chinese zone of humid subtropical climate, *Sustainable Cities and Society*. 52 (2020): 101840. <https://doi.org/10.1016/j.scs.2019.101840>
- [15] B. Rosti, A. Omidvar, N. Monghasemi, Optimal insulation thickness of common classic and modern exterior walls in different climate zones of Iran, *Journal of Building Engineering*. 27 (2020): 100954. <https://doi.org/10.1016/j.jobee.2019.100954>
- [16] J. Hou, T. Zhang, Z. Liu, L. Zhang, H. Fukuda, Application evaluation of passive energy-saving strategies in exterior envelopes for rural traditional dwellings in northeast of Sichuan hills, China, *International Journal of Low-Carbon Technologies*. 17 (2022): 342–355.
- [17] China Statistical Yearbook 2020. <http://www.stats.gov.cn/tjsj/ndsj/2020/indexch.htm>, 2021 (accessed 14 August 2021).
- [18] Sichuan Statistical Yearbook 2020. <http://tjj.sc.gov.cn/tjnj/cs/2020/zk/indexch.htm>, 2021 (accessed 14 August 2021).
- [19] N.A. Kurekci, Determination of optimum insulation thickness for building walls by using heating and cooling degree-day values of all Turkey’s provincial centers, *Energy and Buildings*. 118 (2016): 197-213. <https://doi.org/10.1016/j.enbuild.2016.03.004>
- [20] L. Derradji, K. Imessad, M. Amara, F.B. Errebai, A study on residential energy requirement and the effect of the glazing on the optimum insulation thickness, *Applied Thermal Engineering*. 112 (2017): 975-985. <http://dx.doi.org/10.1016/j.applthermaleng.2016.10.116>
- [21] M. Ozel, Cost analysis for optimum thicknesses and environmental impacts of different insulation materials, *Energy and Buildings*. 49 (2012): 552-559. <https://doi.org/10.1016/j.enbuild.2012.03.002>
- [22] A.M. Raimundo, N.B. Saraiva, A.V.M. Oliveira, Thermal insulation cost optimality of opaque constructive solutions of buildings under Portuguese temperate climate, *Building and Environment*. 182 (2020): 107107. <https://doi.org/10.1016/j.buildenv.2020.107107>
- [23] D. D. Agostino, F. De. Rossi, M. Marigliano, C. Marino, F. Minichiello, Evaluation of the optimal thermal insulation thickness for an office building in different climates by means of the basic and modified “cost-optimal” methodology. *Journal of Building Engineering*, 24 (2019): 100743. <https://doi.org/10.1016/j.jobee.2019.100743>
- [24] J. Yu, C. Yang, L. Tian, D. Liao, A study on optimum insulation thicknesses of external walls in hot summer and cold winter zone of China, *Applied Energy*. 86.11 (2009): 2520-2529.

CHAPTER 5. DETERMINE INSULATION THICKNESS OF EXTERIOR ENVELOPES FOR THE TRADITIONAL DWELLINGS IN NORTHEAST OF SICHUAN HILLS

<https://doi.org/10.1016/j.apenergy.2009.03.010>

- [25] X. Liu, Y. Chen, H. Ge, P. Fazio, G. Chen, X. Guo, Determination of optimum insulation thickness for building walls with moisture transfer in hot summer and cold winter zone of China, *Energy and Buildings*. 109 (2015): 361-368. <https://doi.org/10.1016/j.proeng.2017.10.153>
- [26] Y. Geng, X. Han, H. Zhang, L. Shi, Optimization and cost analysis of thickness of vacuum insulation panel for structural insulating panel buildings in cold climates, *Journal of Building Engineering*. 33 (2021): 101853. <https://doi.org/10.1016/j.jobe.2020.101853>
- [27] N. Daouas, A study on optimum insulation thickness in walls and energy savings in Tunisian buildings based on analytical calculation of cooling and heating transmission loads, *Applied Energy*. 88.1 (2011): 156-164. <https://doi.org/10.1016/j.apenergy.2010.07.030>
- [28] Ministry of Housing and Urban-Rural Development of the People's Republic of China, Standard for weather data of building energy efficiency JGJ/T 346-2014, China Architecture & Building Press, Beijing, 2014.
- [29] Ministry of Housing and Urban-Rural Development of the People's Republic of China, Design standard for energy efficiency of residential buildings in hot summer and cold winter zone JGJ134-2010, China Architecture & Building Press, Beijing, 2010.
- [30] J.A. Duffie, W.A. Bechman, *Solar energy and thermal process*, New York, 1991.
- [31] M.K. Urbikain, M.G. Davies, A frequency domain estimation of wall conduction transfer function coefficients, *Energy & Buildings*. 51.AUG.(2012):191-202. <https://doi.org/10.1016/j.enbuild.2012.05.005>
- [32] U.S. Department of Energy, *EnergyPlus™ version 8.7 documentation input output reference*, 2016.
- [33] D.B. Crawley, L.K. Lawrie, F.C. Winkelmann, W.F. Buhl, Y.J. Huang, C.O. Pedersen, R.K. Strand, R.J. Liesen, D.E. Fisher, M.J. Witte, *Energyplus: creating a new-generation building energy simulation program*, *Energy and Buildings*. 33.4(2001):319-331. [https://doi.org/10.1016/S0378-7788\(00\)00114-6](https://doi.org/10.1016/S0378-7788(00)00114-6)
- [34] A.A. Serageldin, A. Abdeen, M.S. Ahmed, A. Radwan, S. Ookawara, Solar chimney combined with earth to-air heat exchanger for passive cooling of residential buildings in hot areas, *Solar Energy*. 206(2020):145-162. <https://doi.org/10.1016/j.solener.2020.05.102>
- [35] H. Huang, W.I.B.W.M. Nazi, Y. Yu, Y. Wang, Energy performance of a high-rise residential building retrofitted to passive building standard – A case study, *Applied Thermal Engineering*. 181 (2020): 115902. <https://doi.org/10.1016/j.applthermaleng.2020.115902>
- [36] X. Liu, *Engineering Economy (3rd Edition)*, China Architecture & Building Press, Beijing, 2015

CHAPTER 5. DETERMINE INSULATION THICKNESS OF EXTERIOR ENVELOPES FOR THE TRADITIONAL DWELLINGS IN NORTHEAST OF SICHUAN HILLS

- [37] J. Zhu, D.A.S. Chew, S. Lv, W. Wu, Optimization method for building envelope design to minimize carbon emissions of building operational energy consumption using orthogonal experimental design (OED), *Habitat International*. 37 (2013): 148-154. <https://doi.org/10.1016/j.habitatint.2011.12.006>
- [38] K. Chen, *Design and Analysis of Experiments* (2nd Edition), Tsinghua University Press, Beijing, 2005
- [39] Weather Data Download - Sichuan Nanchong 574110 (CSWD). https://energyplus.net/weather-location/asia_wmo_region_2/CHN/CHN_Sichuan.Nanchong.574110_CSWD, 2021 (Accessed 10 November 2021).
- [40] S. Chen, M.D. Levine, H. Li, P. Yowargana, L. Xie, Measured air tightness performance of residential buildings in North China and its influence on district space heating energy use, *Energy and Buildings*. 51 (2012):157-164. <https://doi.org/10.1016/j.enbuild.2012.05.004>
- [41] E. Cuce, Role of airtightness in energy loss from windows: experimental results from in-situ tests, *Energy and Buildings*. 139 (2017): 449-455. <https://doi.org/10.1016/j.enbuild.2017.01.027>
- [42] Ministry of Housing and Urban-Rural Development of the People's Republic of China, Design standard for energy efficiency of rural residential buildings GB/T 50824-2013, China Architecture & Building Press, Beijing, 2012.
- [43] J. Xu, *Chengdu Engineering Cost Information*, Sichuan University Press, Chengdu, 2021
- [44] A. F. Siegel, *Practical Business Statistics* (Seventh Edition), Academic Press, 2017. <https://doi.org/10.1016/C2015-0-00463-4>
- [45] M. Jowkar, H.B. Rijal, A. Montazami, J. Brusey, A. Temeljotov-Salaj, The influence of acclimatization, age and gender-related differences on thermal perception in university buildings: Case studies in Scotland and England, *Building and Environment*. 179 (2020): 106933. <https://doi.org/10.1016/j.buildenv.2020.106933>
- [46] M. Luo, W. Ji, B. Cao, Q. Ouyang, Y. Zhu, Indoor climate and thermal physiological adaptation: Evidences from migrants with different cold indoor exposures, *Building and Environment*. 98 (2016): 30-38. <https://doi.org/10.1016/j.buildenv.2015.12.015>
- [47] B. Cheng, Y. Fu, M. Khoshbakht, L. Duan, J. Zhang, S. Rashidian, Characteristics of thermal comfort conditions in cold rural areas of china: A case study of stone dwellings in a tibetan village, *Buildings*. 8.4 (2018): 49. <https://doi.org/10.3390/buildings8040049>
- [48] C. Buonocore, R. De Vecchi, V. Scalco, R. Lamberts, Influence of recent and long-term exposure to air-conditioned environments on thermal perception in naturally-ventilated classrooms, *Building and Environment*. 156 (2019): 233-242. <https://doi.org/10.1016/j.buildenv.2019.04.009>
- [49] M. Jowkar, R.D. Dear, J. Brusey, Influence of long-term thermal history on thermal comfort

CHAPTER 5. DETERMINE INSULATION THICKNESS OF EXTERIOR ENVELOPES FOR THE TRADITIONAL DWELLINGS IN NORTHEAST OF SICHUAN HILLS

- and preference, *Energy and Buildings*. 210.Mar.(2020):109685.1-109685.12. <https://doi.org/10.1016/j.enbuild.2019.109685>
- [50] Y. Wu, H. Liu, B. Chen, B. Li, R. Kosonen, J. Jokisalo, T. Chen, Effect of long-term thermal history on physiological acclimatization and prediction of thermal sensation in typical winter conditions, *Building and Environment*. 179(2020):106936. <https://doi.org/10.1016/j.buildenv.2020.106936>
- [51] B. Lin, Z. Wang, Y. Liu, Y. Zhu, Q. Ouyang, Investigation of winter indoor thermal environment and heating demand of urban residential buildings in China's hot summer–Cold winter climate region, *Building and Environment*. 101 (2016): 9-18. <https://doi.org/10.1016/j.buildenv.2016.02.022>
- [52] J. Han, W. Yang, J. Zhou, G. Zhang, Q. Zhang, D. J. Moschandreas, A comparative analysis of urban and rural residential thermal comfort under natural ventilation environment, *Energy and Buildings*. 41.2 (2009): 139-145. <https://doi.org/10.1016/j.enbuild.2008.08.005>
- [53] X.A.C. Yan, J.L. B, J.K. C, Understanding differences in thermal comfort between urban and rural residents in hot summer and cold winter climate, *Building and Environment*. 165(2019): 106393. <https://doi.org/10.1016/j.buildenv.2019.106393>
- [54] C. Xu, S. Li, X. Zhang, S. Shao, Thermal comfort and thermal adaptive behaviours in traditional dwellings: A case study in Nanjing, China, *Building and Environment*. 142 (2018): 153-170. <https://doi.org/10.1016/j.buildenv.2018.06.006>
- [55] Z. Wang, R. de Dear, B. Lin, Y. Zhu, Q. Ouyang, Rational selection of heating temperature set points for China's hot summer–Cold winter climatic region, *Building and Environment*. 93 (2015): 63-70. <https://doi.org/10.1016/j.buildenv.2015.07.008>

CHAPTER 5. DETERMINE INSULATION THICKNESS OF EXTERIOR ENVELOPES FOR THE TRADITIONAL DWELLINGS IN NORTHEAST OF SICHUAN HILLS

Nomenclature

Nomenclature	C_i	Material cost of insulation, (CNY/m ³)	
q	Heat loss per unit area of exterior wall, (W/m ²)	C_p	Labor cost of insulation, (CNY/m ²)
U	Overall heat transfer coefficient of exterior wall, [W/(m ² K)]	P_D	Dynamic investment payback period, (year)
T_{cal}	Calculated indoor constant temperature, (°C)	i_0	Benchmark discount rate, (%)
$Q_{w,H}$	Annual heating energy demand per unit area of the exterior wall, (J/m ²)	T'	Number of the first year with positive cumulative discounted value
$Q_{w,C}$	Annual cooling energy demand per unit area of the exterior wall, (J/m ²)	t'	Number of the last year with negative cumulative discounted value
CDD	Cooling degree-day, (°C·d)	CI	Cash inflow, (CNY/year)
HDD	Heating degree-day, (°C·d)	CO	Cash outflow, (CNY/year)
T_{cal}	Indoor calculated temperature, (°C)	P/F	Present-value compound interest factor
R_i	Heat transfer resistance of internal surface, [(m ² K)/W]	\dot{Q}_i	Convective internal loads, (J)
R_{wt}	Heat transfer resistance of exterior wall without insulation, [(m ² K)/W]	h_i	Inside surface coefficient of heat transfer, [W/(m ² K)]
R_e	Heat transfer resistance of external surface, [(m ² K)/W]	C_z	Heat capacity of zone air and internal thermal mass, [J/(kg K)]
EER	Energy efficiency ratio of the cooling system	C_p	Zone air specific heat, [J/(kg K)]
η	Comprehensive heating energy efficiency quota	C_T	Heat capacity multiplier, [J/(kg K)]
λ_{ins}	Thermal conductivity of insulation material, [W/(m K)]	\dot{m}_{inf}	Zone infiltration mass flow rate, (kg/s)
C_E	Electricity cost, (CNY/kWh)	A_i	Zone surface area, (m ²)
E_C	Annual cooling electric expense per unit area of exterior walls, (CNY/m ²)	\dot{Q}_{sys}	Air systems load, (J)
E_H	Annual heating electric expense per unit area of exterior walls, (CNY/m ²)	\dot{Q}_{load}	Total heating and cooling loads, (J)
C_{ins}	Retrofit cost of exterior walls insulation, (CNY/m ²)	T_∞	Temperature of Outdoor air, (°C)
N_e	Service life of insulation material, (year)	T_{zi}	Interzone air temperature, (°C)
i	Increase rate of electricity cost, (%)	t	temperature, (°C)
d	Market discount rate, (%)	ρ_{air}	Air density, (kg/m ³)
N_L	Term of loan, (year)		Abbreviations

CHAPTER 5. DETERMINE INSULATION THICKNESS OF EXTERIOR ENVELOPES FOR THE TRADITIONAL DWELLINGS IN NORTHEAST OF SICHUAN HILLS

Nomenclature (Cont)

D	Ratio of down payment to initial investment, (%)	PCDI	Per capita disposable income
M_s	Ratio of first year miscellaneous costs to initial investment, (%)	PWF	Present worth factor
R_v	Ratio of resale value at the end of the analysis period to initial investment, (%)	NPV	Net present value
N_{min}	Years over which mortgage payments contribute to the analysis period, (year)	EPS	Expanded polystyrene
S	Economic benefit brought by increasing the insulation material, (CNY/m ²)	SW	Stone wool board
x	Thickness of insulation material, (m)	PU	Polyurethane foam
x_{op}	Optimum economic thickness of insulation material, (m)	XPS	Extruded polystyrene
T_{si}	Inside surface temperature, (°C)	PF	Phenolic foam
T_z	Zone air temperature, (°C)	HSCW	Hot summer and cold winter climate zone
T_{sup}	Air system supply air temperature, (°C)	AVOVA	analysis of variance

CHAPTER 5. DETERMINE INSULATION THICKNESS OF EXTERIOR ENVELOPES F
OR THE TRADITIONAL DWELLINGS IN NORTHEAST OF SICHUAN HILLS

CHAPTER 6. PARAMETRIC AND ECONOMIC ANALYSIS OF PHASE CHANGE
MATERIALS (PCM) ON ENERGY SAVING FOR TRADITIONAL DWELLINGS IN
NORTHEAST OF SICHUAN HILLS

Chapter 6

Parametric and Economic Analysis of Phase Change Materials (PCM) on Energy Saving for Traditional Dwellings in Northeast of Sichuan Hills

CHAPTER 6. PARAMETRIC AND ECONOMIC ANALYSIS OF PHASE CHANGE
MATERIALS (PCM) ON ENERGY SAVING FOR TRADITIONAL DWELLINGS IN
NORTHEAST OF SICHUAN HILLS

Chapter 6. Parametric and Economic Analysis of Phase Change Materials (PCM) on Energy Saving for Traditional Dwellings in Northeast of Sichuan Hills

6. Parametric and Economic Analysis of Phase Change Materials (PCM) on Energy Saving for Traditional Dwellings in Northeast of Sichuan Hills	6-1
6.1 Introduction.....	6-1
6.2 Materials and methods	6-3
6.2.1 Simulation model	6-3
6.2.2 Model validation	6-5
6.2.3 Evaluation indicator	6-7
6.3 Results and discussion.....	6-7
6.3.1 Effect of PCM melting temperature and location on energy saving	6-7
6.3.2 Effect of PCM thickness on energy saving	6-8
6.3.3 Effect of PCM phase transition temperature radius on energy saving	6-9
6.3.4 Effect of PCM latent heat on energy saving.....	6-10
6.3.5 Effect of PCM density on energy saving.....	6-11
6.3.6 Effect of PCM thermal conductivity on energy saving	6-12
6.3.7 Effect of PCM specific heat on energy saving	6-13
6.3.8 Comparison of energy-saving performance between recommended PCM and present PCM products.....	6-14
6.3.9 Economic analysis of PCM selection.....	6-15
6.3.10 Selection of PCM for this study region.....	6-19
6.4 Summary	6-20
Reference	6-22

CHAPTER 6. PARAMETRIC AND ECONOMIC ANALYSIS OF PHASE CHANGE
MATERIALS (PCM) ON ENERGY SAVING FOR TRADITIONAL DWELLINGS IN
NORTHEAST OF SICHUAN HILLS

6. Parametric and Economic Analysis of Phase Change Materials (PCM) on Energy Saving for Traditional Dwellings in Northeast of Sichuan Hills

6.1 Introduction

The energy consumption of the building sector occupies nearly 40% of global energy consumption [1], while in China, total energy consumption of the whole building process in 2018 was 2.147 billion tce, accounting for 46.5% of the total national energy consumption, of which 1 billion tce was consumed during the building operation phase [2]. Meanwhile, rural buildings contribute 24% of building energy consumption during the operation phase [2], therefore it is an essential approach to achieving carbon neutral by reducing energy consumption of rural buildings. However, it is challenging because the energy demand in rural regions is growing owing to the increased income and desire for a more comfortable indoor thermal environment for local residents. In order to control the building energy consumption, lowering heating and cooling loads is unavoidable since the major portion of the energy consumption in buildings is related to them [3], and globally, energy consumption for space heating and cooling even exceeds 40% and 61% of energy demand in commercial and residential buildings, respectively [4]. Additionally, it is imperative to enhance their thermal performance considering that the heat loss of exterior envelopes can count for 60%-80% of the total building heat loss [5].

Currently, there are extensive studies focusing on applying thermal energy storage (TES) to realize energy conservation, where phase change material (PCM) is an effective TES medium due to its large amount of latent heat [6,7] and broad phase change temperature range [8]. Hence the application of PCM has vast potential to reduce energy demand of buildings because it is able to phase change in a particular temperature range and then alleviate the impact of outdoor temperature variation on the indoor environment, thereby lower energy demand for heating and cooling, and improve occupant thermal comfort [9,10]. Preceding related research has manifested the remarkable contribution of incorporating PCM into building envelopes to control both heating load [11, 12] and cooling load [9, 13-14]. The result obtained by Nghana and Tariku [15] demonstrated that the application of PCM can lower heating energy demand by up to 57% during winter. In another optimization study of PCM parameters for U.S. buildings, annual heat gain even could be reduced by 35.6% and 47.2% when the proper transition temperature and location of PCM were adopted in Denver and Billings, respectively [9]. Nevertheless, sometimes the optimal PCM for lowering cooling load may have a negative impact on heating load reduction, and vice versa. For example, also in the study carried out by Kishore et. al [9], the amount of heat loss increased in Denver and Billings although application of PCM created a remarkable reduction of cooling demand, therefore evaluating thermal performance of PCM based on the whole year period perspective is essential. By evaluating the impact of PCM-drywalls on energy-saving effect for residential buildings in European climates, Soares et. al [13] concluded that an optimal solution of using PCM to decrease annual energy consumption can be found for each climate, and PCM-drywalls were particularly suitable for Mediterranean climate, even 62% of energy saving could be obtained for the Csb-Coimbra climate, while 10%-46% of energy-saving rate was achieved for other climates. The above studies display the great energy-saving potential of PCM, however, the effect of PCM is not necessarily positive on energy conservation. Tunçbilek et al. [14] found that energy saving can be

CHAPTER 6. PARAMETRIC AND ECONOMIC ANALYSIS OF PHASE CHANGE MATERIALS (PCM) ON ENERGY SAVING FOR TRADITIONAL DWELLINGS IN NORTHEAST OF SICHUAN HILLS

up to 12.8% when proper transition temperature and thickness of PCM were adopted under the intermittent cooling operation, whereas any phase transition temperature above 26°C had a negative impact on energy-saving performance of PCM. In addition, Kishore et al. [6,9] also concluded that unsuitable parameters of PCM should not be suggested for energy saving.

Preceding studies demonstrate that the energy-saving performance of PCM is determined jointly by its thermophysical parameters, building construction and the climate background, while inappropriate parameter values even have a negative impact on the exploit of PCM for energy saving, thus the parametric analysis of PCM is imperative. Currently, there are abundant studies about these influencing parameters. Zhou and Eames [16] carried out simulation works for a lightweight building in the UK, optimized the melting temperature of phase change material wallboard and finally found energy-saving rate can be as high as 40% compared to the ordinary building during summer. Except for melting temperature, thermal conductivity and latent heat of PCM were analyzed in the research conducted by Li et al. [17], they concluded the above three parameters can greatly influence the performance of PMC-based walls. Xie et al. [18] discussed the effect of phase change range on the performance of PCM and discovered the optimal phase change range of each month was different, therefore they suggested the performance of PCM should be evaluated during an entire year. In order to acquire a better energy-saving performance of PCM throughout a whole year, Wang et. al [19] investigated the performance of PCM wallboards in air-conditioned lightweight buildings in Shanghai and optimized melting temperature for different rooms. According to the previous studies, it's no doubt that many parameters related to PCM itself can affect the thermal performance of PCM when it is employed in building envelopes, generally including installation location, phase transition temperature, thickness, latent heat, density, thermal conductivity, and specific heat capacity, however, only a few scholars comprehensively analyzed these parameters rather than only a part of the influencing parameters. Kishore et al. [6] investigated the influence of eight parameters on the thermal performance of PCM, but they aimed to discuss the load modulation caused by PCM. In a numerical study conducted by Liu et. al [20], seven parameters were optimized step by step, and their influences on the performance of lightweight buildings were evaluated.

Based on the above literature review, we can find that the optimal parameters of PCM incorporated into envelopes are greatly affected by the climates and the thermal property of building construction. For example, the optimal melting peak temperature of PCM when it is utilized in warmer climates tends to be higher than that of colder climates [13]. And for the installation position of PCM, it is recommended to be closer to the interior for a heating purpose [21,22] and be installed on the exterior side of walls for the cooling purpose [21], whereas some studies found the mid-element position was better based on annual performance [20, 23]. The disparity of the thermal performance of PCM fitted into different positions displays the proper location of PCM depending on the climate characteristics and the consequential application purpose. Additionally, the thermal property of exterior walls also has a certain impact on the thermal performance of PCM [24, 25], indicating that the optimal parameter of PCM employed for buildings with dissimilar construction may be unique even though these buildings are located in the same climate zone. Hence it is necessary to carefully optimize the relevant parameters of PCM when it is incorporated into building

CHAPTER 6. PARAMETRIC AND ECONOMIC ANALYSIS OF PHASE CHANGE MATERIALS (PCM) ON ENERGY SAVING FOR TRADITIONAL DWELLINGS IN NORTHEAST OF SICHUAN HILLS

envelopes, thereby improving its thermal performance and contribution to building energy saving. On the other hand, the current economic analysis of the application of PCM is not insufficient [11,12], and sometimes PCM is not even recommended when considering its high cost and long payback period from the economic perspective even though it can lower energy consumption to some extent [25-27], thus economic evaluation of applying PCM is crucial, especially in the rural region where has backward economic development. Furthermore, many common evaluation parameters, such as the investment payback period, economic benefits during particular periods are related to local economic circumstances [25-26, 28-30], indicating that the results of economic evaluation are distinctive for different regions even though the same material is employed, thus the economic evaluation should be carried out based on the local economic condition. Consequently, we aim to obtain the optimal parameters of PCM to exploit its energy-saving potential for traditional dwellings in northeast of Sichuan hills, China, and carry out the corresponding economic evaluation to provide decision-makers with some references. In this paper, the total eight parameters related to PCM itself are analyzed, that is, PCM location in the wall, melting temperature, thickness, phase transition temperature radius, latent heat, density, thermal conductivity, and specific heat. We initially determine the default values of these parameters and their variation range based on the common values of these parameters employed in the preceding relevant research. Then their optimal values are detected based on their contribution to energy saving with the help of EnergyPlus. Finally, we evaluate the investment payback period and economic benefits during the service life (25 years) of the PCM with recommended parameters via the dynamic investment payback period (DPP) method and further discuss the corresponding economic results of PCM whose values of these influencing parameters fluctuate in different degree compare to the recommended one. The optimal parameters combination of PCM this paper determined can provide some references for engineers to develop new PCM products which are more suitable for traditional dwellings in northeast of Sichuan hills, China, and the detailed economic analysis results are able to help policy-makers or residents select proper PCM products from the current market as well.

6.2 Materials and methods

6.2.1 Simulation model

A traditional dwelling model was built as the base model for dynamic simulation by EnergyPlus (shown in Table 6-1). The building is facing south and the width of the living room (the middle room) is 4.8m, the rest of the rooms are 4.5m, respectively, and the depth of all of the rooms is 6m. In addition, the construction of exterior walls is the common construction form of local traditional dwellings, consisting of three layers from outside to inside: gypsum plaster layer (20mm), clay layer (100mm) and gypsum plaster (20mm). The roof heat transfer coefficient and air change rate (ACH) of the simulation model satisfy the minimum limits required by JGJ134-2010 [33], that is, the heat transfer coefficient of roof is $0.5 \text{ W}/(\text{m}^2 \text{ K})$ and ACH equals 1 per hour. The calculated indoor temperature in winter and in summer is 18°C and 26°C , respectively [33,34]. For this base building, annual heating load and cooling load is $79.11 \text{ kWh}/\text{m}^2$ and $14.78 \text{ kWh}/\text{m}^2$, respectively, so the annual energy demand for space heating and cooling of base model is $93.89 \text{ kWh}/\text{m}^2$. Additionally, the thermophysical properties of walls materials used for simulation are shown in Table 6-2.

CHAPTER 6. PARAMETRIC AND ECONOMIC ANALYSIS OF PHASE CHANGE MATERIALS (PCM) ON ENERGY SAVING FOR TRADITIONAL DWELLINGS IN NORTHEAST OF SICHUAN HILLS

Table 6-1 Setting details of original model.

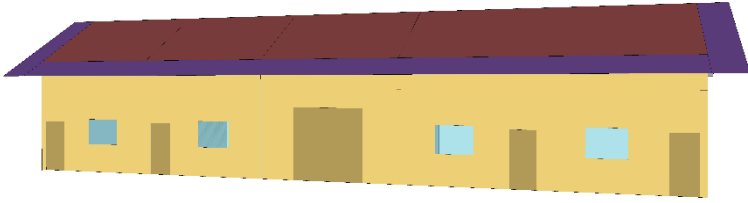
Model parameter	Detail
Three-dimensional model	
Exterior wall construction	20mm gypsum plaster (outside layer) + 100mm clay +20mm gypsum plaster
Roof thermal resistance	2 m ² K/W [33]
Air change rate	1 h ⁻¹
Heating thermostat	18°C
Heating load	78.54 kWh/m ²
Cooling thermostat	26°C
Cooling load	13.78 kWh/m ²
Total energy demand	92.32 kWh/m ²

Table 6-2 Thermophysical parameters of wall materials.

Material	Thickness/x	Thermal conductivity/ λ	Density/ ρ solid(liquid)	Specific heat/ C_p	Melting temperature/ t_m	Latent heat/ L_p
	mm	W/(m K)	kg/m ³	J/(kg K)	°C	kJ/kg
Gypsum plaster	20	0.76	1500	1050	/	/
Clay	100	0.76	1600	1010	/	/
Plywood	5	0.17	600	2510	/	/
EPS	20	0.039	20	1380	/	/
Natural TCM [35]	20	0.5(0.25)	1300	1785	18-26	216

Table 6-3 displays the relevant parametric values of PCM for analysis in subsection 6.3, including default value and varies range of each influencing parameter. These values are summarized based on the literature review [REF]. In subsection 6.3, the thermophysical parameters of default PCM are consist with the default value in the Table 6-3, while the parametric analysis is carried out according to the varies range of parameter. And then, the next parameter optimization analysis is on the basis of the former optimized parameter. In addition, the melting temperature means the center point of phase-transition temperature range, while the phase transition radius stands for the temperature difference between the lowest (highest) transition temperature and melting temperature. For example, the melting temperature of default PCM is 18 °C, while the default phase transition radius is 2 °C, then the phase transition temperature of the default PCM is 16-20 °C. And in order to improve the calculation efficiency, the values of density and conductivity for solid and liquid phase are not diverse in parametric analysis.

Table 6-3 Range and default value of PCM material parameters used for the parametric analysis.

PCM parameter	Unit	Default value	Range for parametric analysis	Interval of parameter range
Location	/	inside	inside, outside	/
Melting temperature	°C	18	8-24	1
Thickness	mm	20	5-20	5
Phase transition radius	°C	2	2-8	1
Latent heat	kJ/kg	100	50-250	50
Density	kg/m ³	1000	500-2000	250
Conductivity	W/(m K)	0.5(solid), 0.25(liquid)	0.1-0.5	0.1
Specific heat	J/(kg K)	1500	1000-2500	500

6.2.2 Model validation

The reliability and accuracy of EnergyPlus in predicting PCM performance have been verified by a lot of researches [12-13, 25-26]. In this study, an experimental test that combining the real PCM product with walls has been carried out, and a validation model was built up by EnergyPlus, while errors between the simulated results and the measured results were assessed. The experimental test was carried out at Qingdao (36.27 °N, 120.67 °E), China during September, 2021. PCM product is Natural TCM, and its thermal performance parameters are shown in Table 6-2. Figure 6-1 presents the details of the experiment and Figure 6-2 displays the validation results. It is apparent that the trends of simulated values and measured values are basically similar. In order to assess the error more exactly, the normalized mean bias error (*NMBE*) and coefficient of variation of the root mean square error [*CV(RMSE)*] of simulation model were calculated by Eq. 6-1 and Eq. 6-2, while their values were -1.8 and 8.8%, respectively. According to [39], the computer model shall have an *NMBE* of 10% and *CV(RMSE)* of 30% when the hourly calibration data are used, and both of them of validation model are satisfied. This validation work further verifies the reliability and accuracy of the CondFD solution algorithm and PhaseChangeHysteresis module embedded in EnergyPlus, and they will be employed in the following analysis works.

CHAPTER 6. PARAMETRIC AND ECONOMIC ANALYSIS OF PHASE CHANGE MATERIALS (PCM) ON ENERGY SAVING FOR TRADITIONAL DWELLINGS IN NORTHEAST OF SICHUAN HILLS

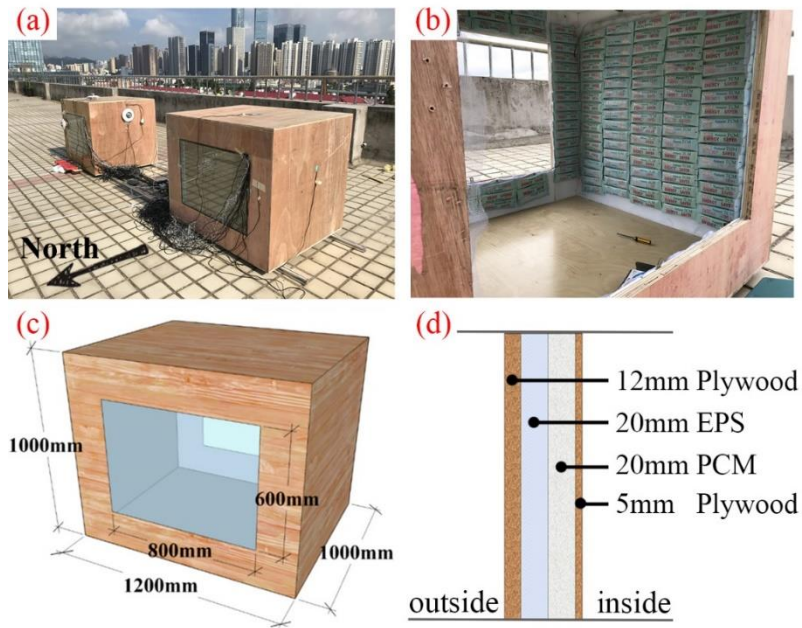


Figure 6-1 Experimental details for performance of natural TCM.

$$NMBE = \frac{\sum_{i=1}^n (y_i - \bar{y}_i)}{(n-1) \times \bar{y}} \times 100 \quad (6-1)$$

$$CV(RMSE) = 100 \times \frac{\sqrt{\sum (y_i - \bar{y}_i)^2 / (n-1)}}{\bar{y}_i} \quad (6-2)$$

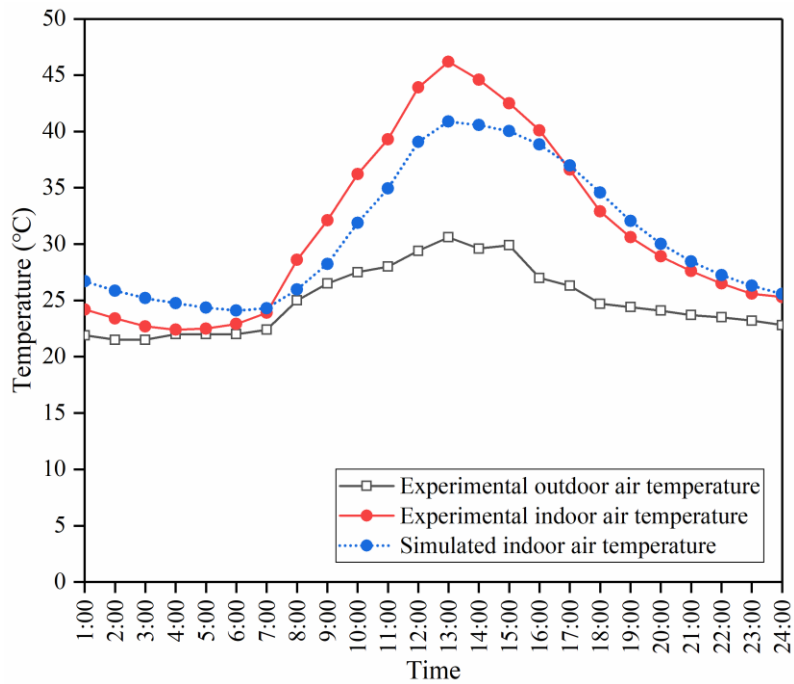


Figure 6-2. Results of experimental and simulated indoor air temperature.

CHAPTER 6. PARAMETRIC AND ECONOMIC ANALYSIS OF PHASE CHANGE MATERIALS (PCM) ON ENERGY SAVING FOR TRADITIONAL DWELLINGS IN NORTHEAST OF SICHUAN HILLS

6.2.3 Evaluation indicator

The saving rate (S) of annual energy demand which is consisted of annual heating load and annual cooling load is used as the evaluation indicator in this study. It is defined by Eq. 6-3, reflecting the energy-saving effect of PCM application compared to the base model.

$$S = \frac{E_{base} - E_{pcm}}{E_{base}} \times 100\% \quad (6-3)$$

where:

S means saving rate of energy demand, %;

E_{base} stands for annual energy demand of base model (without PCM), kWh/m²;

E_{pcm} stands for annual energy demand of model combined with PCM, kWh/m².

6.3 Results and discussion

6.3.1 Effect of PCM melting temperature and location on energy saving

According to the review of previous research, we know that the optimal position of PCM depends on the application purpose of PCM to some extent because the position of PCM determines the degree of its interaction with the ambient environment. In detail, for cooling purposes, PCM is recommended close to the exterior [21] since it can interact very efficiently with the exterior environment and the heat stored by PCM cannot efficiently move to the indoor room due to the thermal resistance of the wall insulation, likewise, PCM close to the interior is better for heating purpose since it can interact with the indoor environment effectively and the heat stored by PCM can hardly lose due to the thermal resistance of wall insulation. And in this part, the optimal location of PCM for traditional dwellings in this region was analyzed, while in consideration of the convenience of construction, only two locations were discussed. One location of PCM is between inner gypsum plaster and clay, which is close to the indoor room, represented as inside PCM, another is between clay and outer gypsum plaster, which is close to the outdoor environment, represented as outside PCM. Except for the location, melting temperature also has a great impact on the thermal performance of PCM, and it can be found in previous relevant studies that different combinations of melting temperature and location will lead to diverse annual energy demand [9, 16]. Therefore, the effects of location and melting temperature on PCM performance are comprehensively discussed in this part, and the results are shown in Figure 6-3.

From Figure 6-3, regardless of location and melting temperature, the application of PCM can obviously save energy demand of the building, however, there is an optimal melting temperature for diverse locations of PCM. For the outside PCM, the maximum saving rate of annual energy demand can be up to 14.22% when the melting temperature is 11°C, while for the inside PCM, a saving rate of 16.89% can be obtained when the optimal temperature of 14°C is adopted. It's obvious that when considering the final saving rate of energy demand, there is the optimal combination of location and temperature even though the variation trend of melting temperature for both outside PCM and inside PCM is similar. It also reveals that location and melting temperature have a joint influence on the

CHAPTER 6. PARAMETRIC AND ECONOMIC ANALYSIS OF PHASE CHANGE MATERIALS (PCM) ON ENERGY SAVING FOR TRADITIONAL DWELLINGS IN NORTHEAST OF SICHUAN HILLS

thermal performance of PCM, which is consistent with the findings in [9,16]. Furthermore, it can be found the outside PCM performs better when the melting temperature is below 13°C. Taking the melting temperature of 11°C as an example, the heating load of inside PCM and outside PCM is 70.84kWh/m² and 68.54 kWh/m², respectively, while the cooling load is 10.9 kWh/m² and 10.65 kWh/m², respectively. The reason for this phenomenon is that the phase transition temperature range of PCM is 9-13°C when the melting temperature is 11°C, and in winter, the occurrence frequency of 9-13°C in the outdoor environment is much higher than that in the indoor room. And in this condition, outside PCM, which is close to the outdoor environment is affected by the outdoor air temperature intensely and can store more energy than PCM nearing the indoor room, where the thermostat remains 18°C in winter.

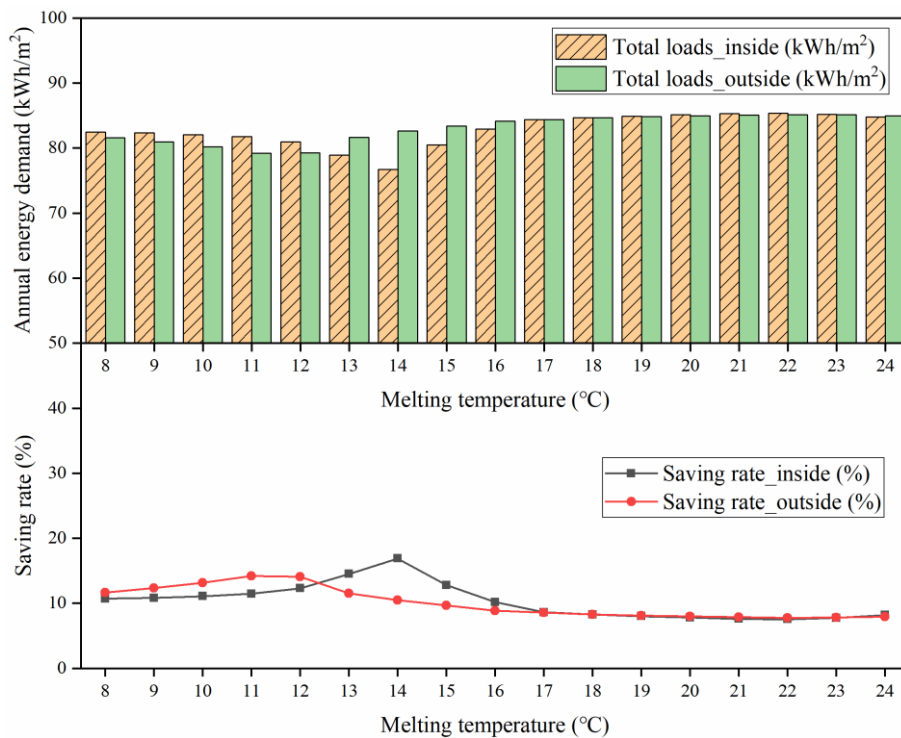


Figure 6-3. Effect of PCM location and melting temperature on the energy demand.

6.3.2 Effect of PCM thickness on energy saving

Based on the optimized location (inside) and melting temperature (14°C) of PCM, the effect of PCM thickness on energy saving is discussed in this subsection, and the results are displayed in Figure 6-4. This study varies the PCM thickness from 5-20mm with an interval of 5mm. From Figure 6-4, both heating load and cooling load decrease as PCM thickness becomes larger. It's logical because a thicker PCM has a larger thermal energy storage capacity per unit surface area of the wall, and with a higher thermal energy storage capacity, it can store and release more heat during the period when the ambient temperature is in the range of its phase transition temperature. Therefore, the thicker PCM can provide more heat for indoor rooms in winter and transfer more heat in summer, thereby reducing more heating load and cooling load.

According to Figure 6-4, a PCM of 5mm is able to save about 7.19% of total heating and cooling

CHAPTER 6. PARAMETRIC AND ECONOMIC ANALYSIS OF PHASE CHANGE MATERIALS (PCM) ON ENERGY SAVING FOR TRADITIONAL DWELLINGS IN NORTHEAST OF SICHUAN HILLS

loads. As for PCM of 10mm, 15mm, and 20mm, the saving rate is 10.77%, 14.49%, and 16.89%, respectively. We can realize that the growth rate of saving rate is not linear, and when the thickness passes 10mm, the thicker the PCM is the lower the growth rate of saving rate is, therefore, we can conclude that the thicker PCM may not be the better selection when its cost is in consideration. And this is one of the reasons that the thickness of PCM is rarely exceeding 20mm in the relevant published papers. But in this part, we only evaluate the saving rate, so the thickness of 20mm, which is common in the relevant research, is suggested and will be employed in the following parametric analysis.

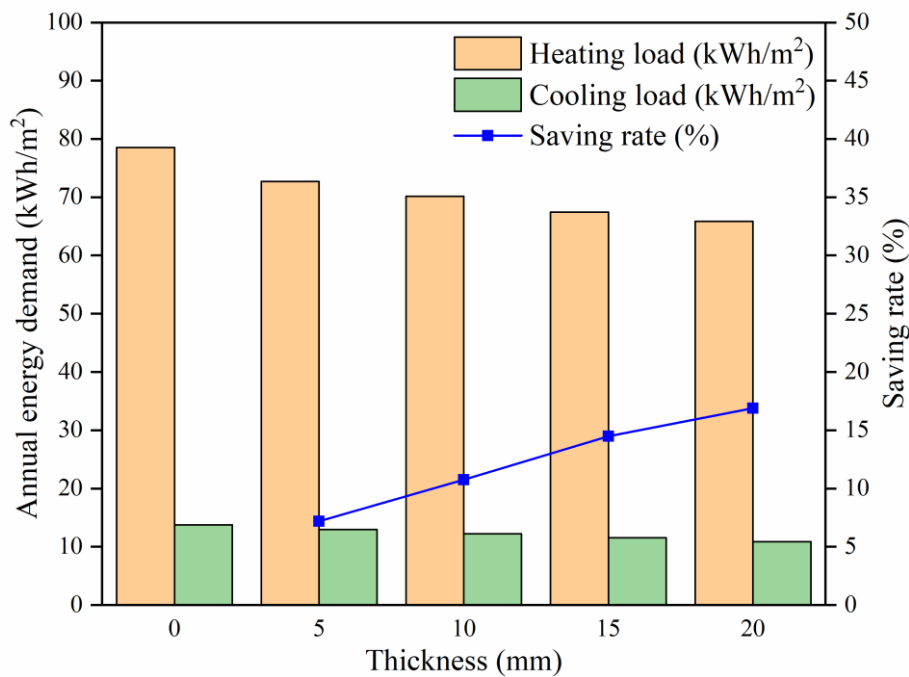


Figure 6-4. Effect of PCM thickness on the energy demand.

6.3.3 Effect of PCM phase transition temperature radius on energy saving

Phase transition temperature radius determines the phase transition temperature range of PCM in conjunction with melting temperature, and the higher value of this parameter leads to a wider phase transition temperature range. The larger transition temperature range of PCM implies that the activate time of PCM will be longer because the frequency of PCM temperature in the range of transition temperature range is growing. Therefore, it is rational that both heating load and cooling load decrease as the phase transition temperature radius becomes larger (see Figure 6-5).

Compared to the base model, which doesn't apply PCM, PCM creates a notable energy-saving effect. However, there is hardly any change in the saving rate of the annual energy demand due to the variation in the phase transition temperature radius. From Figure 6-5, the corresponding saving rate of phase transition temperature radius from 2°C to 8°C is 16.89%, 16.96%, 17%, 17.04%, 17.05%, 17.08% and 17.11%, respectively. The best condition (phase transition temperature radius equals 8°C) only saves 0.22% of the annual energy demand of the base model more than when the phase transition temperature radius equals 2°C, and their corresponding annual energy demand is

CHAPTER 6. PARAMETRIC AND ECONOMIC ANALYSIS OF PHASE CHANGE MATERIALS (PCM) ON ENERGY SAVING FOR TRADITIONAL DWELLINGS IN NORTHEAST OF SICHUAN HILLS

76.52kWh/m² and 76.73kWh/m², respectively. It's obvious that the phase transition temperature range has a minor effect on the annual heating and cooling loads of traditional dwellings in this region, and this finding is also consistent with the discovery in [10, 20].

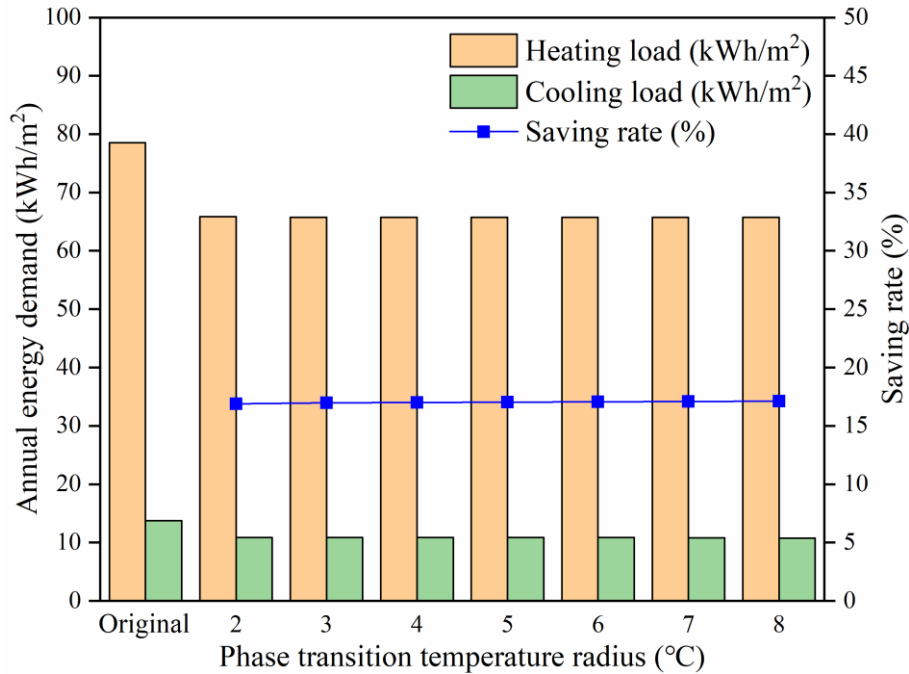


Figure 6-5. Effect of PCM phase transition temperature radius on the energy demand.

6.3.4 Effect of PCM latent heat on energy saving

Latent heat determines the amount of energy that PCM can store per unit mass. This study varies latent heat from 50 kJ/kg to 250 kJ/kg with a gap of 50 kJ/kg. We can note that increasing the latent heat results in a greater saving effect than phase change temperature radius on heating load as well as cooling load even though the saving rate of them grows slowly. According to the results shown in Figure 6-6, the saving rate of the annual energy demand is 16.37%, 17.11%, 17.28%, 17.41%, and 17.55%, respectively, corresponding to the latent heat from 50 kJ/kg to 250 kJ/kg. The latent heat of 250 kJ/kg displays the best energy-saving performance among these discussion ranges even though the increasing speed of saving rate declines after latent heat surpasses 100 kJ/kg and the annual energy demand when latent heat equals 250 kJ/kg is only 1.09 kWh/m² lower than that when the latent heat is 50 kJ/kg. Therefore, 250 kJ/kg of latent heat is suggested in this part based on its energy-saving performance.

CHAPTER 6. PARAMETRIC AND ECONOMIC ANALYSIS OF PHASE CHANGE MATERIALS (PCM) ON ENERGY SAVING FOR TRADITIONAL DWELLINGS IN NORTHEAST OF SICHUAN HILLS

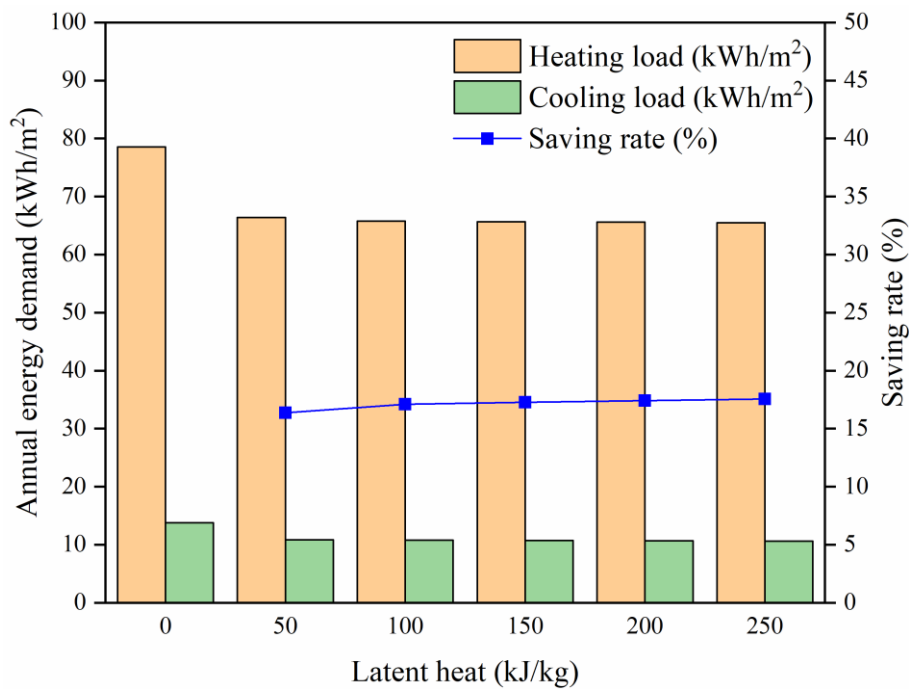


Figure 6-6. Effect of PCM latent heat on the energy demand.

6.3.5 Effect of PCM density on energy saving

The density of PCM reflects the amount of PCM per unit volume, and further determines the energy storage capacity of PCM per unit volume. We vary the density of PCM from 500 kg/m³ to 2000 kg/m³ with a gap of 250 kg/m³ to discuss the effect of mass density on the energy-saving performance, and Figure 6-7 depicts their relation. It's notable that the relationship between density and saving rate is neither linear nor parabolic according to Figure 6-7. From the simulation results, the cooling load decreases with density enlarges. As for the heating load, it reduces at first, but it suddenly ups to a higher level (66.95 kWh/m²) compared to the beginning (65.72 kWh/m²) when the density achieves 1250 kg/m³, and then it reduces again, and finally, the heating load equals to 66.68 kWh/m² when the density is 2000 kg/m³, therefore it is obvious that the variation of heating load leads to no obvious regularity of the saving rate of the annual energy demand. However, we can still conclude that the lowest density (1250 kg/m³) has worse performance than other values of density although the saving rate fluctuates irregularly with the density variation, and it's better to select PCM at least with the density of 500 kg/m³ for this region. Additionally, there still exists the best selection of mass density. When the mass density is set as 1000 kg/m³, the heating load and cooling load are 65.5 kWh/m² and 10.62 kWh/m², respectively, while the saving rate of the annual energy demand is able to achieve 17.55%. Hence, a density of 1000 kg/m³ is recommended in order to maximize the energy-saving effect.

CHAPTER 6. PARAMETRIC AND ECONOMIC ANALYSIS OF PHASE CHANGE MATERIALS (PCM) ON ENERGY SAVING FOR TRADITIONAL DWELLINGS IN NORTHEAST OF SICHUAN HILLS

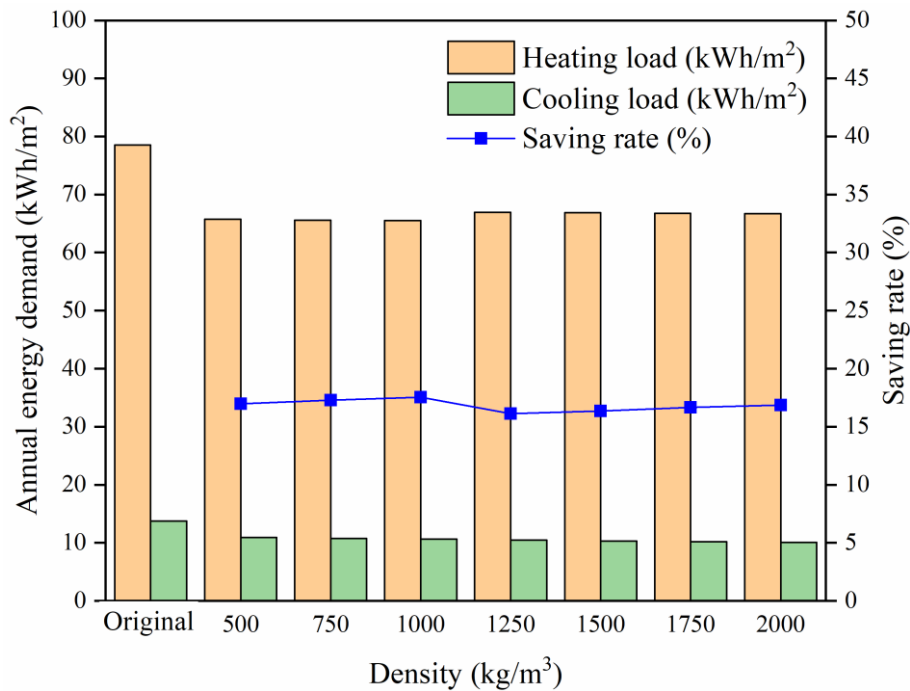


Figure 6-7. Effect of PCM density on the energy demand.

6.3.6 Effect of PCM thermal conductivity on energy saving

The thermal conductivity of material reflects its ability to transfer heat regardless of the material category (the traditional insulation material or PCM), and the phase state of material (solid phase or liquid phase). Higher thermal conductivity indicates a better ability to transfer heat, in other words, compared to the material with lower conductivity, high-conductivity materials have a worse ability to resist heat loss in winter and reduce heat gain in summer. Therefore, the thermal performance of PCM with conductivity variation depicted in Figure 6-8 is logical that both heating load and cooling load are growing with the thermal conductivity becoming larger. And unlike some other parameters which have a minor impact on the energy-saving effect, such as phase transition temperature radius, latent heat, and specific heat, thermal conductivity has a manifest influence on the thermal performance of PCM.

From Figure 6-8, the saving rate of the annual energy demand is 21.91%, 13.76%, 10.31%, 8.41%, and 7.2%, respectively, corresponding to the thermal conductivity from 0.1-0.5. W/(m K). And even though the downward trend of saving rate gradually flattens with larger thermal conductivity, the PCM with 0.1 W/(m K) still has excellent performance on energy saving compared with that with 0.5 W/(m K) – the saving rate of 0.1 W/(m K) is about 3 time of that of 0.5 W/(m K). Therefore, a lower thermal conductivity of PCM is better from the view of energy saving, while Li et al. [17] and Ji et al. [44] also obtained the same observation results. Hence, 0.1 W/(m K) of thermal conductivity is recommended in this study.

CHAPTER 6. PARAMETRIC AND ECONOMIC ANALYSIS OF PHASE CHANGE MATERIALS (PCM) ON ENERGY SAVING FOR TRADITIONAL DWELLINGS IN NORTHEAST OF SICHUAN HILLS

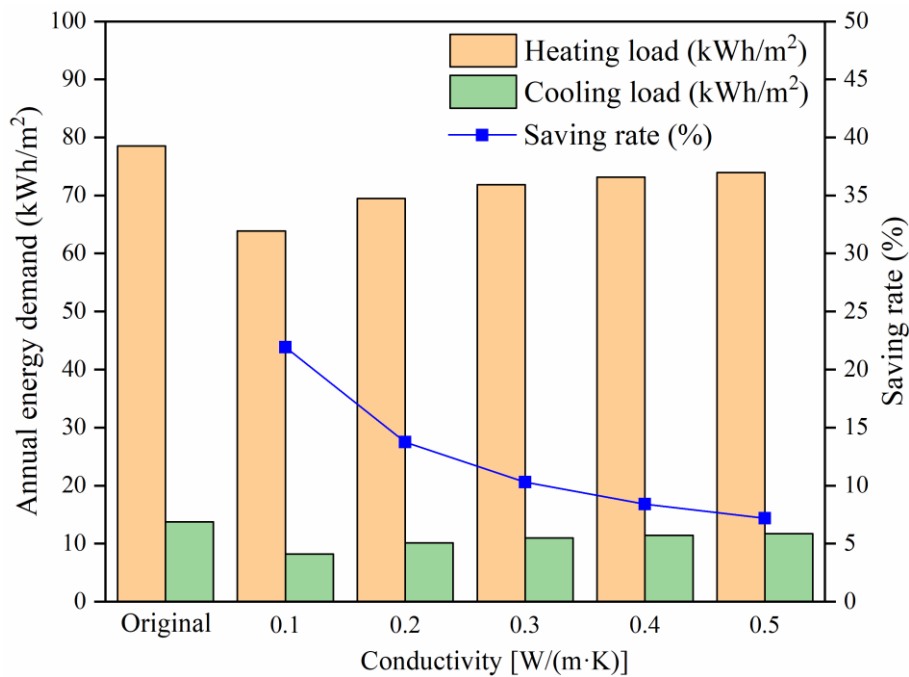


Figure 6-8. Effect of PCM thermal conductivity on the energy demand.

6.3.7 Effect of PCM specific heat on energy saving

Figure 6-9 depicts the influence of the specific heat on the annual energy demand. It's apparent that there is hardly any change in both heating load and cooling load due to the variation of specific heat. The heating load declines from 63.89 kWh/m² to 63.84 kWh/m² and cooling load decreases from 8.32 kWh/m² to 8.03 kWh/m² when the specific heat enlarges from 1000 J/(kg K) to 2000 J/(kg K), while the corresponding saving rate of 1000 J/(kg K), 1500 J/(kg K), 2000 J/(kg K) and 2500 J/(kg K) is 21.78%, 21.91%, 22.04% and 22.15%, respectively. It is an expected result that the difference caused by specific heat variation is minor because the magnitude of specific heat is much lower than the latent heat capacity, which can be seen according to the material thermophysical parameters shown in Table 6-3. Therefore, the specific heat isn't the important parameter for the thermal performance of PCM, but 2500 J/(kg K) is still suggested in this study because it has the best performance although its corresponding saving rate is only 0.37% higher than that corresponding to 1000 J/(kg K).

CHAPTER 6. PARAMETRIC AND ECONOMIC ANALYSIS OF PHASE CHANGE MATERIALS (PCM) ON ENERGY SAVING FOR TRADITIONAL DWELLINGS IN NORTHEAST OF SICHUAN HILLS

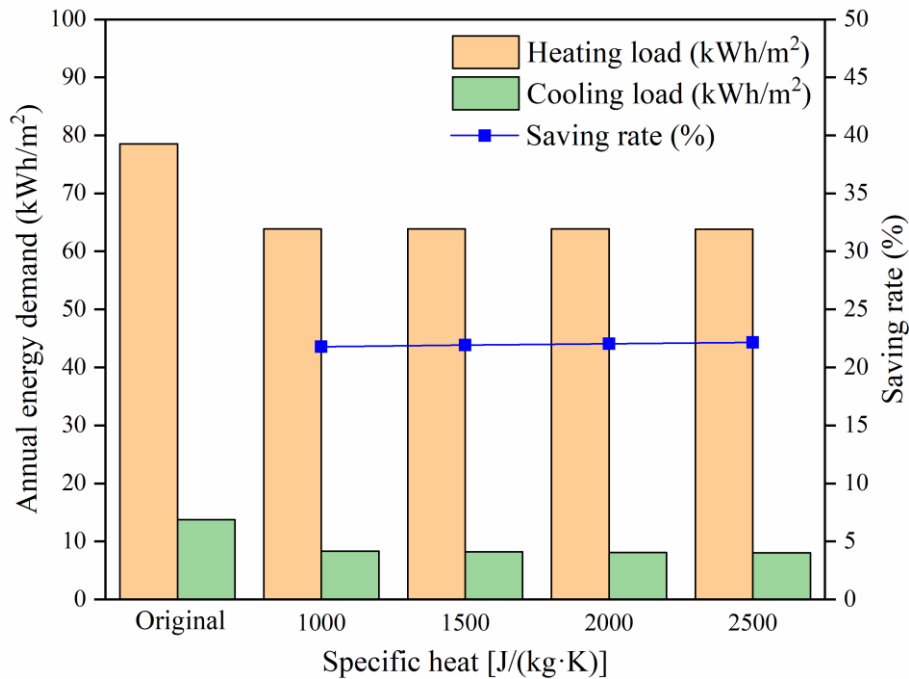


Figure 6-9. Effect of PCM specific heat on the energy demand.

6.3.8 Comparison of energy-saving performance between recommended PCM and present PCM products

In order to assess the advantage of the recommended PCM with optimal parameters obtained by the above analysis, we compared its energy-saving performance with other PCM products. Table 6-4 displays the thermophysical parameters of each PCM and their corresponding saving rate. It is apparent that recommended PCM has the best energy-saving performance, its saving rate is even 9.5 times higher than the worst-performing PCM (PCM18). Additionally, we can note that few PCM products have a thermal conductivity as low as 0.1 W/(m K), but thermal conductivity affects the annual energy demand greatly, therefore recommended PCM with lower thermal conductivity can reduce much more energy demand compared to other products. These results prove that PCM with suitable parameters can decline more energy demand, indicating that it is imperative to develop PCM products based on their application purpose and climate background.

Table 6-4. Parameters and the corresponding energy saving rate of different PCM products.

PCM products	Thermal conductivity W/(m K)	Density kg/m ³	Specific heat J/(kg K)	Phase transition temperature °C	Latent heat kJ/kg	Saving rate %
Recommended PCM	0.1	1000	2500	6-22	250	22.15
Natural TCM [35]	0.5(solid) 0.25(liquid)	1300	1785	18-26	216	9.23
PCM18 [45]	5.6	850	3131	11-22	73	2.10

Table 6-4. Parameters and the corresponding energy saving rate of different PCM products (Cont).

BioPCM [46]	2.5(solid)	1400(solid)	4500(solid)	17-33	175	11.89
	0.15(liquid)	850(liquid)	2200(liquid)			
RT15 [47]	0.2	880(solid)	2000	10-17	155	13.11
		770(liquid)				
RT27 [48]	0.24(solid)	870(solid)	2500	28-30	179	12.97
	0.15(liquid)	781.5(liquid)				

6.3.9 Economic analysis of PCM selection

The above analysis demonstrates the significant energy-saving potential of PCM with appropriate parameters, but the fact that PCM generally has a high price cannot be ignored, therefore it's necessary to evaluate the economic benefits of using PCM for this region that has a backward economy. Hence, the dynamic investment payback period (N_e) and the economic benefits (S_{pcm}) are calculated in this part to provide some references for decision-makers. In addition, there is no PCM product whose parameters absolutely match the optimal values recommended before in the current market, indicating that the economic analysis results of PCM with optimal parameters are not completely appropriate for PCM products in the present market since the energy-saving performance of PCM fluctuates greatly because of the influencing parameters variation. In order to provide a broader reference, we take the optimal combination of parameters as the baseline, then the values of each influencing parameter were adjusted upward and downward by 25% and 50% (other parameters still take their optimal value except for the study parameter), respectively, and Table 5 displays their corresponding payback period and economic benefits. Additionally, the location of PCM is close to the indoor room (between the inner wall surface and clay wall), and the calculation method is depicted in subsection 2.5, the PCM price is set as 8.3 CNY/kg (1.3 USD/kg) [27] and the service life of PCM is set as 25 years.

We can note that there are minor reductions in the payback period (less than 1 year) when melting temperature (F1), phase transition temperature radius (F3), latent heat (F4), and specific heat (F7) enlarge by 25% and 50% according to Table 5, and their corresponding economic benefits grow to diverse degrees. For example, increasing F1 by 50% can create more economic benefits of 30.1%, while expanding F3 to the same amplitude only brings approximately 5.6% of the increase in economic benefits. Amongst these four parameters, the improvements of economic benefits for phase transition temperature radius (F3), latent heat (F4), and specific heat (F7) are consistent with the findings obtained in the above parametric analysis, that is, economic benefits logically increase as the values of these parameters expand since there is a positive correlation between their variations and the amount of energy saved, thereby the larger their values are, the more energy can be saved, and then the corresponding economic benefits improved. By contrast, the economic increment caused by the growing melting temperature (F1) is not in keeping with the previous parametric analysis results that have already demonstrated the melting temperature (14°C) is optimal, which means that economic benefits should be decreasing regardless of whether the melting temperature rises or declines based on the previous results, however, the reality is that the economic benefits

CHAPTER 6. PARAMETRIC AND ECONOMIC ANALYSIS OF PHASE CHANGE MATERIALS (PCM) ON ENERGY SAVING FOR TRADITIONAL DWELLINGS IN NORTHEAST OF SICHUAN HILLS

only decrease when the melting temperature drops, while there is a real increase of economic benefits as the melting temperature raises. It indicates that among the rest of the parameters, including thickness (F2), phase transition temperature radius (F3), latent heat (F4), density (F5), thermal conductivity (F6), and specific heat (F7), there exist one or more parameters which can jointly affect the energy-saving performance of PCM with the melting temperature (F1), in other words, there is one or more parameter has some impacts on the energy-saving contribution of melting temperature. In order to explain this phenomenon, we review a lot of relevant papers and find some discoveries that are probably able to help us to comprehend it. Xie et. al [49] explored the correlation between thermal conductivity and utilization rate of latent heat (URLH) of PCM and finally found there was the optimal point of thermal conductivity when PCM was utilized for buildings, in other words, the thermal conductivity of PCM is not the higher the better, and meanwhile, they also noted that phase transition cannot occur when the value of thermal conductivity was very low and then PCM was equivalent to a layer of thermal insulation material. A similar conclusion was obtained by another work. Xu et. al [50] proposed two concepts – relative depth of activation, and time rate of activation, to evaluate the latent heat utilization of PCM, and then optimized the thermal conductivity of PCM according to them. And finally, they concluded that from the perspective to maximize the matching degree between PCM and its specific application background, the thermal conductivity is not certainly the bigger the better or the smaller the better when PCM is employed in buildings. According to these phenomena, we infer that reducing thermal conductivity leads to some negative impacts on latent heat utilization, thereby reducing the energy-saving effects, then the improvement of melting temperature is able to offset this negative influence to some extent since there will be more points inside PCM layer whose temperatures are within the phase transition temperature range, in other words, the activation degree of PCM becomes larger to some extent as melting temperature raises when the thermal conductivity of PCM is very small. Therefore, the economic benefits certainly improve as the melting temperature increases compare to the baseline.

As for thickness (F2), density (F5), and thermal conductivity (F6), the smaller their values are the shorter their investment payback period and the corresponding economic benefits become higher. For instance, when the thickness of PCM drops from 20mm to 10mm, its payback period reduces by 4.5 years while the corresponding economic benefit raises 51.5%. It demonstrates that PCM thickness is not certainly the thicker the better when considering the economic factors since the cost of PCM increases greatly and the corresponding economic benefits created by improving thickness cannot offset it. Similarly, 500 kg/m³ of density saves more money than 1000 kg/m³ although the energy demand increases by 0.68kWh/m². This result occurs logically because the reduction amount of PCM cost is greatly larger than the value of the corresponding additional energy consumption caused by lowering the density, therefore the final economic benefits rise from 18.16 CNY/m² to 97.6 CNY/m² and the payback period drops from 21.7 years to only 9.6 years. In addition, thermal conductivity reflects the resistant capacity of PCM for heat transfer, and the lower its value is, it can decrease much more heat gain in summer and heat loss in winter, thereby the corresponding energy demand reduces from 73.41 kWh/m² to 63.97 kWh/m² when thermal conductivity reduces from 0.1 W/m K to 0.05 W/m K, and then its economic benefits surges from 18.16 CNY/m² to 105.57 CNY/m² and the payback period decreases by 8 years. It displays the enormous economic potential

CHAPTER 6. PARAMETRIC AND ECONOMIC ANALYSIS OF PHASE CHANGE MATERIALS (PCM) ON ENERGY SAVING FOR TRADITIONAL DWELLINGS IN NORTHEAST OF SICHUAN HILLS

to develop low thermal conductivity PCM for buildings. Furthermore, the detailed economic analysis also demonstrates the influence degree of each thermophysical parameter of PCM on the economic benefits. The variation of thermal conductivity has the greatest impact on final economic benefits that a 50% reduction of it can improve the economic benefits by 4.8 times the original one. The density of PCM also has a significant influence, and a 50% reduction for it increases the economic benefit by 4.4 times. Except for these two parameters, a 50% reduction of thickness increases 50% of economic benefits, and the variation of economic benefits caused by the change of the rest parameters is not more than $\pm 30\%$. Additionally, some important phenomena also should be noted in Table 5 that the payback period for thickness (F2), density (F5), and thermal conductivity (F6) is longer than the reference payback period (25 years) after their values exceed a certain value, meaning their benefits will still be negative after the 25 years. These results indicate that thermal conductivity, density, and thickness of PCM are the three crucial parameters for economic benefits, and this detailed economic evaluation can provide a useful reference for decision-makers when they select PCM products in the present market.

Table 6-5 Dynamic investment payback period and economic benefits of PCM with different parameters.

	-50%		-25%		Base		+25%		50%	
	N_e	S_{pcm}	N_e	S_{pcm}	N_e	S_{pcm}	N_e	S_{pcm}	N_e	S_{pcm}
F1	22.6	12.5	22.3	14.6	21.7	18.16	21.1	22.2	20.9	23.6
F2	17.2	27.5	19.4	26.1	21.7	18.16	24.3	4.6	27	-13.2
F3	22	16.5	21.8	17.3	21.7	18.16	21.6	18.7	21.6	19.2
F4	22.2	14.9	22.0	16.5	21.7	18.16	21.5	19.6	21.3	21.0
F5	9.6	97.6	15.2	58.1	21.7	18.16	29.4	-22.1	39	-62.7
F6	13.4	105.6	17.4	53.1	21.7	18.16	26.5	-6.9	31.9	-25.5
F7	22.2	15.3	21.9	16.9	21.7	18.16	21.5	19.3	21.4	20.4

Note: F1: melting temperature of PCM, °C; F2: thickness of PCM, mm; F3: phase transition temperature radius of PCM, °C; F4: latent heat of PCM, kJ/kg; F5: density of PCM, kg/m³; F6: thermal conductivity of PCM, W/m K; F7: specific heat of PCM, J/(kg K); N_e : dynamic payback period, year; S_{pcm} : the amount of saving money produced by the application of PCM during 25 years, CNY/m².

As effective thermal energy storage (TES) medium, phase change material (PCM) has been widely concerned about due to its energy-saving potential for buildings. However, the application of PCM does not necessarily reduce energy consumption if inappropriate parameters are employed [6,9,14], therefore selecting proper parameters of PCM based on the application purpose is crucial. In order to obtain the optimal PCM parameters for traditional dwellings in northeast of Sichuan hills, China, eight parameters related to PCM itself, including PCM location in the wall, melting temperature, thickness, phase transition temperature radius, latent heat, density, thermal conductivity, and specific heat, were optimized in this study. According to the detailed parametric analysis, we find that some parameters (phase transition temperature radius, latent heat, and specific heat) have minor influences on the energy-saving performance of PCM, whereas the variation of

CHAPTER 6. PARAMETRIC AND ECONOMIC ANALYSIS OF PHASE CHANGE MATERIALS (PCM) ON ENERGY SAVING FOR TRADITIONAL DWELLINGS IN NORTHEAST OF SICHUAN HILLS

other parameters (melting temperature, thickness, and thermal conductivity) can greatly affect the thermal performance of PCM. These influence degrees of parameter variations on the thermal performance of PCM are consistent with some preceding relevant studies [10, 20]. As for the location of PCM, setting PCM close to the inner surface is better in this region, which is match the opinion proposed by Al-Yasiri and Szabó [21] that PCM should be installed closer to the interior for heating purposes. Next, a further work that compares the energy-saving effect of PCM with optimal parameters obtained before with some PCM products in the present market was carried out, and the comparison results demonstrate PCM with optimal parameters has a significant advantage, which once again proves the necessity to develop PCM whose parameters are appropriate to the local climate and building characteristics. On the other hand, the economic analysis results of PCM can provide useful references to decision-makers due to the high costs of PCM, while the present relevant economic analysis is insufficient [11,12]. Additionally, the previous economic analysis of the recommended PCM only discussed the economy of the certain PCM with fixed parameters [25,26], whereas the variations of parameters have a certain impact on the energy-saving performance of PCM and thereby change the economic benefits, therefore the economic evaluation results are inaccurate for PCM products whose parameters are not completely matched with the recommended PCM. Hence, the reference value of economic analysis results is limited because there may be no PCM product in the present market whose parameters exactly match the optimal parameters. In order to further improve the reference values of economic analysis, we not only evaluated the payback period and economic benefits of recommended PCM but assessed the economic performance of other PCM whose parameters has a varying extent of deviation relative to the recommended PCM. These detailed economic analysis results clearly demonstrate the effect of variation of these thermophysical parameters on the payback period and final economic benefits, which can help decision-makers select the relatively proper PCM products from the current market.

An unexpected result caused by melting temperature variation then occurs when we evaluate the payback period and economic benefits, that is, the improvement of melting temperature does not lead to a reduction of economic benefits, by contrast, energy demand decreases as melting temperature rises, which means the optimal temperature determined in parametric analysis part is not the best anymore. We inferred the reason for this phenomenon is that the effect of each parameter on energy demand is not independent, there exist one or more factors that interact with melting temperature and jointly affect the energy-saving performance of PCM. By the preceding research conducted by Xie et al. [49] and Xu et al. [50], we can notice that the thermal conductivity of PCM has a great impact on the utilization rate of latent heat, while the lower thermal conductivity may lead to the utilization rate of latent heat dwindles to zero, and then PCM is equivalent to a layer of traditional insulation material and does not exploit its unique advantages of storing and releasing heat. Based on this fact, we speculate that 14°C is the optimal melting temperature corresponding to the thermal conductivity equals to the default value, and when thermal conductivity declines to only 0.1 W/m·K while melting temperature is still 14°C, the utilization rate of latent heat consequentially decreases, in other words, there is much less point inside PCM layer whose temperature is within the phase transition temperature range as thermal conductivity lowers from default value to a lower value, while the increase of melting temperature at this time can activate more points and then offset this negative influence to some degree, and finally exhibits the much

CHAPTER 6. PARAMETRIC AND ECONOMIC ANALYSIS OF PHASE CHANGE MATERIALS (PCM) ON ENERGY SAVING FOR TRADITIONAL DWELLINGS IN NORTHEAST OF SICHUAN HILLS

higher economic benefits and shorter payback period shown in Table 5. Hence a further investigation that whether there is an interaction effect between melting temperature and thermal conductivity in terms of energy-saving performance of PCM are involved in our further works.

6.3.10 Selection of PCM for this study region

Undeniably, the prohibitive price is an important factor limiting the widespread use of PCM, and thermal conductivity, density and thickness are assumed the three crucial parameters affecting the final economic benefits based on the above detailed economic analysis. Amongst these three parameters, density and thickness are able to directly affect the investment of material cost of PCM since they determine the mass of PCM. Furthermore, we have already known from Figure 6-4 that energy saving rate of annual energy demand grows as thickness increases, but their correlation is not linear, meaning the growth of energy saving benefits gradually slows down with higher thickness, however, the cost of PCM surges with thickness as a linear law, thereby there exists a possibility that thinner PCM is able to create higher economic benefits. Additionally, higher density means heavier mass of PCM per unit volume, then its cost increases as density enlarges, but the fact shown in Figure 6-7 cannot be ignored, that is, there is minor difference of the saving rate of annual energy demand among PCM with varies density, which implying that the money saved by changing density cannot offset the corresponding additional investment cost, therefore, a lower density probably performs better in terms of economic benefits. Hence, considering the economic development of this region is relatively backward, we conduct a deep economic analysis based on the perspective of actual project in order to find the more suitable values of thickness and density for this region.

Table 6-6 displays the economic evaluation results of PCM with different thickness (values of other parameters are the same as the recommended PCM shown in Table 6-4). The calculation method of economic benefits is explained in Chapter 3, the electricity price is 0.52 CNY/kWh; meanwhile, considering in an actual project, the investment cost for fixing PCM not only includes the material cost of PCM itself, but also covers the corresponding labor cost and other related costs, therefore, the total investment costs shown in Table 6-6 and Table 6-7 include the material costs of PCM and gypsum plaster, and corresponding labor costs, and thereby there are some discrepancies in the following economic benefits compared to the previous results. In Table 6-6, the corresponding economic benefits of different thickness confirm the previous inference, that is, thicker PCM doesn't mean the better economic benefits even though the thicker PCM is, more energy can be saved, and therefore 5mm is recommended for PCM used in this region.

Based on the recommended thickness (5mm), we also calculate economic benefits corresponding to density variation (other parameters of PCM are the same as values shown in Table 6-4 except for thickness), and results are presented in Table 6-7. It is apparent that low density of PCM is better and 500 kg/m³ is recommended for this region based on these results. Furthermore, we can deeply analyze the reason of the phenomenon that density can greatly affect the final economic benefits which is discovered before according to Table 6-7. The saving rate of energy demand increases as density grows, meaning the annual total energy demand decreases, and thereby the larger the density is, the saved money caused by PCM becomes more, but notably, the increased saved money is not more than 10 CNY per year whereas the corresponding additional costs of PCM exceeds 2000 CNY.

CHAPTER 6. PARAMETRIC AND ECONOMIC ANALYSIS OF PHASE CHANGE MATERIALS (PCM) ON ENERGY SAVING FOR TRADITIONAL DWELLINGS IN NORTHEAST OF SICHUAN HILLS

These results certainly demonstrate that the improvement of energy-saving effect caused by increasing density of PCM cannot balance out the additional investment cost, therefore the variation of density can lead to a great fluctuation of economic benefits.

Table 6-6 Economic benefits of PCM with different thickness.

Thickness mm	Saving rate of energy demand %	Saved money per year CNY/a	Total investment cost CNY/m ²	Economic benefits after 25 years CNY/m ²
5	7.3	291.9	320.3	-259.5
10	13.2	526.1	434.0	-324.3
15	18.1	719.5	547.6	-397.6
20	22.2	880.5	661.2	-477.7

Table 6-7 Economic benefits of PCM with different density.

Density mm	Saving rate of energy demand %	Saving money per year CNY/a	Total investment cost CNY/m ²	Economic benefits after 25 years CNY/m ²
500	7.0	279.4	263.5	-205.3
750	7.2	285.9	291.9	-232.3
1000	7.3	291.9	320.3	-259.5
1250	7.5	297.5	348.7	-286.7
1500	7.6	302.7	377.1	-314.0
1750	7.7	307.9	405.6	-341.4
2000	7.9	312.6	434.0	-368.8

6.4 Summary

Phase change material (PCM) is an effective thermal energy storage (TES) medium due to its large amount of latent heat and broad phase change temperature range, thus the application of PCM has vast potential to reduce the energy demand of buildings because it is able to phase change in a particular temperature range and then alleviate the impact of outdoor temperature variation on the indoor environment, thereby lower energy demand for heating and cooling, and improve occupant thermal comfort. Hence there are extensive studies focusing on utilizing PCM to realize energy conservation. Although there are extensive studies focusing on incorporating PCM into buildings to lower energy consumption, the thorough optimization analysis for parameters related to PCM itself and the corresponding economic evaluation are still insufficient.

In this chapter, the total of eight parameters of PCM, including location, melting temperature, thickness, phase transition temperature radius, latent heat, density, thermal conductivity, and specific heat, were analyzed. We varied their values in a predetermined range and investigated the effects of their variation on the annual energy demand of traditional dwellings in northeast Sichuan hills, China, and then a detailed economic analysis, which predicted the investment payback period and economic benefits of PCM with different parameters, was conducted. Furthermore, considering

CHAPTER 6. PARAMETRIC AND ECONOMIC ANALYSIS OF PHASE CHANGE MATERIALS (PCM) ON ENERGY SAVING FOR TRADITIONAL DWELLINGS IN NORTHEAST OF SICHUAN HILLS

the high cost of PCM, we discussed a more economic selection of PCM for this study region. Eventually, we obtain the following findings:

- It is more recommended to place the PCM on the inside of the wall in the climatic background of this region. The saving rate of the annual energy demand of inside PCM with its optimal melting temperature (14°C) is 16.89%, higher than that of outside PCM with its optimal melting temperature (14.22%).
- Recommended PCM with the optimal combination of parameters is able to reduce 21.81% of annual energy demand, which can lower 8%-20% of original annual energy demand more than PCM products in the present market. It certainly proves that it is imperative to develop the appropriate PCM product based on its application background and purpose.
- Thickness, phase transition temperature radius, latent heat, and specific heat of PCM have a positive correlation with the energy-saving performance of PCM, while there is a negative correlation between the thermal conductivity of PCM and its energy-saving effect, and density of PCM doesn't present the regular link with annual energy demand. Additionally, variations of phase transition temperature radius, latent heat, and specific heat have minor impacts on the annual energy demand.
- Thermal conductivity, density, and thickness are the three crucial parameters affecting the economic benefits of PCM application. When decreasing their values by 50% based on the optimal values for energy saving, the corresponding economic benefits can increase by 480%, 440%, and 50%, respectively; but when increasing their values by 50%, their investment payback period exceeds 25 years.
- There exists a potential interplay between thermal conductivity and melting temperature of PCM in terms of energy-saving purposes for buildings, that is, changing the value of one parameter probably leads to a consequential variation of the optimal value of another parameter. And this interplay between thermal conductivity and melting temperature of PCM will be explored in our future research.
- Lastly, PCM with 5mm of thickness and 500 kg/m³ of density, while other parameters remain the optimal value is recommended for traditional dwellings in this region, that is, location, melting temperature, thickness, phase transition temperature radius, latent heat, density, thermal conductivity, and specific heat of the recommended PCM is inside, 14°C, 5mm, 8°C, 250 kJ/kg, 500 kg/m³, 0.1 W/(m K), and 2500 J/(kg K), respectively.

CHAPTER 6. PARAMETRIC AND ECONOMIC ANALYSIS OF PHASE CHANGE MATERIALS (PCM) ON ENERGY SAVING FOR TRADITIONAL DWELLINGS IN NORTHEAST OF SICHUAN HILLS

Reference

- [1] N. Zhu, Z. Ma, S. Wang, Dynamic characteristics and energy performance of buildings using phase change materials: a review, *Energy Conversion and Management*. 50 (2009) 3169–3181. doi: <https://doi.org/10.1016/j.enconman.2009.08.019>
- [2] China Building Energy Consumption Research Report (2020). <https://www.cabee.org/site/content/24021.html>, 2022 (Accessed 28 April 2022).
- [3] S.E. Kalnæs, B.P. Jelle, Phase change materials and products for building applications: a state-of-the-art review and future research opportunities, *Energy and Buildings*. 94 (2015) 150–176. doi: <https://doi.org/10.1016/j.enbuild.2015.02.023>
- [4] D. Ürge-Vorsatz, L.F. Cabeza, S. Serrano, C. Barreneche, K. Petrichenko, Heating and cooling energy trends and drivers in buildings, *Renewable and Sustainable Energy Reviews*. 41 (2015) 85–98. doi: <https://doi.org/10.1016/j.rser.2014.08.039>.
- [5] X. Meng, B. Yan, Y. Gao, J. Wang, W. Zhang, E. Long, Factors affecting the in situ measurement accuracy of the wall heat transfer coefficient using the heat flow meter method, *Energy and Buildings*. 86 (2015) 754-765. doi: <https://doi.org/10.1016/j.enbuild.2014.11.005>.
- [6] R.A. Kishore, M.V.A. Bianchi, C. Booten, J. Vidal, R. Jackson, Parametric and sensitivity analysis of a PCM-integrated wall for optimal thermal load modulation in lightweight buildings, *Applied Thermal Engineering*. 187 (2021) 116568. doi: <https://doi.org/10.1016/j.applthermaleng.2021.116568>
- [7] D. H. Yu, Z. Z. He, Shape-remodeled macrocapsule of phase change materials for thermal energy storage and thermal management, *Applied Energy*. 247 (2019) 503e516. doi: <https://doi.org/10.1016/j.apenergy.2019.04.072>
- [8] E. Solgi, Z. Hamedani, R. Fernando, B. M. Kari, A parametric study of phase change material characteristics when coupled with thermal insulation for different Australian climatic zones, *Building and Environment*. 163 (2019) 106317. doi: <https://doi.org/10.1016/j.buildenv.2019.106317>
- [9] R.A. Kishore, M.V.A. Bianchi, C. Booten, J. Vidal, R. Jackson, Optimizing PCM-integrated walls for potential energy savings in US buildings, *Energy and Buildings*. 226 (2020) 110355. doi: <https://doi.org/10.1016/j.enbuild.2020.110355>
- [10] R. A. Kishore, M.V.A. Bianchi, C. Booten, J. Vidal, R. Jackson, Modulating thermal load through lightweight residential building walls using thermal energy storage and controlled precooling strategy, *Applied Thermal Engineering*. (2020) 115870. doi: <https://doi.org/10.1016/j.applthermaleng.2020.115870>
- [11] K. Faraj, M. Khaled, J. Faraj, F. Hachem, C. Castelain, A review on phase change materials for thermal energy storage in buildings: Heating and hybrid applications, *Journal of Energy Storage*. 33 (2021) 101913. doi: <https://doi.org/10.1016/j.est.2020.101913>

CHAPTER 6. PARAMETRIC AND ECONOMIC ANALYSIS OF PHASE CHANGE MATERIALS (PCM) ON ENERGY SAVING FOR TRADITIONAL DWELLINGS IN NORTHEAST OF SICHUAN HILLS

- [12] Y. Li, N. Nord, Q. Xiao, T. Tereshchenko, Building heating applications with phase change material: A comprehensive review, *Journal of Energy Storage*. 31 (2020) 101634. doi: <https://doi.org/10.1016/j.est.2020.101634>
- [13] N. Soares, A.R. Gaspar, P. Santos, J.J. Costa, Multi-dimensional optimization of the incorporation of PCM-drywalls in lightweight steel-framed residential buildings in different climates, *Energy and Buildings*. 70 (2014) 411-421. doi: <http://dx.doi.org/10.1016/j.enbuild.2013.11.072>
- [14] E. Tunçbilek, M. Arıcı, Michal. Krajčák, S. Nižetić, H. Karabay, Thermal performance based optimization of an office wall containing PCM under intermittent cooling operation, *Applied Thermal Engineering*. 179 (2020) 115750. doi: <https://doi.org/10.1016/j.applthermaleng.2020.115750>
- [15] B. Nghana, F. Tariku, Phase change material's (PCM) impacts on the energy performance and thermal comfort of buildings in a mild climate, *Building and Environment*. 99 (2016) 221-238. doi: <http://dx.doi.org/10.1016/j.buildenv.2016.01.023>
- [16] D. Zhou, P. Eames, Phase Change Material Wallboard (PCMW) melting temperature optimisation for passive indoor temperature control, *Renewable Energy*. 139 (2019) 507-514. doi: <https://doi.org/10.1016/j.renene.2019.02.109>
- [17] Z.X. Li, A. A. Al-Rashed, M. Rostamzadeh, R. Kalbasi, A. Shahsavar, M. Afrand, Heat transfer reduction in buildings by embedding phase change material in multi-layer walls: Effects of repositioning, thermophysical properties and thickness of PCM, *Energy Conversion and Management*. 195 (2019) 43-56. doi: <https://doi.org/10.1016/j.enconman.2019.04.075>
- [18] J. Xie, W. Wang, J. Liu, Song Pan, Thermal performance analysis of PCM wallboards for building application based on numerical simulation, *Solar Energy*. 162 (2018) 533-540. doi: <https://doi.org/10.1016/j.solener.2018.01.069>
- [19] H. Wang, W. Lu, Z. Wu, G. Zhang. Parametric analysis of applying PCM wallboards for energy saving in high-rise lightweight buildings in Shanghai, *Renewable Energy*. 145 (2020) 52-64. doi: <https://doi.org/10.1016/j.renene.2019.05.124>
- [20] Z. Liu, J. Hou, X. Meng, B.J. Dewancker, A numerical study on the effect of phase-change material (PCM) parameters on the thermal performance of lightweight building walls, *Case Studies in Construction Materials*. 15 (2021) e00758. doi: <https://doi.org/10.1016/j.cscm.2021.e00758>
- [21] Q. Al-Yasiri, M. Szabó, Incorporation of phase change materials into building envelope for thermal comfort and energy saving: A comprehensive analysis, *Journal of Building Engineering*. 36 (2021) 102122. doi: <https://doi.org/10.1016/j.jobe.2020.102122>
- [22] X. Jin, M.A. Medina, X. Zhang, Numerical analysis for the optimal location of a thin PCM layer in frame walls, *Applied Thermal Engineering*. 103 (2016) 1057-1063. doi: <http://dx.doi.org/10.1016/j.applthermaleng.2016.04.056>

CHAPTER 6. PARAMETRIC AND ECONOMIC ANALYSIS OF PHASE CHANGE MATERIALS (PCM) ON ENERGY SAVING FOR TRADITIONAL DWELLINGS IN NORTHEAST OF SICHUAN HILLS

- [23] A. Vukadinović, J. Radosavljević, A. Đorđević, Energy performance impact of using phase-change materials in thermal storage walls of detached residential buildings with a sunspace, *Solar Energy*. 206 (2020) 228-244. doi: <https://doi.org/10.1016/j.solener.2020.06.008>
- [24] Z. Liu, J. Hou, Y. Huang, J. Zhang, X. Meng, B. J. Dewancker, Influence of phase change material (PCM) parameters on the thermal performance of lightweight building walls with different thermal resistances, *Case Studies in Thermal Engineering*. 31 (2022) 101844. doi: <https://doi.org/10.1016/j.csite.2022.101844>
- [25] K. Saafi, N. Daouas, Energy and cost efficiency of phase change materials integrated in building envelopes under Tunisia Mediterranean climate, *Energy*. 187 (2019) 115987. doi: <https://doi.org/10.1016/j.energy.2019.115987>
- [26] X. Mi, R. Liu, H. Cui, S. A. Memon, F. Xing, Y. Lo, Energy and economic analysis of building integrated with PCM in different cities of China, *Applied Energy*. 175 (2016) 324-336. doi: <https://doi.org/10.1016/j.apenergy.2016.05.032>
- [27] F. Souayfane, P. H. Biwole, F. Fardoun, P. Achard, Energy performance and economic analysis of a TIM-PCM wall under different climates, *Energy*. 169 (2019) 1274-1291. doi: <https://doi.org/10.1016/j.energy.2018.12.116>
- [28] J. Hou, T. Zhang, Z. Liu, L. Zhang, H. Fukuda, Application evaluation of passive energy-saving strategies in exterior envelopes for rural traditional dwellings in northeast of Sichuan hills, China, *International Journal of Low-Carbon Technologies*. 17 (2022) 342-355. <https://doi.org/10.1093/ijlct/ctac007>
- [29] J. Hou, T. Zhang, Z. Liu, C. Hou, H. Fukuda, A study on influencing factors of optimum insulation thickness of exterior walls for rural traditional dwellings in northeast of Sichuan hills, China, *Case Studies in Construction Materials*. 16 (2022) e01033. doi: <https://doi.org/10.1016/j.cscm.2022.e01033>
- [30] X. Liu, *Engineering Economy (3rd Edition)*, China Architecture & Building Press, Beijing, 2015.
- [31] Weather Data Download - Sichuan Nanchong 574110 (CSWD). https://energyplus.net/weather-location/asia_wmo_region_2/CHN/CHN_Sichuan.Nanchong.574110_CSWD. 2022 (Accessed 28 April 2022).
- [32] Ministry of Housing and Urban-Rural Development of the People's Republic of China, Standard for weather data of building energy efficiency JGJ/T 346-2014, China Architecture & Building Press, Beijing, 2014.
- [33] Ministry of Housing and Urban-Rural Development of the People's Republic of China, Design standard for energy efficiency of residential buildings in hot summer and cold winter zone JGJ134-2010, China Architecture & Building Press, Beijing, 2010.
- [34] Ministry of Housing and Urban-Rural Development of the People's Republic of China, Code for thermal design of civil building GB50176-2016, China Architecture & Building Press,

CHAPTER 6. PARAMETRIC AND ECONOMIC ANALYSIS OF PHASE CHANGE MATERIALS (PCM) ON ENERGY SAVING FOR TRADITIONAL DWELLINGS IN NORTHEAST OF SICHUAN HILLS

Beijing, 2016.

- [35] Products information of Natural TCM. TCM Manufacturing - Natural TCM Energy Saver (tcm-energysaver.com) 2022 (Accessed 28 April 2022).
- [36] M. K. Urbikain, M. G. Davies, A frequency domain estimation of wall conduction transfer function coefficients, *Energy and Buildings*. 51 (2012) 191-202. doi: <https://doi.org/10.1016/j.enbuild.2012.05.005>
- [37] U.S. Department of Energy, EnergyPlus™ Version 22.1.0 Documentation Input Output Reference, 2022.
- [38] U.S. Department of Energy, EnergyPlus™ Version 22.1.0 Documentation Engineering Reference, 2022.
- [39] ASHRAE, A. G, Guideline 14-2002: Measurement of Energy and Demand Savings. ASHRAE, Atlanta, 2022.
- [40] H. Huang, W.I.B.W.M. Nazi, Y. Yu, Y. Wang, Energy performance of a high-rise residential building retrofitted to passive building standard – a case study, *Applied Thermal Engineering*. 181 (2020) 115902. doi: <https://doi.org/10.1016/j.applthermaleng.2020.115902>
- [41] A.A. Serageldin, A. Abdeen, M.S. Ahmed, A. Radwan, S. Ookawara, Solar chimney combined with earth to-air heat exchanger for passive cooling of residential buildings in hot areas, *Solar Energy*. 206 (2020) 145–162. doi: <https://doi.org/10.1016/j.solener.2020.05.102>
- [42] Y. Geng, X. Han, H. Zhang, L. Shi, Optimization and cost analysis of thickness of vacuum insulation panel for structural insulating panel buildings in cold climates, *Journal of Building Engineering*. 33 (2021) 101853. doi: <https://doi.org/10.1016/j.job.2020.101853>
- [43] L. Zhang, C. Hou, J. Hou, D. Wei, Y. Hou, Optimization analysis of thermal insulation layer attributes of building envelope exterior wall based on DeST and life cycle economic evaluation, *Case Studies in Thermal Engineering*. 14 (2019) 100410. <https://doi.org/10.1016/j.csite.2019.100410>
- [44] R. Ji, Z. Zou, M. Chen, Y. Zheng, S. Qu, Numerical assessing energy performance for building envelopes with phase change material, *International Journal of Energy Research*. 43 (2018) 6222-6232. doi: <https://doi.org/10.1002/er.4293>
- [45] R. Ye, R. Huang, X. Fang, Z. Zhang, Simulative optimization on energy saving performance of phase change panels with different phase transition temperatures, *Sustainable Cities and Society*. 52 (2020) 101833. doi: <https://doi.org/10.1016/j.scs.2019.101833>
- [46] M. T. Plytaria, C. Tzivanidis, E. Bellos, I. Alexopoulos, K. A. Antonopoulos, Thermal Behavior of a Building with Incorporated Phase Change Materials in the South and the North Wall, *Computation*. 7 (2019) 2. doi: <https://doi.org/10.3390/computation7010002>
- [47] C. Araújo, A. Pinheiro, M. F. Castro, L. Bragança, Phase Change Materials as a solution to improve energy efficiency in Portuguese residential buildings, *IOP Conf. Series: Materials*

CHAPTER 6. PARAMETRIC AND ECONOMIC ANALYSIS OF PHASE CHANGE MATERIALS (PCM) ON ENERGY SAVING FOR TRADITIONAL DWELLINGS IN NORTHEAST OF SICHUAN HILLS

Science and Engineering. 251 (2017) 012110. doi: <https://doi.org/10.1088/1757-899X/251/1/012110>

- [48] D. Qi, L. Pu, F. Sun, Y. Li, Numerical investigation on thermal performance of ground heat exchangers using phase change materials as grout for ground source heat pump system, *Applied Thermal Engineering*. 106 (2016) 1023-1032. doi: <https://doi.org/10.1016/j.applthermaleng.2016.06.048>
- [49] X. Xie, B. Xu, X. Chen, G. Pei, Turning points emerging in the effect of thermal conductivity of phase change materials on utilization rate of latent heat in buildings, *Renewable Energy*. 179 (2021) 1522-1536. doi: <https://doi.org/10.1016/j.renene.2021.07.129>
- [50] B. Xu, X. Xie, G. Pei, X. Chen, New view point on the effect of thermal conductivity on phase change materials based on novel concepts of relative depth of activation and time rate of activation: The case study on a top floor room, *Applied Energy*. 266 (2020) 114886. doi: <https://doi.org/10.1016/j.apenergy.2020.114886>

Chapter 7

Passive Application of Solar Energy for Traditional Dwellings in Northeast of Sichuan Hills

Chapter 7. Passive Application of Solar Energy for Traditional Dwellings in
Northeast of Sichuan Hills

Chapter 7. Passive Application of Solar Energy for Traditional Dwellings in Northeast of Sichuan Hills

7. Passive Application of Solar Energy for Traditional Dwellings in Northeast of Sichuan Hills	7-1
7.1 Introduction.....	7-1
7.2 Energy-saving potential of Trombe wall (T-wall) strategy	7-3
7.2.1 Description of T-wall.....	7-3
7.2.2 Simulation results.....	7-5
7.3 Energy-saving potential of on-top sunspaces application	7-6
7.3.1 Description of on-top sunspaces (OS).....	7-6
7.3.2 Simulation results.....	7-8
7.4 Summary	7-9
Reference	7-11

Chapter 7. Passive Application of Solar Energy for Traditional Dwellings in
Northeast of Sichuan Hills

7. Passive Application of Solar Energy for Traditional Dwellings in Northeast of Sichuan Hills

7.1 Introduction

This subsection describes the heat transfer model of the building exterior envelopes in detail, which can help us find more strategies to lower energy demand of buildings. The heat transfer process of opaque exterior envelope such as walls and roofs can be viewed as a one-dimensional unsteady heat conduction process. Let x be the coordinate of the thickness direction of the wall, and its heat balance differential equation can be expressed as Eq. (7-1):

$$\frac{\partial t}{\partial \tau} = a \frac{\partial^2 t}{\partial x^2} \quad (7-1)$$

$$a = \frac{\lambda}{\rho C} \quad (7-2)$$

where:

a is thermal diffusivity, m^2/s ;

t is temperature, $^{\circ}\text{C}$; τ is time, s ;

λ is thermal conductivity, $\text{W}/(\text{m K})$;

ρ is density kg/m^3 ;

C is specific heat, $\text{J}/(\text{kg K})$.

It is clear that the thermophysical properties of the envelope materials directly affect the rate and amount of heat transfer in space and time. As for building envelopes, enhancing the overall thermal resistance of the wall is the main means to suppress the impact of outdoor temperature on the indoor, therefore reducing the overall heat transfer coefficient of the wall is the main method currently applied, which includes adding insulation materials with lower thermal conductivity or raising the thickness of the wall to improve the thermal inertia. In consideration of the accessibility and practicability of energy-saving renovation of traditional dwellings, the energy-saving strategy of adding insulation material can be widely applied to local traditional dwellings, and the application of insulation materials is analyzed in Chapter 5. Furthermore, phase change material (PCM) can transfer heat in the time dimension by storing and releasing heat rely on its phase transition property, thus weakening the impact of outdoor temperature fluctuations on the indoor environment, while the energy-saving potential of PCM is also discussed in Chapter 6. In addition, the variation of indoor and outdoor temperature as the heat transfer boundary of building envelopes has a direct influence on the heat balance of building envelopes. So define $x = 0$ as the outside surface of the envelope and $x = \delta$ as the inside surface of the envelope, then the boundary condition of outdoor and indoor can be expressed as Eq. (7-3) and Eq. (7-4), respectively:

$$\alpha_{out} [t_{out}(\tau) - t(0, \tau)] = -\lambda \left. \frac{\partial t}{\partial x} \right|_{x=0} \quad (7-3)$$

$$\alpha_{in}[t(\delta, \tau) - t_{in}(\tau)] = -\lambda \left. \frac{\partial t}{\partial x} \right|_{x=\delta} \quad (7-4)$$

$$t_{out}(\tau) = t_e + \frac{\alpha I}{\alpha_{out}} \quad (7-5)$$

where:

α_{out} is convective heat transfer coefficient of the outside surface, (W/m² K);

α_{in} is convective heat transfer coefficient of the inside surface, (W/m² K);

$t_{out}(\tau)$ is solar-air temperature, °C; $t_{in}(\tau)$ is indoor air temperature, °C;

δ is thickness of wall, m; t_e is outdoor air temperature, °C;

α is solar radiation absorptivity of outer surface ;

I is solar radiation intensity, (W/m²);

$t(x, \tau)$ represents temperature at each point in the wall , °C.

Based on the above equations, we know that the thermal performance of exterior envelopes has a direct impact on the energy demand of building, and Chapter 5 and Chapter 6 focuses upgrading the thermophysical properties of exterior envelopes by both traditional insulation material and innovative phase change material (PCM), however, the thermal performance of building exterior envelopes is not only determined by their thermophysical properties but also affected by the ambient environment. Thus we can further improve the thermal performance of exterior envelopes by changing the outdoor boundary condition via some strategies.

According to Eqs. (7-3) - (7-4), it is obvious that improving thermal performance of the outside surface of building envelopes by utilizing renewable energy, such as solar radiation, can significantly enlarge the heat gain of building envelopes in winter while keeping the indoor temperature comfortable, thus it can dramatically lower the heating load for buildings with high heating demand. Hence, enhancing the heat gain of the exterior surface of the envelope is an important focus of the energy-saving strategies proposed in this study. And by review preceding related studies, we have noted that the solar thermal utilization is the most commonly used passive strategy in rural China in terms of using renewable energy to reduce the usage of fossil [1], while the mainly strategies to passively utilize solar energy include adding sunrooms, adjusting the solar radiation absorption coefficient of outside surfaces, installing Trombe wall (T-wall) and setting on-top sunspaces. Si et al. [2] installed the Trombe wall (T-wall) on the south façade of an elementary school dormitory building in Qinghai Province, China, and the experimental and simulation results revealed that this strategy raised the indoor temperature by 4.5°C-10°C in winter, which reduced the building heat load effectively. Zhang et al. [3] did a case study to discuss the effect of T-wall design factors on energy consumption, and the final results showed that up to 72% of annual building energy consumption could be saved by using T-wall with the optimum combination of design factors. Hou [4] analyzed the effect of using additional sunrooms in Tibetan traditional dwellings located in Sichuan Northwestern Plateau by investigation and simulation. The eventual results displayed that installing the additional sunroom with a depth

of 1.2m on the south façade could improve indoor temperature by 5°C-10°C in winter. Simoes et al. [5] revealed that T-wall system contributed to a reduction of more than 20% in heating demand without compromising the cooling season in Mediterranean climates. Bevilacqua et al. [6] found that in a moderate climate, such as Pisa, percentage reductions of heating requirements of up to 35.5% for the single-story building have been obtained for the high-insulated building by using T-wall. Wang et al. [7] analyzed the application potential of on-top sunspaces installed on the roof in serve cold zone, and the ultimate results showed that the rational on-top sunspaces could save about 42.8% for total building energy consumption.

Predicting the heating and cooling performance of the T-wall is always one of the main research focuses. Based on the literature review, the range of the heating and cooling load reductions of the building or experimental model is within 12.7-94% and 14.8-73%, respectively. Yu et al. [8,9] determined that the total reduced heat loadings for PC-T-wall, TC-T-wall, and PTC-T-wall are 309.8, 204.7, and 296.1 MJ/m², respectively. Zhou et al. [10] evaluated the thermal performance of a new ventilated T-wall integrated with phase change materials in a building in China. This had resulted in a reduction in the cooling loading (14.8%) and heating loading (12.7%) when the fusion temperatures of PCMs in exterior and interior PCM wallboards were 26°C and 22°C, respectively. Dabaieh and Elbably [11] optimized a classical T-wall, and the new design reduces the heating and cooling loading by 94% and 73%, respectively. Bojic et al. [12] reported that building with a T-wall could save 20% annual energy consumption during the heating season. Abbassi et al. [13] reported that rooms equipped with 4 m² and 8 m² T-walls reduced the annual heating energy consumption by 50% and 77% under the Tunisian climate, respectively. Ma et al. [14] found that the composite T-wall with optimized ventilation can reduce the annual energy cost by up to 3.7% compared to the composite T-wall without air supply.

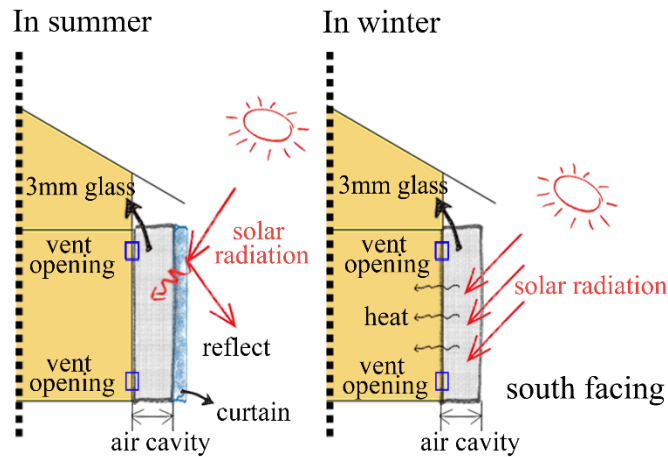
Taking into account local topographic characteristics that there are basically hills and mountains and the lower economic development of this region, two passive energy-saving strategies with low requirements for additional space— Trombe wall (T-wall) and on-top sunspaces are proposed and their application effects are evaluated in this chapter. We introduce the T-wall strategy and propose the recommended parameters by analyzing the impacts of its influencing parameters on energy-saving effect. Then we describe the on-top sunspaces (OS) strategy and its energy-saving potential in subsection 7.3. Finally, the findings and recommended parameters about these two strategies are summarized in subsection 7.4.

7.2 Energy-saving potential of Trombe wall (T-wall) strategy

7.2.1 Description of T-wall

Figure 7-1 displays the working method of T-wall and Figure 7-2 shows the corresponding model, and we apply a classical T-wall, including additional glazing wall outside the wall, and vent openings on the exterior wall. Glazing of T-wall is 3mm ordinary glass, with U-factor of 5.2 W/m² K. The height of each vent opening is 100mm, the distance between vent opening and the corresponding top (bottom) edge of room is 100mm, and the distance between vent opening and left (right) edge is still 100mm [6]. In order to utilize the warmer air heated by solar radiation in winter, the vent opening will be open in daytime and be close at night, while in summer, it remains close

all the time to prevent excessive heat from entering the room. According to the boundary condition equations, air in the T-wall zone can be heated by solar radiation, then the temperature of outside surface of building walls will be consequentially improved, which is positive for winter but negative for summer, thus we also considerate to alleviate the harmful impact on exterior walls in summer by utilizing shade control, that is, using curtains with high reflective coating solar reflectance is set as 0.8 [15,16] to reflect solar radiation and thereby lower the outside surface temperature of building walls in summer. Additionally, the thickness of air cavity of T-wall determines amount of heated air, which may has a potential effect on energy-saving effect of T-wall based on other research. Hence, we analyze the influence of air cavity thickness on the energy-saving performance of T-wall, and evaluate the application effect of shade control in subsection 7.2.2; meanwhile, in consideration that the glazing properties have great impact on the energy-saving effect, we also compare the effects of T-wall when the ordinary glass and low-e glass used in terms of energy-saving effect and economic benefits and results are shown in subsection 7.2.2.



Vent opening schedule:

- In summer: always close (with shade control);
- In winter: open in daytime; close in nighttime.

Figure 7-1. Diagram of Trombe wall (T-wall) strategy for base building.

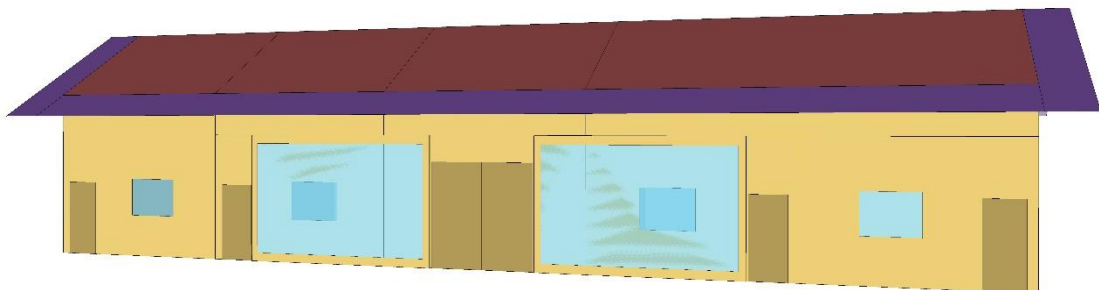


Figure 7-2. Application of Trombe wall (T-wall) on the base model.

7.2.2 Simulation results

Figure 7-3 displays the annual heating load and cooling load of different air cavity thickness, while Figure 7-3(a) shows the results when the shade control is not employed and Figure 7-3(b) presents the results when using the shade control. It is clear that annual heating load decreases when T-wall is fixed whether the shade control is applied or not, but the heating load hardly changes as thickness of air cavity from 50mm expands to 150mm, meaning the air cavity thickness has minor influence on the energy demand, in detail, the heating load of 50mm, 100mm, and 150mm air cavity is 71.83 kWh/m², 71.93 kWh/m², and 72.03 kWh/m², therefore, 50mm of air cavity thickness will be adopted in the following research, and the saving rate of heating load is 11.5%. As for cooling load, it appears an opposite performance compared to heating load. Although the air cavity thickness still cannot significantly influence the annual cooling load, the cooling load grows compared to the base model. From Figure 7-3(a), the annual cooling load corresponds to 50mm, 100mm, and 150mm air cavity thickness is 21.62 kWh/m², 21.56 kWh/m², and 21.51 kWh/m², respectively, while their increasing rate is 15.4%, 15.1%, and 14.8%, respectively. Then the total annual heating load and cooling load is 93.45 kWh/m², 93.49 kWh/m², and 93.54 kWh/m², while compared to the original model without T-wall, whose annual load is 99.89 kWh/m², the energy-saving rate is only 6.5%, 6.4% and 6.3%, respectively. It is apparently that the increase amount of cooling load offset a part of the saved amount of heating load, diminishing the energy-saving effect in winter, therefore, adopting shade control to alleviate this harmful effect in summer is crucial. By using the shade control described in subsection 7.2.1, the cooling loads of varies air cavity thickness dramatically decrease as shown in Figure 7-3(b) even though they are still a bit of higher than the original model without T-wall. In detail, the cooling load is 19.25 kWh/m², 19.23 kWh/m², and 19.22 kWh/m² corresponds to air cavity thickness of 50mm, 100mm, and 150mm, respectively, their corresponding saving rate is about -2.7%, -2.6%, and -2.5%, respectively. And when the shade control is applied, the saving rate of annual energy demand is 8.79%, 8.71%, and 8.62% for T-wall with air cavity thickness of 50mm, 100mm, and 150mm, increasing by approximately 36% compared to when the shade control doesn't utilized. Hence, 50mm of air cavity thickness and shade control are employed in the following research.

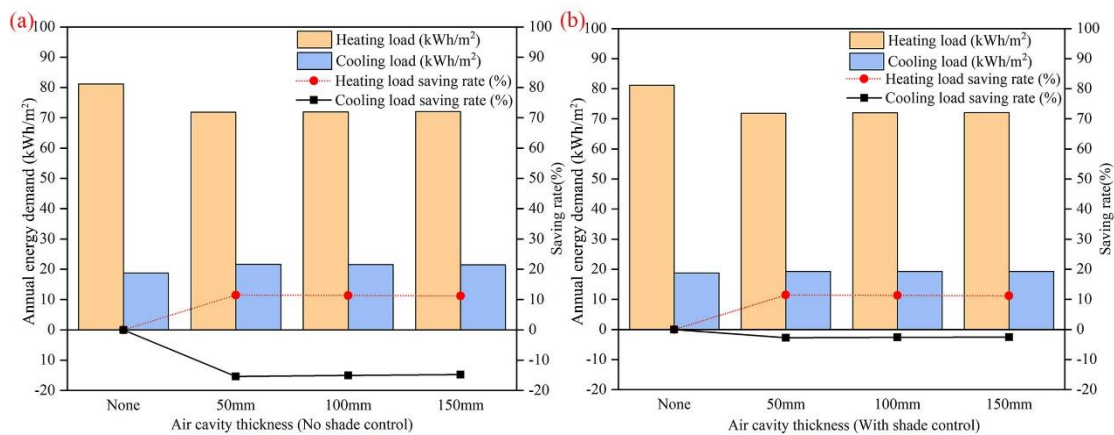


Figure 7-3. Annual heating load and cooling load vs. air cavity thickness and shade control of T-wall.

We replace the glazing of T-wall from ordinary glass to low-e glass and simulate the corresponding annual energy demand by EnergyPlus, then the corresponding economic benefits are calculated by using the dynamic investment payback period (DPP) method, and results are shown in Table 7-1. No doubt that using low-e glass as T-wall glazing is able to lower more amount of energy demand, and its saving rate of annual energy demand increases by approximately 38% compared to the saving rate of ordinary glazing; meanwhile, the corresponding saved money of low-e glass is 142.5 CNY more than ordinary glass per year. However, the payback period of ordinary glass and low-e glass is 2.2 years and 10.7 years, respectively, and the corresponding economic benefits after 25 years are 5341.2 CNY and 3701.2 CNY, respectively. These unsatisfactory economic results of low-e glass occur due to its high cost, that is, the price of 3mm ordinary glass is only 36 CNY/m², while the low-e glass is 200 CNY/m², and thus the total investment cost of ordinary glass and low-e glass is 1184 CNY and 5284 CNY (including the same cost of curtain investment), respectively. In detail, the total investment of low-e glass is 4100 CNY higher than that of ordinary glass, whereas the saved money per year of low-e glass is only 142.5 CNY higher than that of ordinary glass, thus it's difficult to compensate the additional investment cost by the extra saved money especially in an inflationary economic context. Consequently, we still adopt the ordinary glass as T-wall glazing based on the economic evaluation between the ordinary glass and low-e glass.

Table 7-1 Economic evaluation of different glazing type of T-wall.

Glazing type	Saving rate of annual energy demand (%)	Saved money per year (CNY/a)	Total investment cost (CNY)	Economic benefits after 25 years (CNY)
Ordinary	8.8	378.0	1184	5341.2
Low-e	12.1	520.5	5284	3701.2

7.3 Energy-saving potential of on-top sunspaces application

7.3.1 Description of on-top sunspaces (OS)

Application of T-wall improves the outdoor boundary condition of exterior envelopes in vertical dimension, meanwhile we can also change the boundary condition of the top horizontal surface of air-conditioned room by some strategies. On-top sunspaces can make full use of the solar radiation received by the roof in winter and reduce the heating load according to the study by Wang et al. [17]. In consideration of the installation of on-top sunspaces does not affect the daily life of local residents since the current use frequency of local attic is low, the on-top sunspaces (OS) are employed and their energy-saving effects are evaluated. Figure 7-4 demonstrates the work method of on-top sunspaces (OS) strategy, and it includes two part, one part is glazing on the roof, while another part is 30mm of expanded polystyrene board (EPS) fixed on the ceiling, acting as a role of thermal mass. Furthermore, no doubt that the expanded polystyrene board (EPS) will resist the warm air in the attic to transfer into the rooms in winter although it can avoid heat gain in summer. Therefore, we can use fans to blow the warm air into rooms in order to improve the efficiency of the warm air in the attic. However, considering the backward economic development of this research region, we only focus on the passive energy-saving strategies, and thereby no fans are combined in this strategy.

In addition, only two bedrooms adopt OS as shown in Figure 7-5.

The glass area is expressed as the window-roof ratio (WRR), representing the ratio of the glazing area to the area of the roof where it is located. In order to reduce heat gain in summer, blinds with the reflective coating (solar reflectance is set as 0.8 [15,16] are used as the shade control method. It can be found according to Figure 7-4 that on-top sunspaces make the attic temperature rise due to getting more solar radiation and the ceiling floor with insulation material plays a role in thermal mass in winter, then the heat can be absorbed by the thermal mass and through the heat conduction of the ceiling to warm the bedroom, and reduces the heating load in final. Furthermore, the influences of WRR variation and shade control on the heating load and cooling load are evaluated with the help of EnergyPlus, and results are analyzed in 7.3.2.

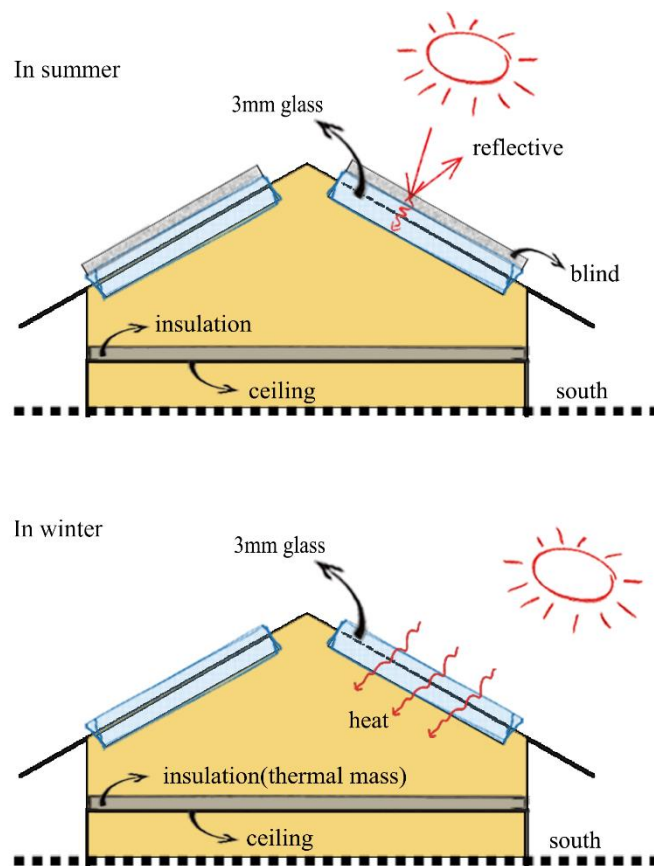


Figure 7-4. Diagram of on-top sunspaces (OS) strategy for base building.

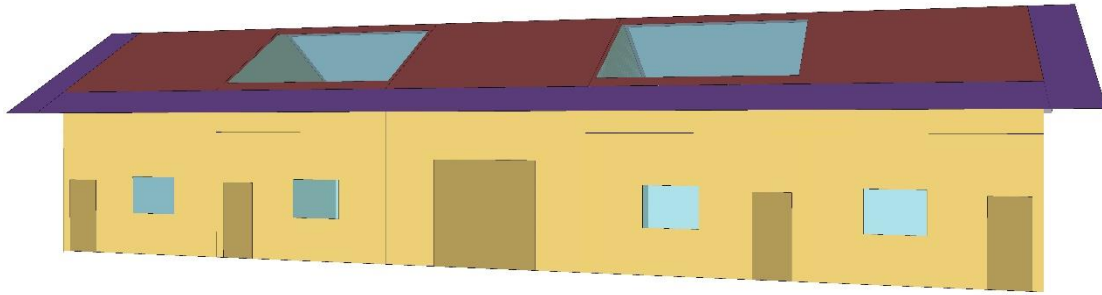


Figure 7-5. Application of on-top sunspaces (OS) on the base model.

7.3.2 Simulation results

Figure 7-6 demonstrates the heating load and cooling load of different glazing areas. The energy-saving rates of the heating load grows with the increase of WRR, and they are 12.9%, 14.7%, and 16.3% when the values of WRR are 25%, 50%, and 75%, respectively, however, the larger the WRR, the greater the increase in cooling load in summer if shade control doesn't be applied, although cooling load decreases 0.33 kWh/m² when WRR equals 25%, the increase rate of cooling load can achieve 10.5% and 23% when WRR equals 50% and 75%, respectively. Furthermore, similar to the T-wall strategy, shade control can efficiently diminish the harmful impacts in summer. As Figure 7-6 shown, when shade control is applied, the saving rate of annual energy demand surges from 7.5% to 14.2% when WRR equals 75%. It can be noted that although the cooling load of 75% of WRR (20.38 kWh/m²) is a bit higher than that of WRR equals 25% (19.47 kWh/m²), the total saving rate of WRR equals 75% is still better, this phenomenon occurs because the larger the glazing area of OS, the heating load is lower, while the amount of the heating load demand is greatly larger than the cooling load, thus the amount of extra saved heating load with WRR increases is higher than increased cooling load amount caused by increasing the glazing area of OS. Finally, we recommend using on-top sunspaces (OS) on the roof of bedrooms with shade control, and meanwhile, the WRR is suggested as 75%.

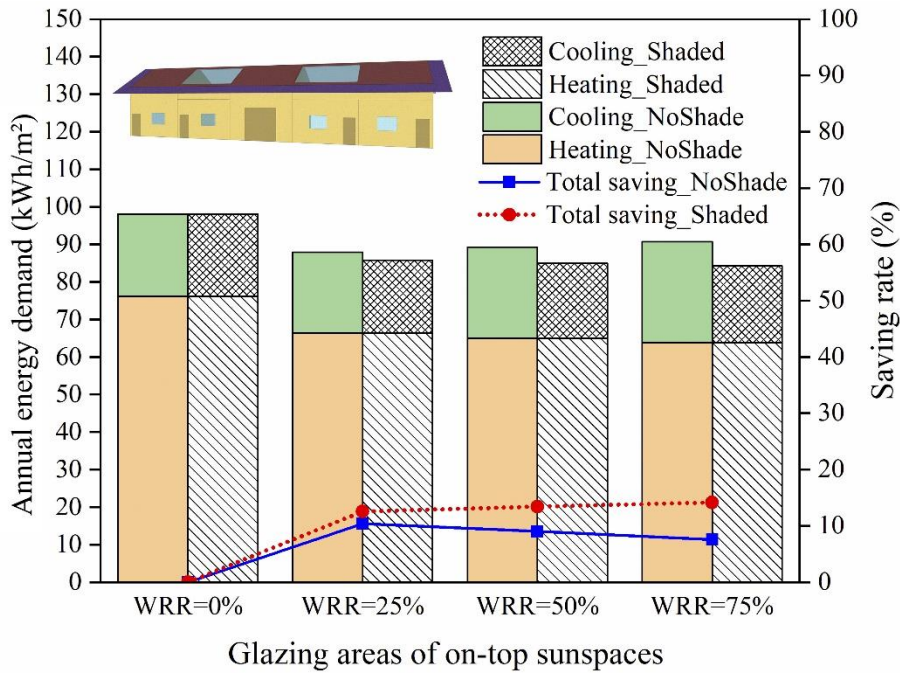


Figure 7-6. Energy-saving effect of the OS on heating and cooling load vs. glazing area.

7.4 Summary

According to the related research, using renewable energy can directly reduce the usage of fossil and the most commonly used passive strategy in rural China is solar thermal utilization. In this chapter, two passive solar utilization methods – Trombe wall strategy (T-wall) and on-top sunspaces strategy (OS) were evaluated. We discussed the impact of thickness of air cavity, the utilization of shade control, and the glass category of T-wall glazing on the energy-saving effect of T-wall, as for on-top sunspaces strategy, we also analyzed the influence of the glazing area variation and shade control on the energy-saving effect of the on-top sunspaces strategy. Based on the analysis in this chapter, we can obtain the following results:

- The thickness of air cavity for Trombe wall strategy (T-wall) has minor influence on the energy-saving effect of T-wall, and considering the investment cost, 50mm of air cavity thickness is recommended for this study region.
- Using low-e glass as T-wall glazing is able to lower more amount of energy demand, and its saving rate of annual energy demand increases by approximately 38% compared to the saving rate of ordinary glazing, whereas its payback period (10.7 years) is longer than that of ordinary glass (2.2 years), and meanwhile, its corresponding economic benefits after 25 years (3701.2 CNY) is also less than that of ordinary glass (5341.2 CNY). Therefore, ordinary glass is recommended as the glazing of T-wall strategy.
- The energy-saving rates of the annual energy demand grows with the increase of the glazing area. Saving rates of annual energy demand are 12.9%, 14.7%, and 16.3% when the values of WRR are 25%, 50%, and 75%, respectively, and 75% of WRR is recommended.

- Shade control can greatly decrease the cooling load for both T-wall strategy and OS strategy. And when the shade control is applied, the saving rate of annual energy demand is 8.79% for T-wall with air cavity thickness of 50mm. Moreover, when shade control is applied, the saving rate of annual energy demand for OS surges from 7.5% to 14.2% when WRR equals 75%.

Reference

- [1] Lin Y, Zhao L, Yang W, Hao X, Li C. A review on research and development of passive building in China. *Journal of Building Engineering*, 2021; 42: 102509. doi: <https://doi.org/10.1016/j.job.2021.102509>.
- [2] Si P, Lv Y, Rong X, Shi L, Yan J, Wang X. An innovative building envelope with variable thermal performance for passive heating systems. *Applied Energy*, 2020; 269: 115175. doi: <https://doi.org/10.1016/j.apenergy.2020.115175>.
- [3] Zhang L, Hou Y, Liu Z, Du J, Xu L, Zhang G, Shi L. Trombe wall for a residential building in Sichuan-Tibet alpine valley – a case study. *Renewable Energy*, 2020; 156: 31–46. doi: <https://doi.org/10.1016/j.renene.2020.04.067>.
- [4] Hou J (2019). Optimization of indoor thermal environment in winter for traditional Tibetan dwellings in the Sichuan Northwestern Plateau. Master Dissertation, Sichuan Agricultural University, China. doi: <https://doi.org/10.27345/d.cnki.gsnyu.2019.000693>.
- [5] Simes N, Manaia M, Simes I. Energy performance of solar and trombe walls in mediterranean climates. *Energy*, 2021; 121197. doi: <https://doi.org/10.1016/j.energy.2021.121197>
- [6] Bevilacqua P, Benevento F, Bruno R, Arcuri N. Are trombe walls suitable passive systems for the reduction of the yearly building energy requirements?. *Energy*, 2019; 185, 554-566.
- [7] Wang W, Yuan M, Li Y, Li C. Numerical Investigation on the Impact of an On-top Sunspace Passive Heating Approach for Typical Rural Buildings in Northern China. *Solar Energy*, 2019; 186: 300–310. doi: <https://doi.org/10.1016/j.solener.2019.05.013>.
- [8] B. Yu, Q. Jiang, W. He, Z. Hu, H. Chen, J. Ji, G. Xu, The performance analysis of a novel TC-Trombe wall system in heating seasons, *Energy Convers. Manag.* 164 (2018) 242e261, doi: <https://doi.org/10.1016/j.enconman.2018.02.093>.
- [9] B. Yu, J. Yang, W. He, M. Qin, X. Zhao, H. Chen, The performance analysis of a novel hybrid solar gradient utilization photocatalytic-thermal-catalytic-Trombe wall system, *Energy* 174 (2019) 420e435, doi: <https://doi.org/10.1016/j.energy.2019.02.121>.
- [10] Y. Zhou, C.W.F. Yu, G. Zhang, Study on heat-transfer mechanism of wallboards containing active phase change material and parameter optimization with ventilation, *Appl. Therm. Eng.* 144 (2018) 1091e1108, doi: <https://doi.org/10.1016/j.applthermaleng.2018.04.083>.
- [11] M. Dabaieh, A. Elbably, ScienceDirect Ventilated Trombe wall as a passive solar heating and cooling retrofitting approach ; a low-tech design for off-grid settlements in semi-arid climates, *Sol. Energy* 122 (2015) 820e833, doi: <https://doi.org/10.1016/j.solener.2015.10.005>.
- [12] M. Bojić, K. Johannes, F. Kuznik, Optimizing energy and environmental performance of passive Trombe wall, *Energy Build.* 70 (2014) 279e286, doi: <https://doi.org/10.1016/j.enbuild.2013.11.062>.

- [13] F. Abbassi, N. Dimassi, L. Dehmani, Energetic study of a Trombe wall system under different Tunisian building configurations, *Energy Build.* 80 (2014) 302e308, doi: <https://doi.org/10.1016/j.enbuild.2014.05.036>.
- [14] Q. Ma, H. Fukuda, X. Wei, A. Hariyadi, Optimizing energy performance of a ventilated composite Trombe wall in an office building, *Renew. Energy* 134 (2019) 1285e1294, doi: <https://doi.org/10.1016/j.renene.2018.09.059>.
- [15] UIUC L. 2010. EnergyPlus documentation: output details and examples. US Department of Energy. pp. 279.
- [16] ASHRAE H. 2001. ASHRAE fundamentals handbook. Atlanta, GA, USA: American Society of Heating Refrigeration and Air-Conditioning Engineers. pp. 710.
- [17] Wang W, Yuan M, Li Y, Li C. Numerical Investigation on the Impact of an On-top Sunspace Passive Heating Approach for Typical Rural Buildings in Northern China. *Solar Energy*, 2019; 186: 300–310. doi: <https://doi.org/10.1016/j.solener.2019.05.013>.

Chapter 8

Tech-economic Analysis of Comprehensive Energy- saving Strategies

Chapter 8. Tech-economic Analysis of Comprehensive Energy-saving Strategies

8. Tech-economic Analysis of Comprehensive Energy-saving Strategies	
8.1 Introduction.....	8-1
8.2 Evaluation of energy-saving and economic potential of comprehensive energy-saving strategies	8-1
8.3 Influence of building orientation on energy-saving and economic potential	8-10
8.4 Energy-saving and economic potential for the tested building	8-12
8.5 Summary	8-14
Reference	8-16

8. Tech-economic Analysis of Comprehensive Energy-saving Strategies

8.1 Introduction

In this chapter, we employ different combinations of energy-saving strategies proposed in Chapter 5 to Chapter 7, and firstly, their energy-saving potential and the corresponding payback period and economic benefits are evaluated in section 8.2 via EnergyPlus and dynamic payback period method. Then in section 8.3, we take the strategy with best economic performance as example and discuss the influences of orientation variation on the energy-saving and economic effects. And finally, we employ the most recommended strategy to optimize the real tested building described in Chapter 4 and evaluate the energy-saving and economic potential to further validate the effectiveness of the recommended strategy, results are shown in section 8.4.

8.2 Evaluation of energy-saving and economic potential of comprehensive energy-saving strategies

8.2.1 Description of energy-saving strategies

Before we evaluated the energy-saving effect of individual strategy, such as employing insulation materials, phase change materials (PCM), Trombe wall (T-wall) and on-top sunspaces (OS) in Chapter 5 to Chapter 7. In order to thoroughly evaluate these strategies, we combine these strategies in different ways and numbered each one, detailed information are shown in Table 8-1.

In Table 8-1, we can see S1, S9, S13, and S15 are individual energy-saving strategy, corresponds to insulation materials, PCM, T-wall and OS, respectively, and other strategies are a combination of these four individual strategies in different ways. Additionally, the recommended parameter values of S1, S9, S13, and S15 are employed. In detail, the insulation strategy (S1) adds 81mm of polyurethane foam (PU) for exterior walls, and meanwhile adds 121mm of polyurethane foam (PU) for roof; S2 uses 5mm of phase change material (PCM), with density of 500 kg/m³, phase transition temperate of 6-22°C, thermal conductivity of 0.1 W/(m K), specific heat of 2500 J/kg K, and latent heat of 250 kJ/kg; S13 installs Trombe wall (T-wall) on the south walls of air-conditioned rooms, and the air cavity is 50mm, while glazing adopts 3mm ordinary glass, and meanwhile, curtains with high reflectivity coating are utilized as shade control to alleviate the harmful impact from solar radiation in summer; as for S15, on-top sunspaces (OS) are set on two bedrooms, with WRR equals 75%, similarly, 3mm ordinary glass is adopted and blinds with high reflectivity coating are used, and meanwhile, 30mm of expanded polystyrene board (EPS) fixed on the ceiling, playing a role of thermal mass.

Table 8-1 Contents of each energy-saving strategy.

	S1	S2	S3	S4	S5	S6	S7	S8	S9	S10	S11	S12	S13	S14	S15
Insulation	●	●	●	●	●	●	●	●							
PCM		●			●	●		●	●	●	●	●			
T-wall			●		●		●	●		●		●	●	●	
On-top sunspaces				●		●	●	●			●	●		●	●

8.2.2 Description of simulation model

In order to improve efficiency of lots of simulation works, some model settings, for example, airtightness or air change rate, are not unify in each chapter, while in this chapter, they are unified to ensure that the evaluation results are comparable for each energy-saving strategy. Table 8-2 shows the settings of the base model, which stands for the present building without any energy-saving strategies employed. The construction of exterior walls and roof is consistent with the reality, and the corresponding thermophysical parameters of related materials are shown in Table 8-3 (thermophysical parameters of PCM are described in subsection 8.2.1). According to Design standard for energy efficiency of residential buildings in hot summer and cold winter zone JGJ 134-2010 [1], heating thermostat should be set as 18°C and cooling thermostat should be 26°C when predicting the heating and cooling load of building, and meanwhile, air change rate (ACH) should be 1 per hour, therefore airtightness of this model is equivalent to ACH is 1 h⁻¹. Moreover, the weather condition boundary is CSWD data of Nanchong [2-3], and the heating load and cooling load of the base model is 81.11 kWh/m² and 18.74 kWh/m², respectively, thus the annual energy demand of the base model is 99.85 kWh/m². Additionally, air-conditioned area of 82.8m² (not the total floor area of 217.8 m²) is employed to evaluate the energy-saving and economic effects in the following parts.

Table 8-2 Information of the base model.

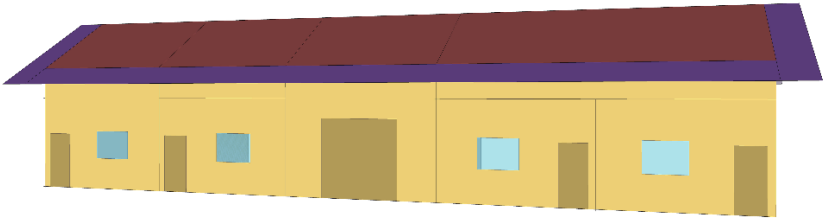
Model description	Detail
Three-dimensional model	
Floor area	217.8 m ²
Air-conditioned area	82.8 m ²
Orientation	Facing south
Exterior wall construction	20mm gypsum plaster (outside layer) + 100mm clay +20mm gypsum plaster
Roof construction	Roof tiles
Airtightness	1 h ⁻¹
Heating thermostat	18 °C
Cooling thermostat	26 °C
Heating load	81.11 kWh/m ²
Cooling load	18.74 kWh/m ²

Table 8-3 Thermophysical parameters of materials for simulation [4].

Building material	Calculation parameters		
	Heat conduction coefficient/ λ	Specific heat capacity/C	Density/ ρ_0
	W/(m K)	kJ/kg K	kg/m ³
Clay	0.76	1.01	1600
Gypsum plaster	0.76	1.05	1500
Roof board	0.14	2.51	500
Roof tiles	0.47	1.01	1200
Crushed stone concrete	1.28	0.92	2100
Expanded polystyrene (EPS)	0.039	1380	20
Polyurethan foam (PU)	0.024	550	35
Glazing	Heat transfer coefficient/U	Solar heat gain coefficient/SHGC	Transmittance of visible light
	W/(m ² K)		
Window	4.7	0.85	0.9
T-wall and OS glass	5.2	0.72	0.9

8.2.3 Energy-saving and economic potential of energy-saving strategies

Table 8-4 demonstrates the heating load, cooling load, and annual energy demand of each strategy. It is apparent that all of these 15 energy-saving strategies can achieve the aim that lower the annual demand of the building. From these results, we can note that the heating load decreases whatever strategy is utilized although there is a significant difference in the degree of their effects. And for the four individual strategies (S1, S9, S13, and S15), S1 of economic insulation material application has the excellent energy-saving rate of both heating load and cooling load, it can save 99.26% of heating load and even decline the cooling load to zero, and all of other strategies which involve the insulation strategy also create significant reductions of both heating load and cooling load. Amongst these strategies, S2 (insulation and PCM) saves the most amount of heating load (99.30%), even higher than saving rate of heating load obtained by S1. The heating load difference between S1 and S2 proves that PCM enhances the energy-saving effects of heating load of adding insulation, even though the difference is minor, and meanwhile, compared to S9 which only employs PCM, combining insulation materials (S2) performs better, implying that the combination of these two strategies is better than applying them separately in terms of energy-saving effects. However, not all individual strategies combined with the insulation strategy (S1) can result in an improved energy savings. For example, S3 which simultaneously adopts insulation materials with economic thickness and installs T-wall decrease less heating load and less cooling load than S1, indicating that T-wall weaken the energy-saving effects of insulation materials. This phenomenon occurs since vent openings of T-wall lead more air infiltration although it allows warm air to enter room in winter, and meanwhile the glass of vent opening has higher value of thermal conductivity than exterior walls, thereby there is much more heat loss in winter and heat gain in summer, and then improves

CHAPTER 8. TECH-ECONOMIC ANALYSIS OF COMPREHENSIVE ENERGY-SAVING STRATEGIES

the heating load and cooling load. Similarly, the combination of on-top sunspaces and insulation material (S4) also has a worse saving rate of both heating load and cooling load than only applying insulation strategy (S1). We infer that the reason of this occurrence is that the glazing of on-top sunspaces boosts the gross heat transfer coefficient of roof although they don't lead to extra air infiltration like T-wall does, therefore the temperature of indoor air in the attic spaces of S4 will be lower in winter while be higher in summer compared to the attic indoor air of S1, then the heating load and cooling load for air-conditioned rooms increase consequentially, and thereby saving rate of S4 is a bit lower than that of S1. Then from the results of S9, S10, and S13, we can notice that T-wall helps PCM decrease heating load from 76.66 kWh/m² to 68.41 kWh/m² and meanwhile, PCM offsets the negative impacts of T-wall in summer, that is, cooling load of T-wall (S13) declines from 19.25 kWh/m² to 18.57 kWh/m², meaning both heating load and cooling load of S10 cut down. Furthermore, PCM plays a similar role to alleviate the harmful effect in summer for on-top sunspaces, then the saving rate of cooling load for on-top sunspaces (S15) improves from -8.7% to -3.36% with an increase amount of 5.34%, implying there probably exists a synergy between PCM and on-top sunspaces. As for the performance of T-wall strategy and on-top sunspaces strategy, results of S14 show their combination can create more benefits, especially for cooling load, which is higher than original base building when T-wall strategy (S13) and on-top sunspaces (S15) are separately utilized, whereas when they are combined the value of saving rate of cooling load becomes positive from negative. Additionally, S5, S6, and S12 are strategies which integrate three individual strategies, and S8 is the comprehensive strategy integrate all of four individual strategies, while amongst them, S6 has a best saving effect for the annual energy demand of 97.98%, followed by S5 (93.76%) and S8 (93.81%) whose results are almost similar, S12 is worst with saving rate of annual energy demand of 25.85%. Based on the above results, we can conclude that adding insulation materials with economic thickness for exterior walls and roof contributes the largest portion of the energy savings for both heating load and cooling load. And an obvious example is S12, which uses all of these individual strategies expect for the insulation strategy, while comparing its saving rate of energy demand to that of S8 that integrates all of these four individual strategies, we can notice that the energy-saving rate of S12 is 25.85% whereas that of S8 is 93.81%, implying the crucial effect of insulation strategy for energy saving.

From the clear results shown in Table 8-4 and the above analysis, we can realize the best strategy is S2 in terms of the performance of annual energy demand, that is, adding insulation material (polyurethane foam) with economic thickness for exterior walls and roof, and simultaneously installing phase change material (PCM) on the exterior walls. However, we also need to notice that the saving rate of the comprehensive strategy (which combine two or more individual strategies) does not exactly equal to the sum of the energy-saving rate of each involved strategy, for instance, although the sum of the saving rate of heating demand corresponding to S1 (only employing insulation strategy) and S9 (only employing PCM strategy) exceeds 100%, the combination strategy (S2) still cannot decline the heating load to zero. This fact further indicates that when the investment cost is under consideration, the economic performance of each strategy may not be consistent with that of energy-saving effects since the investment cost of each energy-saving strategy is divergent while sometimes their energy-saving effects are similar, meaning the corresponding saved money

CHAPTER 8. TECH-ECONOMIC ANALYSIS OF COMPREHENSIVE ENERGY-SAVING STRATEGIES

is similar, thus the final economic benefits will perform diversely. Hence, we also carry out the economic evaluation of each strategy, including their dynamic payback period and economic benefits after 25 years. Table 8-4 displays the saved money caused by the application of these energy-saving strategies with the electricity price of 0.52 CNY/kWh, and the last column presents the total investment cost of each strategy based on the material and labor cost listed in Table 8-5. Additionally, the expenditure on these energy-saving strategies is a one-time investment that does not involve loans, and the calculation methods of dynamic payback period and economic benefits are clearly explained in Chapter 3.

Table 8-4 Annual energy demand, saved money per year and investment cost of each energy-saving strategy.

Strategy	Heating load (Saving rate) kWh/m ²	Cooling load (Saving rate) kWh/m ²	Energy demand (Saving rate) kWh/m ²	Saved money per year CNY/m ²	Investment cost CNY/m ²
Baseline	81.11	18.74	99.85	/	/
S1	0.6 (99.26%)	0 (100%)	0.6 (99.40%)	51.6	621.0
S2	0.57 (99.30%)	0 (100%)	0.57 (99.43%)	51.6	884.5
S3	3.08 (96.20%)	0.31 (98.35%)	3.39 (96.6%)	50.2	635.3
S4	1.7 (97.90%)	0.32 (98.29%)	2.02 (97.98%)	50.9	584.8
S5	2.97 (96.34%)	0.29 (98.45%)	3.26 (93.76%)	50.2	797.5
S6	1.68 (97.93%)	0.34 (98.19%)	2.02 (97.98%)	50.9	722.3
S7	4.77 (94.12%)	1.46 (92.21%)	6.23 (93.76%)	48.7	599.1
S8	4.69 (94.22%)	1.49 (92.05%)	6.18 (93.81%)	48.7	761.3
S9	76.66 (5.49%)	18.09 (3.47%)	94.75 (5.11%)	2.7	263.5
S10	68.41 (15.66%)	18.57 (0.91%)	86.98 (12.89%)	6.7	277.8
S11	59.53 (26.61%)	19.37 (-3.36%)	78.90 (20.98%)	10.9	297.4
S12	56.36 (30.51%)	17.68 (5.66%)	74.04 (25.85%)	13.4	311.7
S13	71.85 (11.42%)	19.25 (-2.72%)	91.1 (8.76%)	4.6	14.3

Table 8-4 Annual energy demand, saved money per year and investment cost of each energy-saving strategy (Cont).

S14	59.67 (26.43%)	18.27 (2.51%)	77.94 (21.94%)	11.4	48.2
S15	63.82 (21.32%)	20.37 (-8.70%)	84.19 (15.68%)	8.1	33.9

Table 8-5 Unit costs of materials and labor [5-6]

Material	Material cost		Labor cost	
	Unit	Price per unit (CNY)	Unit	Price per unit (CNY)
Gypsum plaster	m ³	480	m ²	27.4
Polyurethane foam (PU)	m ³	550	m ²	38.5
Expanded polystyrene (EPS)	m ³	442	m ²	24.6
Roof wooden board	m ²	45 (includes labor cost)		
Ordinary glass	m ²	36	day	60
Curtains / blinds	m ²	8 (includes labor cost)		
Phase change material (PCM)	kg	8.3	m ²	38.5

Figure 8-1 and Figure 8-3 display the dynamic payback period and final economic benefits after 25 years of each energy-saving strategy. Obviously, S9 and S10 whose dynamic period even exceeds 100 years should not be considered from the perspective of economy; meanwhile, S11 and S12 with dynamic payback period of 48.3 years and 53.7 years, respectively, also have a longer payback period than the reference value of 25 years. These unsatisfactory payback periods mainly caused by the expensive price and the relatively lower energy-saving effects of PCM compared by insulation materials, while the dynamic payback period of S2 (21.8 years) can prove this inference. Although the investment cost of S2 ups to 884.5 CNY/m², which is 2.8-3.3 times of that of S9, S10, S11, and S12, the saving rate of S2 is much higher than others and then the consequential saved money per year of S2 can achieve 51.6 CNY/m², whereas the saved money per year of S9, S10, S11, and S12 is 2.7 CNY/m², 6.7 CNY/m², 10.9 CNY/m², and 13.4 CNY/m², respectively, and only account for 5-26% of saved money per year of S2, therefore we can conclude that insulation strategy can balance out the high cost of PCM and the dynamic payback period is less than the reference year, though PCM strategy is also employed. The shortest payback period of 2.1 years belongs to S14 that integrates both T-wall (S13) and on-top sunspaces (S15), and meanwhile, dynamic payback period of S13 and S15 is 2.2 years and 3.4 years, respectively. Although the energy-saving rate and the consequential saved money per year of S13, S14, and S15 perform worse than S1 (only insulation material used), their payback period are shorter than that of S1 instead due to their lower cost of investment compared to insulation materials. In detail, the saved money per year of S2 can be up to 51.6 CNY/m² but the corresponding investment cost even ups to 621 CNY/m², by contrast, although the saved money per year of S13, S14, and S15 is only 4.6 CNY/m², 11.4 CNY/m², and 8.1 CNY/m², which only accounts for 8-22% of that of S1, their investment costs of 14.3 CNY/m², 48.2 CNY/m², and 33.9 CNY/m² are much less than S2, accounting for 2.3-7.8% of that of S2, thus these strategies with lower energy-saving rate can balance out the investment expenditure more quickly.

Additionally, the dynamic payback period of S2 that saves the largest amount of annual largest energy demand is 21.8 years, whereas the dynamic payback period of S1 is approximately 8 years shorter than S2, showing that investment expenditure can be recovered in a shorter period of time if PCM is not employed, and this result also proves the related inference expressed in the last paragraph.

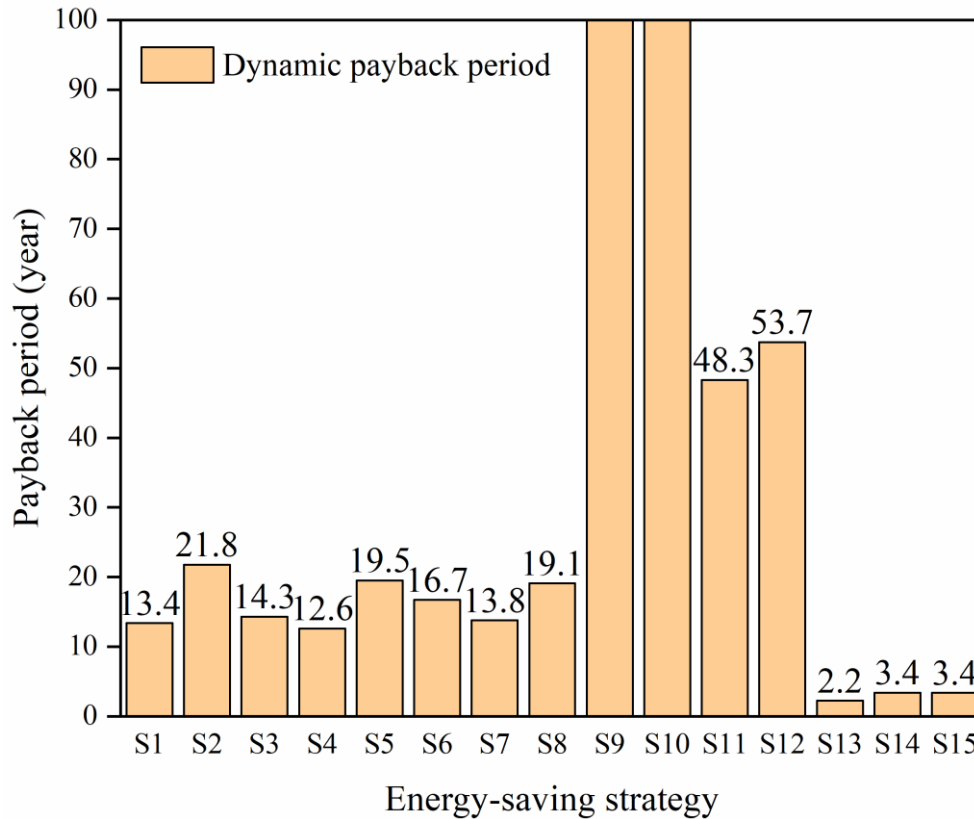


Figure 8-1. Dynamic payback period of each energy-saving strategy.

It's no doubt that different calculation method can lead to distinct value of payback period for each energy-saving strategy, which can further affect the final judgment made by decision-makers and thus an appropriate calculation method can provide results closer to the reality as a reference for making decisions. Hence, based on these results of dynamic investment payback period (DPP), we can compare it to the results obtained by simple payback period method (SPP). Unlike dynamic investment payback period taking into account the value of money [7-8], simple payback period (SPP) is calculated by directly dividing the initial investment cost by the annual saved money for electricity [8-10]. SPP of S9, S10, S11, and S12 is 97.6 years, 41.5 years, 27.3 years, and 23.3 years, respectively, all of these results are much less than results of DPP, and SPP results of S10 and S12 are even lower than half of their DPP values. Moreover, the payback period of S12 obtained by SPP is even shorter than the reference value of 25 years, and if only considering whether the payback period is within the reference years, which means that the results calculated by SPP and DPP methods will lead to completely opposite conclusions. As for S1 and S2, their payback period based on SPP calculation is shorter than DPP, and meanwhile, the difference between their SPP is only 5.1

years, which also less than that of DPP (8.4 years). Similarly, S3, S4, S5, S6, S7, and S8 also have a less payback period when simple payback period (SPP) method is employed. The appearance of smaller values of SPP results is logical since it doesn't consider the effect of time on the value of money. In detail, the saved money per year of energy-saving strategies is converted to the present value for the calculation year to reflect the time value of money in DPP method, while in the present economic background, the value of benchmark discount rate is positive, meaning an inflation phenomenon and also implying that the value of saved money caused by energy-saving strategies declines over time. However, the calculation results obtained by SPP is not certainly smaller than that of DPP method, for instance, S13, S14, and S15 have a longer payback period when SPP method is used, and we infer the reason of this phenomenon is that in the DPP method, based on the year with non-negative cumulative discounted value first appeared, the accurate result is further obtained based on the cumulative discounted value of the last year and the net present flow discounted value in the present year, and the detailed calculation procedure is depicted in Chapter 3; whereas in SPP method, the investment cost is directly divided by the saved money per year, meaning the result is the end of the year when investment cost is recovered and thereby the result cannot reflect the fact if the investment cost is recovered before the end of this year, thus its result is not as accurate as it of DPP. Hence the calculation results obtained by DPP are much closer to reality and more accurate while the results calculated by SPP are more ideal and relatively crude.

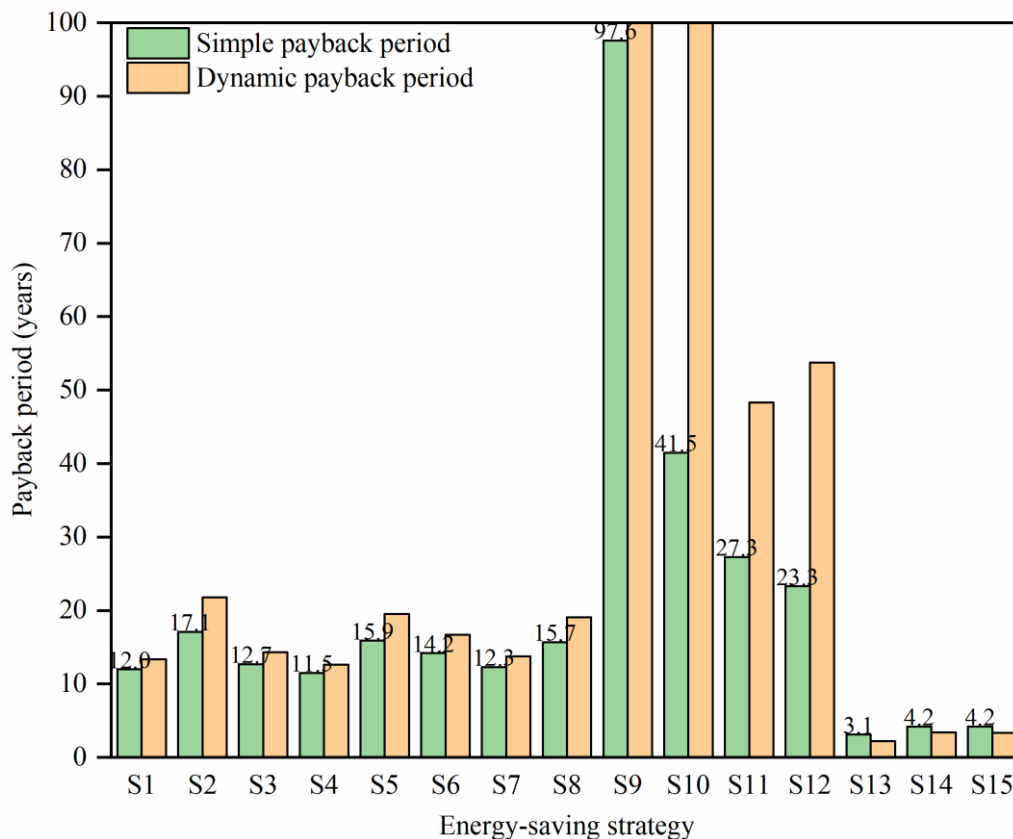


Figure 8-2. Comparison of simple payback period (SPP) and dynamic payback period (DPP) for each energy-saving strategy.

CHAPTER 8. TECH-ECONOMIC ANALYSIS OF COMPREHENSIVE ENERGY-SAVING STRATEGIES

Payback period is a crucial reference factor for making decisions on general investment projects, while for these energy-saving strategies that will continue to bring economic benefits once they are implemented, meaning the energy-saving strategies can still create electric charge savings benefits beyond the payback years, therefore an assessment of their economic benefits over a long time can provide a highly useful reference for decision-makers and help them make more desirable decisions. Hence the corresponding economic benefits that each energy-saving strategy obtained over 25 years are evaluated based on dynamic payback period (DPP) calculation method and results are presented in Figure 8-3. Amongst these strategies, S9, S10, S11, and S12 have a negative economic benefits owing to the prohibitive expenditure of PCM. Furthermore, S1 of only insulation strategy is utilized is able to save money of 324 CNY/m², however, the strategy S2 only can only save 61 CNY/m² once PCM is added because the expensive investment cost of PCM negates the great benefits brought by insulation strategy. The above results corroborate that utilizing PCM to save building energy is not cost-effective in the current economic environment. As for S13, S14, and S15, although they can balance out the initial investment cost in a very short period of time, their economic benefits are not the highest in the long run, demonstrating a fact that a shorter payback period does not certainly mean an excellent economic benefit, and further proving the necessity of assessing economic benefits for each energy-saving strategy. Lastly, the best benefit is neither created by the strategy that declines the largest energy demand (S2), nor by S1 which only adding insulation materials with the optimal economic thickness or by S8 who combines all of four individual strategies, but by S4, which includes optimal insulation material (S1) and on-top sunspaces (S15). The economic benefits of S4 can achieve 347 CNY/m², approximately 7.1% higher than that of S1 (324 CNY/m²), and about 4.7 times higher than S2 (61 CNY/m²). Although the annual energy demand of S4 is 1.42 kWh/m² higher than S1, meaning the saved money per year by S4 is about 0.7 CNY/m² less than S1, however, the investment cost of S4 is also cheaper than that of S1. According to Table 8-4, it is notable that the cost of S4 (584.8 CNY/m²) is 36.2 CNY/m² lower than that of S1 (621 CNY/m²), and it is apparent that the amount of cost saving is far larger than the electricity cost of extra energy load consumed, thus S4 creates the greatest economic benefits rather than S1. Consequently, we can know that economic evaluation results not only determined by the energy-saving effects but greatly affected by the investment expenditure and economic background, and meanwhile, payback period and economic benefits are two important reference factors whereas they are not certainly consistent with each other, therefore both of them should be deeply evaluated and in this study, S4 which using polyurethane foam of 81mm for exterior walls, adding polyurethane foam of 121mm for roof and meanwhile, setting sunspaces with WRR equals 75% is the most cost-effective strategy for traditional dwellings in northeast of Sichuan hills, China.

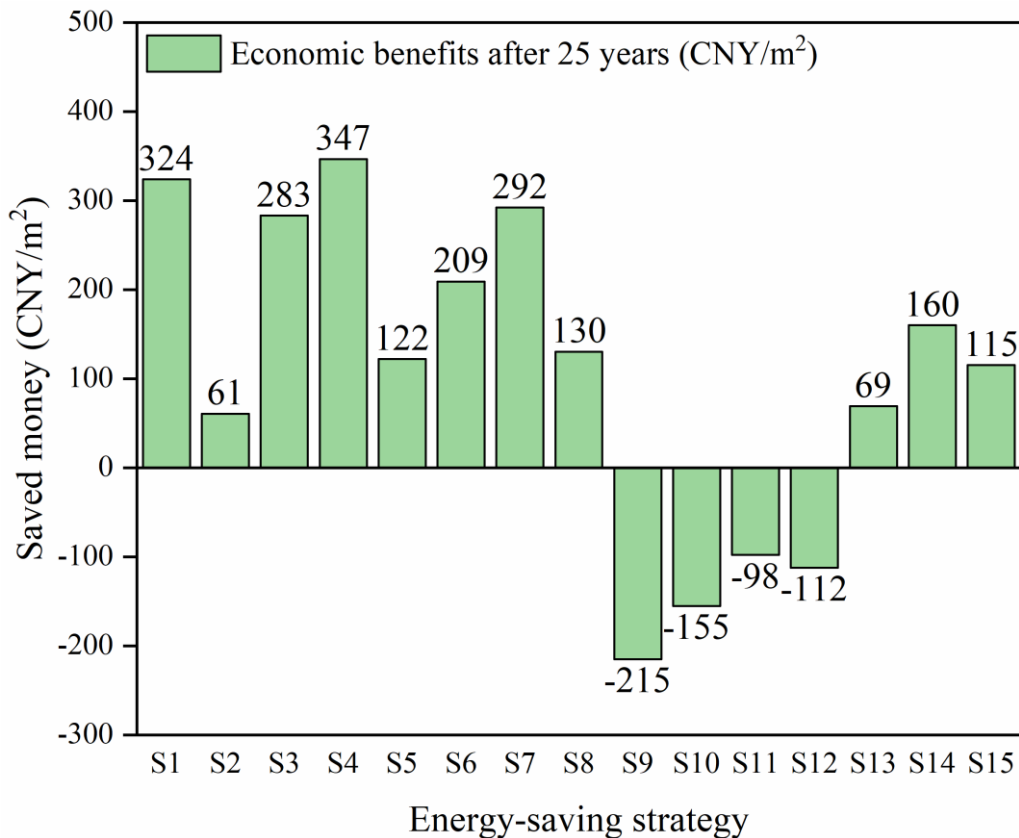


Figure 8-3. Economic benefits after 25 years of each energy-saving strategy.

8.3 Influence of building orientation on energy-saving and economic potential

Building orientation is one of the important factors affecting building energy demand. Although Li et al. [11] selected public buildings in China as research objects to analyze effects of building orientation on building energy consumption and asserted that orientation was not the significant factor for energy consumption variation compared to other design factors, such as thermophysical parameters of exterior envelopes, wall/window ratio, and shape coefficient, the influence of building orientation still cannot be ignored. For instance, Hu et al. [12] proved that energy consumption was closely related to the building orientation in hot summer and cold winter zone (HSCW) based on simulation, and the energy consumption of building when faces south was about 15% lower than which faces north. Similarly, Odunfa et al. [13] found that building with North-South orientation could lower 4.87% of energy demand than that with East-West building orientation. In addition, Ji et al. [14] carried out a simulation analysis of cooling, heating, lighting system, and annual energy consumption of a dormitory of a university located in Shandong province, China and observed that the amount of annual energy consumption increased as orientation varied from south to north. In northeast of Sichuan hills, China, the construction of local traditional dwellings always tends to conform to the terrain since the research area is hilly terrain with limited flat land. As a result, the orientation of the local rural traditional buildings is usually not facing south, whereas the previous analysis results are obtained based on building facing south, thus the energy-saving and economic

CHAPTER 8. TECH-ECONOMIC ANALYSIS OF COMPREHENSIVE ENERGY-SAVING STRATEGIES

evaluation results are not sufficiently accurate for buildings with different orientation. In order to analyze the influence caused by building orientation on the energy-saving and economic potential and ensure the efficiency of the recommended energy-saving strategy, this part discusses the influence of building orientation on the effect of energy-saving strategy based on the base model adopted S4 strategy. The model is rotated in the clockwise and counterclockwise direction, respectively, and each rotation angle is 15° during the rotation process, while the corresponding energy demands of each building orientation are displayed in Table 8-6 and Figure 8-4.

The simulation results displayed in Figure 8-4 and Table 8-6 reveal that orientation affects the effect of energy-saving strategy to some extent. 0° stands for the energy demand of building facing south, while the corresponding energy demand of other orientation increases as orientation variation. In detail, the increase rate of energy demand is 1%, 2%, 5%, 8%, 10%, and 11%, from 15° to 90° (clockwise), while for counterclockwise, the corresponding increase rate is 1%, 3%, 5%, 6%, 7%, and 6%, respectively. Based on these results, the angle of building north and actual north is within $\pm 30^\circ$ has less impact on the energy demand. Furthermore, from detailed data shown in Table 8-6, we can notice that heating load hardly varies whatever rotation angle is, whereas cooling load becomes larger with orientation variation, and similar variations of heating load and cooling load occur in another research conducted by Hu et. al [15]. We are try to explain this performance of cooling load is because that the cooling load accounts for a small portion of the annual energy demand, therefore the annual energy demand is less affected by building orientation. In addition, although there is an 11% energy increase rate of energy consumption when under the worst situation when the research model rotates clockwise 90° (facing east), there is still an obvious saving rate (97.6%) of the annual energy demand compared to the primitive building without any energy-saving strategy. Consequently, these strategies still have a broad application prospect in this region although building orientation has some impacts on their effects.

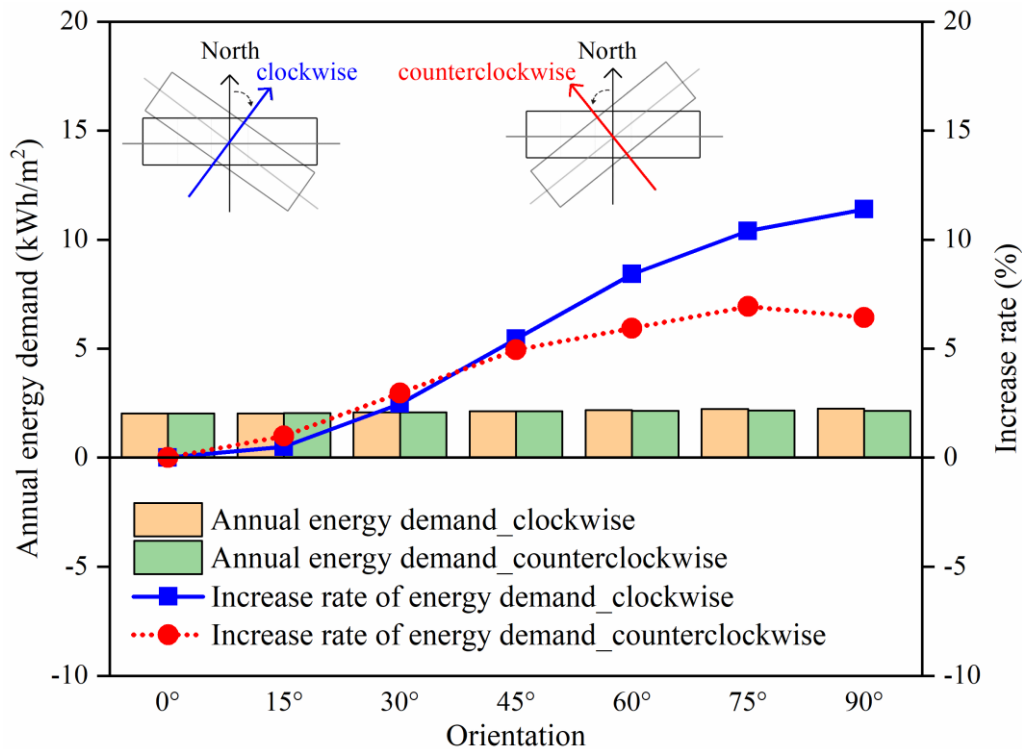


Figure 8-4. Influence of building orientation on the energy-saving effect of the optimal strategy.

Table 8-6 Heating load, cooling load, and annual energy demand of building with different orientation.

	Clockwise			Counterclockwise		
	Heating load kWh/m ²	Cooling load kWh/m ²	Annual energy demand kWh/m ²	Heating load kWh/m ²	Cooling load kWh/m ²	Annual energy demand kWh/m ²
0°	1.7	0.32	2.02	1.7	0.32	2.02
15°	1.7	0.33	2.03	1.71	0.33	2.04
30°	1.7	0.37	2.07	1.73	0.35	2.08
45°	1.7	0.43	2.13	1.73	0.39	2.12
60°	1.71	0.48	2.19	1.73	0.41	2.14
75°	1.72	0.51	2.23	1.73	0.43	2.16
90°	1.72	0.53	2.25	1.72	0.43	2.15

8.4 Energy-saving and economic potential for the tested building

We have already obtained the appropriate energy-saving strategy (S4) for this region which can almost reduce the annual energy demand to zero based on thorough energy-saving and economic evaluation in the previous parts, however, building shape coefficient also has great impact on the building energy consumption [14], therefore considering that there are other floor plan forms for

local dwellings and meanwhile, building orientation is varies, it is necessary to use a real building to further verify the energy savings and economic potential of the recommended energy-saving strategy. Hence, we take the tested building described in Chapter 3 as example, and evaluate its energy demand and economic performance pre and post renovation in this part, additionally, there is a fact to note that there is an angle of 60° (counterclockwise) between the north orientation of the tested building and the actual north orientation. Figure 8-5 displays the post renovation for tested building, the insulation materials (polyurethane foam) of 81mm and 121mm are fixed on exterior walls and roof, respectively, and meanwhile, on-top sunspaces with WRR of 75% are set on the roof of air-conditioned rooms. And finally, Table 8-7 summarizes the related results of energy demand and economic assessment.

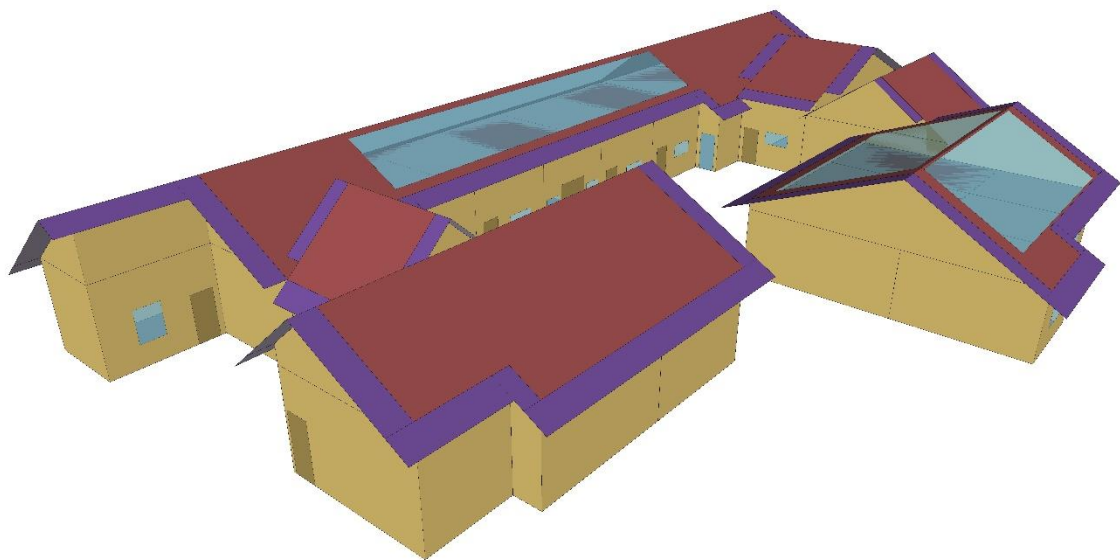


Figure 8-5. Diagram of tested building adopted S4 strategy.

According to the detailed calculation results shown in Table 8-7, both heating load and cooling load drop, and the saving rate of energy demand can achieve approximately 75.2%. Compared to the base building, the saving rates of heating load, cooling load, and annual energy demand are smaller, and we infer that there are two reasons. Firstly, we have already know that building orientation has an obvious influence on cooling load, the orientation of tested building makes it has a higher cooling load than it faces south, while the cooling load almost occupies 30% of the total annual energy demand whereas that of base building is 18%, therefore cooling load variation of tested building has a greater impact on the annual energy demand. Another most important reason is that the complex floor plan of tested building leads to the larger shape coefficient and irregular surfaces, further resulting in more self-shading of the building itself, which has a harmful impact for building to absorb more solar heat in winter. Additionally, although the energy-saving rate of S4 utilized in tested building is smaller than the base building, the dynamic investment payback period is only 9.1 years, which is even 3.5 years shorter than that of base building, and its economic benefits after 25 years is 412.8 CNY/m^2 , approximately 20% higher than that of base building. Eventually, we can conclude that the recommended strategy (S4) proposed in this study has substantial energy-

saving and economic benefits even for other local traditional dwellings with complex floor plan and unfavorable building orientation.

Table 8-7 Energy-saving and economic benefits of pre and post renovation for tested building.

Scenarios	Heating load (Saving rate) kWh/m ²	Cooling load (Saving rate) kWh/m ²	Energy demand (Saving rate) kWh/m ²	Saved money per year CNY/m ²	Investment cost CNY/m ²	Payback period year	Economic benefits after 25 years CNY/m ²
Pre	79.38	33.63	113.01	/	/	/	/
Post	19.41 (75.55%)	8.66 (74.25%)	28.07 (75.16%)	44.2	395.8	9.1	412.8

8.5 Summary

In Chapter 5, Chapter 6, and Chapter 7, we only discussed the energy-saving potential and their influencing factors of four individual strategies, including adding insulation materials with economic thickness for exterior walls and roof, adopting phase change material (PCM) with optimal parameter combination for exterior walls, fixing Trombe wall (T-wall) on the south façade, and setting on-top sunspaces (OS) on roofs of rooms. In this chapter, we obtained 15 strategies by making different combinations of these 4 individual strategies and then, we comprehensively evaluated their energy-saving potential, investment payback period, and economic benefits after 25 years with the help of EnergyPlus and dynamic investment payback period method (DPP). Considering that the building orientation of local traditional dwellings is diverse, we further assessed the influence of building orientation on the energy-saving effects and economic potential. Furthermore, we also took the actual tested building as an example, simulated its annual energy demand pre and post renovation by the recommended strategy, and calculated the corresponding economic benefits to prove the effective of the recommended energy-saving strategy. Eventually we obtained the following results.

- In terms of the performance of annual energy demand, the best strategy is S2, that is, adding insulation material (polyurethane foam) with economic thickness for exterior walls and roof, and simultaneously installing phase change material (PCM) on the exterior walls. Its saving rate of annual energy demand can up to 99.43%.
- In terms of the dynamic payback period, S13 that only T-wall strategy is adopted has the shortest payback period of only 2.2 years, whereas S9 (PCM), S10 (PCM and T-wall), S11 (PCM and OS), and S12 (PCM, T-wall and OS) cannot balance out their investment during the reference year of 25 years.
- The results of investment payback period obtained by DPP which considering the time value of the currency are much closer to reality and more accurate while the results calculated by SPP are more ideal and relatively crude. In detail, S1 (insulation), S2 (insulation and PCM), S3 (insulation and T-wall), S4 (insulation and OS), S5 (insulation, PCM and T-wall), S6

CHAPTER 8. TECH-ECONOMIC ANALYSIS OF COMPREHENSIVE ENERGY-SAVING STRATEGIES

(insulation, PCM and OS), S7 (insulation, T-wall and OS), S8 (all four individual strategies), S9 (PCM), S10 (PCM and T-wall), S11 (PCM and OS), and S12(PCM, T-wall and OS) have a less payback period when simple payback period method (SPP) is employed, by contrast, S13 (T-wall), S14 (T-wall and OS), and S15 (OS) has a longer payback period obtained by simple payback period method (SPP).

- In terms of economic benefits after 25 years calculated by dynamic payback period method (DPP), S4 (insulation and OS) can achieve the highest one of 347 CNY/m², followed by S1 of 324 CNY/m² (insulation), and S7 of 292 CNY/m² (insulation, T-wall and OS).
- Although building orientation has some impacts on their effects these strategies still have a broad application prospect in this region. The angle of building north and actual north is within $\pm 30^\circ$ has less impact on the energy demand. In addition, although there is an 11% energy increase rate of energy consumption when under the worst situation that the research model rotates clockwise 90° (facing east), there is still an obvious saving rate (97.6%) of the annual energy demand compared to the primitive building without any energy-saving strategy.
- Although the energy-saving rate of S4 utilized in the actual tested building (75.16%) is smaller than the base building (99.43%), the dynamic investment payback period is only 9.1 years, which is even 3.5 years shorter than that of the base building, and its economic benefits after 25 years is 412.8 CNY/m², approximately 20% higher than that of base building.

Reference

- [1] Ministry of Housing and Urban-Rural Development of the People's Republic of China, Design standard for energy efficiency of residential buildings in hot summer and cold winter zone JGJ134-2010, China Architecture & Building Press, Beijing, 2010.
- [2] Weather Data Download - Sichuan Nanchong 574110 (CSWD). https://energyplus.net/weather-location/asia_wmo_region_2/CHN/CHN_Sichuan.Nanchong.574110_CSWD, 2021
- [3] Chinese Standard Weather Data (CSWD). 2021. Available at <https://www.energyplus.net/weather/sources#CSWD>.
- [4] Ministry of Housing and Urban-Rural Development of the People's Republic of China. 2016. Code for thermal design of civil building GB50176-2016. Beijing: China Architecture & Building Press.
- [5] Xu J. 2021. Chengdu Engineering Cost Information. Chengdu: Sichuan University Press.
- [6] Sichuan Province material price information reporting and publishing system. 2021. Available at <http://202.61.90.35:8032/>. Accessed 15 October 2021.
- [7] Y. Geng, X. Han, H. Zhang, L. Shi, Optimization and cost analysis of thickness of vacuum insulation panel for structural insulating panel buildings in cold climates, *Journal of Building Engineering*. 33 (2021): 101853. <https://doi.org/10.1016/j.job.2020.101853>.
- [8] X. Liu, *Engineering Economy* (3rd Edition), China Architecture & Building Press, Beijing, 2015.
- [9] A.A. Serageldin, A. Abdeen, M.S. Ahmed, A. Radwan, S. Ookawara, Solar chimney combined with earth to-air heat exchanger for passive cooling of residential buildings in hot areas, *Solar Energy*. 206(2020):145-162. <https://doi.org/10.1016/j.solener.2020.05.102>
- [10] H. Huang, W.I.B.W.M. Nazi, Y. Yu, Y. Wang, Energy performance of a high-rise residential building retrofitted to passive building standard – A case study, *Applied Thermal Engineering*. 181 (2020): 115902. <https://doi.org/10.1016/j.applthermaleng.2020.115902>
- [11] R. Li, X. Cheng, X. Huang, D. Yuang, Reflections on the Optimal Building Orientation Based on the Analysis of Cooling-Heating Loads Affected by Solar Parameters, *Architectural Journal*. 2020 (11): 99-104. doi: <https://doi.org/10.19819/j.cnki.ISSN0529-1399.202011018>
- [12] D. Hu, D. Chen, P. Shan, F. Huang, H. Huang. Influence of Residential Building Orientations to Energy Consumption in Hot Summer and Warm Winter Zone, *Architectural Journal*. 2017 (45): 57-60.
- [13] K. M. Odunfa, T. O. Ojo, V. O. Odunfa, O. S. Ohunakin, Energy Efficiency in Building: Case of Buildings at the University of Ibadan, Nigeria, *Journal of Building Construction and Planning Research*. 2015 (3): 18-26. doi: <http://dx.doi.org/10.4236/jbcpr.2015.31003>
- [14] W. Ji, J. Wang, Y. Xie. Influence of Dormitory Building Orientation on Energy Consumption in Cold Zones: Taking the Dormitory of Shandong Jianzhu University as an Example, *Architectural Journal*. 2022 (50): 34-41.
- [15] Y. Hong, C. I. Ezech, W. Deng, S. H. Hong, Z. Peng, Y. Tang. Correlation between Building Characteristics and Associated Energy Consumption: Prototyping Low-Rise Office Buildings in Shanghai, *Energy and Buildings*. 2020(217): 1-13. doi: <https://doi.org/10.1016/j.enbuild.2020.109959>

Chapter 9

Conclusion

CHAPTER 9. CONCLUSION

Chapter 9. Conclusion

9. Conclusion	9-1
---------------------	-----

CHAPTER 9. CONCLUSION

9. Conclusion

The energy consumption of the building sector occupies nearly 40% of global energy consumption, while in China, the total energy consumption of the whole building process in 2018 was 2.147 billion tce, accounting for 46.5% of the total national energy consumption, of which 1 billion tce was consumed during the building operation phase. Meanwhile, rural buildings contribute 24% of building energy consumption during the operation phase, therefore it is an essential approach to reduce energy consumption and carbon emission by lowering energy demand of rural buildings. According to the field investigation, traditional dwellings located in northeast of Sichuan hills always has thermal performance of exterior envelopes which cannot be satisfied with the related energy efficiency standard, thus causing high annual energy demand and the poor indoor thermal environment. In order to determine appropriate energy-saving renovation strategies for traditional dwellings in this region, we carried out thorough tech-economic evaluation for a set of energy-saving strategies. The main work and results can be summarized as follows.

In **Chapter 1, Research Background and Purpose of the Study**, we reviewed the energy consumption situation for the world and China, and further introduced the share of energy consumption for building sector in China. Next we explained the climate background of the research region – northeast of Sichuan hills, and analyzed the challenge for lowering energy consumption in this region. Then we also introduced the current population and economic development of the research region. Based on the previous research background of the research region, we clarified the purpose, significance, and research structure of this study.

In **Chapter 2, Literature Review**, we reviewed a lot of previous published studies to find appropriate energy-saving strategies for traditional dwellings in this research region. Firstly, we summarized the heat transfer process through opaque envelopes of buildings, and then we determined three directions to realize the goal of energy saving based on these fundamental theories. Therefore, the related research on applying insulation system, phase change material (PCM), and solar radiation to reduce the energy demand of buildings were reviewed in the rest parts of this chapter.

In **Chapter 3, Methodology**, we introduced the detail information about traditional dwellings in this research region based on the field investigation carried on January and July, 2017, and the arrangement of the experimental work, then a base model used for discussing the energy-saving strategies was established and depicted. Next, we also clarified the calculation process of all of research methods we used in this study, including the core formula for the dynamic simulation program – EnergyPlus, the principle of orthogonal experiment design (OED) and the thorough calculation process of analysis of variance (AVOVA), and the principle and calculation method to obtain a dynamic investment payback period (DPP) and the corresponding economic benefits.

In **Chapter 4, Thermal Performance of the Tested Building**, we analyzed the recorded data of the actual tested building, including the outdoor air temperature and relative humidity, indoor air temperature and relative humidity, outside and inside surface temperatures of exterior walls, and outside and inside surface temperature of the roof. Then we calculated the theoretical values of some

basic thermal indicators of exterior envelopes, including the heat transfer coefficient of the present exterior walls and roof, the thermal inertia of the present exterior walls and roof, and the temperatures of the inner surface of the exterior wall and the inner surface of the roof, and further compared these values with the requirements proposed by the related energy efficiency standard. Moreover, in order to deeply comprehend the indoor environment of the current local traditional dwellings in this region, we also simulated the indoor air temperature throughout the whole year by EnergyPlus.

In **Chapter 5, Determine Insulation Thickness of Exterior Envelopes for the Traditional Dwellings in Northeast of Sichuan Hills**, we derived the calculation method of the optimum economic thickness of insulation materials for building exterior walls in northeast of Sichuan hills, then calculated the optimal economic thickness for exterior walls of five commonly used insulation materials, including expanded polystyrene (EPS), stone wool board (SW), polyurethane foam (PU), extruded polystyrene (XPS), and phenolic foam (PF). Next, we compared and ranked the importance of all of the factors which could affect the optimum thickness by orthogonal test and analysis of variance (AVOVA). Furthermore, we discussed the correlation between the optimal economic thickness of insulation materials for roof and the optimal economic thickness of insulation materials for exterior walls and finally, we determined the recommended ratio of their optimal economic thickness.

In **Chapter 6, Parametric and Economic Analysis of Phase Change Materials (PCM) on Energy Saving for Traditional Dwellings in Northeast of Sichuan Hills**, we selected the total of eight parameters of PCM, including location, melting temperature, thickness, phase transition temperature radius, latent heat, density, thermal conductivity, and specific heat, then varied their values in a predetermined range and investigated the effects of their variation on the annual energy demand of traditional dwellings in northeast Sichuan hills, and finally obtained the optimal combination of the parameters of PCM. Furthermore, considering the high cost of PCM, we also discussed a more economic selection of PCM for this study region.

In **Chapter 7, Passive Application of Solar Energy for Traditional Dwellings in Northeast of Sichuan Hills**, we proposed two strategies – Trombe wall (T-wall) and on-top sunspaces (OS) and assessed their energy-saving performances. We discussed the impact of thickness of air cavity, the utilization of shade control, and the glass category of T-wall glazing on the energy-saving effect of T-wall, as for on-top sunspaces strategy, we also analyzed the influence of the glazing area variation and shade control on the energy-saving effect of the on-top sunspaces strategy. Finally, we determined the optimal parameters of these two strategies.

In **Chapter 8, Tech-economic Analysis of Comprehensive Energy-saving Strategies**, we obtained 15 strategies by making different combinations of four individual strategies proposed in Chapter 5-7 and then, we comprehensively evaluated their energy-saving potential, investment payback period, and economic benefits after 25 years with the help of EnergyPlus and dynamic investment payback period method (DPP). Considering that the building orientation of local traditional dwellings is diverse, we further assessed the influence of building orientation on the

energy-saving effects and economic potential. Furthermore, we also took the actual tested building as an example, simulated its annual energy demand pre and post renovation, and calculated the corresponding economic benefits to prove the effective of the recommended energy-saving strategy.

In **Chapter 9, Conclusion** has been presented.

Finally, we can obtain the following main findings:

- The optimum thickness of expanded polystyrene (EPS), stone wool board (SW), polyurethane foam (PU), extruded polystyrene (XPS), and phenolic foam (PF) is 0.114m, 0.105m, 0.081m, 0.098m and 0.113m, respectively.
- Polyurethane foam is the preferred insulation material among these five commonly used insulation materials in this region. Its economic benefit can achieve 306.7 CNY/m² during 25 years while its dynamic payback period is 7.8 years.
- The optimum thickness of roof insulation material is 1.5 times of the optimum economic thickness of walls insulation.
- PCM with optimal parameters can save about 22.15% of annual energy demand, and this saving rate is 9-20% higher than others.
- The thermal conductivity, density, and thickness are three crucial parameters affecting the economic benefits of PCM.
- The most economic strategy for this region is combining insulation materials and on-top sunspaces, the corresponding economic benefit can up to 347 CNY/m² (\approx 51.8 USD/m²) and 412.8 CNY/m² (\approx 61.6 USD/m²) for the base model and tested building, respectively.

To summary, this study aims to find some efficient and economic strategies for traditional dwellings in northeast of Sichuan hills, China to lower their energy demand. And the significance of this study are summarized as following:

1. Derive the formula for calculating the optimum economic thickness of insulation materials used for exterior walls. Then determine the optimum thickness of five commonly used insulation materials by this calculation formula, results can be directly adopted by residents, engineers, or decision-makers for this region.
2. Rank the important degree of influencing factors of optimum economic thickness of insulation materials and determine the most significant influencing factor. This exploration is rare in the previous relevant work. Results can provide some new insights into the energy-saving retrofit and offer some data references for residents and policy-makers.
3. Evaluate the energy-saving and economic potential of phase change material (PCM) utilization in this region, and determine three crucial factors affecting the economic benefits of PCM. Results can help decision-makers comprehend the application effect of this innovation materials and provide useful economic references for them.

4. Determine the optimal parameters for each energy-saving strategy, and propose the most economic retrofit strategy for traditional dwellings in this region. Results can help residents or decision-makers select the relatively appropriate energy-saving strategy to retrofit the traditional dwellings in this region, and thereby decrease the energy demand of the building.